THE ROLE OF THE METASTASIS SUPPRESSOR TETRASPANIN CD82/KAI1 IN TRASTUZUMAB-MEDIATED CELLULAR RESPONSES

By

EVA MCGROWDER

A thesis submitted to the Division of Cancer Studies at the University of Birmingham for the degree of DOCTOR OF PHILOSOPHY

Cancer Research UK Institute for Cancer Studies

University of Birmingham

June 2012

ABSTRACT

The metastasis suppressor CD82/KAI1, a member of the tetraspanin family of transmembrane proteins has previously been shown to associate with ErbB2 (Odintsova et al. 2003). We hypothesised that CD82 could potentiate the efficacy of Herceptin by either regulating the distribution and dynamics of the ErbB2/Herceptin complex or by modifying the recruitment of signalling molecules to the plasma membrane. The role of CD82 in Herceptin-mediated cellular responses was investigated using ErbB2-positive breast cancer cell lines expressing varying levels of CD82. We found that ectopic expression of CD82 resulted in a poor cellular response to Herceptin treatment, redistribution of ErbB2 and an increase in phosphorylation of ErbB2, Src and proteins of the mitogen-activated protein kinase (MAPK) signalling cascade in a manner that was independent of the Ras proteins. The CD82-mediated effect on ErbB signalling was found to be specific to the MAPK pathways, as the phosphoinositide 3-kinase (PI3K) pathway was unaffected by ectopic expression of CD82. Taken together, our results demonstrate that CD82 negatively modulates the cellular response of ErbB2-positive breast cancer cells to Herceptin treatment by not only regulating the distribution of the ErbB2 receptor, but also its phosphorylation and activation of downstream signalling pathways, particularly the MAPK pathway.

FOR MY FAMILY

ACKNOWLEDGEMENTS

Firstly, I would like to express my immense gratitude to my family for the love, belief, support and patience they have shown me over the years. I never would have reached this stage without them by my side. Secondly, I am very grateful to my supervisors, Dr Elena Odintsova and Dr Fedor Berditchevski for giving me the opportunity to undertake my PhD studies in their laboratory and also for their wisdom and guidance throughout this project. Thirdly, I would like to thank Dr Thorsten Wohland, Professor William J. Gullick, Dr Michael A. White, Dr Hélène Conjeaud, Dr Osamu Yoshie and Dr Eric Rubinstein, for kindly providing us with plasmids and antibodies used for this work. I am also grateful to Dr Hanna Romanska for helping me with the analysis of the 3-dimensional cultures. Fourthly, I express my profound thanks to all my dear friends and colleagues with whom I had the pleasure of working with or indeed disturbing, especially, Dr Dale Powner, Dr Vera Novitskaya, Dr Ruzica Bago, Dr Rafal Sadej, Dr Sven Petersen, Dr Gouri Baldwin, Professor David Blackbourn, Dr Simon Joel, Dr Adedayo Oke, Dr Jude Fitzgibbon, Dr Csaba Bödör, Professor Gordon Gibson and Gordon Ryan for their encouragement and support and for never being too busy for me whenever I needed their help. I am also thankful to all my other friends; Izabela Bombik, Elvie Solen and Michael Parks for all the banter and humour that always lightened my heart and made life in Birmingham much more enjoyable. Last but not least, I would like to thank the University of Birmingham, School of Medicine for funding my studies. This work would not have been done without all those mentioned above and I thus extend my deepest appreciation to you all.

TABLE OF CONTENTS

LIST OF FIGURES

LIST OF TABLES

ABBREVIATIONS

µg	Microgram
µl	Microlitre
3D	Three dimensions
AC	Adenocarcinoma
ADCC	Antibody-dependent cellular cytotoxicity
ADU	Arbitrary densitometry units
AP	Adaptor protein
AP1	Activator protein 1
APC	Antigen presenting cell
APS	Ammonium persulfate
AR	Amphiregulin
Asn/N	Asparagine
BSA	Bovine serum albumin
BTC	Betacellulin
CAS	Crk-associated substrate
CCG	Cysteine-cysteine-glycine motif
CO_2	Carbon dioxide
CR	Cysteine-rich
CRUK	Cancer Research UK
DARC	Duffy antigen receptor for chemokines
dH_2O	Distilled water
DMEM	Dulbecco's Modified Eagle's Medium
DMSO	Dimethyl sulfoxide
EC	Extracellular
ECL Plus	Enhanced chemiluminescence plus
ECM	Extracellular matrix
EDTA	Ethylenediaminetetraacetic acid
EGF	Epidermal growth factor
EGFR	Epidermal growth factor receptor
EPR	Epiregulin
ER	Estrogen receptor
Erk	Extracellular signal-regulated kinase
ERM	Ezrin-radixin-moesin
EVH1	Enabled/VASP homology domain 1
FACS	Fluorescence activated cell sorting
FAK	Focal adhesion kinase
FBS	Fetal bovine serum
FcR	Fc receptor
FDA	Food and Drug Administration
FEVR	Familial exudative vitreoretinopathy
FITC	Fluorescein isothiocyanate
FN	Fibronectin
FRAP	Fluorescence recovery after photobleaching
GAP	GTPase-activating protein
GDP/GTP	Guanosine di-(tri)-phosphate

GEF	Guanosine nucleotide exchange factor
GFP	Green fluorescent protein
Gln/Q	Glutamine
Glu/E	Glutamic acid
GPCR	G-Protein coupled receptor
Grb2	Growth factor receptor-bound protein 2
GTPγS	Non-hydrolysable GTP analogue
HA	Haemagglutinin
HB-EGF	Heparin-binding EGF-like growth factor
HC	Herceptin
HCl	Hydrochloric acid
HEPES	4-(2-hydroxyethyl)-1-piperazineethanesulfonic acid
HGF	Hepatocyte growth factor
hGH	Human growth hormone
HGNC	HUGO Gene Nomenclature Committee
HI – FBS	Heat-inactivated foetal bovine serum
HrG	Heregulin
HTLV-1	Human T-cell leukaemia virus-1
IBC	Invasive breast carcinoma
ICAM-1	Intracellular cell adhesion molecule-1
IDC	Invasive ductal carcinoma
IGF	Insulin-like growth factor
IGF-1R	Insulin-like growth factor-1 receptor
IgG	Immunoglobulin G
IMP	Impedes mitogenic signal propagation
IP	Immunoprecipitation
JNK	Jun N-terminal kinase
K	Lysine
kDa	Kilodalton
KSR1	Kinase suppressor of Ras 1
L	Luminal breast cancer subtype
LN	Laminin
LR	Leucine-rich
mAbs	Monoclonal antibodies
MAPK	Mitogen-activated protein kinase
MDM2	Murine double minute 2
MES	2-(*N*-morpholino)ethanesulfonic acid
M_f	Mobile fraction
MHC	Major histocompatibility complex
mIgG	Mouse immunoglobulin G
MKP-1	MAPK phosphatase-1
mTOR	Mammalian target of rapamycin
NA	Numerical aperture
Na_3VO_4	Sodium orthovanadate
$Na_4P_2O_7$	Tetrasodium pyrophosphate
NaF	Sodium fluoride
NGF	Nerve growth factor
NRGs	Neuregulins
PBS	Phosphate buffered saline
PBS-T	Phosphate buffered saline with Tween-80

PDK1	Phosphoinositide-dependent kinase-1
PE	Phycoerythrin
PFA	Paraformaldehyde
PHA	Phytohaemagglutinin
PI3K	Phosphatidylinositol-3-kinase
PI4KII	Type II phosphatidylinositol 4-kinase
PIP2	Phosphatidylinositol-4,5-bisphosphate
PIP3	Phosphatidylinositol-3,4,5-trisphosphate
PKC	Protein kinase C
PMSF	Phenylmethylsulfonyl fluoride
PP2A	Protein phosphatase-2A
PR	Progesterone receptor
PRAPA	Precision red advanced protein assay
ProHB-EGF	Membrane-bound heparin-binding EGF-like growth factor
PTB	Phosphotyrosine binding
PTEN	Phosphatase and tensin homolog deleted on chromosome 10
Puro	Puromycin
RBD	Ras binding domain
RDS	Retinal dystrophy syndrome
RKIP	Raf kinase inhibitor protein
ROI	Region of interest
RTK	Receptor tyrosine kinase
S	Serine
SDS	Sodium dodecyl sulphate
SDS-PAGE	Sodium dodecyl sulphate polyacrylamide gel electrophoresis
SH2	Src homology 2 domain
Shc	Src homology 2 domain-containing protein
shRNA	Short-hairpin ribonucleic acid
SOS	Son of sevenless
SPRED	Sprouty-related proteins with an EVH1
T	Threonine
TBS-T	Tris buffered saline with Tween-80
TEMED	Tetramethylethylenediamine
TERMs	Tetraspanin enriched microdomains
TGF-α/β	Transforming growth factor-alpha and beta
TI-VAMP	Tetanus neurotoxin-insensitive vesicle-associated membrane protein
TKI	Tyrosine kinase inhibitor
TM	Transmembrane domain
TNF-α	Tumour necrosis factor-alpha
TSP-1	Thrombospondin-1
UP	Uroplakin
V	Valine
V/V	Volume to volume
VCAM-1	Vascular cell adhesion molecule-1
VEGF	Vascular endothelial growth factor
WB	Western blotting
W/V	Weight to volume
WinMDI	Windows multiple document interface
Y	Tyrosine
Zeo	Zeocin

1 INTRODUCTION

1.1 Introduction to cancer

Cancer is a generic name used to denote a variety of malignant neoplastic diseases that stem from different cell types. It is a progressive disease that involves numerous alterations in the genetic material of normal cells, that ultimately leads to transformed cancer cells with a growth advantage over their neighbouring non-transformed cells (Hanahan and Weinberg 2000;Hanahan and Weinberg 2011).

1.1.1 Breast cancer

Breast cancer is the most common cancer in the United Kingdom (UK), preceding prostate, lung and colorectal cancers, which all together account for more than half (59%) of all new cases of cancer (Office of National Statistics) (http://www.ons.gov.uk/ons/publications/re-reference-tables.html?edition=tcm%3A77-251462). In 2007-2009, there were 47,809 (30.6%) registered cases of breast cancer in the UK out of a total of 156,254 cases of all malignancies registered in women. Of all the cancers registered in the UK during the same period, breast cancer had the highest incidence rate of 124 cases per 100,000 women preceding lung cancer which is the second highest registered type of cancer in women for which only 39 cases were registered per 100,000 women (Office of National Statistics)

(http://www.ons.gov.uk/ons/rel/cancer-unit/cancer-incidence-and-mortality/2007-2009/stb-cancer-incidence-and-mortality.html). Breast cancer is a heterogeneous disease which encompasses several pathological entities with distinct clinical behaviour. Based on gene expression profile analysis using microarrays, breast cancer can be classified into five groups according to their expression pattern, namely: luminal A, luminal B, normal breast-like, ErbB2-positive and basal-like. Of the five types of breast cancer, luminal A carcinomas are considered to have a better prognosis compared to basal-like, which is the most aggressive subtype (Geyer et al. 2009;Tavassoli 2010). The human mammary gland consists of two distinct types of epithelial cells; basal and luminal epithelial cells. The former can be immunohistochemically distinguished from luminal, by staining with antibodies against the basal cytokeratins 5/6, whilst the latter cells stain positive for the luminal cytokeratins 8/18. Cytokeratins are widely used as biomarkers due to their tissue specific expression (Perou et al. 2000).

1.1.1.1 Luminal subtypes

The luminal subtypes are hormone receptor-expressing breast carcinomas. Luminal A cancers are positive for the hormone receptors; oestrogen receptor (ER^+) and progesterone receptor (PR^+), but do not overexpress ErbB2, therefore are considered to be ErbB2 negative ($ErbB2^-$). In contrast, luminal B cancers are ER^+, PR^+ and $ErbB2^+$ (Brenton et al. 2005;Carey et al. 2006;Carey 2010;Millikan et al. 2008). These types of breast cancers are treated with endocrine therapy such as Tamoxifen and generally have a good prognosis

compared to other breast cancer subtypes. However, there are variations between the two luminal groups in their response to treatment, whereby luminal B tumours generally have a worse prognosis, with high proliferative rates than luminal A (Brenton et al. 2005).

1.1.1.2 Triple-negative breast cancer

Triple-negative breast cancer is a subtype that is negative of the three main breast cancer markers; ER^-, PR^- and $ErbB2^-$. It can be classified into two sub-groups, basal-like and non-basal-like, according to the expression of cytokeratins 5/6 and the epidermal growth factor receptor (EGFR) (Yamamoto et al. 2009). The basal-like subtype shows gene expression patterns reminiscent for normal basal epithelial cells of the breast. These include, positive immunohistochemistry staining for the breast basal cytokeratins 5/6, ER negative, low expression levels of ErbB2 (thus considered $ErbB2^-$), and overexpression of EGFR. Conversely, the non-basal-like subgroup of triple-negative breast cancer is cytokeratins 5/6-negative and also EGFR-negative (Brenton et al. 2005;Geyer et al. 2009;Yamamoto et al. 2009). Triple-negative breast cancers display an aggressive clinical behaviour, with high recurrence rates within the first five years post diagnosis and a worse outcome compared to tumours of other subgroups. This could be due to the fact that no therapeutic target has been confirmed yet for this subtype as compared to the targeted therapy available for the hormone receptor-positive and ErbB2-positive breast cancer subtypes; endocrine therapy and Herceptin, respectively (Geyer et al. 2009).

1.1.1.3 The ErbB2-enriched subtype

ErbB2 positive breast cancers are characterised by overexpression of the ErbB2 receptor and whether they harbour amplification of the *ErbB2* gene. These tumours are also often ER and PR negative (Carey 2010;Geyer et al. 2009;Schnitt 2010). However, not all ErbB2-enriched breast cancers are classified into the ErbB2-enriched category; ErbB2-driven breast cancers that express both the luminal and ErbB2 gene clusters are categorised into the luminal subtypes rather than in the ErbB2-enriched subtype (Carey 2010). The ErbB2-enriched subtype of breast cancer carries a poor prognosis. However, the incorporation of Herceptin, a monoclonal antibody against ErbB2 into adjuvant chemotherapy improved disease-free survival in some cases of this subgroup, thus demonstrating the effectiveness of targeted therapy at improving outcome (Brenton et al. 2005;Carey 2010;Hudis 2007;Olopade et al. 2008). Both ErbB2 and Herceptin will be discussed further in the next sections.

1.2 The ErbB receptor tyrosine kinase family

The epidermal growth factor (EGF) family of receptor tyrosine kinases (RTKs) comprises of four members, namely, EGFR/ErbB1/HER1, ErbB2/Neu/HER2, ErbB3/HER3 and ErbB4/HER4, located on chromosomes 7p12; 17q11.2-q12; 12q13; and 2q33.3-q34, respectively (Figure 1.1) (Robinson et al. 2000). From henceforth, they will be referred to as EGFR and ErbB receptors accordingly. This receptor family was originally named the ErbB family due to their homology

to the v-erbB oncogene of the avian erythroblastosis virus (Citri and Yarden 2006;Roskoski, Jr. 2004). Receptor tyrosine kinases are single-pass transmembrane receptors with an extracellular ligand binding domain, a single transmembrane domain and an intracellular tyrosine kinase domain, flanked by a juxtamembrane and a C-terminal regulatory region (Figure 1.2) (Burgess et al. 2003;Li and Hristova 2010).

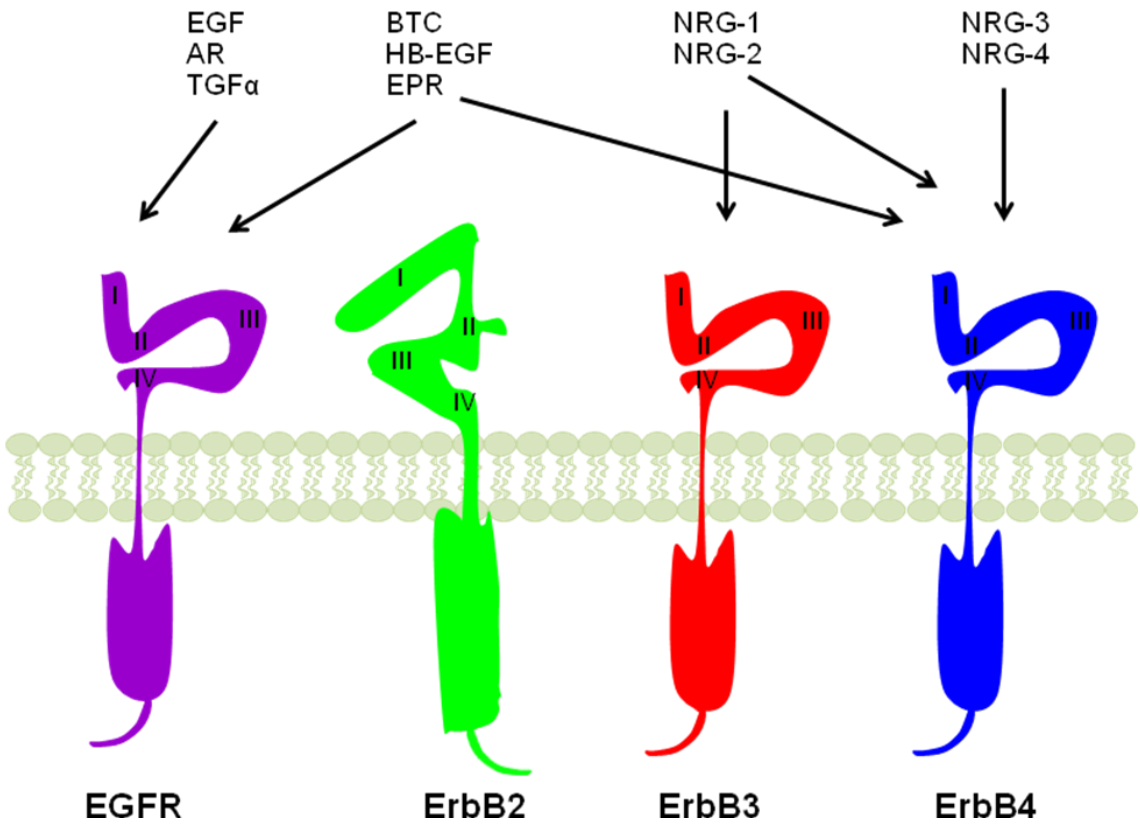

Figure 1.1: The ErbB family of receptor tyrosine kinases.

The four family members of the epidermal growth factor (EGF) family of receptor tyrosine kinases and the binding specificity of the EGF-related growth factor ligands. There is currently no EGF-related growth factor ligand known to bind to ErbB2. The extracellular domain of all family members consists of four subdomains I-IV; of which, domains I and III are important for ligand binding, domain II also known as the dimerisation arm, is important for receptor-receptor interactions and domain IV is involved in receptor auto-inhibition. In the absence of a ligand, the receptors exist in a tethered auto-inhibitory conformational state whereby subdomains II and IV interact, thus burying and inhibiting the dimerisation arm from interacting with neighbouring ligand-bound ErbB receptors. ErbB2 however, exists in a fixed conformation resembling the ligand-bound state with the dimerisation arm exposed and thus permanently poised for receptor-receptor interactions. Abbreviations of ligands: EGF - epidermal growth factor; AR - amphiregulin; TGF-α - transforming growth factor-alpha; BTC - betacellulin; HB-EGF - heparin-binding EGF-like growth factor; EPR - epiregulin; and NRGs - neuregulins 1, 2, 3 and 4 (also known as heregulins (HrG) 1-4. This figure was adapted from Burgess et al. and Hynes et al. (Burgess et al. 2003;Hynes and Lane 2005).

1.2.1 Structural features of the ErbB extracellular domain

The ErbB proteins belong to subclass I of the RTK superfamily and are characterised by four main structural features namely, the extracellular domain, a transmembrane region, a tyrosine kinase domain, and the C-terminal region (Barros et al. 2010;Blume-Jensen and Hunter 2001;Bublil and Yarden 2007) (Figure 1.2). The extracellular region of the ErbB proteins comprises four subdomains of two different types: the leucine-rich (L) domains (L1 and L2); and the cysteine-rich (CR) domains (CR1 and CR2), which are organised in the order of L1-CR1-L2-CR2 (Burgess et al. 2003;Jorissen et al. 2003). The alternative nomenclature of these domains is I-II-III-IV, which is what will be used from henceforth in this thesis, respectively (Figures 1.1 and 1.2). The structural characteristics of each domain type include the six-turn β-helical configuration capped at each end by an α helix, specific for the L domains (domains I and III). The CR domains consist of multiple disulphide-bonded modules, with domain II containing 8 whilst domain IV contains 7 of these disulphide-bonded modules. Domain II is important for receptor dimerisation and is often referred to as the dimerisation arm since one of its disulphide-bonded modules (module 5) protrudes out as a point of contact with an active dimerisation partner. Domains I and III are required for ligand binding, whereas subdomains II and IV are involved in receptor auto-inhibition (Burgess et al. 2003).

When the receptor is non-activated (i.e. not ligand-bound), it takes on a tethered conformational state whereby autoinhibitory intramolecular interactions occur between subdomains II and IV that result in burying and thus occlusion of the dimerisation arm, which impedes it from interacting with the dimerisation arm of an active (ligand-bound) neighbouring binding partner (Ferguson et al. 2003). Ligand binding involves domains I and III, whereby a single growth factor molecule simultaneously interacts with domains I and III of the same receptor. Upon binding, it causes rearrangement of the domains to give rise to an extended conformation resulting in the exposure of the dimerisation arm, thus facilitating homo- or heterodimerisation (Ferguson et al. 2003;Linggi and Carpenter 2006;Roskoski, Jr. 2004).

Structural studies of the extracellular region of ErbB2 revealed specific features that differed from structures of other family members. Firstly, it was revealed that the auto-inhibitory tethering interaction between subdomains II and IV that is observed with the other inactive family members, is absent in the ErbB2 extracellular structure. The ErbB2 receptor is thus locked in a fixed conformation resembling the ligand-bound state seen with other family members, whereby the dimerisation arm is exposed (Figure 1.1) (Cho et al. 2003;Garrett et al. 2003). This indicates that ErbB2 is permanently poised to interact with other ErbB ligand-bound receptors, thus rendering it as the preferred partner for heterodimerisation with other ErbB receptors (Burgess et al. 2003;Cho et al. 2003;Ferguson et al. 2003;Garrett et al. 2003). Secondly, these studies also revealed that domains I and III are in close proximity to one another in the ErbB2 structure, even closer than what was observed with the

ligand-bound structure of EGFR. In the ErbB2 conformation, the ligand-binding sites on domains I and III are in direct contact with one another thereby hindering any possible interaction of a ligand. Thirdly, key residues in domain IV of the ErbB2 extracellular region were found to be different from those of other family members. For example, Gly563 that is conserved in EGFR, ErbB3 and ErbB4 was found to be replaced by Pro572 in the extracellular region of ErbB2. This is thought to account for the lack of the auto-inhibitory tether between domains II and IV (Cho et al. 2003;Garrett et al. 2003).

On the other hand, a recent study by Alvarado and colleagues argued against the notion that ErbB2 lacks auto-inhibition. The authors revealed evidence to suggest that the direct interaction between domains I and III of the extracellular region of ErbB2 is autoinhibitory as it occludes the ligand binding site (Alvarado et al. 2009).

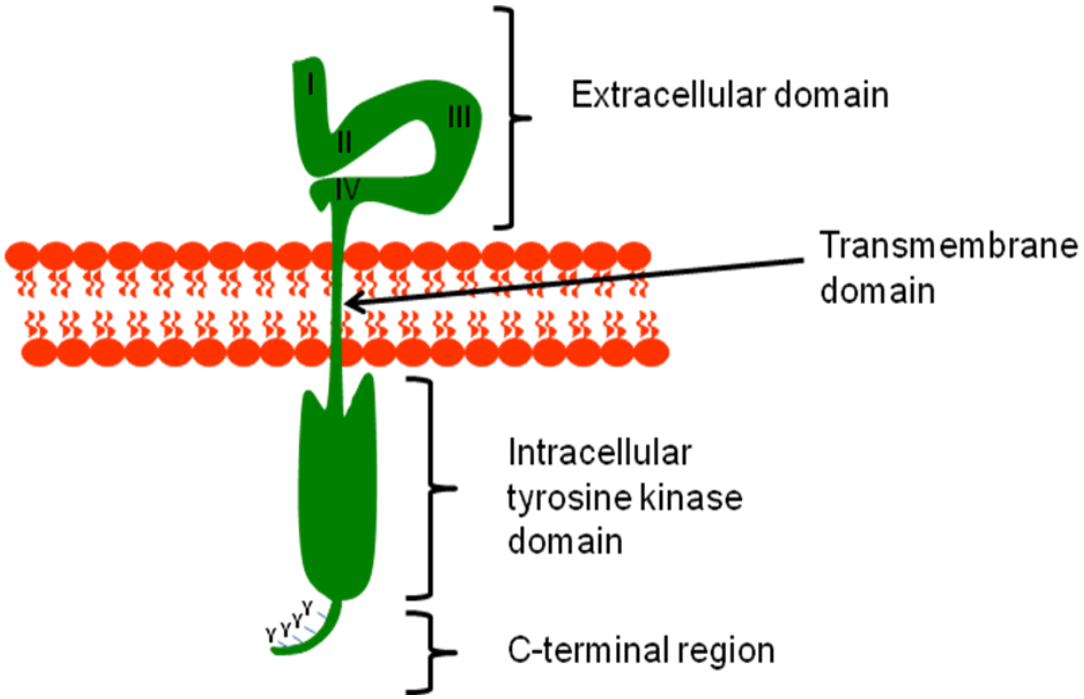

Figure 1.2: Structural features of ErbB proteins.

ErbB proteins share four main structural features: the N-terminal extracellular domain for ligand binding, which also comprises the four subdomains (I-IV) that are important for ligand binding and structural conformation; a transmembrane domain; an intracellular tyrosine kinase domain; and a C-terminal tail for tyrosine phosphorylation, which also serve as docking sites for phosphotyrosine-binding effector molecules. The example shown here is of an unliganded receptor in a tethered auto-inhibitory conformational state. This figure was adapted from Burgess et al. (Burgess et al. 2003).

1.2.2 ErbB Ligands

The characteristics of RTK proteins include ligand binding and the subsequent tyrosine kinase activation, which couples the receptors to downstream intracellular signalling cascades thereby facilitating the relay of signals from the extracellular space to the intracellular space, through phosphorylation of downstream effectors. There are at least 13 ligands known to bind to ErbB receptors, with various specificities (Figure 1.1). These include EGF, transforming growth factor-alpha (TGF-α) and amphiregulin (AR), which specifically bind to EGFR with high affinity and no other ErbB family members. Other ligands include betacellulin (BTC), epiregulin (EPR) and heparin-binding EGF-like growth factor (HB-EGF), which are known to bind both EGFR and ErbB4. The neuregulins (also known as heregulins) make up the other group of ErbB ligands, whereby neuregulins (NRG) 1 and NRG2 bind both ErbB3 and ErbB4, whilst NRG3 and NRG4 specifically bind ErbB4 exclusively (Barros et al. 2010;Linggi and Carpenter 2006).

1.2.3 ErbB receptor dimerisation and downstream signalling

A study by de Vos and colleagues into the mechanisms of ligand-induced dimerisation of the human growth hormone (hGH) receptor led to a paradigm that a single ligand binds simultaneously to two receptor molecules to form a 1:2 (ligand:receptor) complex, thereby mediating dimerisation (de Vos et al. 1992). Conversely however, later studies analysing the binding of EGF to the

epidermal growth factor receptor revealed that one EGF molecule binds to the extracellular region of one receptor molecule to form a 2:2 (ligand:receptor) dimer complex (Ferguson et al. 2003;Lemmon et al. 1997). Ligand binding to the extracellular region of the receptor via domains I and III induces a structural conformational change that results in the exposure of the dimerisation arm (domain II), which is the first point of contact between two receptors in a dimer (Figure 1.3). It is proposed that further contact occurs between the kinase domains of the two receptors within a dimer complex thereby inducing activation of their kinase activity and the subsequent transphosphorylation of the receptors at multiple tyrosine phosphorylation sites located within the C-terminal tail (Barros et al. 2010;Hynes and Lane 2005). Recent structural studies of EGFR suggest that the kinase domain of EGFR can dimerise to form two types of kinase-domain conformation states, inactive symmetric and active asymmetric dimmers (Bessman and Lemmon 2012;Mi et al. 2011;Zhang et al. 2006). In the asymmetric dimer, the C-terminal lobe of one monomer kinase domain interacts with the N-terminal lobe of the other monomer kinase domain (Mi et al. 2011;Zhang et al. 2006).

ErbB receptors function as homodimers through association between two identical receptors, or heterodimers through association with their cognate family members. Thus the four family members can interact to form 10 distinct states comprising four homodimers (EGFR/EGFR, ErbB2/ErbB2, ErbB3/ErbB3 and ErbB4/ErbB4) and six heterodimers (EGFR/ErbB2, EGFR/ErbB3, EGFR/ErbB4, ErbB2/ErbB3, ErbB2/ErbB4 and ErbB3/ErbB4) (Roskoski, Jr. 2004;Yarden and Sliwkowski 2001). The phosphorylated tyrosine residues then

serve as docking sites for numerous adaptor proteins that contain Src homology 2 (SH2) domains or phosphotyrosine-binding (PTB) domains. Examples of such adaptor molecules include the Src homology 2 domain-containing (Shc) protein, p85 and the growth factor receptor-bound protein 2 (Grb2). Recruitment of adaptor proteins to these phosphorylated sites couples activated receptors to various downstream signalling pathways. The two main signalling pathways associated with the ErbB receptors are the mitogen-activated protein kinase (MAPK) and the phosphoinositide 3-kinase (PI3K) pathways, which promote proliferation and survival. Coupling to the MAPK pathway is through adaptor proteins Shc and Grb2, whilst the PI3K pathway can be activated via docking of p85, the regulatory subunit of PI3K onto activated receptors (Hynes and Lane 2005;Olayioye et al. 2000). There is an overlap in the adaptor molecules recruited to the receptors; however individual ErbB receptors have the ability to preferentially associate with some effector proteins than others, thus ensuring specificity in the signalling potential of these receptors (Hynes and MacDonald 2009). For example, out of the four ErbB family members, ErbB3 is the most efficient activator of the PI3K pathway due to the presence of six docking sites for the p85 subunit of PI3K (Hynes and MacDonald 2009;Olayioye et al. 2000;Stern 2008). The C-terminus domain of ErbB3 contains six YXXM motifs (Y – tyrosine; X – any amino acid; M – methionine), which when phosphorylated serve as a docking site for the SH2 domain of p85 (Olayioye et al. 2000;Smirnova et al. 2012).

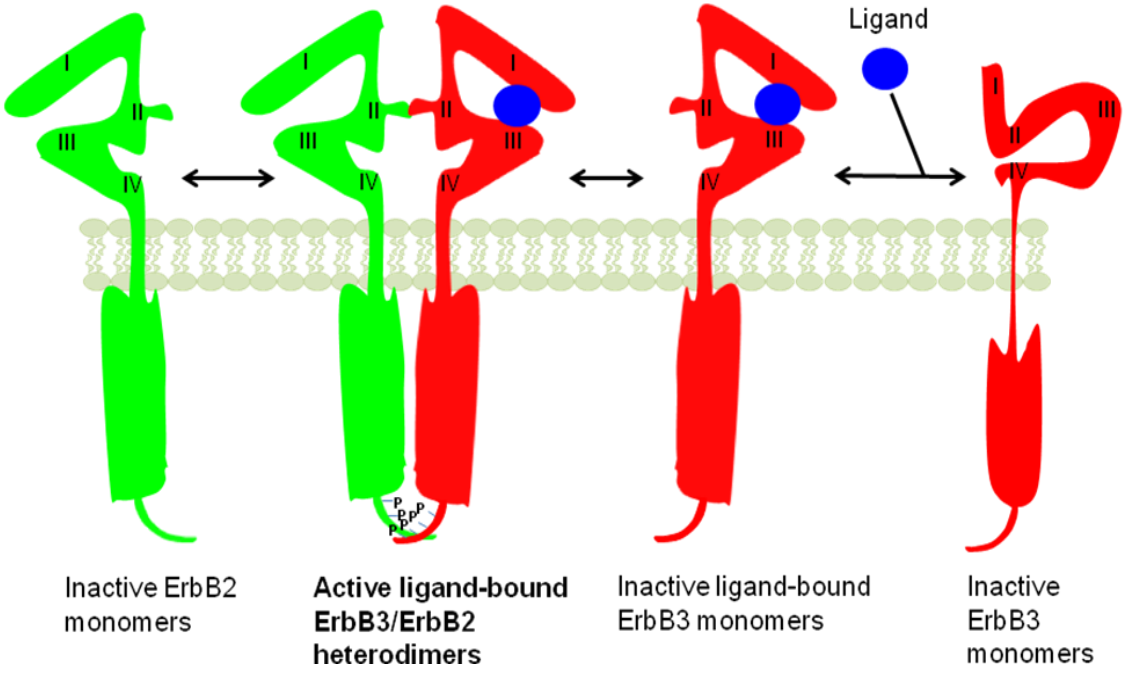

Figure 1.3: Ligand-induced heterodimerisation of ErbB2 and ErbB3.

In the absence of a ligand, ErbB3 monomers are inactive due to the tethered autoinhibitory intramolecular interactions involving domains II/IV. However, ligand binding to domains I/III induces domain rearrangement leading to the exposure and extension of the dimerisation arm of domain II. The extended configuration of the resulting ligand-bound monomer makes it suitably poised for intermolecular interactions, but it remains inactive until dimerisation. In the example shown above, ErbB3 dimerises with ErbB2 thereby forming an active heterodimer. Such an association induces receptor autophosphorylation. This figure was adapted from Burgess et al. (Burgess et al. 2003).

1.2.3.1 The PI3K pathway and breast cancer progression

The presence of six docking sites for the p85 regulatory subunit of PI3K in the C-terminal tail of ErbB3 is not enough to activate the PI3K pathway, since ErbB3 is deemed kinase-dead due to a non-functional kinase domain. Therefore, signalling via the PI3K pathway requires the formation of ErbB3 heterodimers with other ErbB receptors such as ErbB2. Once ErbB2/ErbB3 heterodimers are formed, the PI3K signalling cascade can be activated via docking of p85 to active ErbB3 receptors (Figure 1.4). Upon recruitment of p85, p110 which is the catalytic subunit of the PI3K protein, phosphorylates phosphatidylinositol-4,5-bisphosphate (PIP2) to phosphatidylinositol-3,4,5-trisphosphate (PIP3). The latter is a crucial second messenger that recruits Akt to the plasma membrane for activation (Dillon et al. 2007;Manning and Cantley 2007;Yuan and Cantley 2008). This reaction is antagonised by PTEN (phosphatase and tensin homolog deleted on chromosome 10), which negatively regulates the intracellular levels of PIP3 and thus Akt activity. Once generated, PIP3 binds phosphoinositide-dependent kinase-1 (PDK1) at the plasma membrane, which then phosphorylates the kinase domain of Akt at Threonine (T) 308. Full activation of Akt is achieved following phosphorylation at a second residue, serine (S) 473 by PDK2. Activated Akt can then translocate to the cytoplasm and nucleus where it phosphorylates downstream effector proteins such as the murine double minute 2 (MDM2), or the cell cycle inhibitors $p27^{Kip1}$ and $p21^{WAF1}$, ultimately leading to promotion of cell growth and survival (Figure 1.4) (Dillon et al. 2007;Manning and Cantley 2007).

The PI3K pathway is deregulated in many human cancers through mutations such as activating mutations of the *PIK3CA* gene encoding the p110 catalytic subunit, which are observed in 20-25% of primary breast tumours (Hynes and MacDonald 2009). The pathway is also affected by loss-of-function mutations in the tumour suppressor gene *PTEN*. Both types of mutations result in elevated levels of PIP3 and Akt activation, ultimately leading to cellular transformation (Blume-Jensen and Hunter 2001;Hynes and MacDonald 2009;Stern 2008). In most human cancers including breast cancer, *PTEN* is one of the most frequently mutated genes (Chow and Baker 2006). ErbB2 overexpressing breast cancers are reported to maintain elevated PI3K activity, particularly through the oncogenic ErbB2/ErbB3 heterodimer signalling unit (Hynes and MacDonald 2009).

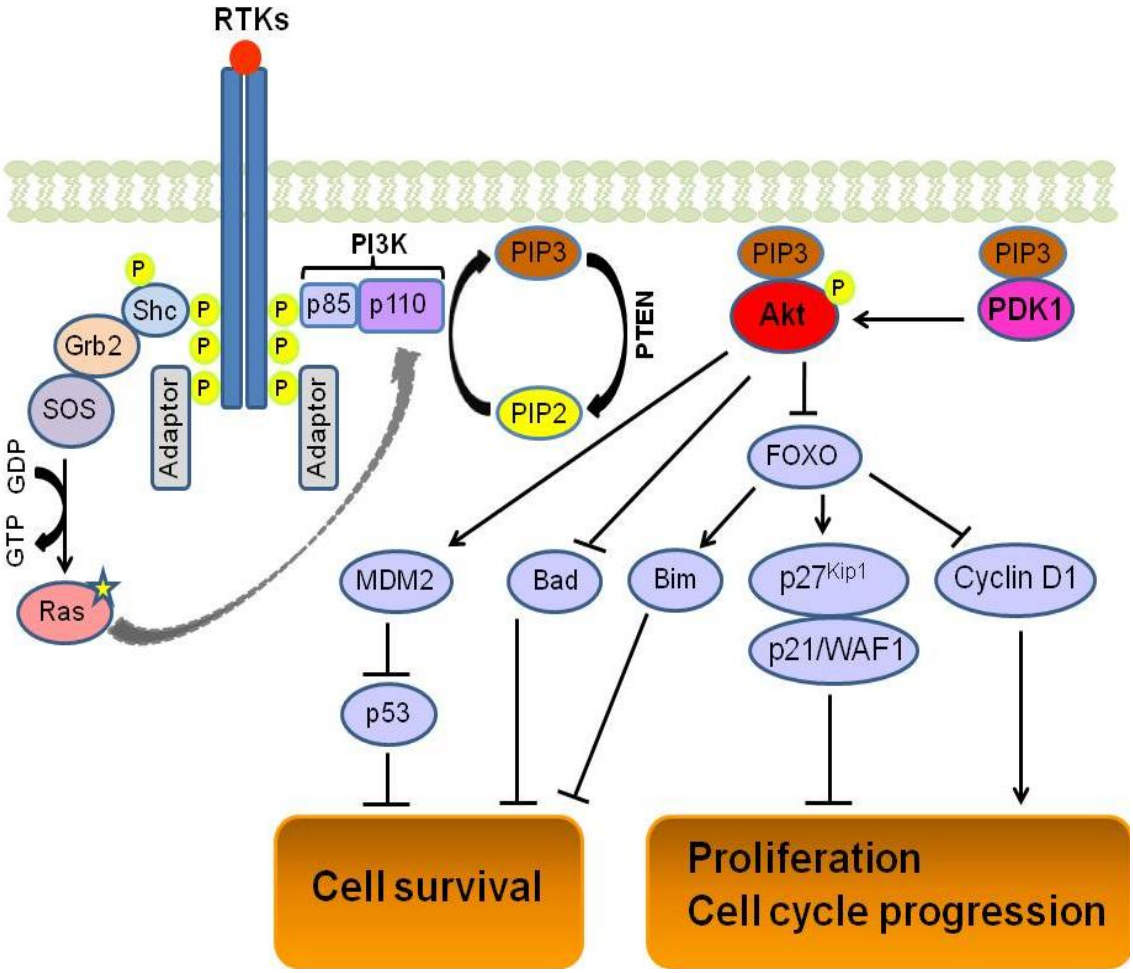

Figure 1.4: The PI3K/Akt signalling pathway.

Schematic representation of the PI3K/Akt signalling pathway from activated receptor tyrosine kinases (RTKs). Lines represent either activation (arrow head) or inactivation/inhibition (blunt end). Abbreviations: Bad - Bcl-2-associated death promoter; Bim - Bcl-2 interacting mediator of cell death; FOXO - Forkhead Homeobox type O; GDP/GTP - guanosine-di-(tri)-phosphate; Grb2 - growth factor receptor-bound 2; KIP1 – kinase inhibitor protein 1; MDM2 - murine double minute 2; PDK1 - phosphoinositide-dependent protein kinase 1; PI3K - phosphoinositide-3 kinase; PIP2/PIP3 - phosphatidylinositol-di-(tris)-phosphate; PTEN - phosphatase and tensin homolog deleted on chromosome ten; Shc - Src homology 2 domain containing; SOS - son of sevenless; WAF1 – wild-type p53 activated-fragment 1. This figure was adapted from Baselga (Baselga 2011).

1.2.3.2 MAPK signalling

The mitogen-activated protein kinase (MAPK) pathways function downstream of cell surface receptors thereby enabling cells to mediate signal transduction from extracellular environmental stimuli such as growth factors or cellular stress into intracellular signalling cascades thus regulating key functions such as cell proliferation, survival and differentiation (Gehart et al. 2010;Mebratu and Tesfaigzi 2009;Roberts and Der 2007). There are at least six distinct groups of MAPK proteins that have been characterised in mammals and these include extracellular signal-regulated kinases (Erk1/2); Erk3/4; Erk5; Erk7/8, Jun N-Terminal kinase (JNK1/2/3) and the p38 kinase isoforms α/β/γ/δ (Dhillon et al. 2007). The MAPK signalling network comprises of a three-tier protein kinase module that involves a series of protein phosphorylation. An external stimulus causes activation of a MAPK kinase kinase (MAPKKK), which in turn phosphorylates a MAPK kinase (MAPKK) that subsequently phosphorylates and thus activate a terminal MAPK with effects on downstream targets such as transcription factors (Figure 1.5) (Dhillon et al. 2007;Roberts and Der 2007).

Upstream of the MAPK pathway is Ras, a small GTPase. Ras proteins act as molecular switches, that turn signalling pathways on or off by cycling between inactive guanosine diphosphate (GDP)-bound and active guanosine triphosphate (GTP)-bound states. Guanosine nucleotide exchange factors (GEFs) such as son of sevenless (SOS) mediate the signal-induced conversion of the inactive to active state by stimulating the exchange of GDP to the more

abundant GTP (Mor and Philips 2006). Upon receptor activation, SOS is recruited to the receptor via the adaptor protein Grb2 thereby inducing the conversion of GDP bound to Ras for GTP and thus Ras activation (Figure 1.6). Additionally, the activation state of Ras is also partly self-limited by its intrinsic GTPase activity through the action of GTPase activating proteins (GAPs), which increase the catalytic activity of Ras to revert from the GTP-bound active state to the inactive GDP-bound state. The actions of both GEFs and GAPs therefore regulate the duration of Ras signalling by allowing the signal to be switched on and off, thereby controlling the duration of the signal (Fehrenbacher et al. 2009;Mor and Philips 2006;Omerovic and Prior 2009).

Once activated, GTP-bound Ras can then affect many downstream effector proteins including Raf, a serine/threonine MAPKKK. Activation of Raf leads to phosphorylation of MEK1/2, a dual-specificity MAPKK which then in turn, phosphorylates and activates Erk1/2 MAPK on threonine and tyrosine residues. Erk1/2 are serine/threonine kinases, which when activated can phosphorylate a wide range of substrates, both nuclear and cytoplasmic (Figures 1.5 and 1.6) (Fehrenbacher et al. 2009;Roberts and Der 2007). The MAPK signalling cascades emanate from multiple receptors including the ErbB receptors, insulin-like growth factor-1 receptor (IGF-1R) and G-protein coupled receptors (GPCR); and can therefore be activated by various stimuli. MAPK signalling can thus induce a range of biological responses, depending on the type of activated receptor and stimuli. Indeed, it has previously been reported that stimulation of neuronal PC12 cells with nerve growth factor (NGF) induced cellular

differentiation; whilst stimulation of the same cells with EGF resulted in cell proliferation (Marshall 1995;Sacks 2006).

Scaffold proteins play a critical role in regulating MAPK signalling by assembling these signalling molecules into a complex, which not only enables rapid relay of signals, but also ensures a degree of specificity through isolation of these signalling modules from each other and thus limiting crosstalk between different pathways (Dhanasekaran et al. 2007;Sacks 2006). Kinase suppressor of Ras 1 (KSR1) is one of the scaffold proteins involved in the Erk signalling pathway. It is a multidomain protein that binds all three-tier kinases (Raf/MEK/Erk) of the Erk pathway (Figure 1.6). In resting cells, KSR1 is retained in the cytoplasm via its constitutive association with MEK1/2, the core domain of protein phosphatase-2A (PP2A), 14-3-3 and the Ras-responsive E3-ubiquitin ligase, IMP (impedes mitogenic signal propagation). Ras activation induces IMP auto-polyubiquitination, which is subsequently degraded. This leads to dephosphorylation of KSR1 at serine 392 by PP2A, thereby reducing its interaction with 14-3-3 (Matheny et al. 2004). Consequently, the KSR1-MEK1/2 complex is released to translocate to the plasma membrane where it interacts with Raf and Erk thus facilitating their activation (Dhanasekaran et al. 2007;Kolch 2005).

Besides regulation of Erk signalling via KSR sequestration, the ERK pathway can also be regulated by specific proteins that inhibit protein interactions between members of this pathway. These endogenous inhibitors include Raf kinase inhibitor protein (RKIP), which inhibits MEK phosphorylation by binding

to both Raf and MEK, thereby hindering their interaction. Other inhibitor proteins include Sprouty and SPRED (Sprouty-related proteins with an EVH1 (Enabled/VASP homology domain-1) domain), which when phosphorylated, bind and sequester Grb2 thereby impairing the recruitment of SOS to the active receptors, ultimately inhibiting Ras activation (Kim and Bar-Sagi 2004;Kolch 2005). Furthermore the duration of MAPK signalling activation is determined by a balance between phosphorylation and dephosphorylation of the kinases. Serine/threonine phosphatases such as PP2A and the dual-specificity protein phosphatases such as the MAPK phosphatase (MKP)-1, inhibit the activity of the MAPK kinases such as MEK1/2 and Erk1/2 by removing their activating phosphates thereby reversing their activation (Westermarck et al. 2001).

Aberrant regulation of MAPK signalling is correlated with cancer. For example, it is estimated that mutations in the Erk signalling pathway are found in at least 30% of human breast cancers (Roberts and Der 2007;Whyte et al. 2009). Constitutive activation of the Erk pathway can occur due to mutations in the *b-raf* gene that results in constitutive activation of the catalytic activity of B-Raf. Mutations in the *RAS* genes that lock the protein in the active GTP-bound state are found in 30% of human cancers. Furthermore, overexpression of growth factors and their cognate receptors can also lead to hyperstimulation of these signalling pathways (Dhillon et al. 2007;Fehrenbacher et al. 2009;McCubrey et al. 2007;Roberts and Der 2007).

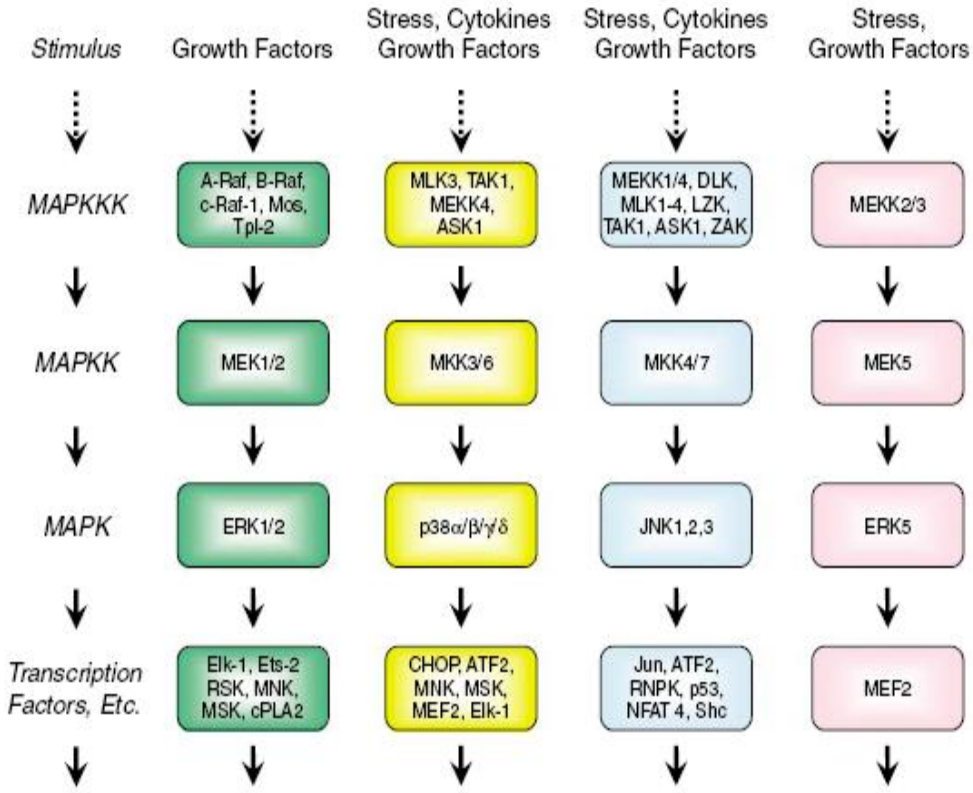

Figure 1.5: The MAPK signalling cascades.

Schematic overview of the MAPK signalling network, represented as a three-tier (MAPKKK-MAPKK-MAPK) protein kinase module. Shown are the Erk1/2, p38, JNK and Erk5 signalling pathways. This figure was obtained from Roberts et al. (Roberts and Der 2007).

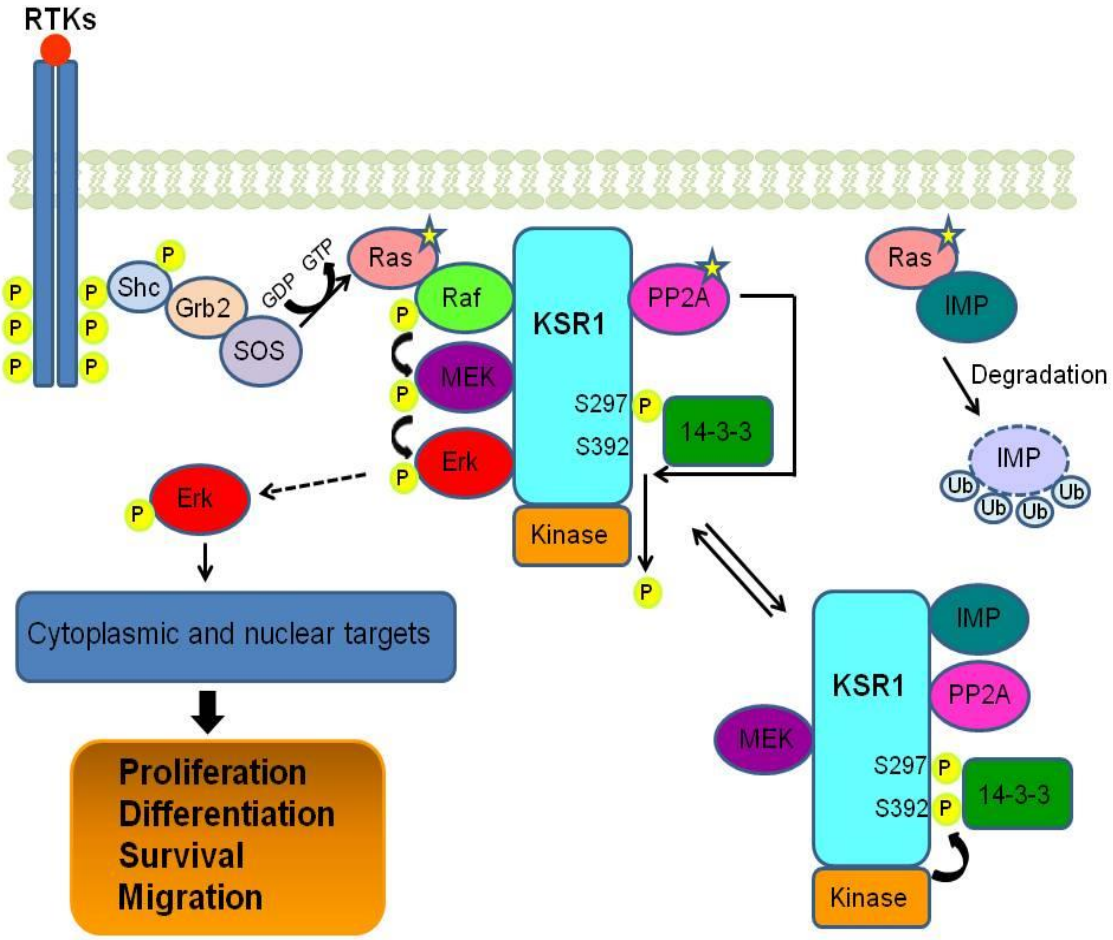

Figure 1.6: Erk signalling and KSR1 regulation.

Schematic representation of the Erk signalling pathway from activated receptor tyrosine kinases (RTKs). Mitogenic signals are propagated from the extracellular space to the intracellular compartments via a series of protein phosphorylation. In resting cells, kinase suppressor of Ras 1 (KSR1) is retained in the cytoplasm via its association with 14-3-3 and the E3-ubiquitin ligase IMP (impedes mitogenic signal propagation). Ras activation induces dephosphorylation of KSR1 and degradation of IMP, thus facilitating membrane translocation of KSR1 followed by the subsequent assembly and activation of the Raf-MEK-Erk signalling module. Phosphorylated Erk can affect numerous cytoplasmic and nuclear targets, ultimately leading to a wide range of biological responses. This figure was adapted from Kolch (Kolch 2005).

1.2.4 ErbB2 and breast cancer

The *ErbB2* gene is located on chromosome 17q and encodes a protein of 185kDa belonging to the EGFR family of RTKs as described in section 1.2. Overexpression and/or gene amplification of ErbB2 is observed in at least 20-25% of invasive breast cancers and this is associated with a poor prognosis and a reduced disease-free survival period (Chang 2010;Freudenberg et al. 2009;Schmitt 2009). ErbB2 overexpression is correlated with breast cancer progression, since ErbB2 is generally either absent or expressed at low levels in benign breast lesions. Its expression is reported to be an important event in the early stages of malignant transformation (Freudenberg et al. 2009). Benign breast lesions are relatively common, with only a very small proportion of these cases progress to invasive breast carcinoma (IBC). It is therefore important to identify and begin treatment of such lesions at an early stage in order to prevent the development of lethal IBC. ErbB2 expression status is one of the ways of determining disease stage; and this is also seen as a very important prognosis factor that can predict response to different therapeutic targets. Patients with benign breast lesions that have *ErbB2* gene amplification have an increased risk of developing IBC (Freudenberg et al. 2009;Schmitt 2009). All these factors highlight ErbB2 as an important therapeutic target.

1.2.4.1 ErbB2-targeted therapies

The importance of ErbB2 in particular to the progression of a subset of breast cancers generated great interest in the development of ErbB2-targeted cancer therapeutics over the years. These include the monoclonal antibody Trastuzumab which binds the extracellular portion of ErbB2; and small molecule tyrosine kinase inhibitors (TKIs) such as Lapatinib, which inhibit the intracellular kinase activity (Hynes and MacDonald 2009;Ignatiadis et al. 2009).

1.2.4.1.1 Lapatinib

Lapatinib is a reversible TKI targeting the kinase domain of both EGFR and ErbB2, thus inhibiting receptor activation and consequently downstream signalling via the MAPK and PI3K/Akt pathways (Freudenberg et al. 2009). Currently, Lapatinib is approved for patients with advanced ErbB2-positive breast cancer who have been previously treated with other anticancer drugs. As a small molecule, Lapatinib is capable of crossing the blood-brain barrier and could therefore have activity against breast cancer metastases to the brain (Kroep et al. 2010).

1.2.4.1.2 Trastuzumab

Trastuzumab (Herceptin) is the first of its kind; a recombinant humanised IgG1 monoclonal antibody directed at the extracellular domain of ErbB2. From

henceforth, Trastuzumab will be referred to by its trade name, Herceptin. Initially, Herceptin was identified through screening of various monoclonal antibodies against ErbB2 including the murine antibody 4D5, of which a humanised version, Herceptin was subsequently developed (Fendly et al. 1990;Ignatiadis et al. 2009;Spector and Blackwell 2009).

In vivo studies using xenografts of ErbB2-overexpressing breast cancer cell lines in mice and clinical trials involving patients with ErbB2-overexpressing metastatic breast cancer demonstrated activity of Herceptin as a single agent and in combination with a range of chemotherapeutic agents (Pegram et al. 1999;Pegram et al. 1998;Pegram et al. 2004;Yeon and Pegram 2005). Further trials comparing treatment regimens of chemotherapy alone against Herceptin-chemotherapy combinations as first line therapy for women with ErbB2-overexpressing metastatic breast cancer revealed that Herceptin enhanced the activity of first-line chemotherapy and provided a survival advantage for patients of up to eight months (Routledge et al. 2006).

In 1998, Herceptin was approved by the United States Food and Drug Administration (FDA) for use in patients with ErbB2-overexpressing metastatic breast cancer as monotherapy (second-line treatment) or in combination with paclitaxel (as first-line treatment) (Yeon and Pegram 2005).

1.2.4.1.2.1 Mechanisms of action

Although the exact mechanisms of action of how Herceptin exerts its therapeutic effects are not fully elucidated, several mechanisms have been proposed to account for its anti-tumour activity, based on preclinical and clinical studies (Spector and Blackwell 2009;Valabrega et al. 2007).

1.2.4.1.2.1.1 Attenuation of cell signalling

It has been proposed that Herceptin could act by reducing receptor signalling via the PI3K/Akt signalling pathway (Valabrega et al. 2007). As discussed in previous sections, the PI3K/Akt pathway is an important target in breast cancer management as it regulates numerous cellular functions including proliferation, cell cycle progression and survival (Figure 1.4). Several studies have demonstrated that Herceptin inhibits cellular signalling via the PI3K pathway by inhibiting Akt phosphorylation (Le et al. 2005a;Nagata et al. 2004). This in turn leads to G1 cell cycle arrest due to the induction of $p27^{Kip1}$, a cyclin-dependent kinase inhibitor that controls cell cycle progression by inhibiting the activity of cyclin-CDK complexes (Lane et al. 2000;Le et al. 2003;Le et al. 2005b).

1.2.4.1.2.1.2 Immune-mediated response

The mechanism of action by which Herceptin induces its anti-tumour cytostatic and possibly cytotoxic effects *in vivo* could be due to the activation of antibody-

dependent cellular cytotoxicity (ADCC). This immune-mediated response of ADCC occurs when Herceptin bound to the extracellular domain of ErbB2 on tumour cells recruits immune effector cells such as natural killer cells to the tumour microenvironment through its Fc domain. Immune effector cells such as monocytes and macrophages express both activation (FcγRIII) and inhibitory (FcγRIIB) Fcγ receptors. Natural killer cells, which are the main cell type involved in ADCC, express only the FcγRIII activation receptors on their cell surface and not the inhibitory FcγRIIB counterpart (Clynes et al. 2000;Hudis 2007). It has been proposed that activation of immune effector cells through the engagement of Herceptin to Fcγ receptors via its Fc domain is important for the anti-tumour activity of Herceptin. The recruited and activated natural killer cells can induce apoptosis of the Herceptin-bound tumour cells through secretion of cytoplasmic granule toxins such as perforin and granzymes (Smyth et al. 2005;Valabrega et al. 2007). In agreement with this proposed mechanism, a preclinical study by Clynes and colleagues demonstrated that treatment with Herceptin of mice bearing ErbB2-overexpressing xenografts, in which the Fc receptor was deleted, resulted in a marginal effect on tumour volume when compared to the Herceptin effect in the control group (Clynes et al. 2000). Additionally, a pilot clinical study by Gennari and colleagues demonstrated the importance of a functional immune system for the efficacy of Herceptin (Gennari et al. 2004).

1.2.4.1.2.1.3 Inhibition of ErbB2 ectodomain cleavage

As previously mentioned, the molecular weight of full length ErbB2 is 185kDa. In ErbB2 overexpressing breast cancer, the ErbB2 receptor can undergo proteolytic cleavage of its extracellular domain thus resulting in a truncated membrane-bound fragment termed $p95^{ErbB2}$. This truncated fragment of ErbB2 has a functional kinase domain, is phosphorylated and is therefore capable of signalling (Scaltriti et al. 2007). A study by Molina and colleagues demonstrated that Herceptin can inhibit both basal and chemically-induced ErbB2 ectodomain cleavage thereby inhibiting formation of phosphorylated $p95^{ErbB2}$ (Molina et al. 2001).

1.2.4.1.2.1.4 Inhibition of angiogenesis

During the early stages of tumour development, tumour cells can proliferate up to a size of 1-2mm in the absence of their own vascularisation. However, once a tumour reaches a certain mass, it can induce the formation of new blood vessels from pre-existing ones, a process called neovascularisation. These new blood vessels can therefore supply tumour cells with more nutrients to facilitate further growth (Leber and Efferth 2009). Tumour cells can induce angiogenesis through activation and thus stimulation of endothelial cells to secrete pro-angiogenic factors (Cook and Figg 2010). A study by Izumi and colleagues demonstrated that Herceptin treatment induced vasculature regression and normalisation in a murine xenograft tumour model of overexpressing ErbB2.

These authors found that Herceptin markedly reduced vessel diameter and tumour volume when compared to a control antibody (Izumi et al. 2002). Furthermore, gene expression analysis of angiogenesis-related genes revealed that Herceptin treatment resulted in reduced expression of pro-angiogenic factors including vascular endothelial growth factor (VEGF) and increased expression of the anti-angiogenic factor, thrombospondin-1 (TSP-1) (Izumi et al. 2002).

1.2.4.1.2.2 Mechanism of resistance

The response rates to Herceptin monotherapy range from 11-26% in patients with ErbB2-positive metastatic breast cancer, thus indicating that a vast majority of patients do not respond to Herceptin as a single agent (Kruser and Wheeler 2010;Valabrega et al. 2007). However, combinations of Herceptin with taxanes such as paclitaxel or docetaxel increase the response rates ranging from 50-80% (Valabrega et al. 2007). The underlying issue with Herceptin therapy is that the majority of patients who initially respond to Herceptin-based regimens develop resistance within the first year of treatment initiation. There is thus a need to elucidate the molecular mechanisms underlying Herceptin-induced resistance in order to improve patient survival and also to identify groups of patients that are likely to develop resistance to such regimens. This would save treatment costs and the unnecessary exposure to side effects such as cardiotoxicity. Several potential mechanisms to Herceptin resistance have been proposed as discussed below (Mukohara 2011;Valabrega et al. 2007).

1.2.4.1.2.2.1 Impaired access of Herceptin to the ErbB2 epitope

There is evidence in the literature to suggest that tumour cells acquire resistance to Herceptin by limiting access of the antibody to its epitope. Although Herceptin has been shown to inhibit cleavage of the ErbB2 extracellular domain (Molina et al. 2001), resistance to Herceptin is reported in $p95^{ErbB2}$-positive breast cancer patients. Specifically, Scaltriti and colleagues investigated response to Herceptin in breast cancer patients, xenografts and cell lines expressing either $p95^{ErbB2}$ or full length ErbB2. From these studies, the authors collectively found that $p95^{ErbB2}$-expression correlated with resistance to Herceptin (Scaltriti et al. 2007). In a separate study, Nagy and colleagues observed that a Herceptin-resistant breast cancer cell line expressed high levels of MUC4, a membrane-associated mucin, the levels of which, inversely correlated with the Herceptin binding capacity (Nagy et al. 2005).

These studies demonstrate that Herceptin is not effective in a subset of breast cancer that either lacks the ErbB2 epitope for Herceptin through ectodomain shedding or in which the epitope is hindered. For such patients, alternative treatment regimens such as tyrosine kinase inhibitors like Lapatinib would be more appropriate than Herceptin.

1.2.4.1.2.2.2 Loss of PTEN

PTEN is a phosphatase that antagonises PI3K function by de-phosphorylating phosphatidylinositol-3,4,5 trisphosphate (PIP3) at the site that recruits Akt to the plasma membrane; thereby it negatively regulates Akt activity (Figure 1.4). Nagata and colleagues previously reported that PTEN activation contributes to the anti-tumour activity of Herceptin. These authors demonstrated that treatment of ErbB2-overexpressing breast cancer cells with Herceptin enhanced the membrane localisation of PTEN and thus its activation. This correlated with a reduction in the inhibitory tyrosine phosphorylation of PTEN, following Herceptin treatment (Nagata et al. 2004).

In a separate study by Esteva and colleagues whereby PTEN expression status was evaluated in a cohort of patients with ErbB2-positive metastatic breast cancer, loss of PTEN expression was observed in 52% tumours of 137 patients. Furthermore, these authors found that loss of PTEN significantly correlated with resistance to Herceptin (P=0.028) and shorter survival time (P=0.008), particularly in patients receiving Herceptin as first-line therapy (Esteva et al. 2010).

1.2.4.1.2.2.3 Alternative signalling

The insulin-like growth factor-1 receptor (IGF-1R) is a member of the type II family of growth factor receptors. Ligand binding to the receptor can lead to

activation of PI3K and MAPK signalling pathways, thereby promoting cell proliferation and survival (Lu et al. 2004). Data from *in vitro* studies in the literature suggest that cross talk occurs between IGF-1R and ErbB2 receptors and that this is associated with resistance to Herceptin (Huang et al. 2010;Jin and Esteva 2008;Lu et al. 2001;Lu et al. 2004;Nahta et al. 2005). Specifically, a study by Nahta and colleagues demonstrated that stimulation of Herceptin-sensitive and resistant breast cancer cells with IGF-1 resulted in a rapid increase in phosphorylation of ErbB2 and downstream pathways. This was particularly observed in the Herceptin-resistant cells than in the sensitive cells. Furthermore, these authors demonstrated that chemically-induced inhibition of IGF-1R tyrosine kinase activity restored sensitivity of resistant cells to Herceptin (Nahta et al. 2005).

A study by Shattuck and colleagues implicated the Met receptor in resistance to Herceptin. In this study, the authors demonstrated co-expression of the Met receptor with ErbB2 in breast cancer, and also that depletion or inhibition of Met enhanced Herceptin-mediated growth inhibition (Shattuck et al. 2008).

Collectively, the above described mechanisms of resistance to Herceptin and the associated studies clearly demonstrate that the use of Herceptin as a single agent is not sufficient in the management of breast cancer. These mechanisms highlight the requirement of alternative treatment regimens involving a range of combinations with multiple targets, in order to combat resistance.

1.3 Tetraspanins

1.3.1 The Tetraspanin superfamily

Tetraspanins belong to a superfamily of small four transmembrane proteins, comprising 33 members in mammals (Table 1.1) (Hemler 2008;Romanska and Berditchevski 2011). These membrane proteins are ubiquitously expressed across a range of species, including fungi, *Drosophila, Caenorhabditis elegans* and mammals (Hemler 2001;Levy and Shoham 2005b). Furthermore, all nucleated cells express tetraspanins on their cell membranes (Levy and Shoham 2005a;Wright et al. 2004b). Some tetraspanins such as CD9, CD81 and CD151 have an extensive, though not ubiquitous cell and tissue distribution, whilst other tetraspanins belonging to specialised structures have a restricted pattern of expression. These include the uroplakins UP1a and UP1b, found on the membrane of the urothelium and the proteins encoded by the retinal dystrophy syndrome (RDS) genes, RDS/peripherin and Rom-1, which are localised on the outer segment of the photoreceptor structure (Charrin et al. 2009).

HGNC approved gene symbol	Alternative names	Chromosome
TSPAN1	TM4-C, NET-1, TSP-1	1p34.1
TSPAN2	FLJ12082, TSN2, TSP-2	1p13.1
TSPAN3	TM4-A, TM4SF8.1,2, TSP-3	15q24.3
TSPAN4	TM4SF7, NAG-2, TSP-4	11p15.5
TSPAN5	NET-4, TSP-5	4q23
TSPAN6	T245, TM4SF6, TSP-6	Xq22
TSPAN7	CD231, A15, MXS1, CCG-B7, TALLA-1, TM4SF2, DXS1692E	Xp11.4
TSPAN8	TM4SF3, CO-029, D6.1	12q14.1-q21.1
TSPAN9	NET-5	12p13.33-32
TSPAN10	Oculospanin (OCSP)	17q25.3
TSPAN11	Human form may not be expressed; mouse only (CD151-like)	12p11.21
TSPAN12	TM4SF12, NET-2	7q31.31
TSPAN13	NET-6, FLJ22934, TM4SF13	7p21.1
TSPAN14	DC-TM4F2, BC002920, NEW2, TMSF14	10q22.3
TSPAN15	NET-7, 2700063A19Rik, TMSF15	10q22.1
TSPAN16	TM4-B, TM-8, TMSF16	19p13.2
TSPAN17	CAD35489, FBox23 (FBX23), SB134, BC067105, NEW3, TM4F17	5q35.3
TSPAN 18	BAB55318, AK027715.1, NEW6	11p11.2
TSPAN19	XP_084868	
TSPAN20	Uroplakin Ib (UPIb), UPK1	3q13.3-q21
TSPAN21	Uroplakin Ia (UP1a), UPIA, UPKA, MGC14388	19q13.13
TSPAN22	Peripherin, RDS, RP7, AVMD, PRPH, AOFMD, PRPH2	6p21.2-p12.3
TSPAN23	Rom1, ROSP1	11q13
TSPAN24	CD151 (2 variants; UTR) PETA3, SFA1, gp27	11p15.5
TSPAN25	CD53, MOX44	1p13
TSPAN26	CD37, GP52-40	19p13-q13.4
TSPAN27	CD82, Kangai1, R2, 4F9, C33, IA4, ST6, GR15, KAI1, SAR2	11p11.2
TSPAN28	CD81, TAPA-1, S5.7	11p15.5
TSPAN29	CD9, BA2, P24, GIG2, MIC3, MRP-1, BTCC-1, DRAP-27	12p13.3
TSPAN30	CD63, MEL1, ME491, granulophysin, LAMP3, OMA81H, MLA1, neuroglandular Ag (NGA) LIMP	12q12-q13
TSPAN31	SAS	12q13.3
TSPAN32	TSSC6 (3 variants; UTR) PHEMX, MGC22455	11p15.5
TSPAN33	MGC50844, Penumbra, New7	7q32.3

Table 1.1: The nomenclature and chromosomal locations of human tetraspanins.

This table was obtained from Romanska et al. (Romanska and Berditchevski 2011).

1.3.1.1 Characteristics of tetraspanins

Not all four transmembrane spanning proteins belong to the tetraspanin superfamily. All tetraspanin family members share key structural features that distinguish them from other four transmembrane proteins, such as stargazin and sarcospan (Min et al. 2006).

1.3.1.1.1 Topology

Tetraspanins are small proteins ranging between 204-355 amino acids in length and comprise of four transmembrane (TM) domains (TM1-4). The key structural features of tetraspanins include short intracellular N- and C-terminal tails of less than 20 amino acid residues; an intracellular loop; a short extracellular loop (EC1) of 13-31 amino acids located between TM1 and TM2; and a large extracellular loop (EC2) of 76-131 amino acids found between TM3 and TM4 (Figure 1.7) (Charrin et al. 2009;Hemler 2005).

In 2001, Kitadokoro et al. described the crystallographic structure of the extracellular domain of tetraspanin CD81 (Kitadokoro et al. 2001). This work revealed a unique structure of the extracellular domain to consist of 5 α-helices (A-E) organised into two subdomains, namely the stalk, comprising of two anti-parallel α-helices, A & E; and the head subdomain comprising α-helices B, C & D. The C and D region of the EC2 domain of CD81 is not structurally conserved amongst all tetraspanins and is thus termed the variable region. In contrast, the

A and B helices are connected by a short loop, and together with the E helix, they form what is known as the constant region of the EC2 domain. This region is conserved within the tetraspanin family and thus serves as the basic structural feature for which the extracellular domains of other tetraspanins are modelled against (Figure 1.7) (Kitadokoro et al. 2001;Miranti 2009).

The EC2 variable region is stabilised by structural motifs including the two disulphide bridges formed between the highly conserved signature motif of tetraspanins, the cysteine-cysteine-glycine (CCG) motif and with two other conserved cysteines (Charrin et al. 2009;Kitadokoro et al. 2001;Zoller 2009). The number of cysteine residues within the EC2 domain varies amongst the tetraspanin family with 4 cysteines being reported for CD81 and another example including CD9. The EC2 domains of most tetraspanins are reported to have 6 cysteines and this includes tetraspanins CD151 and CD82 (Figure 1.7). However, some tetraspanins are reported to contain 7 or 8 cysteine residues resulting in up to 4 disulphide bridges (Charrin et al. 2009;Hemler 2005;Levy and Shoham 2005b). Further to the cysteine residues found in the extracellular loop, tetraspanins contain juxtamembrane cysteine residues which are potential sites for palmitoylation, a post-translational modification involving the covalent linkage of palmitate to cysteine residues. Palmitoylation plays an important role in the organisation of tetraspanins into tetraspanin-enriched microdomains and will be discussed further in the next section (Charrin et al. 2009;Hemler 2005;Levy and Shoham 2005b).

The EC2 domain is important for protein-protein interactions as demonstrated for the interaction between tetraspanin CD151 with α3β1. A study by Berditchevski and colleagues, using a panel of CD151/CD9 chimeras and CD151 mutants demonstrated the importance of the EC2 domain of CD151 in particular the variable region constituting the CCG motif, for the association of CD151 with integrin α3β1. It was also shown in that study that the EC2 domain was not required for tetraspanin-tetraspanin interactions, since its deletion did not abolish the interaction of CD151 with other tetraspanins such as CD9, thereby highlighting the requirement of other structural domains in facilitating tetraspanin-tetraspanin interactions (Berditchevski et al. 2001).

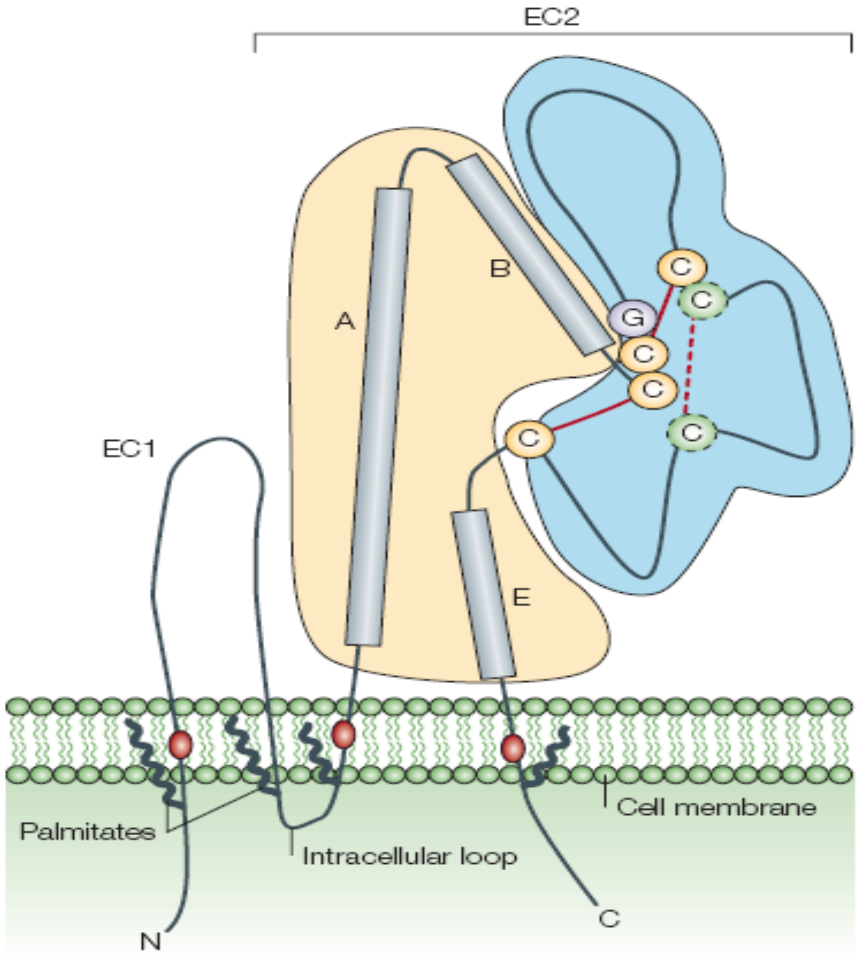

Figure 1.7: Structural features of tetraspanins.

The main characteristic features of tetraspanins include the four transmembrane domains (TM1-4), a small extracellular loop (EC1), an intracellular loop, a large extracellular loop (EC2) and short amino- and carboxyl-terminal tails. The large extracellular loop is subdivided into a constant region (peach) comprising 3 α-helices A, B and E; and a variable region (blue) important for protein-protein interactions. The EC2 variable region comprises several highly conserved amino-acid residues such as the cysteine-cysteine-glycine (CCG) motif found in all tetraspanins. These residues form two to four disulphide bridges (red) with other conserved cysteines, which account for the variations in the EC2 structures of family members. Furthermore, tetraspanins contain polar residues within TM1, 3 and 4 (red balls) for structural stability; potential N-glycosylation sites within the EC2 domain; and intracellular juxtamembrane cysteines which are sites for palmitoylation. This figure was obtained from Hemler (Hemler 2005).

1.3.1.2 Tetraspanin-enriched microdomains

Studies in the 1990s demonstrated the ability of tetraspanins to associate with each other and with other transmembrane proteins. These studies utilised biochemical techniques including immunoprecipitation under a range of detergent conditions, whereby tetraspanins were co-immunoprecipitated with various binding partners (Berditchevski et al. 1996;Rubinstein et al. 1996). Such advances led to the emergence of the concept that tetraspanins organise the plasma membrane to form membrane domains termed, tetraspanin-enriched microdomains (TERMs), also referred to as the tetraspanin web or TEMs. Herein, they will be referred to as TERMs (Figure 1.8) (Charrin et al. 2009;Hemler 2005;Yanez-Mo et al. 2009). Besides tetraspanins, other components of TERMs can be classified into several groups including integrins (such as α3β1) and other adhesion molecules including intracellular and vascular cell adhesion molecules, ICAM-1 and VCAM-1, respectively; members of the immunoglobulin superfamily (such as EWI-2); enzymes (such as metalloproteinases); and signalling molecules (such as EGFR) (Figure 1.8) (Charrin et al. 2009;Yanez-Mo et al. 2009).

Tetraspanins bind to their partner proteins with different levels of interactions which can be classified as primary, secondary or tertiary interactions based on the detergent conditions that are required to disrupt the association (Hemler 2003;Zoller 2009). Partner proteins are defined as those that retain their association with a given tetraspanin even after use of detergent conditions that

disrupt tetraspanin-tetraspanin interactions (Charrin et al. 2009). Primary interactions are direct protein-protein interactions revealed by chemical crosslinking techniques (Kovalenko et al. 2004). Such interactions occur early in biosynthesis presumably within the endoplasmic reticulum. They are often retained in stringent detergent conditions (1% NP-40); and include tetraspanin homodimers, homotrimers, homotetramers as well as heterointeractions with non-tetraspanin proteins. Examples of primary interactions between tetraspanins and non-tetraspanin proteins include CD151 with integrin α3β1; and CD9 or CD81 with EWI-2 (Charrin et al. 2009;Hemler 2003;Hemler 2005;Kovalenko et al. 2004;Zoller 2009).

Primary protein complexes act as building blocks that assemble together forming a network of secondary interactions. These secondary interactions can be distinguished from primary interactions in that they occur late in biosynthesis (Golgi apparatus). They are independent of the EC2 domain, can be stabilised by palmitoylation and furthermore, secondary interactions are disrupted by detergents such 1% Triton X-100 and digitonin, but are maintained under milder detergent conditions such as 1% Brij 96/97. In the literature, it is reported that the majority of tetraspanin interactions are secondary interactions (Hemler 2003;Hemler 2005;Hemler 2008;Kovalenko et al. 2004;Zoller 2009). Several studies have highlighted differences between primary and secondary interactions and also the requirement of palmitoylation for secondary interactions. The study by Berditchevski and colleagues in 2001 demonstrated that even though the EC2 domain of CD151 was important for its association with α3β1 (a primary interaction), its removal did not affect the association of

CD151 with tetraspanins CD9, CD63 and CD81 (secondary interactions) (Berditchevski et al. 2001). Separate studies demonstrated the importance of palmitoylation in facilitating tetraspanin-tetraspanin associations. For example in one study, it was shown that loss of CD151 palmitoylation weakened its association with tetraspanins CD63 and CD81 but did not affect its interaction with α3β1 (Berditchevski et al. 2002). In a separate study, Charrin and colleagues demonstrated that palmitoylation contributed to the association of CD9 with tetraspanins CD81 and CD53, and that mutation of CD9 palmitoylation sites impairs this association (Charrin et al. 2002). These studies therefore demonstrate that secondary interactions involve regions below the extracellular domains, particularly involving the juxtamembrane cysteine residues.

Tertiary interactions are indirect, weak associations that can be disrupted under detergent conditions such as Brij 96/97 and Triton X-100, but are maintained in milder detergents such as 1% Brij-35/58/99 and CHAPS. These interactions are also stabilised by palmitoylation. They include the association of tetraspanins with kinases such as protein kinase C and type II phosphatidylinositol 4 kinase (PI4KII) (Berditchevski et al. 1997;Claas et al. 2001;Mannion et al. 1996;Zhang et al. 2001).

In addition to interacting with various proteins, tetraspanins can also associate with cholesterol and gangliosides. This association accounts for the lipid raft-like property of tetraspanins, whereby some tetraspanins partition in the insoluble, light membrane fractions of sucrose gradients under certain detergent

conditions (Hemler 2003;Yanez-Mo et al. 2009). Lipid rafts are currently described as dynamic nanoscale plasma membrane microdomains with a high level of lipid composition comprising mainly of sphingolipids, phospholipids and cholesterol as well as proteins (Lingwood and Simons 2010;Simons and Gerl 2010;Simons and Sampaio 2011). Components of these microdomains are often defined by their resistance to cold non-ionic detergent lysis such as Triton X-100 (Simons and Gerl 2010;Simons and Ikonen 1997). Unlike the tetraspanin enriched microdomains which have high protein content and thus heavy densities, lipid rafts have lower buoyant densities due to the high lipid content and thus segregate into low density, light membrane fractions of sucrose gradients. Lipid rafts differ from TERMs, which are disrupted by Triton X-100 and tend to segregate into high density, heavy fractions of sucrose gradients (Hemler 2003).

The dynamics and partitioning of tetraspanins and raft components within tetraspanin-enriched microdomains and lipid rafts, respectively can be distinguished by use of fluorescence microscopy techniques such as fluorescence recovery after photobleaching and single-molecule tracking (Espenel et al. 2008;Krementsov et al. 2010). For example, a study by Espenel and colleagues analysed the membrane distribution and dynamics of tetraspanin CD9 within TERMs in comparison to that of CD55, a raft resident protein by using single-molecule tracking in live cells (Espenel et al. 2008). In that study, the authors found that CD9 molecules were distributed on the whole cell surface with localised areas whereby CD9 was enriched. These tetraspanin-enriched areas/microdomains were found to be stable in position

and shape. Furthermore, by comparing the membrane distribution and dynamics of CD9 and CD55, these authors found that the partitioning and dynamics of these two membrane proteins were different, whereby they demonstrated that CD55 was excluded from the tetraspanin-enriched areas/microdomains (Espenel et al. 2008).

A study by Charrin and colleagues demonstrated that tetraspanins (CD9, CD81 and CD82) interact with cholesterol, since extraction with digitonin (a cholesterol precipitating reagent) also precipitated tetraspanin oligomers; and that these interactions were disrupted upon cholesterol depletion (Charrin et al. 2003). Other studies have demonstrated tetraspanins to associate with gangliosides; such as CD9 with ganglioside GM3, an interaction that promotes the association of CD9 with integrin α3 (Kawakami et al. 2002). In a separate study by Odintsova and colleagues, it was demonstrated that inhibition of ganglioside GD1a affected interactions of CD82 with other protein partners. Specifically, the association of CD82 with CD151 was decreased, whilst the CD82-EGFR interaction was enhanced by GD1a inhibition (Odintsova et al. 2006).

The ability of tetraspanins to interact with various partners, bringing them in close proximity with other molecules thereby enhancing the formation and stability of functional complexes such as signalling molecules, has seen this protein family described as ‘molecular facilitators’, regulating various cellular processes through their organisation of the plasma membrane (Maecker et al. 1997). It is through these interactions with themselves and other partner molecules, that tetraspanins are believed to modulate various cellular functions

including adhesion strengthening, effects on signalling, tumour progression, immune cell functions, platelet function, infectious diseases, angiogenesis, oocyte fertilisation, protein trafficking and possibly many more (Zoller 2009). CD82 has been shown to be involved in some of these cellular processes as discussed below.

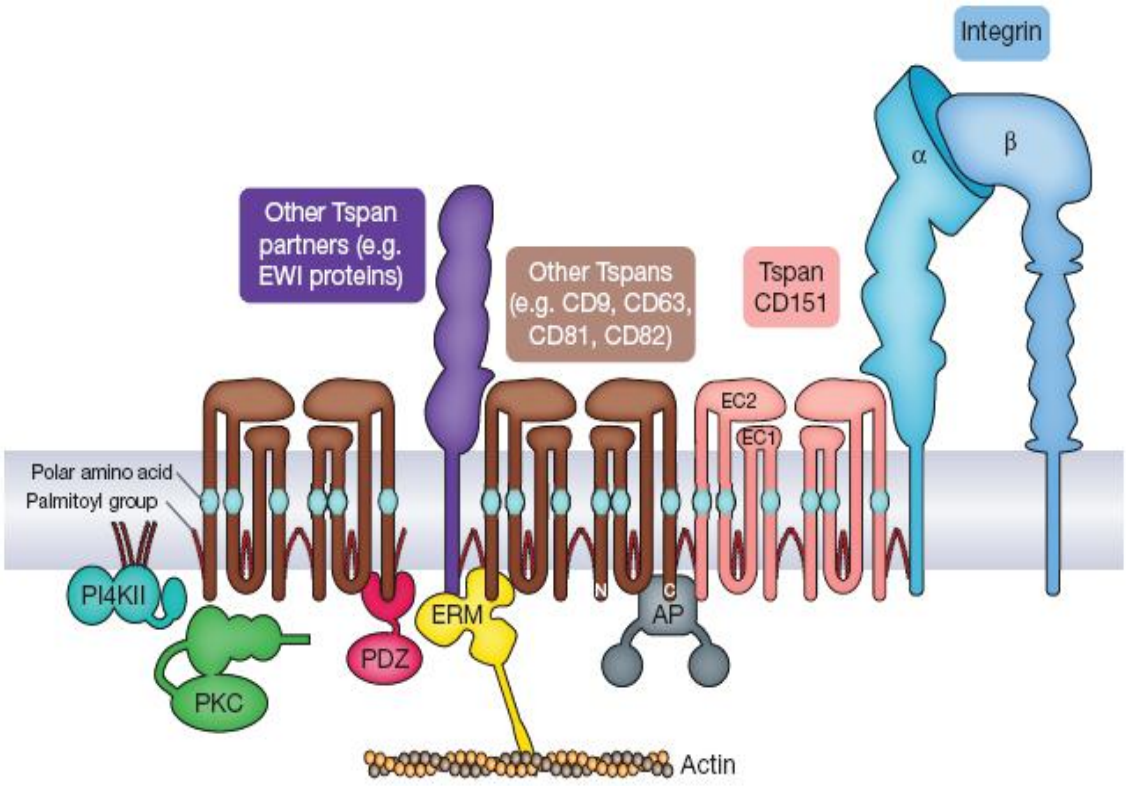

Figure 1.8: Tetraspanin-enriched microdomains.

Tetraspanins organise numerous proteins including other tetraspanins, various transmembrane and cytosolic proteins into complexes termed as tetraspanin-enriched microdomains (TERMs). Integrins such as α3β1 are the major non-tetraspanin partners found in TERMs and can be recruited through their direct association with tetraspanin CD151. Other non-tetraspanin transmembrane partners include immunoglobulin superfamily members such as the EWI proteins (EWI-2 and EWI-F); growth factor receptors such as EGFR and membrane-bound growth factors such as HB-EGF. Cytoplasmic TERM-resident proteins include protein kinase C (PKC), type II phosphatidylinositol 4 kinase (PI4KII), actin-binding ezrin-radixin-moesin (ERM) family proteins, adaptor proteins (AP) and PDZ-domain-containing proteins such as syntenin-1. This figure was obtained from Stipp (Stipp 2010).

1.3.2 CD82

CD82 (formerly known as KAI1, Tspan27) is a membrane glycoprotein belonging to the tetraspanin family (Table 1.1). The human *CD82/KAI1* gene is located on chromosome 11p11.2 and encodes a 267 amino acid protein with a predicted molecular weight of 46-60 kDa due to glycosylation (Figure 1.9) (Dong et al. 1995;Jackson et al. 2005). It was later found that CD82/KAI1 was identical to several antigens that were previously characterised from human lymphocytes. These included R2, an antigen that was highly upregulated in activated T cells (Gaugitsch et al. 1991); C33, a membrane antigen immunoprecipitated by monoclonal antibodies C33 and M104, that was capable of inhibiting syncytium formation induced by human T-cell leukaemia virus type I (HTLV-1) (Fukudome et al. 1992;Imai et al. 1992); and IA4, an antigen widely expressed on the surface of lymphocytes and monocytes (Gil et al. 1992). According to the HUGO Gene Nomenclature Committee (http://www.genenames.org/data/hgnc_data.php?hgnc_id=6210), the currently approved gene symbol and name for *KAI1*, is *CD82*; therefore from henceforth, the KAI1 molecule will be referred to as CD82.

1.3.2.1 Specific structural features of CD82

CD82 contains the characteristic structural features shared by all family members as outlined in Figure 1.7. The bar protein structure illustrates the predicted location of these features for CD82 (Figure 1.9). Like the majority of

tetraspanins, the large extracellular loop (EC2) of CD82 contains six highly conserved cysteines thus forming three disulphide bonds (Figure 1.9; clear) (Charrin et al. 2009). In addition to these cysteine residues, the EC2 region of CD82 also contains three *N*-glycosylation sites, Asparagine (Asn, N)129, Asn157 and Asn198 (Figure 1.9; purple circles) (Liu and Zhang 2006). A report by White and colleagues demonstrated that CD82 was downregulated in more than 50% of the cancer cell lines that were analysed. They also found tissue-specific heterogeneity in the molecular weight of CD82 based on the variability in the protein band pattern as determined by western blot analysis. This was concluded to be due to differences in *N*-linked glycosylation (White et al. 1998).

Twelve tetraspanins including CD82 contain a putative tyrosine-based internalisation sorting motif (YXXΦ) in the C-terminal tail. In the case of CD82, this sequence is YSKV for tyrosine, serine, lysine and valine, respectively (Berditchevski and Odintsova 2007). The YXXΦ motif is recognised by the μ2 chain of the clathrin adaptor protein-2 (AP-2) complex thus suggesting a possible role of this motif in the trafficking of tetraspanins and their associated proteins. However, a study by Xu and colleagues demonstrated that CD82 undergoes lipid-dependent endocytosis, independent from the clathrin pathway (Xu et al. 2009). This study therefore indicates that the YXXΦ motif does not always predict the internalisation pathway.

CD82 is palmitoylated and contains five juxtamembrane cysteine residues located at positions 5, 74, 83, 251 and 253, which are possible sites of palmitoylation (Figure 1.9; yellow circles) (Mazurov et al. 2007;Miranti 2009).

Mutations of these cysteine residues have previously been shown to disrupt protein-protein interactions including the association of CD82 with the HTLV-1 Gag protein. These mutations were also found to reverse the inhibitory effects of wild-type CD82 on cell migration and invasion (Mazurov et al. 2007;Zhou et al. 2004).

The transmembrane regions of tetraspanins including CD82 contain polar residues (Figure 1.9; red circles). Asparagine (Asn, N), glutamine (Gln, Q) and glutamic acid (Glu, E) are the polar residues located in the first, third and fourth transmembrane domains of CD82, respectively (Bari et al. 2009;Bienstock and Barrett 2001). These three polar residues are conserved in all CD82 proteins in vertebrates and are reported to be important for the interactions of CD82 with other tetraspanins such as CD9 and CD151. A study by Bari and colleagues demonstrated that mutations of all three polar residues to alanines markedly reduced the association of CD82 with CD9 and CD151. These authors also found that these polar residues were critical for the motility-inhibitory activity of CD82 since expression of the NQE CD82 mutant resulted in increased cell motility compared to wild-type CD82 (Bari et al. 2009).

Additionally, the 5’ promoter region of the *CD82* gene contains putative binding motifs for several transcription factors including activating protein 2 (AP2), p53 and activating protein 1 (AP1) (Dong et al. 1997). This promoter region is reported to be important in the regulation of CD82 transcription (Dong et al. 1997;Marreiros et al. 2003;Marreiros et al. 2005).

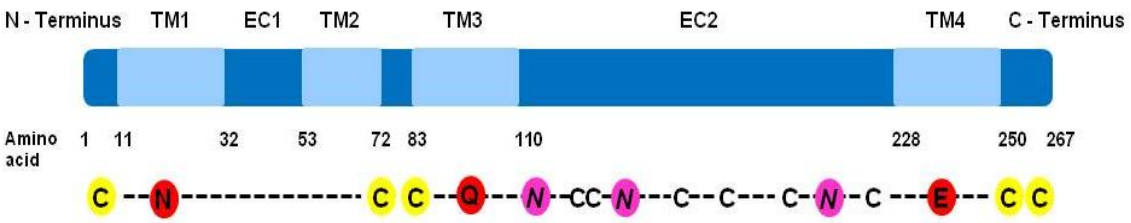

Figure 1.9: Schematic of the CD82 bar protein structure.

The *CD82* gene encodes a 267 amino acid protein. The schematic indicates the location of the main structural features of the CD82 protein including, four transmembrane domains (TM1-4) (pale blue boxes); a short extracellular loop (EC1); a very short intracellular loop located between TM2 and TM3; a large extracellular loop (EC2); short N- and C-termini; juxtamembrane cysteine residues, which are sites for palmitoylation (yellow circles); NQE polar residues (red circles); *N*-glycosylation sites (purple circles); and conserved cysteines including the CCG-motif (clear). This figure was adapted from Bienstock et al. and Jackson et al. (Bienstock and Barrett 2001;Jackson et al. 2005), according to the Universal Protein (UniProt) database (http://www.uniprot.org/uniprot/P27701) in association with the HUGO Gene Nomenclature Committee (HGNC). Abbreviations: C - cysteine; N - asparagine; Q - glutamine; and E - glutamic acid.

1.3.2.2 Effects of CD82 on immune cell signalling

CD82 is abundantly expressed on B and T lymphocytes, granulocytes, monocytes, macrophages and natural killer cells (Wright et al. 2004b). Most of the early studies of CD82 in the 1990s were done in lymphoid cells, whereby it was particularly demonstrated that CD82 expression was upregulated following phytohaemagglutinin (PHA) stimulation of T cells. Furthermore, CD82 was found to inhibit syncytium formation induced by the human T-cell leukaemia virus type I (HTLV-1) (Fukudome et al. 1992;Gil et al. 1992;Imai et al. 1992). These studies suggest a possible role of CD82 in regulating T cells and possible implications on the immune response.

CD82 is reported to interact with a range of immunoreceptors including B-cell and T-cell receptors; peptide receptors - major histocompatibility complex (MHC) class I & II; and co-receptors such as CD4, CD19 and EWI-2 (Table 1.2) (Wright et al. 2004b). CD82 is thought to have a role in regulating T cell signalling through its association with T-cell receptors. Full activation of T cells requires two signals; one generated by the engagement of T cell receptors on T cells with MHC-peptide complexes found on antigen presenting cells (APCs); and the second signal is generated by the association of surface molecules on T cells with those on the APCs. This provides a co-stimulatory signal that leads to a complete T cell immune response involving T cell proliferation and cytokine production (Witherden et al. 2000). Immobilisation of appropriate monoclonal antibodies can provide this second co-stimulatory signal in the absence of

APCs. It has been previously demonstrated that CD82 can deliver a co-stimulatory signal for full activation of T cells resulting in enhanced cytokine production and cell differentiation, when anti-CD82 and anti-CD3 monoclonal antibodies were co-immobilised (Lagaudriere-Gesbert et al. 1998;Lebel-Binay et al. 1995).

The Rho family of GTP-binding proteins including RhoA, Rac and cdc42 is implicated in T cell activation leading to gene transcription and cell differentiation. Like other GTP-binding proteins, their GTPase activity is regulated by the switch between inactive (GDP-bound) to active GTP-bound state, which is in turn regulated by guanosine exchange factor (GEF) molecules such as the Vav family of proteins including Vav1. Furthermore, the activity of GEF molecules and their association with adaptor proteins is regulated by tyrosine phosphorylation. A study by Delaguillaumie and colleagues demonstrated that CD82 engagement promotes T cell signalling involving Rho GTPases; whereby it was demonstrated that CD82 engagement induced tyrosine phosphorylation and association of Vav1 (a Rho-specific GEF) and the adaptor protein SLP76, leading to Rho GTPase activation. Furthermore, the authors demonstrated that inactivation of the Rho GTPases inhibited the CD82-induced formation of membrane extensions (Delaguillaumie et al. 2002).

Collectively, these studies highlight the intermediary role of CD82 in promoting T cell signalling by acting as a co-stimulator through its association with numerous immunoreceptors.

Molecular interactions of CD82

Interacting molecules	References
Tetraspanins	
CD9, CD151	(Bari et al. 2009;Charrin et al. 2003)
CD63	(Hoorn et al. 2012)
CD81	(Charrin et al. 2003;Rubinstein et al. 1996)
CD53	(Charrin et al. 2002)
Molecules of the immune system	
CD4, CD8	(Imai and Yoshie 1993)
CD19	(Horvath et al. 1998)
MHC class I & II	(Lagaudriere-Gesbert et al. 1997)
EWI-2	(Zhang et al. 2003b)
Integrins	
α3β1	(Berditchevski and Odintsova 1999;Odintsova et al. 2000)
α4β1, α6β1	(He et al. 2005;Takahashi et al. 2007)
αLβ2	(Tarrant et al. 2003)
αvβ3	(Ruseva et al. 2009)
Gangliosides	
GM2	(Todeschini et al. 2007)
GM3	(Wang et al. 2007)
Growth factors and growth factor receptors	
ProHB-EGF	(Nakamura et al. 2000)
EGFR	(Odintsova et al. 2000;Odintsova et al. 2006)
ErbB2, ErbB3	(Odintsova et al. 2003)
c-Met	(Takahashi et al. 2007)
Intracellular signalling molecules	
PKC	(Wang et al. 2007;Zhang et al. 2001)
Other molecules	
KITENIN	(Lee et al. 2004b)
DARC	(Bandyopadhyay et al. 2006)
γ-glutamyl transpeptidase	(Nichols et al. 1998)

Table 1.2: Transmembrane and cytosolic molecules that associate with tetraspanin CD82.

Abbreviations: MHC I & II - major histocompatibility complex class I & II; proHB-EGF - membrane-bound heparin-binding EGF-like growth factor; PKC - protein kinase C; KITENIN – KAI1 COOH-terminal interacting tetraspanin; DARC - duffy antigen receptor for chemokines. This table was adapted from Miranti (Miranti 2009).

1.3.2.3 Effects of CD82 on growth factor signalling

Tetraspanins have been previously shown to modulate growth factor signalling. For example, CD82 has been reported to associate with cell surface receptors and thereby regulate their biological activity. A study by Odintsova and colleagues demonstrated that CD82 directly associates with the epidermal growth factor receptor (EGFR); and that ectopic expression of CD82 suppressed EGF-induced morphological changes including lamellipodial extensions and cell migration in epithelial cells (Odintsova et al. 2000). Furthermore, this work also demonstrated that the CD82-mediated attenuation in EGFR signalling correlated with an increased rate of receptor desensitisation through dephosphorylation of the receptor and its downstream signalling molecules; and also with an increase in the rate of ligand-dependent internalisation of the receptor. This negative effect of CD82 on EGF-induced signalling however was not found to affect the initial activation of the receptor, but rather the subsequent desensitisation following activation of the receptor (Odintsova et al. 2000). This group later proposed a molecular mechanism into the specific attenuating effect of CD82 towards EGFR to involve redistribution of the receptor into ganglioside-containing microdomains, as was observed in sucrose gradient fractions. It was also shown that the elevated expression of CD82 resulted in increased surface expression of ganglioside GD1a, which co-localised together with CD82 and EGFR on the plasma membrane (Odintsova et al. 2003). Gangliosides are well-known to play crucial roles in regulating growth factor signalling. Specifically, GD1a has previously been shown to

promote EGFR dimerisation and thus downstream signalling, both in the presence and absence of a ligand (Liu et al. 2004b;Milani et al. 2010;Miljan and Bremer 2002).

Another study by Danglot and colleagues also highlighted the involvement of CD82 in the regulation of EGFR signalling. They demonstrated that the tetanus neurotoxin-insensitive vesicle-associated membrane protein (TI-VAMP) was required for the transport of CD82 from the Golgi apparatus to the cell surface; and that depletion of either TI-VAMP and/or CD82 decreased the cell surface mobility of activated EGFR, which correlated with a decrease in MAPK signalling and also increased endocytosis of the receptor (Danglot et al. 2010).

To further demonstrate the CD82-dependent modulation of EGFR signalling, Wang and colleagues demonstrated that CD82 played a role in promoting the suppression of EGFR signalling by activated PKCα. These authors demonstrated that EGFR is brought in close proximity with PKCα through an ordered complex involving CD82, caveolin-1 and ganglioside GM3. Thereby enabling activated PKCα to phosphorylate EGFR, leading to receptor internalisation and signalling suppression (Wang et al. 2007).

Activation of the c-Met receptor by its ligand, hepatocyte growth factor (HGF) can induce cell proliferation, migration and survival via the PI3K and MAPK signalling pathways. A study by Takahashi and colleagues demonstrated the association of CD82 with c-Met (Takahashi et al. 2007). Furthermore, the authors demonstrated that ectopic expression of CD82 resulted in suppression

of HGF-induced cell migration via the reduced association of signalling adaptor proteins with c-Met, thereby inhibiting activation of downstream signalling pathways (Takahashi et al. 2007).

Collectively, these studies demonstrate that CD82 negatively regulates growth factor signalling, partly through its direct association with growth factor receptors. This interaction appears to be critical for the CD82-mediated attenuation of growth factor signalling. It is possible that through this association, CD82 recruits the growth factor receptors to a multi-molecular complex consisting of negative regulators such as phosphatases to limit signal propagation.

1.3.2.4 Roles of tetraspanins in malignant disease

The ability of tetraspanins to associate with a range of transmembrane and cytoplasmic signalling molecules, recruit them into TERMs and thus modify their activity can have implications in malignant disease. Tetraspanins have been implicated in both progression and suppression of tumours (Boucheix and Rubinstein 2001;Maecker et al. 1997). Some family members such as CD151, Tspan8 and CD37 are reported to promote tumour progression (Lapalombella et al. 2012;Novitskaya et al. 2010;Richardson et al. 2011;Sadej et al. 2009); whilst the expression of others such as CD82 and CD9 is reported to inversely correlate with the metastatic potential of various cancers and is thus indicative of good prognosis (Dong et al. 1997;Jackson et al. 2005;Richardson et al. 2011;Tonoli and Barrett 2005).

1.3.2.4.1 Tetraspanins and tumour progression

CD151 is overexpressed in many tumour types including: breast, pancreatic, non-small cell lung cancer and colorectal cancer; and this is associated with poor prognosis and enhanced metastasis (Yang et al. 2008;Zoller 2009). The expression of CD151 is upregulated in 31% of human breast cancer with even higher expression levels, 40% and 45% in high grade and estrogen receptor-negative tumours, respectively (Yang et al. 2008).

CD151 has previously been reported to be involved in breast cancer tumourigenesis. A study by Sadej and colleagues demonstrated that high expression of CD151 in breast cancers correlated with decreased overall survival, whereby the five-year estimated survival rates for breast cancer patients were reported to be approximately 46% and 80% for CD151-positive and CD151-negative, respectively (Sadej et al. 2009). In that study, the authors further demonstrated the involvement of CD151 in breast cancer tumourigenesis. They found that depletion of CD151 in breast cancer cell lines resulted in a decrease in the tumourigenic potential of these cells when xenotransplanted in athymic nude mice, compared to tumour growth in mice with CD151-positive cells. Additionally, they found that CD151 modulated the response of breast cancer cells to endothelial cell-derived transforming growth factor beta (TGF-β). Thus, CD151 was identified as a key regulator of communication between tumour cells and endothelial cells (Sadej et al. 2009;Sadej et al. 2010). In recent studies, CD151 was shown to regulate

proliferation of non-tumourigenic mammary epithelial cells (Novitskaya et al. 2010). Furthermore, CD151 is reported to be overexpressed in subtypes of invasive breast cancer, resulting in poor overall survival and disease-free survival (Kwon et al. 2012).

Together, these findings implicate CD151 in breast cancer tumourigenesis and disease progression. They thus identify CD151 as a potential prognostic marker for breast cancer and a viable therapeutic target in the management of this disease.

1.3.2.4.2 Tetraspanins and tumour suppression

Tetraspanins such as CD82 and CD9 are known to have tumour suppressive activity, whereby it is reported that expression of these tetraspanins inversely correlates with tumour invasion and metastasis in many malignancies including breast cancer (Hemler 2008;Liu and Zhang 2006;Richardson et al. 2011). The role of CD82 as a metastasis suppressor will be discussed further below.

1.3.2.5 CD82 and metastasis suppression

CD82 is ubiquitously expressed in normal human tissue with highest levels of expression being reported to be in lung, liver, prostate, kidney, placenta and bone marrow (Liu and Zhang 2006;Miranti 2009). CD82 is downregulated during the advanced stages of a wide variety of human cancers, both at mRNA and protein levels; and this is strongly correlated with poor prognosis. However,

mechanisms into inactivation of CD82 in human malignancies remain elusive. CD82 was initially proposed to be a prostate-specific metastasis suppressor (Dong et al. 1997;Liu and Zhang 2006;Miranti 2009). However, subsequent studies revealed that CD82 is a suppressor of the metastasis phenotype of many tumours (Jackson et al. 2005).

It has previously been shown that CD82 is downregulated preferentially in estrogen receptor (ER)-positive breast cancers (Huang et al. 2005) and that in such cases, CD82 could be re-inducible with endocrine therapy involving ER-antagonists such fulvestrant (Christgen et al. 2008;Christgen et al. 2009). In prostate cancer mouse models, downregulation of CD82 correlated with increased invasive potential, an effect that was reversed by re-expression of CD82 (El Touny and Banerjee 2007). These findings highlight the suppressive effect of CD82 on tumour cell invasion. The exact mechanisms of how CD82 suppresses metastasis remain unclear, however it has been postulated that the CD82-mediated metastasis suppression could be via its inhibition of cell migration (Miranti 2009).

1.3.2.5.1 CD82 and cell migration

Cell migration can be promoted by multiple signalling pathways including receptor tyrosine kinase and integrin signalling. The latter involves adhesion-dependent signalling molecules such as focal adhesion kinase (FAK); other signalling molecules including Src; adaptor proteins such as $p130^{CAS}$ (Crk-associated substrate) and Crk, which ultimately promote cell detachment and

thus motility (Cabodi et al. 2010;Klemke et al. 1998). Integrins α3β1 and α4β1 are amongst the proteins that have been reported to interact with CD82 (Table 1.2), and this association is thought to be crucial for the function of CD82 as a metastasis suppressor (Jee et al. 2007). The association of $p130^{CAS}$ and Crk is reported to be crucial in facilitating cell migration; whereby it has previously been shown that coexpression of $p130^{CAS}$ and Crk resulted in a significant increase in cell migration on various extracellular matrices (ECM) (Klemke et al. 1998).

Specifically, a study by Zhang and colleagues demonstrated that expression of CD82 in a metastatic prostate cancer cell line reduced the migratory potential of these cells towards fibronectin and laminin ECM. These authors also observed that cells overexpressing CD82 had increased expression of FAK and low levels of $p130^{CAS}$, resulting in decreased formation of the pro-migratory $p130^{CAS}$-Crk complex. They concluded that CD82 inhibited cell motility through the FAK-Src-$p130^{CAS}$-Crk signalling pathway by downregulating the level of $p130^{CAS}$ and thus affecting formation of the pro-migratory $p130^{CAS}$-Crk complex (Zhang et al. 2003a).

Sprouty2 is a member of the Sprouty protein family which are inducible inhibitors of signalling by receptor tyrosine kinases. Once phosphorylated, Sprouty proteins such as Sprouty2 can antagonise the MAPK signalling pathway through sequestration of Grb2. This therefore inhibits the recruitment of the Grb2-SOS complex to the activated receptor, ultimately inhibiting Ras activation (Kim and Bar-Sagi 2004). Overexpression of Sprouty2 has previously

been reported to result in suppression of cell migration via inhibition of MAPK signalling (Lee et al. 2004a). In a separate study by Mu and colleagues, it was demonstrated that CD82 suppresses HGF-induced hepatoma cell migration via up-regulation of Sprouty2. These authors demonstrated that overexpression of CD82 resulted in elevated levels of Sprouty2 and inhibition of cell migration (Mu et al. 2008).

Collectively, these studies demonstrate that CD82 can suppress cell migration via different mechanisms.

1.3.2.6 Other tetraspanin functions

1.3.2.6.1 Oocyte fertilisation

Besides having roles in malignancies, tetraspanins have also been implicated in various normal physiological processes such as oocyte fertilisation. Le Naour and colleagues previously demonstrated that tetraspanin CD9 was essential for oocyte-sperm fusion, whereby the fertility of knockout mice deficient in CD9 ($CD9^{-/-}$) was severely reduced (Le et al. 2000). This group later demonstrated that CD9 was not the only tetraspanin involved in fertilisation, but also CD81. They demonstrated that CD81 knockout mice ($CD81^{-/-}$) also showed a reduction in fertility (40%), though not as severe as that observed in $CD9^{-/-}$ (95%). Mice lacking both CD9 and CD81 (double knockout mice $CD9^{-/-}$ $CD81^{-/-}$) were completely infertile thus indicating that both CD9 and CD81 are required for effective fertilisation (Rubinstein et al. 2006). The expression of CD9 on oocytes

is mainly localised to the membranes of microvilli; and this expression is thought to be required in maintaining the size, shape and density of oocyte microvilli, thereby facilitating sperm-egg fusion (Hemler 2008;Runge et al. 2007).

1.3.2.6.2 Platelet function

Tetraspanins are expressed on the surface of platelets. These include CD9, CD151, CD63, Tspan9 and Tspan32, whereby CD9 is the most highly expressed tetraspanin on platelets (Haining et al. 2011). *In vivo* studies of tetraspanin-deficient mice demonstrated that tetraspanins are essential for modulating normal platelet function. Specifically, a report by Wright and colleagues demonstrated that CD151 knockout mice displayed abnormal haemostasis, whereby *in vivo* tail bleeding studies revealed prolonged bleeding times for CD151-null mice when compared to that for wild-type mice. Furthermore, the authors observed that CD151-null mice had a significantly higher tendency to re-bleed ($P<0.05$), compared to wild-type mice (Wright et al. 2004a). Another study demonstrated that CD151-deficient platelets had a defect in spreading and clot retraction; effects which were proposed to be due to a defect in integrin signalling (Lau et al. 2004).

1.3.2.7 Tetraspanin deficiencies and associated phenotypes in human

Several clinical phenotypes have previously been described in correlation to tetraspanin deficiencies (Lazo 2007). For example, a study by Karamatic and colleagues described rare cases of three individuals who had a single

nucleotide insertion in exon 5 of *CD151*, which caused a frameshift mutation and a premature stop signal at codon 140. The mutation resulted in expression of a truncated protein lacking most of the integrin-binding large extracellular loop. Clinical phenotypes associated with this mutation in the *CD151* gene included β-thalassemia minor, pretibial epidermolysis bullosa, neurosensory deafness and nephritis (Karamatic, V et al. 2004). This study demonstrated that CD151 played a key role in ensuring the integrity of basement membranes in the kidney, skin and inner ear. It also highlights the importance of CD151-integrin associations for the molecular function of CD151.

Tetraspanin TM4SF2 has previously been implicated in X-linked mental retardation, whereby a study by Zemni and colleagues identified mutations in the *TM4SF2* gene located on chromosome Xp11.4 in patients with X-linked mental retardation. These mutations included an inactivating X;2 translocation breakpoint and a nucleotide transition that leads to a premature stop signal. The latter mutation leads to expression of a truncated protein lacking the fourth transmembrane domain and the C-terminal tail (Zemni et al. 2000).

Other phenotypes associated with tetraspanin deficiencies include an immunodeficiency syndrome characterised by recurrent infectious diseases correlated with lack of CD53 antigen expression on neutrophils (Mollinedo et al. 1997). Moreover, mutations in the peripherin/RDS gene have been implicated in a degenerative disease of the retina (van et al. 1999). Additionally, Tspan12 has been shown previously to be required for retinal vascular development whereby *Tspan12*$^{-/-}$ mice exhibited retinal vascular defects when compared to *Tspan12*$^{+/+}$

mice (Junge et al. 2009). It was later found in three Chinese patients that heterozygous mutations in *Tspan12* resulted in autosomal dominant familial exudative vitreoretinopathy (FEVR), a hereditary vitreoretinal disorder characterised by abnormalities in the development of the retinal vessels (Yang et al. 2011). More recently, van Zelm and colleagues reported the first case study of a patient with antibody deficiency syndrome caused by a homozygous CD81 mutation (a homozygous G>A substitution) which resulted in complete lack of CD81 expression on B cells and this resulted in severe nephropathy and hypogammaglobulinemia (van Zelm et al. 2010).

Considering the wide tissue distribution of tetraspanins and their involvement in numerous biological processes, it is perhaps surprising that defects in individual tetraspanins result in relatively mild phenotypes. Since these proteins are known for their association into multimolecular complexes, the mild phenotypes observed from studying individual molecules suggest that perhaps tetraspanins should be studied as a multimolecular unit. Perhaps then, the functional implications of their deficiencies would be more prominent as opposed to those identified for individual molecules.

1.4 Research objectives

Preliminary experiments performed within our group using MCF-7 breast cancer cells demonstrated that overexpression of CD82 modulated the cellular response of these cells to Herceptin treatment. Specifically, activation of the PI3K/Akt pathway was found to be considerably delayed in Herceptin treated CD82-overexpressing cells when compared to control cells. Additionally, it was demonstrated that ErbB2 was readily degraded in the CD82-overexpressing cells following prolonged treatment with Herceptin when compared to control cells. Furthermore, after stimulation with heregulin, the peptide corresponding to the C-terminus of CD82 pulled down phosphorylated proteins within the molecular weight region similar to that of the ErbB proteins (Odintsova E, unpublished results). These findings led to the hypothesis that CD82 could potentiate the efficacy of Herceptin via two possible mechanisms; either by regulating the distribution and dynamics of the ErbB2/Herceptin complex or by modifying the recruitment of signalling molecules to the plasma membrane. Thus the aims of this project were to use breast cancer cell lines (BT474, SKBR3 and ZR75.30) expressing different levels of CD82 in order to:

1. Determine whether ectopic expression of CD82 altered the cellular response of breast cancer cells to Herceptin treatment.
2. Determine whether CD82 affected the distribution and dynamics of ErbB2 on the plasma membrane following Herceptin treatment.
3. Determine whether ectopic expression of CD82 affected signalling downstream of the ErbB2 receptor.

2 MATERIALS AND METHODS

2.1 Cell Culture Methods

2.1.1 Maintenance of cell lines

All cell lines used in this study and their corresponding features are outlined in Table 3.1. Comprehensive information of growth culture medium and supplements for all these cell lines can be found in *Appendix I.* Purchase information of all reagents and chemicals used can be found in *Appendix II.*

Cells were cultured in complete growth medium at 37^{o}C, in a 5% CO_2 humidified incubator. For sub-culturing, growth medium was aspirated and the cell monolayer was briefly rinsed twice with phosphate buffered saline (PBS) to remove traces of serum. Cells were subsequently detached by the addition of 0.05% trypsin-EDTA to the monolayer, followed by incubation at 37^{o}C for 3-5 minutes to facilitate dispersal. Detached cells were resuspended in complete growth medium and pelleted by centrifugation at 400 g for 3 minutes. The supernatant was removed and the resulting pellet was resuspended with culture medium. Appropriate aliquots of the cell suspension were then transferred to a fresh culture vessel and incubated at 37^{o}C, in a 5% CO_2 humidified atmosphere for further propagation.

2.1.2 Cell freezing and thawing

Cells in log phase were prepared for freezing by being detached, collected and centrifuged as described above in section 2.1.1. The supernatant was removed and the resulting cell pellet was resuspended in 1ml of freezing solution (10% dimethyl sulfoxide (DMSO) and 90% heat inactivated-fetal bovine serum (HI-FBS)) *(Appendix I).* The suspension was transferred to a CryoTube^{TM} vial, which was then wrapped in paper towels and stored in a $^{-}80^{o}C$ freezer for at least 24 hours, to ensure that the cells were gradually frozen prior to being transferred to liquid nitrogen for long-term storage.

To recover frozen cells, the cryovials were placed in a $37^{o}C$ water-bath for 2 minutes and the thawed cells were transferred into 9ml of pre-warmed culture medium before centrifugation at 400 g for 3 minutes. The resulting pellet was resuspended with fresh complete medium and seeded onto a tissue culture vessel followed by incubation at $37^{o}C$, in a 5% CO_2 humidified atmosphere. Cells were maintained in culture for a maximum period of 2 months before another batch was recovered.

2.1.3 Mycoplasma testing

Cells in culture were routinely tested for mycoplasma contamination using a MycoAlert® mycoplasma detection kit immediately prior to freezing; a few days after recovery from liquid nitrogen; and at frequent intervals during culture. In

case of detection of mycoplasma infection, the affected cell line(s) were treated with BM-Cyclin, an antibiotic kit for the elimination of mycoplasma from infected cell cultures that has little or no side effects to the cells at the recommended working concentrations. The kit was used according to the manufacturer's guidelines, which involved changing the growth culture medium from the infected cells and replacing it with fresh medium supplemented with BM-cyclin 1 at 10µg/ml and leaving it on the cells for at least three days, after which, it was replaced by fresh culture medium supplemented with BM-cyclin 2 at 5µg/ml for at least four days. The cycle was repeated for at least 2-3 weeks or until the cells eventually tested negative for mycoplasma.

2.1.4 Cell transfection

Transfection experiments were carried out using either FuGene® 6 or GeneJammer® transfection reagents, with cells at 50-80% confluency according to the manufacturer's protocol. Tables 2.1 and 2.2 summarise the manufacturer's guidelines for the volumes of transfection reagent:DNA in preparation of a complex mixture for FuGene and GeneJammer transfection reagents, respectively. For transient transfections, the cells were transfected as above using GeneJammer and were used in the relevant assays 48h post transfection. All plasmids used in this study are summarised in Table 2.3.

Tissue culture vessel	Surface area (cm^2)	Total volume of medium (ml)	Starting volume of FuGene® 6 (µl)		Starting mass of DNA (µg)		Total volume of complex (µl)
			Amount	Range	Amount	Range	
35mm	8	2	3	3 - 9	1	1 - 2	100
60mm	21	6	6	6 - 20	2	2 - 4.5	200
100mm	55	10	18	17 - 51	6	5.6 - 11	600

Table 2.1: Preparation guidelines for FuGene® 6 transfection reagent: DNA complex (3:1 ratio) in various tissue culture vessels.

Tissue culture vessel	Diameter of the well (mm)	Volume of GeneJammer® per well (µl)	Amount of DNA per well (3:2) ratio (µg)	Final volume of transfection mixture (µl/well)	Total volume of medium per well (ml)
12-well	22	1.5	1	50	1.0
60mm	60	6	4	200	6.0
100mm	100	18	12	600	10.0

Table 2.2: Preparation guidelines for GeneJammer® transfection reagent: DNA complex (3:2 ratio) in various tissue culture vessels.

2.1.5 Generation of stable CD82 knockdown cells

CD82-depleted cell lines were generated by infection of ZR75.30 parental cells with viral particles containing short-hairpin RNA (shRNA) that specifically target wild-type CD82 (target sequence 5'-gcacgtccattccgaagactaca - 3'). Viral particles containing CD82-specific shRNA were generated by co-transfecting a plasmid mixture containing the pLVTHM-shCD82 lentiviral vector encoding CD82-specific shRNA, the packaging vector psPAX2 and the envelope plasmid pMD2G into a packaging cell line, HEK 293T cells using FuGene® 6. One day prior to transfection, the cells were detached and re-seeded at a concentration that would achieve a monolayer density of 50-80% confluency, suitable for transfection. Cells were transfected as described above in section 2.1.4 and were incubated at 37^{o}C, 5% CO_2 for 24 hours, after which the culture medium containing the complex mixture was removed and replaced with complete growth medium. The cells were further incubated for at least 48 hours to allow production of virus particles. For cellular transduction, culture medium containing viral particles was collected from the transfected HEK 293T cells, 72 hours post transfection. The monolayer of HEK 293T cells was replenished with fresh medium and incubated further for use later for a second cellular transduction process. The collected medium was centrifuged at 400 g for 3 minutes and the resulting supernatant was filtered through a 0.22 µm filter to remove all traces of 293T cells and debris. Polybrene® (8µg/ml) was added to the filtered supernatant to enhance the efficiency of viral infection. Immediately prior to transduction, growth medium was removed from a 50-80% confluent

monolayer of breast cancer cells, ZR75.30 and was replaced with the above culture medium containing viral titre. The transduced cells were incubated for 24 hours before repeating the transduction steps again with a second batch of viral particles. 24 hours post the second viral transduction, culture medium containing viral titre was removed and the cells were replenished with fresh complete growth medium and cultured further appropriately followed by determination of the knockdown efficiency using flow cytometry and western blot analysis. A knockdown efficiency greater than 50% was considered to be successful and if achieved, the cells were sorted by Fluorescence Activated Cell Sorting (FACS) using an anti-CD82 mAb (IA4) in order to separate and collect a negative population of cells expressing low levels of CD82. These cells were termed ZR75.30/shCD82. A control cell line termed ZR75.30/GFP composed of empty vector was also prepared in parallel to the CD82 knockdown cells. Several batches of cells were frozen down soon after cell sorting for later use. Cells in culture were routinely checked for the level of CD82 knockdown by flow cytometry and western blot analysis. If the knockdown efficiency was being lost during culture, these cells were either re-sorted by FACS for a clear CD82 negative population or another batch of pre-frozen cells was recovered.

2.1.6 Generation of stable cell lines overexpressing CD82

In order to generate stable cell lines overexpressing wild-type CD82, SKBR3 cells were transfected with the pZeoSV-CD82 plasmid using FuGene® 6, as described in section 2.1.4. Stable transfectants of BT474 cells overexpressing wild-type CD82 were generated by using retroviral transduction. This was achieved by co-transfection of 293T packaging cells with a plasmid mixture consisting of the CD82-enconding pBabe-puro-CD82 retrovirus plasmid along with the gag/pol packaging plasmid and the VSV.G envelope plasmid using FuGene 6 according to the manufacturer's protocol. 72h post transfection, culture medium containing the virus was harvested from the packaging cells as described in section 2.1.5 and various dilutions of the virus were used to infect parental BT474 cells overnight. The pZeoSV-CD82 and pBabe-puro-CD82 plasmids respectively contained a zeocin-resistance gene and puromycin-resistance gene important for selection. 24 hours post transfection, culture medium containing the transfection mixture (SKBR3 cells) or virus (BT474 cells) was removed and replaced with complete growth medium supplemented with either 100µg/ml zeocin or 1µg/ml puromycin, for antibiotic resistance selection. The selection medium was replenished every 3 days and the cells were trypsinised and re-seeded at least once a week in order to speed up selection. Following the antibiotic resistance selection period, antibiotic-resistant colonies were pooled together and sorted by FACS using an anti-CD82 mAb (IA4) for the separation and collection of a positive population of cells overexpressing CD82. These cells were termed BT474/CD82^{High} and SKBR3/CD82^{High}. Empty vector

pBabe-puro and pZeoSV transduction/transfection were also carried out to form neotransfected control cell lines, namely, BT474/Puro and SKBR3/Zeo, respectively. All stable cell lines were maintained in complete growth culture medium, supplemented with the appropriate antibiotic, as outlined in *Appendix I*. Several batches of cells were frozen down soon after cell sorting for later use. Cells in culture were routinely checked for the level of CD82 expression by flow cytometry and western blot analysis. If the level of CD82 overexpression was being lost during culture, then these cells were either re-sorted by FACS for a clear CD82-overexpresing population or another batch of pre-frozen cells was recovered.

Plasmid	Source
pLVTHM	Addgene # 12247
psPAX2	Addgene # 12260
pMD2.G	Addgene # 12259
pLVTHM-shCD82wt	Generated in-house
pZeoSV	Invitrogen # V85001
pZeoSV-CD82wt	Generated in-house
pBabe-puro	Addgene # 1764
pBabe-puro-CD82wt	Generated in-house
Gag/pol	Addgene # 14887
VSV.G	Addgene # 14888
pcDNA3.1(+)	Invitrogen # V790-20
pcDNA3.1-CD82wt	Generated in-house
pcDNA3.1-ErbB2-GFP	Kindly provided by Dr T. Wohland (Liu et al. 2007)
pcDNA3.1-EGFR-GFP	Kindly provided by Prof. W. J. Gullick (Kent, UK)
pcDNA3.1-KSR1-HA	Kindly provided by Dr M. A. White (Dallas, Texas)

Table 2.3: Summary of all plasmids used in this study.

2.1.7 Preparation of cells for cell sorting

24 hours prior to cell sorting, confluent monolayers of cells were detached using 0.05% trypsin-EDTA, centrifuged at 400 g for 3 minutes and the cell pellet was resuspended in complete growth culture medium before the cells were re-seeded on to a fresh culture vessel. The following day, the cells were detached using Cell Dissociation Solution, centrifuged as above at 4^{o}C and the cell pellet was resuspended in ice-cold 1% BSA supplemented with primary monoclonal antibodies followed by incubation for 1 hour on ice to allow antibody binding. The cells were then pelleted at 400 g for 3 minutes at 4^{o}C and the resulting cell pellet was washed 3 times with wash buffer (1% BSA/PBS) followed by re-centrifugation as described above. After the last wash, the cells were incubated for 1h in the dark with anti-mouse secondary antibodies conjugated to a fluorophore either fluorescein isothiocyanate (FITC) or phycoerythrin (PE). Following 1 hour incubation on ice in the dark, the cells were centrifuged and washed as described above. After the last wash, the cell pellet was resuspended with ice-cold complete culture medium and then filtered through a 50µm CellTrics® disposable filter to ensure a suspension of single cells. Stained cells were then sorted by FACS using a Beckman Coulter MoFlow high speed cell sorter as following: for CD82^{High} cells, the most positive population of cells was selected; for shCD82 GFP-containing cells, a GFP positive, PE negative population of cells was selected and collected. The sorted population of cells was seeded onto a tissue culture vessel followed by incubation at 37^{o}C, in a 5%

CO_2 humidified atmosphere and henceforth maintained in appropriate growth medium as outlined in *Appendix I*.

2.1.8 Cell proliferation and viability in 2D

To measure cell viability, the cells were seeded onto 6-well plates in complete growth media in the absence of selection antibiotics and maintained at 37^{o}C, 5% CO_2. 24h post seeding, Herceptin was added to the culture medium at the following concentrations: 10, 20, and 50µg/ml followed by further incubation for 72h. Each experiment included non-treated control cells that were grown only in complete culture medium in the absence of Herceptin and were maintained under the same conditions as the test samples. At the end of the incubation period, growth culture medium containing non-viable cells was removed from each well and collected into 15ml centrifuge tubes. Each well of cell monolayer was rinsed twice with PBS followed by trypsinisation. All wash solution was collected along with the non-viable cells in order to minimise loss of cells. The trypsinised cell suspension was collected into previously collected culture medium and centrifuged at 400 g for 3 minutes at room temperature. The resulting cell pellet was resuspended in 1ml of PBS. Cell viability was determined by Trypan Blue® exclusion cell counts using a haemocytometer. One part of cells was mixed with one part of trypan blue. Cell counts were carried out within 3 minutes of mixing with the dye. Cells that were not stained with the blue dye of trypan blue were counted as viable cells and conversely, blue stained cells were counted separately as non-viable cells. The number of cells per 1ml aliquot was equivalent to the cell count within one area of 16

squares of the haemocytometer multiplied by $2x10^4$, accounting for the dilution factor (1:2) of cells with trypan blue. Percentage viability was calculated as: (number of viable cells/ml aliquot divided by the total number of cells/ml aliquot) multiplied by 100. At least three independent experiments were performed.

2.1.9 Cell proliferation and viability in 3D

Cells in log phase were trypsinised and centrifuged at 400 g for 3 minutes at room temperature. The cells were rigorously resuspended in complete growth medium. For growth in collagen, the cell suspension was mixed 1:1 (v/v) with 1.6mg/ml rat tail collagen type I. Three drops of this collagen-cell mix (~$1.5x10^3$cells/40µl drop) were allowed to polymerise at 37^{o}C before culture medium was added over them. For Herceptin treatment, Herceptin (10µg/ml) was added to the growth medium 24h post seeding. The cells were incubated at 37^{o}C, in a 5% CO_2 humidified atmosphere for 14 days to allow colony formation. Culture medium was changed every 3 days and supplemented accordingly with Herceptin.

For growth in Matrigel™, the cells were mixed 1:1 with 2% Matrigel (v/v) and 300µl of this mixture (~$1.5x10^3$cells/300µl) was overlaid on top of a polymerised layer of 100% Matrigel. The cells were incubated at 37^{o}C, 5% CO_2 for 14 days to allow colony formation. For Herceptin treatment, Herceptin at 10µg/ml was prepared in 2% Matrigel and added to the cells 24h post seeding. This was replenished every 3 days. Colonies were analysed using a Zeiss Axiovert 25 microscope and NIS-Elements BR 3.0 laboratory imaging software.

2.1.10 Cell migration assay

Cell migration assays were performed using modified Boyden chambers with Transwell® polycarbonate membrane filter inserts of 8µm pore size, in 24-well tissue culture plates. The outer membrane of the inserts was coated with collagen (17.5µg/ml) overnight at 4^{o}C and washed with PBS before the cells were added. SKBR3/Zeo and SKBR3/CD82^{High} cells were detached using Cell Dissociation Solution, pelleted at 400 g for 3 minutes at room temperature and resuspended to 1x10^{5} cells in 400µl of serum-free DMEM. The pre-coated inserts were assembled matrix side down into 24-well plates before the cells were added to the inner chamber of the inserts. For haptotactic migration assays, cells migrated toward serum-free medium containing no chemoattractant. For chemohaptotactic migration assays, cells migrated either towards complete DMEM medium containing 10% fetal-calf serum (FBS) or serum-free DMEM supplemented with either heregulin (10ng/ml), heparin-binding EGF-like growth factor (HB-EGF) (10ng/ml) or transforming growth factor-beta 1 (TGF-β1) (10ng/ml). For Herceptin treatment, cells were resuspended in serum-free DMEM containing Herceptin (10µg/ml) prior to being added to the Transwell inserts. After 6h incubation at 37^{o}C, 5% CO_2, cells that had not migrated through the filter were removed by swabbing using cotton buds and the inner chamber was washed twice with PBS. Cells that had migrated to the lower surface of the filter were fixed with 3% paraformaldehyde (PFA), permeabilised with 0.1% Triton X-100 followed by three washes with PBS. The nuclei of migrated cells on the outer side of the membrane inserts

were stained using Hoechst 33342. The membranes were removed from the inserts, mounted on to glass slides and analysed using a Nikon Eclipse E600 fluorescence microscope. Images were taken from five random fields per membrane and scored using ImageJ nuclear/cell counter program. Each of the test conditions per experiment was done in duplicate and three independent experiments were carried out. For each cell line, two additional Transwells of cells were used as control for the number of seeded cells prior to the migration assay. The cells in these wells were fixed, permeabilised, stained and mounted as described above after 1h of seeding. Number of migrated cells = the number of nuclei counted per microscopic field, captured at x 20 magnification.

2.1.11 Cell invasion assay

Cell invasion was measured using modified Boyden chambers with Transwell® polycarbonate membrane filter inserts. Matrigel diluted 1:3 in serum-free DMEM was used to coat the outer membranes of the Transwell® inserts; these were then incubated for 40 minutes at 37^{o}C in order for the Matrigel to polymerise before use. Cells resuspended in serum-free DMEM were added to the inner chambers at 1x10^{5} cells in 400µl. The inserts were placed into 24-well plates containing serum-free DMEM supplemented with heregulin (10ng/ml) and incubated at 37^{o}C for 24, 48 and 72h. Cells that invaded through to the outer membrane into Matrigel were processed as described in the migration assay (section 2.1.10). The data was expressed as number of invaded cells per microscopic field from five randomly selected fields per membrane. Each

condition was done in duplicate and at least two independent experiments were performed.

2.1.12 Inhibitor treatments

The MEK inhibitor, U0126 was prepared in dimethyl sulfoxide (DMSO) as a 10mM stock solution, which was subsequently diluted to a working concentration of 10µM in culture medium prior to use. Serum-starved SKBR3/Zeo and SKBR3/CD82^{High} cells were treated with U0126 (10µM) for 30 minutes, 1h and 6h at 37^{o}C, 5% CO_2. DMSO diluted in culture medium to the same solvent concentration as in the inhibitor preparation was added to the inhibitor-free controls. At the end of each incubation period, the cells were lysed as described below in section 2.2.1 of the Materials and Methods. Lysates of equal protein concentration were subjected to SDS-PAGE under reducing conditions followed by western blot analysis to probe for phosphorylated and total proteins.

2.2 Biochemical Methods

2.2.1 Cell Lysis

For western blotting experiments, monolayers of cells in log phase were rinsed twice with PBS. Cellular proteins were then solubilised in Laemmli sample buffer supplemented with protease and phosphatase inhibitors (2mM phenylmethylsulfonyl fluoride (PMSF), 10µg/ml aprotinin, 10µg/ml leupeptin,

5mM sodium fluoride (NaF), 100µM sodium orthovanadate (Na_3VO_4) and 10mM tetrasodium pyrophosphate ($Na_4P_2O_7$)). The lysates were boiled at 94^oC for 10 minutes and stored at $^-80^oC$ until use.

2.2.2 Protein concentration determination

Protein concentration was determined in all samples using the Bio-Rad *Dc* protein assay kit according to the manufacturer's protocol. Bovine serum albumin (BSA) was serially diluted in Laemmli buffer to generate a standard curve of a concentration range of 0.4 – 3.2mg/ml with each protein assay. The protein concentration was determined in all test samples using the BSA standard curve and corrected to the dilution factor of 4.

2.2.3 SDS-PAGE and western blot analysis

Cell lysates with equal amount of protein, along with pre-stained protein markers were resolved on either a 10% or 12% SDS-PAGE (Table 2.4) under reducing or non-reducing conditions; transferred onto nitrocellulose membrane and incubated with appropriate primary antibodies overnight at 4^oC, unless otherwise stated. For reducing conditions, β-mercaptoethanol was added to the samples as a reducing agent at a concentration of 5% of the total sample volume, before the samples were loaded onto polyacrylamide gels. After three washes (20 minutes/wash) at room temperature, using either phosphate buffered saline with Tween-80 (PBS-T) or Tris buffered saline with Tween-80 (TBS-T) wash buffer (*Appendix III*), the membranes were incubated with

species-specific horseradish peroxidase-conjugated secondary antibodies for 1h at room temperature, followed by three washes as detailed above. The wash buffer was removed at the end of the third wash and the membranes were rinsed with distilled water to remove salt residues. Protein bands were visualised using Enhanced Chemiluminescence Plus (ECL Plus) reagent and detected onto Amersham Hyperfilm™ x-ray film. Protein bands were identified according to their molecular weights comparable to the approximate molecular weight ladder of pre-stained protein markers. All non-commercial and commercial antibodies used in this study are summarised in Table 2.5 and Table 2.6, respectively.

% Gel	Volume of reagents (µl)					
	Acrylamide	1M Tris-HCl pH 8.8	20% SDS	dH_2O	APS	TEMED
10%	2500	2800	37.5	2175	37.5	7.5
12%	3000	2800	37.5	1675	37.5	7.5

Table 2.4: Components of a single mini SDS-PAGE running gel.

Antibody	Target antigen	Source	Application
IA4	CD82	Kindly provided by Dr H. Conjeaud (Paris, France)	Immunofluorescence and cell sorting
M104	CD82	Kindly provided by Dr O. Yoshi (Osaka, Japan)	Flow cytometry and Immunoprecipitation
TS82b	CD82	Kindly provided by Dr E. Rubinstein (Villejuif, France)	Western blot

Table 2.5: Non-commercial hybridoma antibodies used in this study.

Antibody Name/Clone	Target antigen	Molecular weight (kDa)	Source	Supplier	Catalogue number
4C5G	PI4K	-	Bovine	LGC Standards	CRL-2538
Akt	Akt 1/2/3	60	Rabbit	Cell Signaling Technology	9272
Alexa Fluor® 488 F(ab')$_2$ fragment	IgG (H+L)	-	Rabbit	Invitrogen	A11070
Anti-Phosphotyrosine (4G10)	Tyrosine-phosphorylated proteins	-	Mouse	Millipore	05-321
CD82/KAI1 (C-16)	C-terminus of KAI1	46	Rabbit	Santa Cruz	sc-1087
c-erbB2 (Ab-17) (Clone e2-4001 + 3B5)	Cytoplasmic domain of ErbB2	185	Mouse	NeoMarkers	MS-730
c-erbB2 (Ab-2) (Clone 9G6.10)	Extracellular domain of ErbB2	185	Mouse	NeoMarkers	MS-229
c-erbB3 (C-17)	ErbB3	185	Rabbit	Santa Cruz Biotechnology	sc-285
EGFR (Ab-15) (Clone H9B4)	Cytoplasmic domain of EGFR	170 (wild type) 145 (vIII variant)	Mouse	NeoMarkers	MS-665
Flotillin-2 (C42A3)	Flotillin-2	49, 58	Rabbit	Cell Signaling	3436
HA-probe (F-7)	HA-epitope tag	-	Mouse	Santa Cruz	sc-7392
HA-probe (Y-11)	HA-epitope tag	-	Rabbit	Santa Cruz	sc-805
KSR1 (H-70)	KSR1	97	Rabbit	Santa Cruz	sc-25416
MEK1/2	MEK1/2	45	Rabbit	Cell Signaling Technology	9122
p38 MAPK	p38α, -β or -γ MAPK	43	Rabbit	Cell Signaling Technology	9212
p44/42 MAPK (Erk1/2)	p44/42 MAPK	42, 44	Rabbit	Cell Signaling Technology	9102
Pan-Ras	H/K/N-Ras	21	Mouse	Cytoskeleton	BK008
Phospho-Akt	pAkt (Ser473)	60	Rabbit	Cell Signaling Technology	9271
Phospho-ErbB2	pErbB2 (Tyr1221/1222)	185	Rabbit	Cell Signaling Technology	2249
Phospho-ErbB2	pErbB2 (Tyr877)	185	Rabbit	Cell Signaling Technology	2241
Phospho-ErbB3 (21D3)	pErbB3 (Tyr1289)	185	Rabbit	Cell Signaling Technology	4791
Phospho-MEK1/2	pMEK(Ser217/221)	45	Rabbit	Cell Signaling Technology	9121
Phospho-p38 MAPK	Ph p38 MAPK (Thr180/Tyr182)	43	Rabbit	Cell Signaling Technology	9211
Phospho-p44/42 MAPK	Ph p44/42 MAPK (Thr202/Tyr204)	42, 44	Rabbit	Cell Signaling Technology	9101
Phospho-SAPK/JNK	pSAPK/JNK (Thr183/Tyr185)	46 (pJNK1) 54 (pJNK2/3)	Rabbit	Cell Signaling Technology	9251
Phospho-Src family	pSrc (Tyr416)	60	Rabbit	Cell Signaling Technology	2101
Polyclonal Goat anti-mouse Igs/HRP	Mouse IgG, IgA, IgM	-	Mouse	Dako	P0447
Polyclonal Goat anti-rabbit Igs/HRP	Rabbit IgG, IgA, IgM	-	Rabbit	Dako	P0448
SAPK/JNK	SAPK/JNK	46 (JNK1) 54 (JNK2/3)	Rabbit	Cell Signaling Technology	9252
Src (36D10)	Src	60	Rabbit	Cell Signaling Technology	2109
β-Actin (Clone AC-15)	β-Actin	42	Mouse	Sigma-Aldrich	A5441

Table 2.6: Commercial antibodies used in this study.

2.2.3.1 Quantitative and statistical analysis of western blot images

Quantification of western blots was carried out using ImageJ software. Blots of the same x-ray exposure time were used during the analysis in order to measure the relative intensity of the bands (Figure 2.1). Statistical significance of analysed data sets from at least three independent experiments was determined with the one-way ANOVA multiple comparison analysis followed by the Tukey-Kramer post-test unless otherwise stated, using GraphPad Prism software (GraphPad software Inc.). Significance was set at $P< 0.05$; and a P value of less than 0.001 was considered to be highly significant. The degree of significance was represented as (*) = $P< 0.05$; (**) = $P< 0.01$; and (***) = $P< 0.001$.

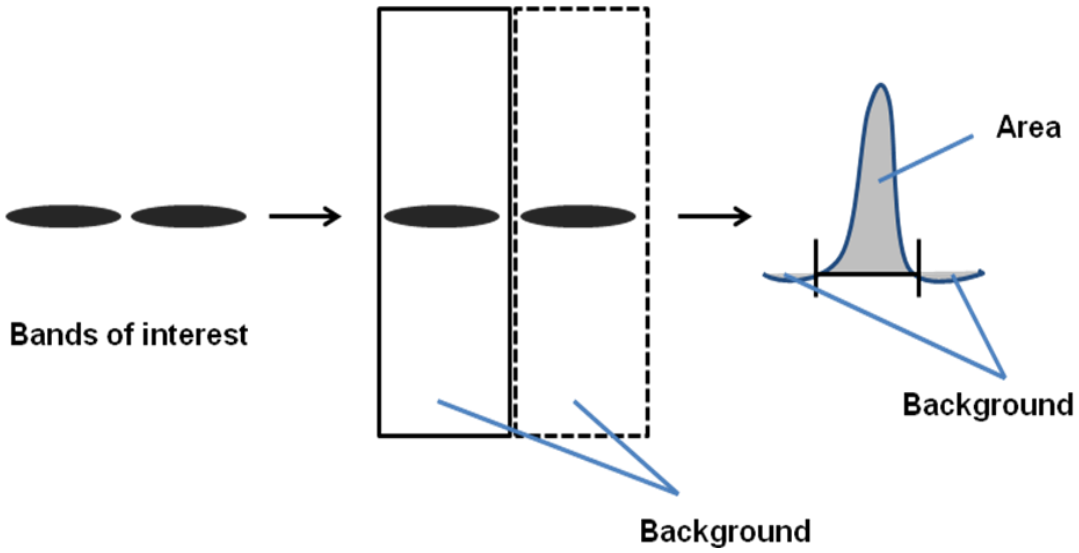

Figure 2.1: Illustrate of quantitative analysis of western blots.

Diagram shows an example of how western blot data was quantitatively analysed using ImageJ imaging software (National Institutes of Health). The intensity of the bands with the same x-ray film exposure time was determined as follows: A box was drawn around the band of interest, taking into account the x-ray film background both above and below the band. The selected region was measured before moving the box onto the next band/lane. The same procedure was applied to all bands and once all lanes were measured, the selected fields were then plotted as graphs, with each enclosed peak corresponding to the intensity of the band from the background. Values of the area under the enclosed peaks were then plotted as bar charts.

2.3 Protein activity

2.3.1 Analysis of cell signalling

For cell signalling experiments cells were incubated under serum-free conditions for 24h. Where indicated, Herceptin (10µg/ml) was added to the culture medium and the cells were incubated for the indicated time intervals followed by lysis in Laemmli buffer as described above.

2.3.2 Kit-based Ras activation assay

2.3.2.1 Sample preparation

SKBR3/Zeo and SKBR3/CD82^{High} cells in log phase were serum-starved overnight prior to the Ras activation assay. The next day, the cells were treated with a Ras activator, heregulin (10ng/ml) for 30min at 37^{o}C, 5% CO_2. At the end of the incubation period, the cells were immediately placed on ice and the cell monolayer was rinsed twice with ice-cold PBS. Cells were scraped into ice-cold lysis buffer, supplemented with 1X protease inhibitor cocktail and immediately clarified by centrifugation at 5000 g; 4^{o}C for 2min. 15µl of lysates was removed for protein quantitation. The remaining cell lysate was transferred into fresh sample tubes and immediately snap frozen in liquid nitrogen before storage at -70^{o}C for future use (see below). The protein concentration in the lysates was determined using Precision Red Advanced Protein Assay (PRAPA) reagent.

The following control reactions were also prepared alongside each Ras activation assay: His-Ras as a quantitation estimate for endogenous Ras; whole cell lysate, as loading controls; positive and negative controls of Ras activity. As a positive control for the pull-down assay of active Ras, the cell lysate was loaded with a non-hydrolysable GTP analogue (GTPγS) and incubated at 37^{o}C for 30mins with gentle rotation, in order to activate Ras. The reaction was terminated using ice-cold stop buffer. The same reaction was carried out for the negative control, by incubating the cell lysate with GDP to inactivate Ras. The sample was then immediately used in the pull-down assay as detailed below in section 2.3.2.2.

2.3.2.2 Active Ras pull-down assay

A commercially available Ras activation assay kit was used to determine Ras activity via a pull-down method involving sepharose beads conjugated with the Ras Binding Domain (RBD) region of the Raf kinase (Raf-RBD beads) (Cytoskeleton, Denver, USA). For the pull-down assay, frozen lysates (from section 2.3.2.1) were thawed in a room temperature water bath and immediately placed on ice upon thawing. Lysates at 300µg protein concentration were added to Raf-RBD beads and incubated for 1h at 4^{o}C, with rotation to allow binding. At the end of the binding reaction, the Raf-RBD beads were pelleted by centrifugation at 5000 g, 4^{o}C for 1min followed by two washes using ice-cold wash buffer. The resultant bead pellet was resuspended with 2X Laemmli buffer containing 5% β-Mercaptoethanol followed by SDS-PAGE and western blot

analysis. Active Ras was detected using mouse anti-Pan Ras monoclonal antibodies.

2.3.3 Immunoprecipitation

Mouse monoclonal antibodies were allowed to bind to goat anti-mouse immunoglobulin G (mIgG)-coupled agarose beads by incubation overnight at 4^{o}C with rotation, prior to the start of the assay. Protein G agarose beads were used as above for binding antibodies raised in rabbit. The next day whilst working on ice, monolayers of cells were rinsed twice with ice-cold PBS and the proteins were solubilised in 1% Brij-98, 1% Triton X-100 or a mixture of Brij-98/Triton X-100 (0.8%/0.2% v/v) lysis buffer supplemented with protease and phosphatase inhibitors as described in section 2.2.1 for 1-3h at 4^{o}C with rotation. The insoluble material was pelleted at 12, 000 g for 10min and the solubilised lysate was precleared by incubation with non-coated agarose beads for 1h at 4^{o}C with rotation. The precleared sample of equal protein concentration was added to pre-washed antibody-conjugated agarose beads and incubated on a rotor wheel at 4^{o}C for overnight binding. The following day, the reaction beads were washed three times with wash buffer and the immune complexes were eluted using 1X Laemmli buffer at room temperature. As loading controls, whole cell lysates of equal protein concentration were prepared in 4X Laemmli buffer alongside the immunoprecipitation samples. Samples were resolved on 10-12% SDS-PAGE under reducing and non-reducing conditions as described in section 2.2.3.

2.4 Cell Fractionation

2.4.1 Lysate preparation

Cells were scraped into PBS, centrifuged at 400 g for 3 minutes at 4^{o}C followed by two washes of the resulting cell pellet with PBS. For lysis with detergent, the washed cell pellet was resuspended in ice-cold 1% Triton X-100, prepared in 25mM MES buffer (2-(*N*-morpholino)ethanesulfonic acid) (pH 6.5) supplemented with 10µg/ml aprotinin, 10µg/ml leupeptin and 2mM PMSF. The suspension was transferred into fresh eppendorf tubes and placed onto a rotor wheel to lyse at 4^{o}C for 30 minutes. For detergent-free mechanical lysis, the washed cell pellet was resuspended in ice-cold sodium carbonate buffer (100mM, pH 11.0) supplemented with 10µg/ml aprotinin, 10µg/ml leupeptin and 2mM PMSF, followed by homogenisation using a Dounce homogeniser and subsequently by sonication. At the end of the lysis period, the sample was successfully passed through a 25G hypodermic needle twenty times, followed by centrifugation at 12, 000 g, 4^{o}C for 1 minute to remove any air bubbles and cell debris. Protein content was measured and equilibrated on the solubilised protein lysate, as detailed in section 2.2.2.

2.4.2 Fractionation in a sucrose gradient

The resulting homogenate from section 2.4.1 was mixed with equal volume of 90% (w/v) sucrose prepared in 25mM MES buffer supplemented with protease

and phosphatase inhibitors, and was overlaid with two volumes of 35% (w/v) sucrose, followed by one volume of 5% sucrose (w/v; both in MES). Samples were centrifuged at 100,000 g for 16 hours at 4^{o}C in a Beckman SW60 rotor. The next day, 10 fractions of 400µl were collected from the meniscus of the gradient into labelled eppendorf tubes. The pellet was resuspended in 400µl of Laemmli buffer supplemented with protease inhibitors. Equal amounts of each fraction were mixed with 4x Laemmli loading buffer and the protein distribution was analysed by SDS-PAGE followed by Western blotting as described in section 2.2.3.

2.5 Staining and imaging methods

2.5.1 Flow cytometry

Sub-confluent cell monolayers were detached using Cell Dissociation Solution, centrifuged at 400 g for 3 minutes and the cell pellet was thoroughly resuspended in ice-cold 1% HI-BSA to ensure a suspension of single cells. Prior to the addition of primary antibodies, the 96-well plate was incubated with 1% HI-BSA for 20 minutes at 4^{o}C in order to block non-specific binding to the wells. At the end of the 20min incubation, the blocking solution was decanted and 150µl of primary mouse monoclonal antibodies (diluted in 1% HI-BSA) or hybridoma supernatant was added to each well; to which 50µl of the cell suspension was subsequently added. Following a gentle mix, the plate was incubated on ice for 1 hour to allow binding. The cells were pelleted at 400 g for 3 minutes at 4^{o}C. The supernatant was decanted and the pellet was washed

three times with wash buffer (1% HI-BSA/PBS). At the end of the last wash, the cell pellet was resuspended with 150µl of anti-mouse FITC- or PE-conjugated secondary antibodies and incubated on ice for 1 hour in the dark. The plate was subsequently centrifuged and the cell pellet was washed three times as described above. After the last wash, the cell pellet was resuspended with 250µl of ice-cold PBS and transferred into FACS tubes containing 250µl of 2% paraformaldehyde (PFA). Stained cells were analysed using a Coulter Epics XL flow cytometer (Becton Dickinson). The data was analysed using Windows Multiple Document Interface (WinMDI) FACS analysis software version 2.9.

2.5.2 Fluorescence recovery after photobleaching (FRAP)

2.5.2.1 Sample preparation

For FRAP experiments, SKBR3/Zeo and SKBR3/CD82^{High} cells were transfected with either EGFR-GFP or ErbB2-GFP. Where indicated, Herceptin (10µg/ml) was added for 1h before FRAP. The cells were seeded on 4-well chambered Lab-Tek coverglass for 48h followed by transfection with the appropriate plasmid using GeneJammer® transfection reagent as described in section 2.1.4 and Table 2.2. Before the experiment, growth medium was replaced by phenol-red-free complete culture medium supplemented with HEPES (4-(2-hydroxyethyl)-1-piperazineethanesulfonic acid) buffer solution to a final concentration of 10mM.

2.5.2.2 FRAP assay and analysis

Live-cell confocal imaging was performed using the Zeiss LSM510 META confocal microscope with a 63x/1.4 NA planapochromat oil objective at 37^{o}C using a temperature-controlled microscope chamber. Two images of the selected cell were taken before GFP in a selected rectangular region of interest (ROI) was continuously bleached for using the 488nm laser line at 60% laser power. The intensity of the laser power was chosen to give >50% loss of fluorescence in the selected bleached region. Image acquisition was at low intensity laser power (488nm laser line at 7% laser power) so as not to affect the recovered fluorescence. Fluorescence recovery in the bleached region was recorded for ~550 sec (70 frames at 7 sec intervals). Only cells expressing moderate levels of GFP-tagged protein were selected for scanning. At least 12 individual cells were bleached and imaged under the same conditions for each FRAP assay; independent experiments were repeated three times. All fluorescence intensities were corrected for background by subtracting the background intensity from the fluorescence intensity within the bleached region. These values were then normalised to the fluorescence intensity prior to the bleaching pulse. The mobile fraction (M_f) was calculated using the following equation $M_f = (F_\infty - F_0) / (F_i - F_0)$, whereby F_i is the initial fluorescence intensity prior to bleaching; F_0 is the fluorescence intensity immediately after bleaching; and F_∞ is fluorescence intensity at the point when recovery reaches a plateau. This equation was previously described by Axelrod and colleagues (Axelrod et al. 1976).

3 RESULTS AND DISCUSSION

3.1 Ectopic expression of CD82 modulates the cellular response of breast cancer cells to Herceptin treatment

3.1.1 Generation of breast cancer cell lines with different expression levels of CD82

In order to investigate the role of CD82 in Herceptin-mediated cellular responses, we established cell lines with different expression levels of CD82 from breast cancer cell lines BT474, SKBR3 and ZR75.30. These cell lines were chosen because they overexpress the ErbB2 receptor which is targeted by Herceptin and also for the fact that they are responsive to Herceptin treatment. Additionally, two of these cell lines (BT474 and SKBR3) have low levels of endogenous CD82 expression. ZR75.30 cells express moderate levels of endogenous CD82 and they were used to study the function of CD82 using a shRNA approach. Table 3.1 summarises the characteristics of these cell lines.

Cell Line	Subtype	ER	PR	ErbB2	PTEN Mutation	PIK3CA Mutation	Ras/Raf Mutations	Tumour Type	Source
BT474	L	+	+	++	No	Yes	No	IDC	CRUK
SKBR3	L	-	-	+++	No	No	No	AC	CRUK
ZR75.30	L	+	-	+++	No	No	No	IDC	CRUK

Table 3.1: Characteristics of the breast cancer cell lines used in this study.

Comprehensive information of propagation medium and supplements for all these cell lines can be found in Appendix I. Abbreviations: AC - adenocarcinoma; ER - estrogen receptor; IDC - invasive ductal carcinoma; L - luminal subtype; PR - progesterone receptor; CRUK - Cancer Research UK. This table was adapted from Hoeflich et al. and Kao et al. (Hoeflich et al. 2009;Kao et al. 2009).

CD82-encoding plasmids were used to generate stable cell lines expressing wild-type CD82; SKBR3 parental cells were transfected with pZeoSV-CD82 plasmids whilst retroviral transduction (using pBabe-puro-CD82 and packaging plasmids) was adapted for BT474 cells as outlined in sections 2.1.4 and 2.1.6 of the Materials and Methods. In the case of BT474 cells, retroviral transduction was used due to low transfection efficiency of this cell line when transfected with the pZeoSV-CD82 plasmid. The pBabe-puro-CD82 and pZeoSV-CD82 plasmids carried a puromycin- or zeocin-resistance gene, respectively. The transduced/transfected cells were selected for antibiotic resistance by culturing in complete growth medium supplemented with either 1µg/ml puromycin (BT474) or 100µg/ml zeocin (SKBR3). Colonies of antibiotic resistant cells were pooled together and tested for the expression levels of CD82 by flow cytometry before cell sorting using the anti-CD82 mouse mAb, IA4 and anti-mouse FITC-conjugated secondary antibodies. These cells were named BT474/CD82^{High} and

SKBR3/CD82^{High}. Control cell lines either transduced or transfected with empty vectors, pBabe puro and pZeoSV were also prepared in parallel to the CD82-overexpressing cells; these control cells were named BT474/Puro and SKBR3/Zeo, respectively. The expression levels of CD82 in sorted cells were tested by western blot analysis as shown in Figure 3.1A. BT474/Puro and SKBR3/Zeo cells were found to express comparable low levels of endogenous CD82 (Figure 3.1A, lanes 1 and 3). In BT474/CD82^{High} cells, the level of CD82 was increased by almost 2-fold when compared to that of BT474/Puro cells (Figure 3.1A, compare lane 1 to 2). This increase in the levels of CD82 was further confirmed by flow cytometry as shown in Figure 3.1B. Isotype control traces are shown in black.

The level of increase in CD82 expression was higher in the SKBR3 cells compared to that of BT474 cells. Western blot analysis and flow cytometry data demonstrates that CD82 was considerably increased in the SKBR3/CD82^{High} cells compared to SKBR3/Zeo cells (Figures 3.1A, compare lanes 3 to 4; 3.1B, right panel). The flow cytometry graph shows a strong shift to the right in the CD82 peak for SKBR3/CD82^{High} cells (pale blue peak) away from that of control cells (dark blue peak). This shift is indicative of at least a 9-fold increase in the surface expression of CD82 in SKBR3/CD82^{High} cells compared to SKBR3/Zeo cells (Figure 3.1B, right panel).

Additionally, this panel of generated cell lines was assessed in order to determine whether overexpression of CD82 affected the expression levels of ErbB2. As expected, these cell lines were found to overexpress the ErbB2

receptor protein, whereby the highest expression levels were observed in the SKBR3 cell lines than in the BT474 cell lines (Figure 3.1C, comparing lanes 3 & 4 to lanes 1 & 2). Furthermore, these data show that CD82 overexpression does not affect the expression levels of ErbB2. The level of ErbB2 in the CD82-overexpressing cells, BT474/CD82^{High} and SKBR3/CD82^{High} was comparable to that in their corresponding control cell lines, BT474/Puro and SKBR3/Zeo (Figure 3.1C). This was further confirmed by flow cytometry as shown in Figure 3.1D.

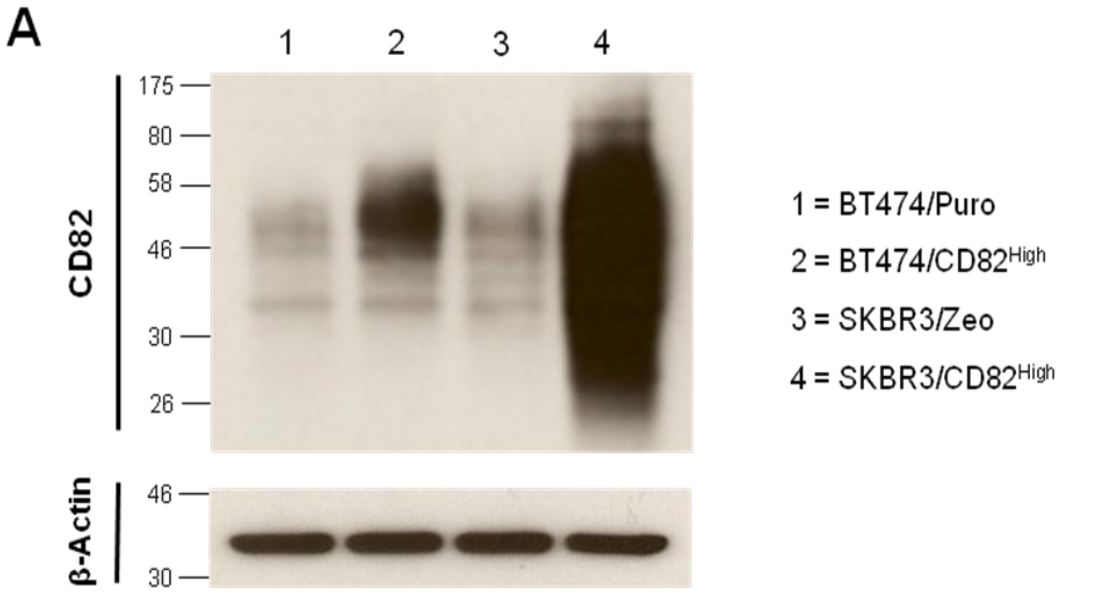
A
1
2
3
4
175
80
58
46
30
26
CD82
46
30
β-Actin
1 = BT474/Puro
2 = BT474/CD82High
3 = SKBR3/Zeo
4 = SKBR3/CD82High

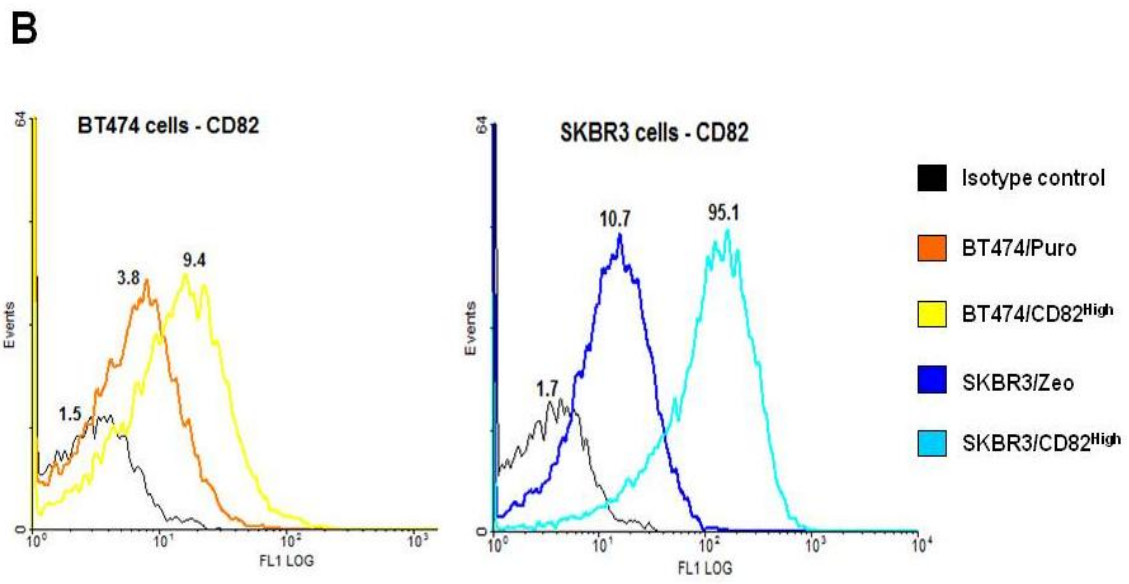
B
BT474 cells - CD82
SKBR3 cells - CD82
Events
FL1 LOG
1.5
3.8
9.4
1.7
10.7
95.1
Isotype control
BT474/Puro
BT474/CD82High
SKBR3/Zeo
SKBR3/CD82High

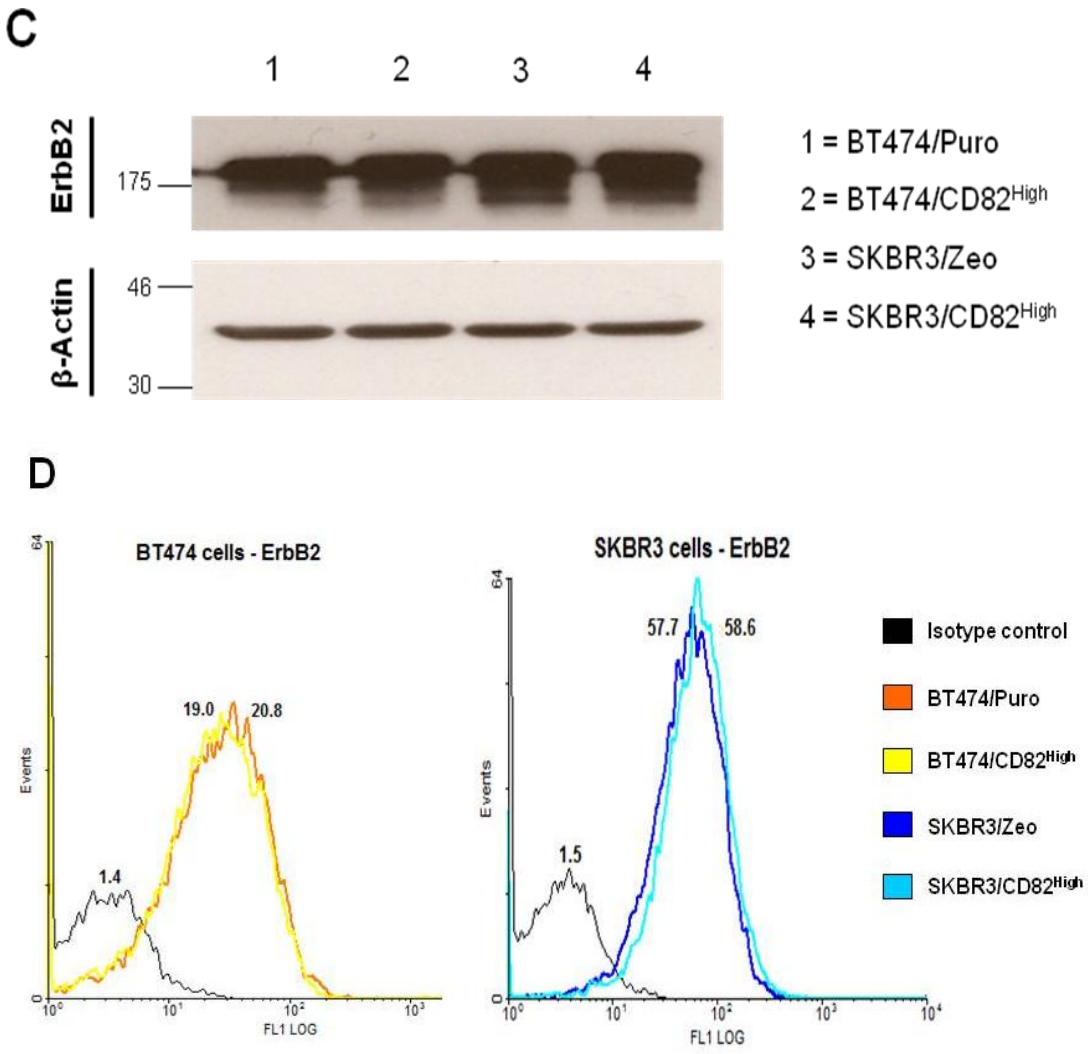

Figure 3.1: Generation of stable CD82-overexpressing breast cancer cells.

The expression levels of CD82 was analysed by western blotting and flow cytometry. (A) & (C) Cell lysates of equal protein concentration were resolved by either 12% SDS-PAGE under non-reducing conditions (CD82) or by 10% SDS-PAGE under reducing conditions (ErbB2) followed by western blotting. CD82 was detected using mouse anti-CD82 monoclonal antibody (mAb), TS82b; whilst ErbB2 was detected using mouse anti-ErbB2 mAb, Ab-17. β-Actin was used as a loading control and verification of equal protein concentration in all samples. (B) & (D) Cells were incubated on ice for 1h with either mouse anti-CD82 (M104) mAb or mouse anti-ErbB2 (Ab-2) mAb. 4C5G monoclonal antibody against phosphatidylinositol 4-kinase was used as an isotype control (black peaks). Cell surface staining of CD82 (B) and ErbB2 (D) were detected by flow cytometry following incubation for 1h on ice with anti-mouse FITC-conjugated secondary antibodies. Data analysis was carried out using WinMDI FACS analysis software (version 2.9).

In addition to CD82-overexpressing cells, a cell line was generated whereby the level of CD82 was stably depleted from ZR75.30 cells. In order to knockdown CD82, ZR75.30 parental cells were infected with lentiviral particles containing shRNA that specifically targets wild-type CD82 as detailed in the Materials and Methods. Following flow cytometry analysis to determine the transduction efficiency, the cells were sorted by FACS using an anti-CD82 mAb (IA4) whereby a negative population of cells expressing low levels of CD82 was collected. These cells were named ZR75.30/shCD82. Control cells (ZR75.30/GFP) were also prepared following infection of ZR75.30 parental cells with lentiviral particles expressing an empty vector. Analysis of the sorted cells by western blot and flow cytometry confirmed that knockdown of CD82 was successfully achieved as shown in Figure 3.2. Western blot analysis shows that the level of CD82 was decreased by at least 80% in ZR75.30/shCD82 cells compared to the control ZR75.30/GFP cells (Figure 3.2, left panel). This was confirmed further by flow cytometry; the graph of which, shows that the peak for CD82 shifted to the left in ZR75.30/shCD82 cells (green peak) away from that of ZR75/GFP cells (red peak) thus indicative of low surface levels of CD82 in the depleted cells (Figure 3.2, right panel). ZR75.30/shCD82 and ZR75.30/GFP cells were used later in the project to confirm some of the CD82-mediated effects and will therefore be discussed in great detail in the later chapters.

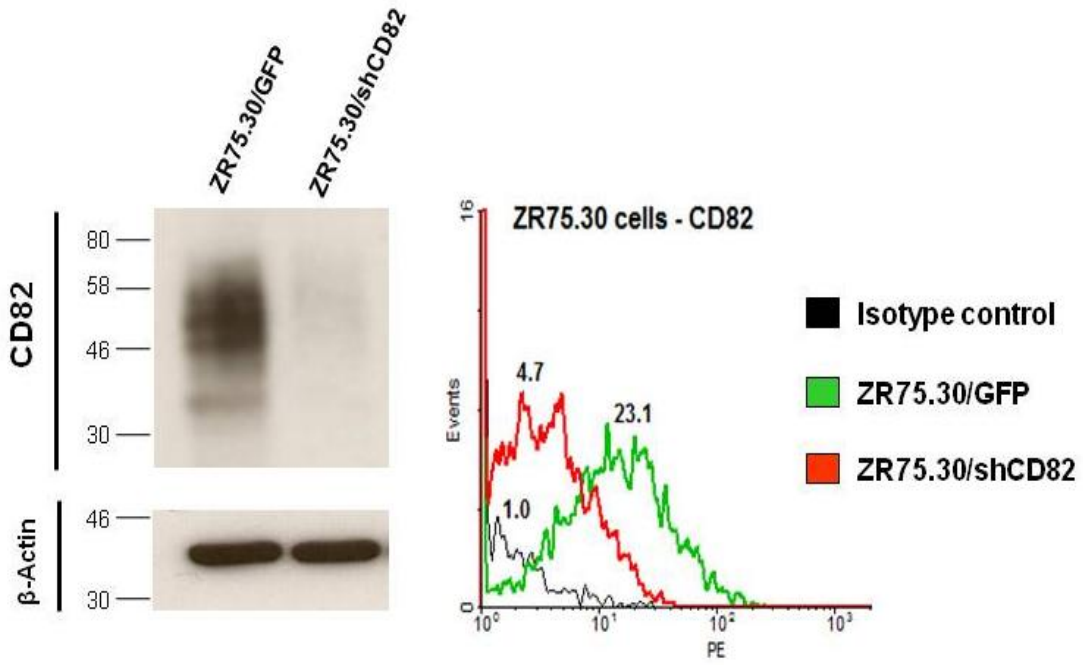

Figure 3.2: Generation of stable CD82-depleted breast cancer cells.

Knockdown of CD82 was analysed by western blotting and flow cytometry. For western blot analysis, lysates were resolved by 12% SDS-PAGE under non-reducing conditions followed by detection using anti-CD82 mAb, TS82b. Cell surface expression of CD82 was determined by flow cytometry using M104, mouse anti-CD82 mAb. Since the ZR75.30 cells were transfected with green fluorescence protein (GFP)-containing plasmids, anti-mouse phycoerythrin (PE)-conjugated secondary antibodies were used for surface staining detection by flow cytometry. Control cells (ZR75.30/GFP) were positive for both GFP and PE; whilst the CD82-depleted cells (ZR75.30/shCD82) were positive for GFP, but negative for PE. Plotted are data following gating for PE. 4C5G monoclonal antibody against phosphatidylinositol 4-kinase was used as an isotype control (black peak).

3.1.2 The cellular response of CD82-overexpressing breast cancer cells to Herceptin treatment when cultured as 2D monolayers

As a starting point, the generated CD82-overexpressing cells (BT474/CD82^{High} and SKBR3/CD82^{High}) were assessed for their response to Herceptin treatment in comparison to control cells (BT474/Puro and SKBR3/Zeo). The cells were treated with increasing concentrations of Herceptin (10, 20 and 50µg/ml) for 72h. Non-treated (Herceptin-free) cells were used as an additional control. At the end of the incubation period, the cells were harvested and counted using Trypan blue staining as outlined in the Materials and Methods section 2.1.8. The effect of Herceptin on cell viability was determined as percentage viable cells at each treatment condition relative to that of non-treated controls.

The percentage of viable cells decreased in response to Herceptin in a concentration-dependent manner (Figure 3.3). Comparison of the response of CD82-overexpressing cells to that of control cells at each concentration of Herceptin revealed subtle differences between the cell line pairs. Specifically, Herceptin at 10µg/ml caused a 23% and 30% decrease in cell viability in BT474/CD82^{High} and SKBR3/CD82^{High}, respectively when compared to control cells, BT474/Puro (6%) and SKBR3/Zeo cells (17%); (Figure 3.3). Further analysis of this data from three independent experiments revealed no statistically significant difference between the cell line pairs in their response to Herceptin treatment at all concentrations ($P>0.05$) as determined by the one-way ANOVA multiple comparison analysis with the Tukey-Kramer post-test,

using GraphPad Prism software, whereby statistical significance was set at $P<0.05$ (Figure 3.3). This suggests that ectopic expression of CD82 did not affect the response of SKBR3 and BT474 cells to Herceptin when cultured as 2D monolayers on plastic. The response of control cells to Herceptin treatment is consistent with other reports, whereby a concentration-dependent decrease in cell viability was also observed in SKBR3 and BT474 cells following Herceptin treatment (Junttila et al. 2009;Pickl and Ries 2009;Tseng et al. 2006). As they were only minimal differences in cellular responses to increasing concentrations of Herceptin (i.e. viability decreased from ~75% at 10µg/ml to ~65% at 50µg/ml), all subsequent experiments were carried out using 10µg/ml of the reagent.

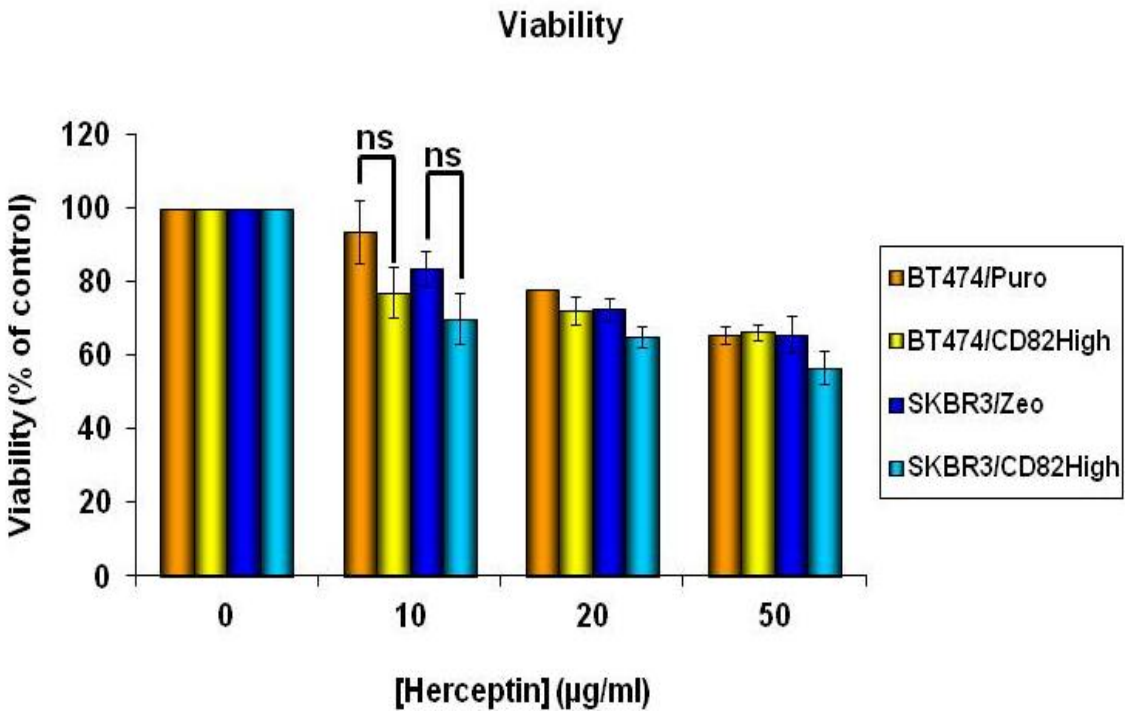

Figure 3.3: The effect of Herceptin on cell viability.

The indicated cell lines were seeded onto 6-well plates for a total of 96h. Herceptin was added to the culture medium at the indicated final concentrations 24h after seeding followed by incubation for a further 72h at 37^{o}C, 5% CO_2. At the end of this incubation period, the cells were detached and counted using Trypan blue. Viable and non-viable cells were counted separately on the basis of trypan blue staining. Cell viability was determined as a ratio of non-stained viable cells from the total number of cells counted per 1ml aliquot, and compared to the non-treated (Herceptin-free) controls as a percentage. Error bars correspond to standard deviation. Statistical comparison between the cell line pairs at each concentration was performed with the one-way ANOVA multiple comparison analysis with the Tukey-Kramer post-test, using GraphPad Prism software, whereby statistical significance was set at $P<0.05$. Data shown is a summary of at least three independent experiments. Abbreviation: ns – not significant ($P>0.05$).

3.1.3 Ectopic expression of CD82 plays a role in the cellular response of ErbB2-positive breast cancer cells to Herceptin treatment when cultured in 3D extracellular matrix substrata

3.1.3.1 The effect of CD82 on cell growth in 3D collagen and its contribution to the cellular response to Herceptin treatment

Tumour growth is promoted by interplay between tumour cells and the surrounding microenvironment. Components of the tumour microenvironment include stromal cells and a protein-rich extracellular matrix (ECM). Cancer cells are routinely grown *in vitro* in 3D extracellular matrix substrata such as collagen and Matrigel in order to recapitulate the *in vivo* architecture and physiological functions of tumour cells (Weigelt and Bissell 2008). In this regard, the effect of CD82 expression on the cellular response to Herceptin treatment was investigated in cells cultured in 3D ECM substrata. SKBR3 and BT474 cells expressing different levels of CD82 were seeded as single cell suspension embedded in collagen and were cultured for 14 days in complete medium to allow formation of colonies. Herceptin (10µg/ml) was added to the culture medium 24h post seeding. Growth medium was replenished every 3 days and was appropriately supplemented with Herceptin. Non-treated (Herceptin-free) cells were used as controls. Each condition was prepared in duplicate. 40 images were captured at high magnification (using a x20 objective for SKBR3; and a x32 objective for BT474 cells) using a Zeiss Axiovert 25 microscope, from which the size and surface area of at least 90 colonies were analysed using the

NIS-Elements BR 3.0 laboratory imaging software; further data analysis was carried out using GraphPad Prism software.

Figure 3.4A shows that SKBR3 cells grown in collagen formed variably sized spherical colonies with smooth edges. SKBR3/CD82^{High} cells formed colonies of significantly smaller size ($P<0.01$) when compared to SKBR3/Zeo cells (Figure 3.4A, top panel). The colony size was reduced by 29% in the CD82-overexpressing cells indicating a profound effect of CD82 on cell proliferation (Figure 3.4B, compare the solid-filled dark blue bar with the chequered light blue bar). BT474 cells grown in collagen formed smaller colonies than SKBR3 cells with slightly irregular edges (Compare Figure 3.4C with 3.4A). Importantly, similar to SKBR3 cells, elevated expression of CD82 in BT474 cells resulted in a 19% reduction in colony size (Figure 3.4D, compare the chequered bar to the solid-filled bar).

As expected, Herceptin treatment resulted in a decrease in cell proliferation reflected by a highly significant ($P<0.001$) reduction in colony size in control cells. Specifically, in SKBR3/Zeo and BT474/Puro cells, incubation with Herceptin caused a 58% and 41% reduction in colony size, respectively (Figures 3.4B and 3.4D, compare the solid-filled bar to the bar with vertical lines, respectively). Surprisingly, the cytostatic effect of Herceptin was less pronounced in the CD82-overexpressing cells: treatment with Herceptin resulted in a 26% and 16% reduction in colony size in SKBR3/CD82^{High} and BT474/CD82^{High} cells, respectively when compared to non-treated cells (Figures 3.4B and 3.4D, compare bars with horizontal lines to the chequered bars). The

fact that the Herceptin-induced cytostatic effect was less pronounced in the CD82-overexpressing cells suggests a probable CD82-mediated resistance mechanism to Herceptin, which at this stage seems to be dependent on the ECM substrata. This notion was investigated further by carrying out similar experiments using 3D Matrigel ECM substrata as described in the subsequent section.

A

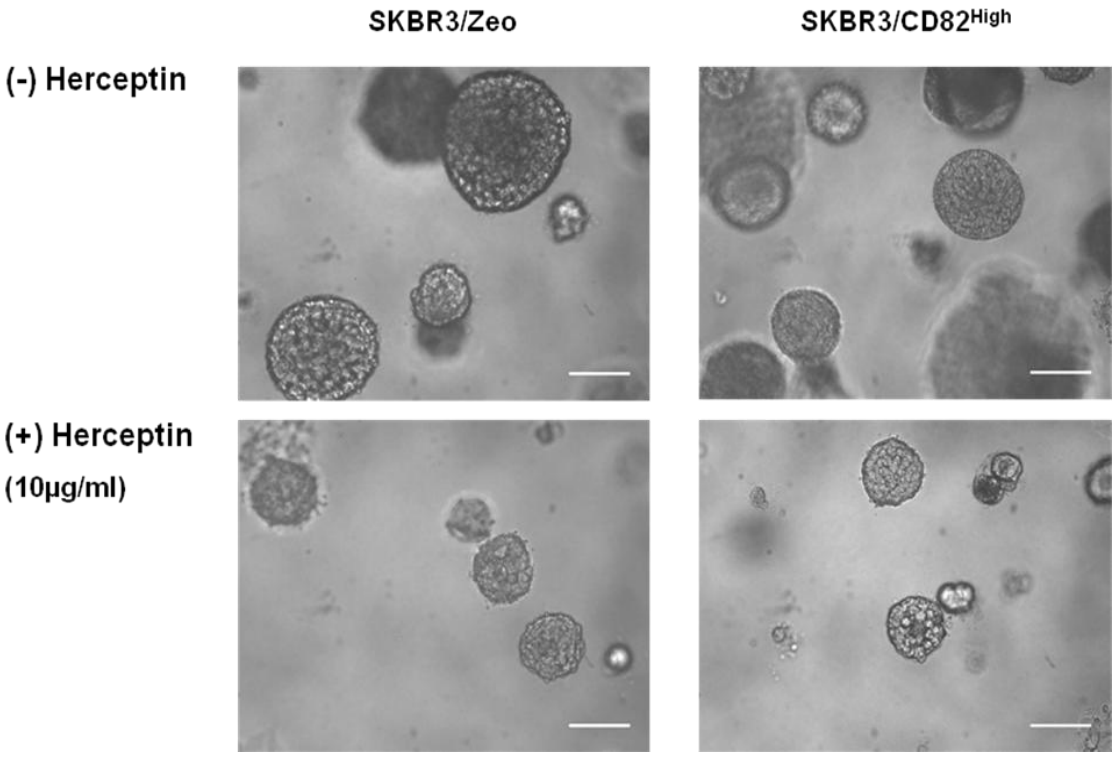
SKBR3/Zeo
SKBR3/CD82High
(-) Herceptin
(+) Herceptin
(10µg/ml)

B

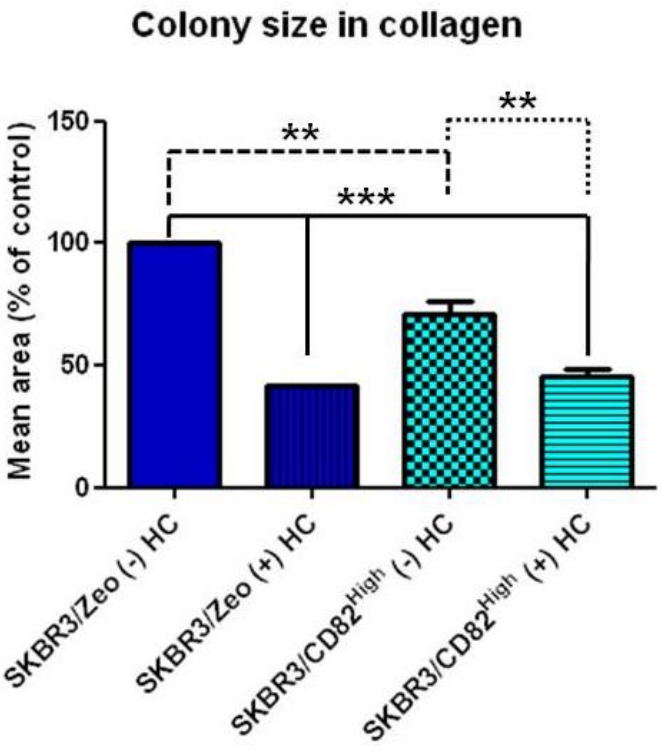
Colony size in collagen
Mean area (% of control)
150
100
50
0
**
**
***
SKBR3/Zeo (-) HC
SKBR3/Zeo (+) HC
SKBR3/CD82High (-) HC
SKBR3/CD82High (+) HC

C

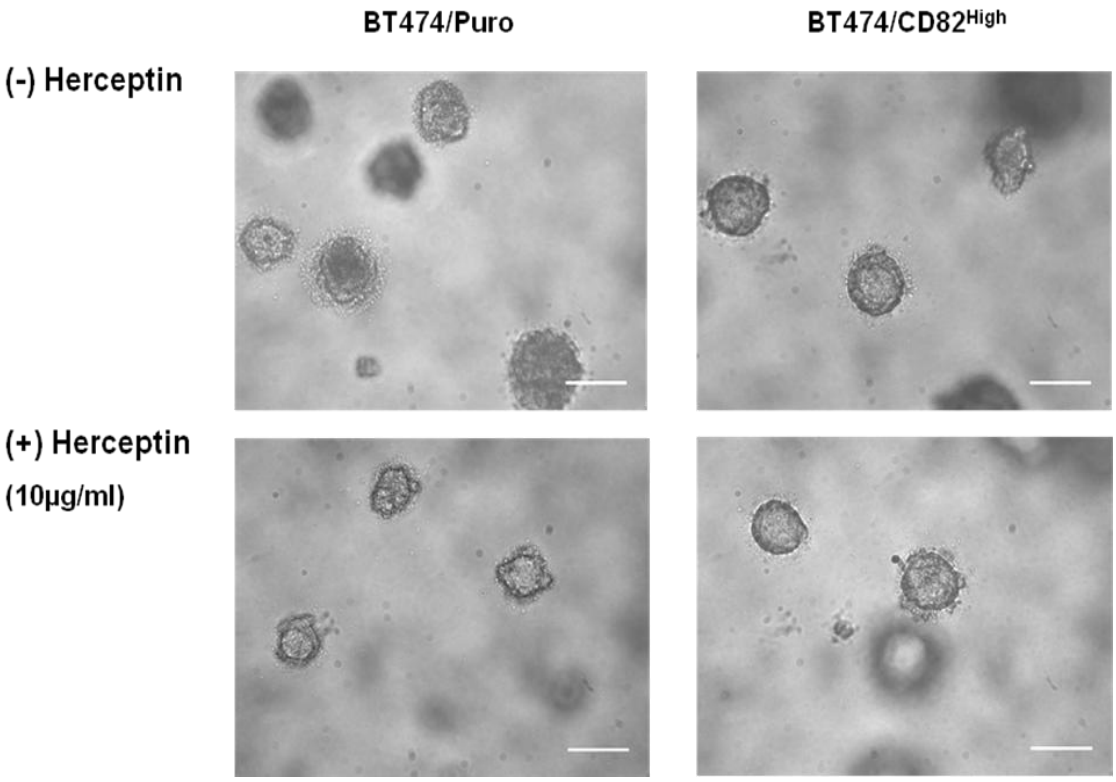
BT474/Puro
BT474/CD82High
(-) Herceptin
(+) Herceptin
(10µg/ml)

D

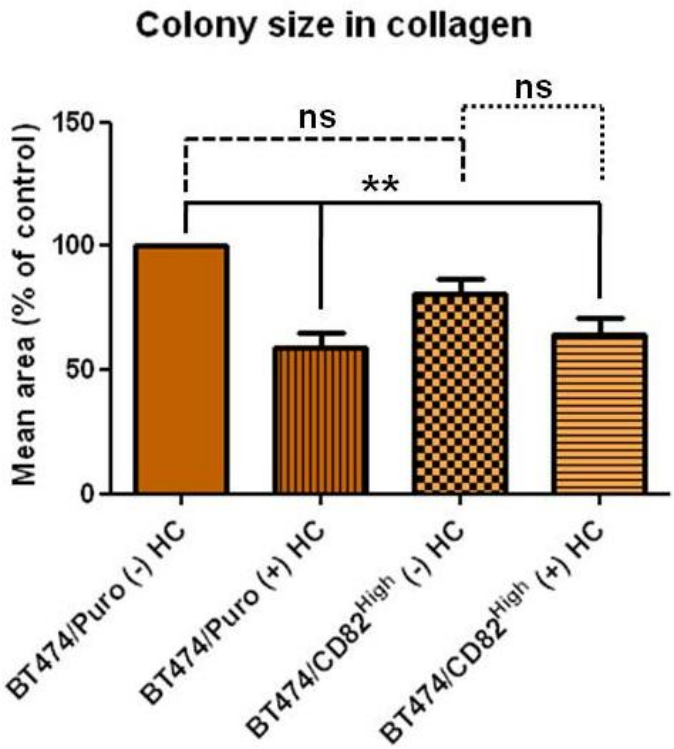
Colony size in collagen
Mean area (% of control)
150
100
50
0
ns
ns
**
BT474/Puro (-) HC
BT474/Puro (+) HC
BT474/CD82High (-) HC
BT474/CD82High (+) HC

Figure 3.4: Ectopic expression of CD82 inhibits cell growth and contributes to the cellular response to Herceptin in 3D collagen.

SKBR3 and BT474 cells were embedded in rat tail collagen type I as described in the Materials and Methods section 2.1.9; and were cultured for 14 days in the presence or absence of Herceptin. Images of the formed colonies were captured using a Zeiss Axiovert 25 microscope with a x 20 objective (A) for SKBR3 cells; and a x 32 objective (C) for the BT474 cells (bar = 200µm). Morphological analysis was performed with the NIH-Elements BR 3.0 laboratory imaging software. 40 images were captured at each condition and the surface area of at least 90 colonies from the captured images was measured. The mean area relative to that of non-treated (Herceptin-free) control cells was plotted as percentage from at least three independent experiments (B & D). Error bars correspond to standard deviation. Asterisks represent the statistical significance as determined by the one-way ANOVA multiple comparison analysis with the Tukey-Kramer post-test, using GraphPad Prism software, whereby statistical significance was set at $P<0.05$; (** $P<0.01$) and (*** $P<0.001$) were considered highly significant. Abbreviations: HC – Herceptin; ns – not significant.

3.1.3.2 The effect of CD82 expression on cell growth and the cellular response to Herceptin of cells cultured in 3D Matrigel

In addition to the 3D collagen studies, the contribution of CD82 on cell growth and the cellular response to Herceptin were investigated in cells cultured in 3D Matrigel ECM substrata. Matrigel is derived from the Engelbreth-Holm-Swarm murine tumour and it is rich in laminin-111, type IV collagen, enactin and proteoglycan. Thus composition of Matrigel resembles that of the basement membrane and therefore can be used *in vitro* to simulate the *in vivo* behaviour of tumour cells (Hughes et al. 2010;Kleinman and Martin 2005;Weigelt and Bissell 2008). In our experiments, both pairs of SKBR3 and BT474 cells were seeded in 3D Matrigel as described in the Materials and Methods (section 2.1.9) and were cultured for 14 days in the presence and absence of Herceptin. Cell proliferation was determined by measuring the perimeter of at least 90 formed colonies, from which surface area was analysed.

Results from these experiments revealed that SKBR3 and BT474 cells grown in 3D Matrigel formed colonies of different morphology: grape-like for the former and compact round-shaped for the latter (Figures 3.5A and 3.5C). Notably, colonies formed by BT474 cells grown in Matrigel were bigger in size (by appearance) than colonies formed in collagen (Compare Figure 3.4C and Figure 3.5C). The pattern of growth in Matrigel due to the ectopic expression of CD82 and the response to Herceptin of both control and CD82-overexpressing SKBR3 and BT474 cells was comparable to that observed in collagen. Firstly,

the expression of CD82 caused a significant reduction in colony size; 30% reduction in SKBR3 and 20% in BT474 cells when compared to controls (Figure 3.5B and Figure 3.5D; compare the chequered bars to the solid-filled bars). Secondly, treatment with Herceptin caused a highly significant ($P<0.001$) reduction in colony size in the control cell lines: 54% and 52% in SKBR3/Zeo and BT474/Puro, respectively compared to non-treated cells (Figures 3.5B and 3.5D; compare the bars of vertical lines to the solid-filled bars). Similar to data for collagen, CD82-overexpressing cells displayed a poor response to Herceptin treatment when compared to non-treated cells: 14% and 13% in SKBR3/CD82^{High} and BT474/CD82^{High}, respectively (Figures 3.5B and 3.5D; compare the bars of horizontal lines to the chequered bars). Collectively, these data from experiments in 3D collagen and Matrigel show a poor response of CD82-overexpressing cells to Herceptin when compared to control cells, thus suggesting that CD82 expression status might play a role in predicting response to Herceptin.

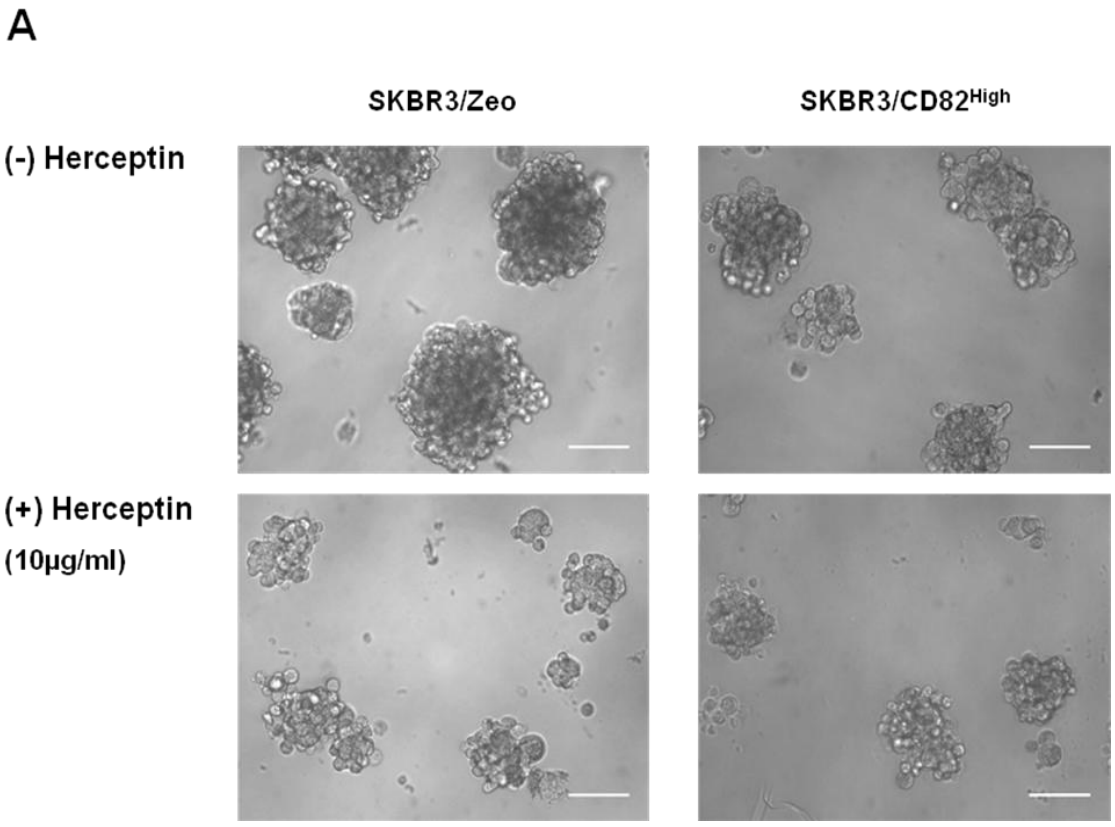
A
SKBR3/Zeo
SKBR3/CD82High
(-) Herceptin
(+) Herceptin
(10µg/ml)

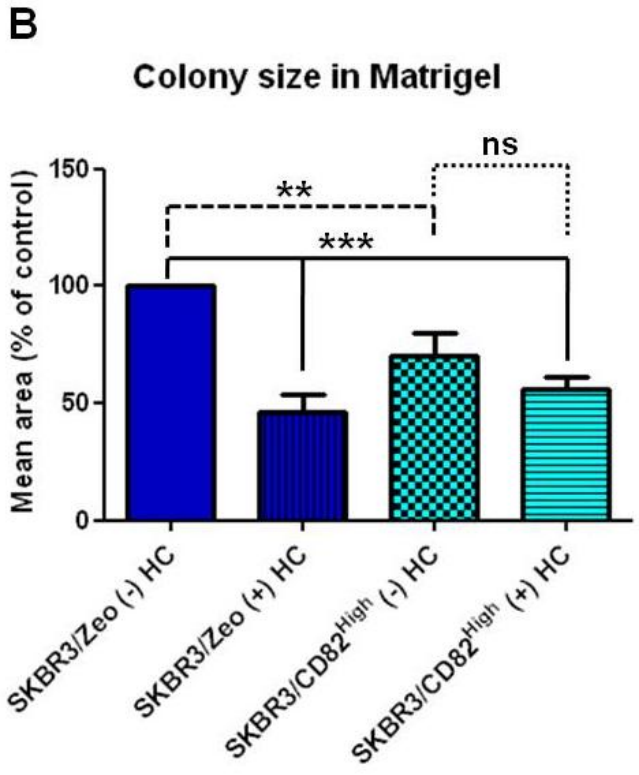
B
Colony size in Matrigel
Mean area (% of control)
150
100
50
0
**
***
ns
SKBR3/Zeo (-) HC
SKBR3/Zeo (+) HC
SKBR3/CD82High (-) HC
SKBR3/CD82High (+) HC

C

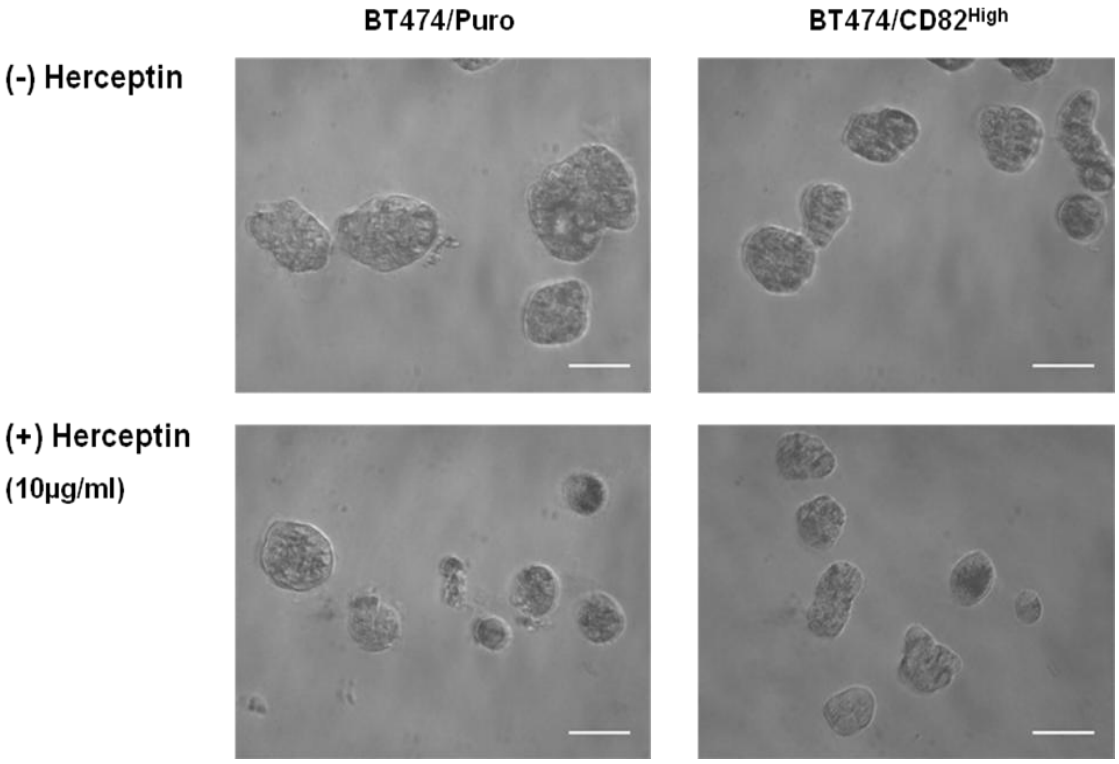
BT474/Puro
BT474/CD82High
(-) Herceptin
(+) Herceptin
(10µg/ml)

D

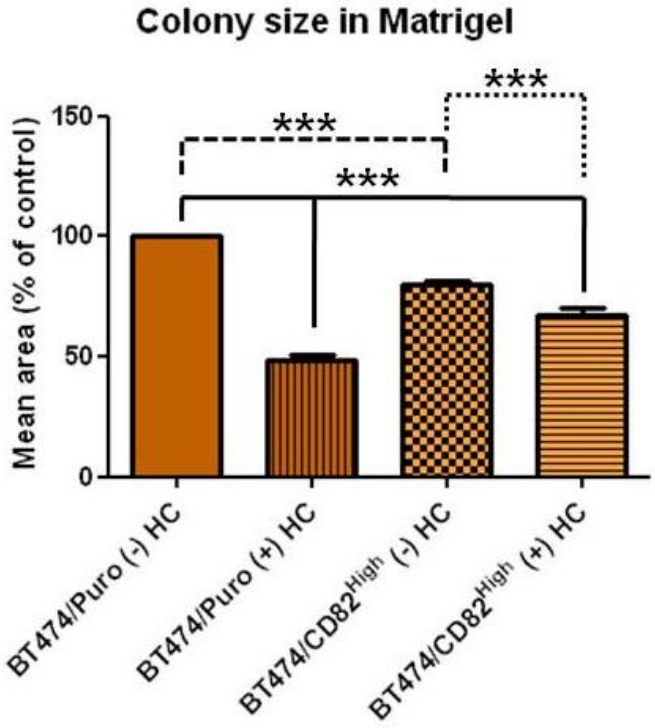
Colony size in Matrigel
Mean area (% of control)
150
100
50
0
***
***
***
BT474/Puro (-) HC
BT474/Puro (+) HC
BT474/CD82High (-) HC
BT474/CD82High (+) HC

Figure 3.5: The effect of CD82 expression on cell growth in 3D Matrigel and its contribution to the cellular response to Herceptin.

Vector control and CD82-overexpressing SKBR3 and BT474 cells were embedded in Matrigel as described in the Materials and Methods under section 2.1.9. The cells were cultured for 14 days in the presence and absence of Herceptin. Images of the formed colonies were captured using a Zeiss Axiovert 25 microscope with a x 20 objective (A) for SKBR3 cells; and a x 32 objective (C) for the BT474 cells (bar = 200µm). Morphological analysis was performed with the NIH-Elements BR 3.0 laboratory imaging software. 40 images were captured at each condition and the surface area of at least 90 colonies from the captured images was measured. The mean area relative to that of non-treated (Herceptin-free) control cells was plotted as percentage from at least three independent experiments (B & D). Error bars correspond to standard deviation. Asterisks represent the statistical significance as determined by one-way ANOVA multiple comparison analysis with the Tukey-Kramer post-test, using GraphPad Prism software, whereby statistical significance was set at $P<0.05$; (** $P<0.01$) and (*** $P<0.001$) were considered highly significant. Abbreviations: HC – Herceptin; ns – not significant.

3.1.4 CD82 suppresses the migration of SKBR3 cells towards various attractants

CD82 is known to suppress cell migration and invasion of cancer cells (Bari et al. 2009;Jee et al. 2007;Zhou et al. 2004). Herein, cell migration assays were performed in order to investigate CD82- and Herceptin-mediated effects on the migration of SKBR3 breast cancer cells. These experiments were performed using a modified Boyden Chamber protocol as described in section 2.1.10 of the Materials and Methods. The cells were left to migrate towards heregulin (HrG) for 6h. Heregulin is a ligand for ErbB3 and ErbB4 and is known to regulate migration. Figure 3.6A demonstrates that the number of cells seeded at the start of the migration assay was comparable for both cell lines used in the assay. Consistent with other studies, ectopic expression of CD82 in SKBR3/CD82^{High} cells significantly inhibited cell migration ($P<0.001$) when compared to control SKBR3/Zeo cells (Figure 3.6B, top panel; and Figure 3.6C, compare the solid-filled dark blue bar with the chequered light blue bar). These data show that CD82 inhibited cell migration towards heregulin by at least 50% in the SKBR3/CD82^{High} cells compared to control cells (Figure 3.6C, compare the solid-filled dark blue bar with the chequered light blue bar).

Next, we investigated whether Herceptin treatment affected cell migration; and if it does, whether CD82 modulated the Herceptin-mediated effect on cell migration. In the assay described above, the cells were left to migrate towards heregulin (10ng/ml) in the presence or absence of Herceptin (10µg/ml) (Figure

3.6B, bottom panel). By considering the SKBR3/Zeo cells first, it is clear that treatment with Herceptin resulted in a highly significant inhibition of cell migration ($P<0.001$) towards heregulin when compared to non-treated cells. Migration was reduced by at least 50% in the Herceptin-treated SKBR3/Zeo cells compared to non-treated cells (Figure 3.6C; compare the solid-filled dark blue bar with the dark blue bar of vertical lines). In contrast, the anti-migratory effect of Herceptin was less pronounced in the CD82-overexpressing cells when compared to non-treated cells. The number of migrated cells towards heregulin was comparable in both non-treated and Herceptin-treated SKBR3/CD82^{High} cells (Figure 3.6C; compare the light blue bar of horizontal lines with the light blue chequered bar). The fact that SKBR3/Zeo cells were responsive to the anti-migratory effect of Herceptin suggests that heregulin-induced migration of SKBR3/Zeo cells is in part, ErbB2-dependent. However, overexpression of CD82 interrupts this mechanism of migration, abrogating the anti-migratory effect of Herceptin and thus rendering the SKBR3/CD82^{High} cells less responsive to Herceptin.

To test the specificity of the CD82-mediated effect on the migration of SKBR3 cells, haptotactic and chemohaptotactic migration assays were carried out using either complete media containing 10% FBS; serum-free media containing no attractant; or serum-free media supplemented with either HB-EGF (10ng/ml) or TGF-β1 (10ng/ml) as chemoattractants. Migration towards heregulin (HrG) was used as a control. These growth factors were chosen because they are reported to regulate migration in many cell types (Kim et al. 2011a;Kim et al. 2011b;Lin et al. 2011) and also for the diversity of the growth factor receptors they bind to:

HB-EGF is a ligand for both EGFR and ErbB4; TGF-β1 is a multifunctional peptide of the transforming growth factor beta superfamily and signals via TGF-β1 type I and type II cell surface receptor (Massague 2008).

As shown in Figure 3.6D, the chemohaptotactic migration of SKBR3/CD82^{High} cells to both HB-EGF and TGF-β1 was remarkably reduced compared with that of SKBR3/Zeo cells. The migratory potential of SKBR3/Zeo cells towards these growth factors was approximately two-fold higher when compared to that of CD82-overexpressing cells (SKBR3/CD82^{High}). Notably, migration towards HB-EGF in SKBR3/Zeo cells was considerably higher than towards TGF-β1 and HrG. However, SKBR3/CD82^{High} cells migrated similarly under all three growth conditions (Figure 3.6D). Surprisingly however, migration of SKBR3/CD82^{High} cells in the presence of complete medium containing 10% FBS was increased by at least 16% compared with that of SKBR3/Zeo cells (Figure 3.6D). These results demonstrate that the initial observation of the CD82-mediated inhibition of cell migration was not limited to heregulin-induced migration, but that it can also be observed with other growth factors including the highly potent chemoattractant, HB-EGF. Furthermore, these data highlight the diversity of the anti-migratory effect of CD82 suggesting that CD82 exerts this effect by not only regulating ErbB2, but also other growth factor receptors, although the observation with fetal-calf serum suggests presence of alternative pro-migratory factors. At this stage however, we were not able to identify this molecule(s) or its corresponding receptor(s).

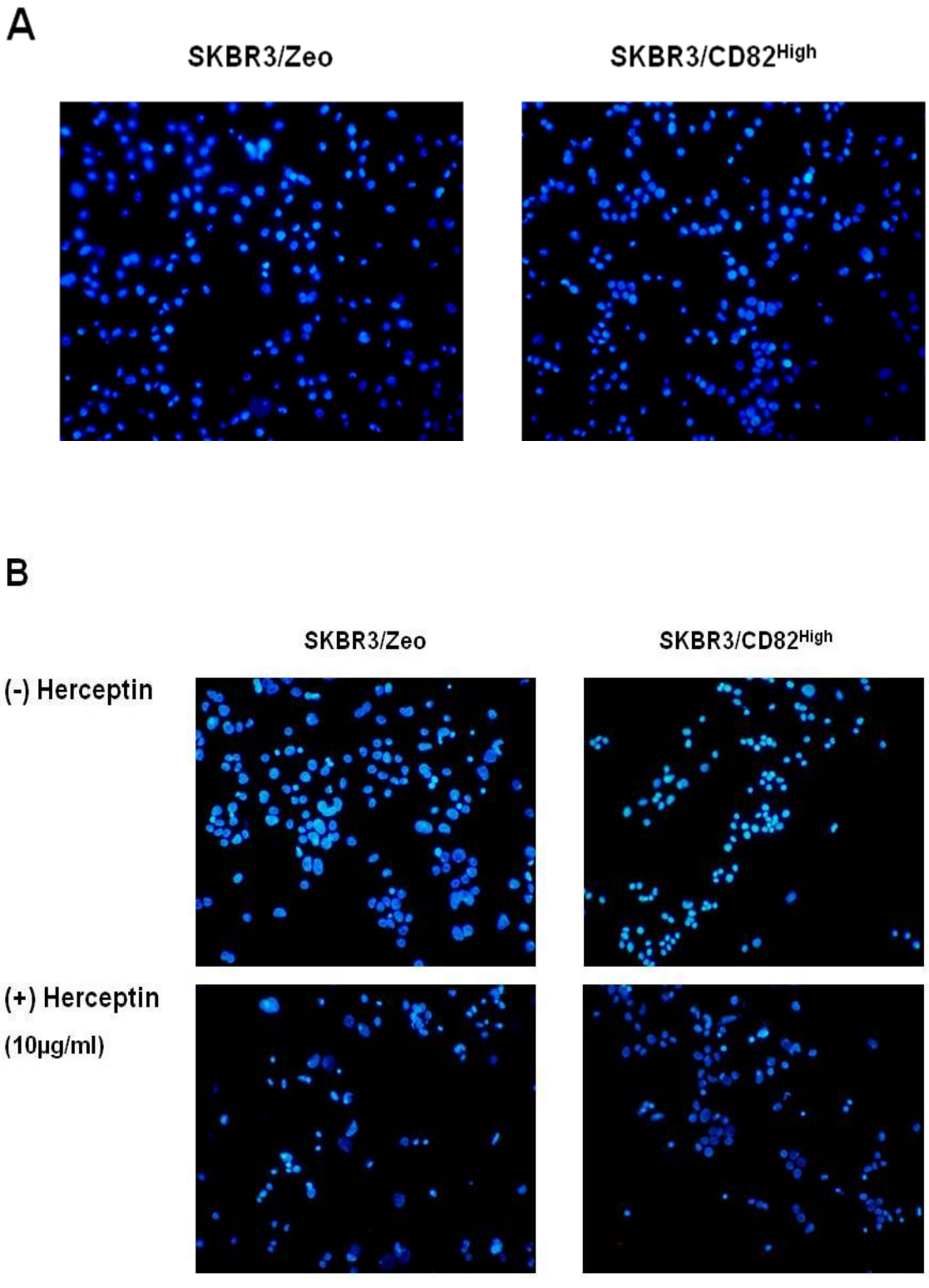
A
SKBR3/Zeo
SKBR3/CD82High
B
SKBR3/Zeo
SKBR3/CD82High
(-) Herceptin
(+) Herceptin
(10µg/ml)

C

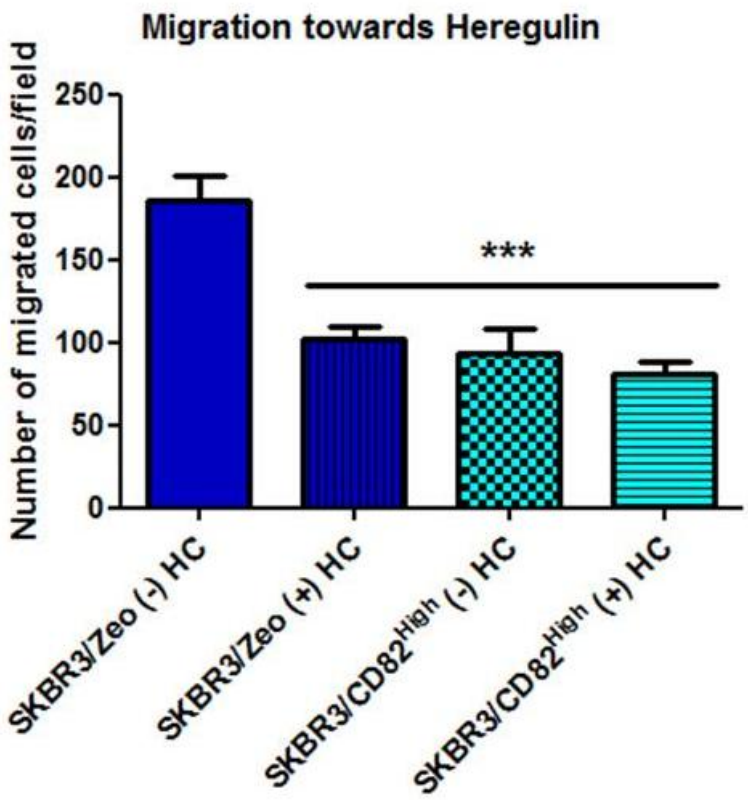
Migration towards Heregulin
Number of migrated cells/field
250
200
150
100
50
0
***
SKBR3/Zeo (-) HC
SKBR3/Zeo (+) HC
SKBR3/CD82High (-) HC
SKBR3/CD82High (+) HC

D

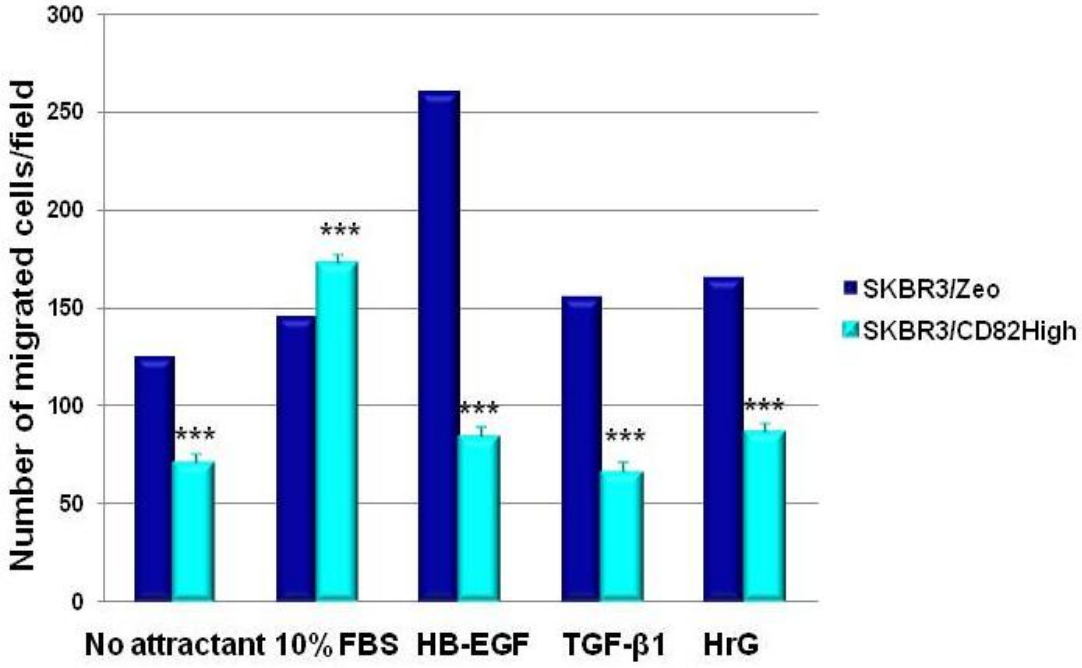
Number of migrated cells/field
300
250
200
150
100
50
0
***
No attractant
10% FBS
HB-EGF
TGF-β1
HrG
SKBR3/Zeo
SKBR3/CD82High

Figure 3.6: Ectopic expression of CD82 and Herceptin treatment suppress the migratory potential of SKBR3 cells.

SKBR3/Zeo and SKBR3/CD82^{High} cells were prepared for migration as described under section 2.1.10 of the Materials and Methods. (A) In parallel to the migration experiments, some cells were prepared on membrane filters as representative of the total number of cells plated for the migration assay. These cells were left to adhere for 1h post seeding, then stained with Hoechst 33342 and mounted onto glass slides. (B and C) For cell migration experiments, the cells were left to migrate for 6h at 37^{o}C, 5% CO_2 towards heregulin (10ng/ml), in the presence or absence of Herceptin (10µg/ml). Images were captured with a x20 objective using a Nikon Eclipse E600 fluorescence microscope. Migration was quantified by counting the number of nuclei from five randomly selected fields per membrane. Each test condition was done in duplicate per experiment and three independent experiments were carried out. Images were scored using ImageJ nuclear/cell counter program. (D) For haptotactic migration assays, cells migrated toward serum-free medium containing no chemoattractant. For chemohaptotactic migration assays, cells migrated either towards complete DMEM medium containing 10% fetal-calf serum (FBS) or serum-free DMEM supplemented with either heregulin (HrG), heparin-binding EGF-like growth factor (HB-EGF) or transforming growth factor-beta 1 (TGF-β1). All growth factors were at a final concentration of 10ng/ml. Number of migrated cells = the number of nuclei counted per microscopic field, captured with a x20 objective. Statistical significance was determined by the one-way ANOVA multiple comparison test with the Tukey-Kramer post-test, using GraphPad Prism software, whereby significance was set at 0.05; (*** P<0.001).

3.1.4.1 CD82 expression inhibits the invasion of SKBR3 cells towards heregulin

In addition to the migration assays, the effect of CD82 expression on the invasiveness of SKBR3 cells was also investigated. In a pilot experiment using control cells (SKBR3/Zeo), the migratory potential of SKBR3 cells over an increasing time interval was examined in order to determine the optimal time point for the basis of the invasion assays. These assays were performed as detailed in section 2.1.11 of the Material and Methods. After incubation for 24, 48 and 72h, cells invaded into the Matrigel were fixed, stained and counted. Figure 3.7A shows that cells invaded into the Matrigel were readily detected after 24h incubation, and that the number of invaded cells increased gradually with time. Since the highest number of invaded cells was detected at 72h in the pilot experiment, this then was the time point used in subsequent invasion assays involving both SKBR3/Zeo and SKBR3/CD82^{High} cells. As expected, ectopic expression of CD82 in SKBR3 cells reduced the invasiveness of these cells by almost 50% (Figures 3.7B and C). Although the invasion assays described here were performed in the absence of Herceptin, it would have been interesting to determine whether Herceptin had an effect on cell invasion, in particular in the CD82-overexpressing cells. Taken together, these data demonstrate an anti-migratory effect of Herceptin and a potent inhibitory effect of CD82 on both cell migration and invasion.

A

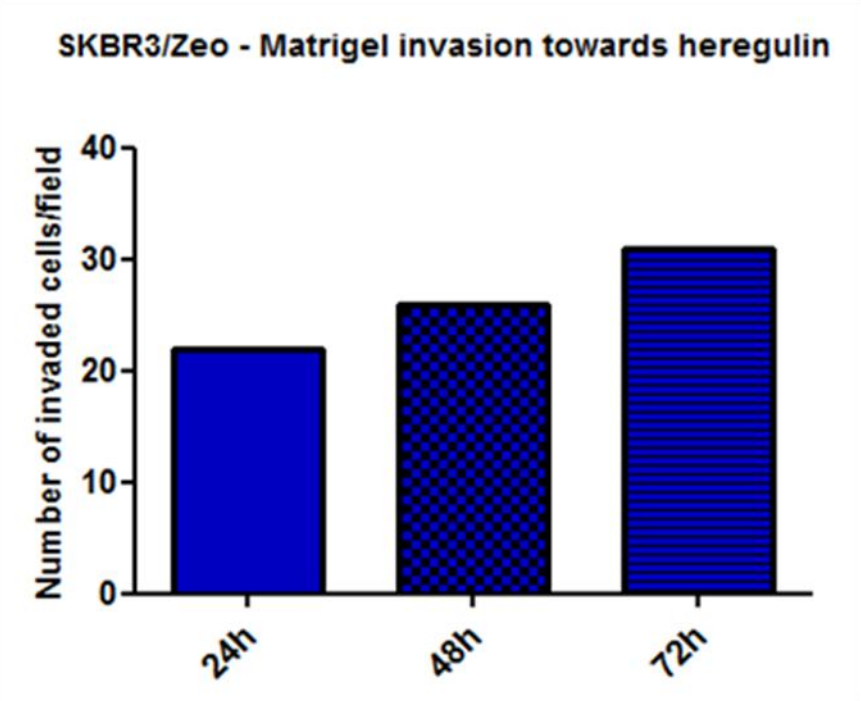
SKBR3/Zeo - Matrigel invasion towards heregulin
Number of invaded cells/field
40
30
20
10
0
24h
48h
72h

B

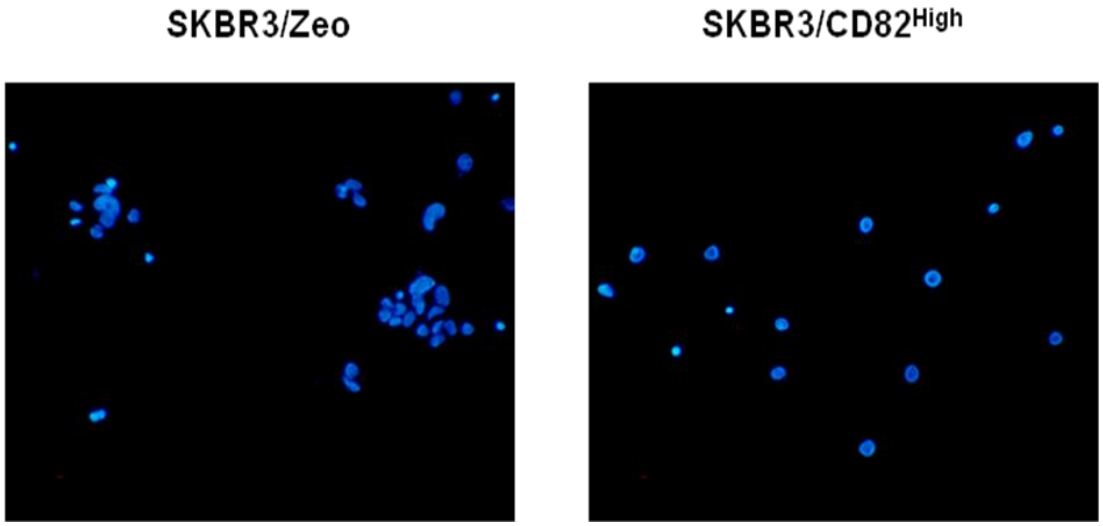
SKBR3/Zeo
SKBR3/CD82High

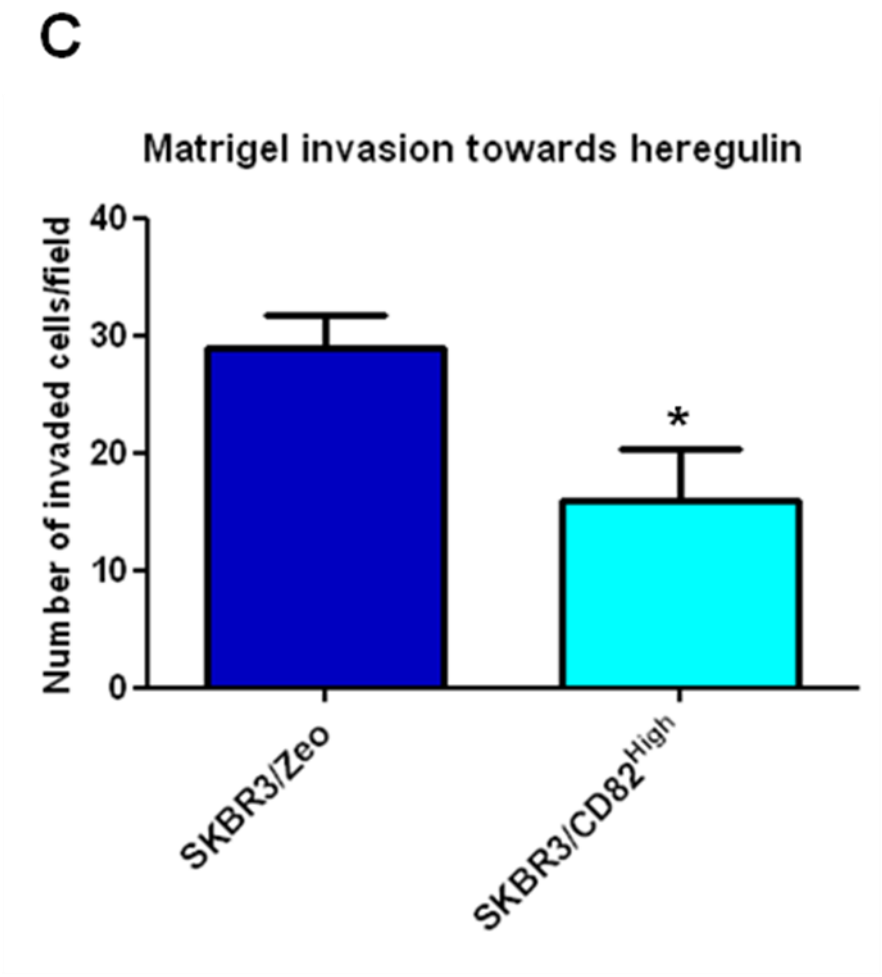

Figure 3.7: CD82 suppresses the invasive potential of SKBR3 cells towards heregulin.

Invasion assays were performed using modified Boyden chambers with polycarbonate membrane filter inserts coated with Matrigel as detailed in section 2.1.11 of the Materials and Methods. (A) Cells were left to invade into the Matrigel using heregulin (10ng/ml) as chemoattractant at 37^{o}C, 5% CO_2 for 24, 48, and 72h. Invaded cells were stained with Hoechst 33342, mounted onto glass slides and counted. (B & C) Matrigel invasion of SKBR3 cells after 72h incubation. Images were captured with a x20 objective using a Nikon Eclipse E600 fluorescence microscope. Invasion was quantified by counting the number of nuclei from five randomly selected fields per membrane. Each test condition was done in duplicate per experiment and at least two independent experiments were carried out. Images were scored using ImageJ nuclear/cell counter program. Number of invaded cells = the number of nuclei counted per microscopic field, captured with a x20 objective. Data shown as mean ± standard deviation. Asterisk represents the statistical significance as determined by a two-tailed, unpaired Student's t test using GraphPad Prism software. Significance was set at 0.05, whereby (*P<0.05).

3.1.5 Discussion

Although Herceptin is currently approved for the treatment of ErbB2-overexpressing metastatic breast cancer, resistance to this drug is a common problem. In addition, several clinical studies demonstrating the activity of Herceptin as monotherapy for this patient group reported low overall (complete and partial) response rates ranging between 12% and 26% (Baselga et al. 1996;Cobleigh et al. 1999;Vogel et al. 2002), indicative that almost two thirds of patients with ErbB2-overexpressing metastatic breast cancer do not respond to Herceptin. The mechanisms by which Herceptin exerts its effects, as well as mechanisms of resistance have been the subject of many studies (Austin et al. 2004;Nahta and Esteva 2007;Pegram et al. 1999;Pickl and Ries 2009;Tseng et al. 2006;Valabrega et al. 2007;Yeon and Pegram 2005). Here, we provide evidence to suggest that tetraspanin CD82 modulates the response of ErbB2-positive breast cancer cell lines to Herceptin. We generated CD82-overexpressing breast cancer cells as a model system to investigate the role of CD82 in the responsiveness of SKBR3 and BT474 cells to Herceptin treatment in several assays including viability, proliferation, migration and invasion. The efficacy of Herceptin has been demonstrated *in vitro* in various ErbB2-positive breast cancer cell lines, including SKBR3 and BT474 cells (Ginestier et al. 2007;Junttila et al. 2009;Tseng et al. 2006;Weigelt et al. 2010). Here, our data demonstrate for the first time that ectopic expression of tetraspanin CD82 negatively modulates the response of SKBR3 and BT474 breast cancer cells to Herceptin.

There is conflicting data regarding the response of breast cancer cells to Herceptin under different culture conditions. For example, a report by Pickl and Ries demonstrated that breast cancer cells including SKBR3 when cultured in 3D extracellular matrix substrata, responded better to the antiproliferative effect of Herceptin than in 2D cultures (Pickl and Ries 2009). However, in a separate study by Weiglet and colleagues, SKBR3 cells were found to be resistant to the anti-proliferative effect of Herceptin when cultured as 3D colonies though they were responsive as 2D monolayers (Weigelt et al. 2010). Herein, we found that the response of control cells (SKBR3/Zeo and BT474/Puro) to Herceptin treatment was in agreement to previously published reports (Junttila et al. 2009;Pickl and Ries 2009;Tseng et al. 2006), whereby cells cultured in 3D ECM substrata responded better to Herceptin treatment than as 2D monolayers. In addition, we observed that ectopic expression of CD82 resulted in a poor response to Herceptin, particularly in cells cultured in 3D ECM as discussed below.

The use of 3D culture models *in vitro* is of physiological relevance, as it enables emulation of *in vivo* cellular structure and function of cancer cells. Such model systems therefore provide rationale to study not only drug response, but also investigation of potential drug targets and elucidation of their molecular mechanisms of action (Schmeichel and Bissell 2003). In this regard, we examined the effect of CD82 expression on proliferation of SKBR3 and BT474 cells grown in 3D extracellular matrix substrata. We found that when the cells were grown in collagen and Matrigel extracellular matrices, ectopic expression

of CD82 resulted in suppression of cell proliferation, as reflected by a decrease in colony size of CD82-overexpressing cells when compared to control cells. These data are indicative of the antiproliferative metastasis suppressive characteristic of CD82. Indeed, these data are in agreement with previously published reports demonstrating the antiproliferative effect of CD82 in other cancer cell lines (Bandyopadhyay et al. 2006;Choi et al. 2009;Joshi et al. 2010;Ruseva et al. 2009). Although CD82 is characterised as a metastasis suppressor protein, the mechanisms by which it exerts its metastasis suppressive function remain to be fully elucidated (Jackson et al. 2005;Miranti 2009;Tonoli and Barrett 2005). Nonetheless, several mechanisms have been proposed in an effort to understand how CD82 suppresses cell proliferation. For example, a study by Bandyopadhyay and colleagues identified Duffy antigen receptor for chemokines (DARC), an endothelial cell surface protein as an interacting partner for CD82. The authors demonstrated that CD82-expressing cancer cells attached to vascular endothelial cells via a CD82-DARC-mediated interaction thus leading to inhibition of tumour cell proliferation and induction of cellular senescence (Bandyopadhyay et al. 2006). Elsewhere, CD82 was reported to downregulate Rac1 and cell proliferation by inhibiting the PI3K/Akt/mTOR signalling pathway (Choi et al. 2009).

In addition to studying the effect of CD82 on cell proliferation in 3D ECM culture models, we also investigated the effect of CD82 expression on cellular response to Herceptin treatment under these culture conditions. When the cells were grown in 3D collagen and Matrigel, we found that CD82-overexpressing cells displayed a weaker response to Herceptin than control cells; this was

consistently observed in both SKBR3 and BT474 cells. However, this CD82-mediated effect on Herceptin response was more prominent in BT474 than SKBR3 cells. The fact that control cells displayed a stronger response to Herceptin than CD82-overexpressing cells indicates that under these culture conditions, control cells rely mainly on ErbB2 in order to proliferate and form colonies, which was significantly inhibited by Herceptin treatment. On the other hand, the expression of CD82 adds a level of complexity to this ErbB2 dependency thus rendering the cells less responsive to Herceptin treatment.

Although these data do not currently offer explanations into the mechanism by which CD82 disrupts this ErbB2-dependent proliferation, it is reasonable to speculate based on the current data and previously published reports. One possible mechanism by which CD82 might modulate the cellular response to Herceptin under 3D cultures is by affecting the compartmentalisation of ErbB2. It has been previously reported that ectopic expression of CD82 caused re-distribution of EGFR into ganglioside-containing microdomains on the plasma membrane (Odintsova et al. 2003). One of the main characteristics of tetraspanins is their ability to interact with one another as well as with other proteins thereby forming tetraspanin-enriched microdomains (TERMs), which are structural platforms that can modulate the activity of component molecules (Hemler 2005;Odintsova et al. 2006;Yanez-Mo et al. 2009). It is feasible that under different 3D culture conditions, membrane microdomains such as TERMs constituting CD82 and its binding partners are formed thus allowing differential clustering of CD82-associated proteins, which can lead to activation of different signalling pathways such as integrin and growth factor signalling. It has been

previously reported that growth of cells under 3D conditions whereby cells are in contact with the extracellular matrix induces interdependency and cross-talk between growth factor receptor and β1 integrin signalling (Bissell et al. 1999;Liu et al. 2004a;Wang et al. 1998;Weaver et al. 1997). Indeed, more recent studies have demonstrated that addition of growth factor receptor and β1 integrin inhibitory agents to breast cancer cells results in a concomitant downregulation of both receptors thus leading to growth arrest (Park et al. 2006;Weigelt et al. 2010). CD82 is widely known to interact with β1 integrins including α3β1, α4β1, α5β1 and α6β1 (Berditchevski 2001). It is therefore possible that in CD82-overexpressing cells, CD82 induces clustering of ErbB2 and β1 thereby promoting cross-talk downstream of these receptors. The consequence of this could be that inhibition of ErbB2 signalling by Herceptin could lead to compensatory mechanisms in the form of β1 signalling thus rendering CD82-overexpressing cells less responsive to Herceptin. Interestingly, we found that BT474 cells express higher levels of α3, α6 and β1 integrins compared to SKBR3 cells; however, ectopic expression of CD82 did not affect the endogenous expression levels of these integrins (Appendix IV – supplementary Figure 1). The fact that BT474 cells express higher integrin levels than SKBR3 cells could explain why the CD82-mediated poor response to Herceptin under 3D culture conditions was more prominent in BT474 than in SKBR3 CD82-overexpressing cells.

Another possible mechanism by which CD82 modulates the cellular response to Herceptin could be that overexpression of CD82 results in hindrance of Herceptin from accessing its epitope on ErbB2. Being that tetraspanins are

small transmembrane molecules and that Herceptin binds to domain IV of the ErbB2 extracellular domain which is also near the plasma membrane, it is feasible that in control cells (SKBR3/Zeo and BT474/Puro) whereby the expression levels of CD82 are low, that Herceptin binds readily or indeed more efficiently to the ErbB2 receptors whilst its binding capacity is limited in the CD82-overexpressing cells. Indeed, it is reported in the literature that epitope inaccessibility is one of the mechanisms of resistance to Herceptin (Valabrega et al. 2007). As mentioned earlier, a study by Nagy and colleagues demonstrated that the binding capacity of Herceptin to ErbB2 was low in a Herceptin-resistant breast cancer cell line. These authors found that the Herceptin-resistant cell lines expressed high levels of MUC4, a membrane-associated mucin known to mask membrane proteins when compared to the sensitive cell lines. Furthermore, they demonstrated that knockdown of MUC4 restored the binding capacity of Herceptin (Nagy et al. 2005). It is thus possible that like MUC4, that CD82 could be masking the Herceptin epitope on ErbB2 in our model system of CD82-overexpressing cells thus rendering these cells less responsive to Herceptin treatment.

One of the hallmarks of cancer is to acquire the capability to invade neighbouring tissue and form metastases at a distant tissue site (Hanahan and Weinberg 2011). In order to form distant metastases, tumour cells must invade the microenvironment, leave the primary tumour and migrate to a secondary site (Leber and Efferth 2009). Cell motility is therefore important during invasion and metastasis. As CD82 has been shown to be a metastasis suppressor (Dong et al. 1995;Jackson et al. 2005;Liu and Zhang 2006), it has also been

shown to inhibit cell migration and the invasiveness of many cancer cell lines (Bari et al. 2009;Jee et al. 2007;Todeschini et al. 2007;Yang et al. 2001;Zhang et al. 2003a). Herein, our data from experiments with SKBR3 cells are consistent with previously reported observations and demonstrate the CD82-mediated suppression of cell migration and invasion using collagen and Matrigel extracellular matrices, respectively. We observed that overexpression of CD82 resulted in a significant reduction ($P<0.001$) in the migratory potential of SKBR3/CD82^{High} cells, when compared to that of SKBR3/Zeo cells.

Furthermore, in an effort to determine whether Herceptin treatment affected cell migration and also whether ectopic expression of CD82 played a role in any Herceptin-mediated inhibition of cell migration, SKBR3/Zeo and SKBR3/CD82^{High} cells were left to migrate in the presence and absence of Herceptin, using heregulin as a chemoattractant. We found that Herceptin significantly ($P<0.001$) inhibited cell migration in SKBR3/Zeo cells, but its anti-migratory effect was less pronounced in SKBR3/CD82^{High} cells. Migration was reduced by at least 50% in the Herceptin-treated SKBR3/Zeo cells compared to non-treated cells; whilst the number of migrated cells was comparable in both non-treated and Herceptin-treated SKBR3/CD82^{High} cells. These data suggest that the heregulin-induced migration of SKBR3/Zeo cells is ErbB2-dependent, which can be inhibited by Herceptin treatment. Since heregulin is a ligand for ErbB3, then heregulin-induced migration of SKBR3/Zeo cells is likely to be due to signalling downstream of ErbB2/ErbB3 heterodimers. However, in the case of CD82 overexpression (SKBR3/CD82^{High}), this ErbB2-mediated mechanism of migration is altered in a way that the cells appear to be less-responsive to the

anti-migratory effect of Herceptin. This suggests that in SKBR3/CD82^{High} cells, the heregulin-induced cell migration may not ErbB2-dependent. Since SKBR3 cells also express EGFR as well as ErbB2 and ErbB3, it is possible that in SKBR3/CD82^{High} cells, heregulin-induced migration is as a result of EGFR/ErbB3 signalling, instead of ErbB2/ErbB3 signalling as proposed for SKBR3/Zeo cells. On the other hand, the poor response of SKBR3/CD82^{High} cells to the anti-migratory effect of Herceptin could be due to signalling via alternative signalling pathways. As discussed earlier for the poor response of SKBR3/CD82^{High} cells to the antiproliferative effect of Herceptin in 3D ECM, it is possible that ectopic expression of CD82 promotes signalling from other receptors other than ErbB2. Notably, this alternative signalling was responsive to the suppressive effect of CD82 on migration in both non-treated and Herceptin-treated cells.

In order to determine the specificity of the anti-migratory effect of CD82 and determine whether it is specific for only ErbB2, we examined the haptotactic and chemohaptotactic migratory potential of SKBR3 cells under serum-free, complete medium with 10% FBS or serum-free medium supplemented with either HB-EGF or TGF-β1 chemoattractants; HrG used as a control. From these experiments, we found that CD82 consistently suppressed migration under all conditions with the exception of 10% FBS; whereby in the latter condition, the CD82-mediated effect was reversed. Since both HB-EGF and HrG are ligands for other members of the EGFR family (EGFR and ErbB4; ErbB3 and ErbB4, respectively), whereby ligand binding induces receptor homo- and hetero-dimerisation of which ErbB2 is the preferred heterodimerisation partner, the

exact specificity of the anti-migratory effect of CD82 for this receptor family is not quite clear. It is widely known that CD82 associates with EGFR, ErbB2 and ErbB3 and that it negatively regulates EGFR signalling (Odintsova et al. 2000). From our current study and reports from others, SKBR3 cells are known to express EGFR, ErbB2 and ErbB3, but not ErbB4; therefore it is feasible that CD82 can suppress migration by regulating either of these receptors. The fact that CD82 also suppressed TGF-β1-induced migration suggests that the anti-migratory effect of CD82 is diverse and is not limited to regulating signalling of just the EGFR family, but also other receptors. However, the reverse result observed with 10% serum is indicative that not all receptors are regulated by CD82.

The complexity into the diverse suppressive effect of CD82 on cell migration is further demonstrated by reports in literature aimed at identifying the mechanism(s) by which CD82 regulates cell migration. For example, Zhang and colleagues identified the FAK-Src- $p130^{CAS}$-CrkII signalling pathway to be responsible for the CD82-mediated suppression of cell migration of a metastatic prostate cancer cell line. They proposed that CD82 suppressed migration in these cells by inhibiting formation of the pro-migratory $p130^{CAS}$-CrkII complex through downregulation of $p130^{CAS}$ expression (Zhang et al. 2003a). Both FAK and Src are reported to play an important role in mediating integrin signalling (Zhao and Guan 2009). In a separate study, Ruseva and colleagues proposed that the association of CD82 with the integrin superfamily in particular integrin αvβ3 contributed to the metastasis suppressive effect of CD82 through inhibition of cell migration as a consequent of enhanced cellular attachment.

The authors demonstrated not only the association of CD82 with αvβ3, but also an increase in αvβ3-mediated cell adhesion and consequently, reduced motility of ovarian cancer cells upon expression of CD82 (Ruseva et al. 2009). Both these studies demonstrate the ability of CD82 to suppress integrin-mediated cell migration. On the other hand, a study by Takahashi and colleagues demonstrated that the association of CD82 with c-Met resulted in suppression of HGF-induced cell migration due to decreased association of signalling adaptor proteins to the c-Met receptor, in the CD82-overexpressing cells (Takahashi et al. 2007).

CD82 is not the only tetraspanin reported to modulate the response of ErbB2-positive breast cancer cells to Herceptin. A recent report by Yang and colleagues demonstrated that knockdown of tetraspanin CD151 sensitised ErbB2-positive breast cancer cells including SKBR3 and BT474 cells to ErbB2-targeted drugs that included Herceptin (Yang et al. 2010). This emerging body of evidence in addition to our findings presented herein is indicative that tetraspanins may play a role in regulating drug sensitivity and thus warrants further studies.

Taken together, our current data suggest a modulatory role of CD82 in the cellular response of ErbB2-positive breast cancer cells to Herceptin treatment possibly by regulating the compartmentalisation of the ErbB2 receptor and/or its downstream signalling. Although the exact mechanism(s) of how CD82 exerts its effects are not yet clear at this stage, the above proposed mechanisms will be investigated further in the following sections.

3.2 The effect of CD82 expression on the distribution and dynamics of ErbB proteins

3.2.1 CD82 interacts with ErbB2 receptor tyrosine kinase

CD82 has previously been shown to associate with the ErbB proteins, however the interaction of CD82 and ErbB2 was found to be cell-type specific (Odintsova et al. 2003). Therefore, it was important for the purpose of this study to determine whether CD82 associated with ErbB2 in our model system of BT474 and SKBR3. Possible interactions of CD82 and ErbB2 were studied by immunoprecipitation as described in the Materials and Methods under section 2.3.3.

Figures 3.8A & C illustrate that ErbB2 coimmunoprecipitated with the anti-CD82 antibody in both control and CD82-overexpressing cells. The amount of ErbB2 in complex with CD82 was significantly ($P<0.001$) higher in SKBR3/CD82^{High} cells when compared to that in SKBR3/Zeo cells (Figure 3.8A, lanes 3 & 4). Densitometric analysis of the blots revealed that at least 17% of total ErbB2 was in complex with CD82 in SKBR3/CD82^{High} cells, when compared to 3% in SKBR3/Zeo cells (Figure 3.8B). In contrast, the amount of ErbB2 that co-immunoprecipitated with CD82 was comparable in both BT474/Puro and BT474/CD82^{High} cells (Figure 3.8C, lanes 3 &4). At least 9% of total ErbB2 was detected to be in complex with CD82 in both BT474/Puro and BT474/CD82^{High} cells (Figure 3.8D). Control experiments show that the anti-CD82 mAb

efficiently precipitated CD82; whereby distinction between control and CD82-overexpressing cells is clearly visible based on the amount of precipitated CD82 (Figures 3.8A & C, lanes 3 & 4, lower panels). The low molecular weight bands (red arrow) detected in the whole cell lysates with the anti-CD82 antibody are likely to be non-specific bands, since they are not detected in the precleared immune complexes (Figures 3.8A & C, compare lanes 1 & 2 and lanes 3 & 4, red arrow). The interaction of CD82 with ErbB2 was confirmed in SKBR3/CD82^{High} cells under different lysis conditions: 1% Brij-98; and a mixture of 0.5% Brij-98 + 0.5% Triton X-100; although the amount of ErbB2 found in complex with CD82 was lower in more stringent detergent conditions (Appendix IV, Supplementary Figure 2). The fact that the ErbB2-CD82 complex is disrupted by more stringent detergent conditions, but is retained in milder detergent conditions (1% Brij-98) suggests that this interaction is not direct.

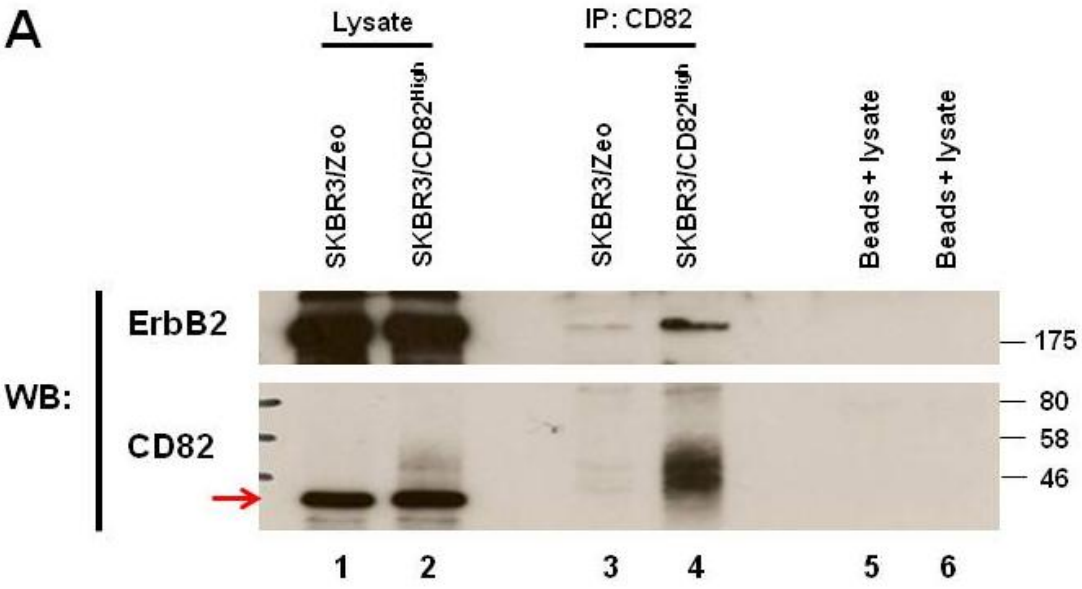
A
Lysate
IP: CD82
SKBR3/Zeo
SKBR3/CD82High
SKBR3/Zeo
SKBR3/CD82High
Beads + lysate
Beads + lysate
WB:
ErbB2
CD82
175
80
58
46
1
2
3
4
5
6

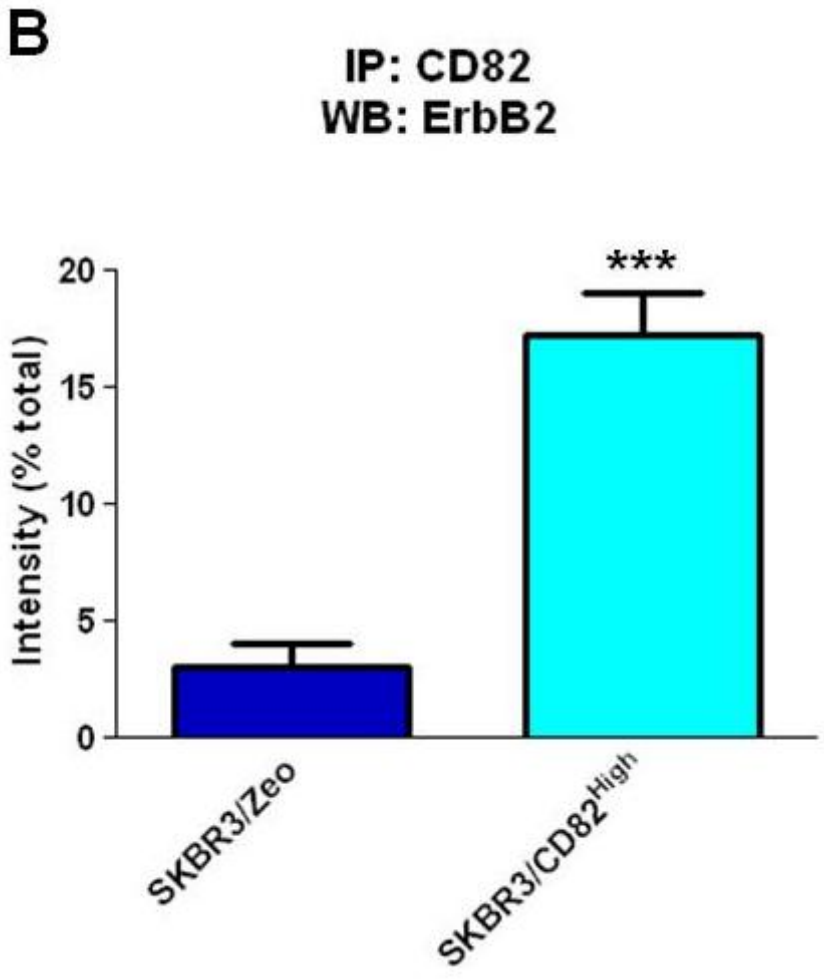
B
IP: CD82
WB: ErbB2
***
Intensity (% total)
20
15
10
5
0
SKBR3/Zeo
SKBR3/CD82High

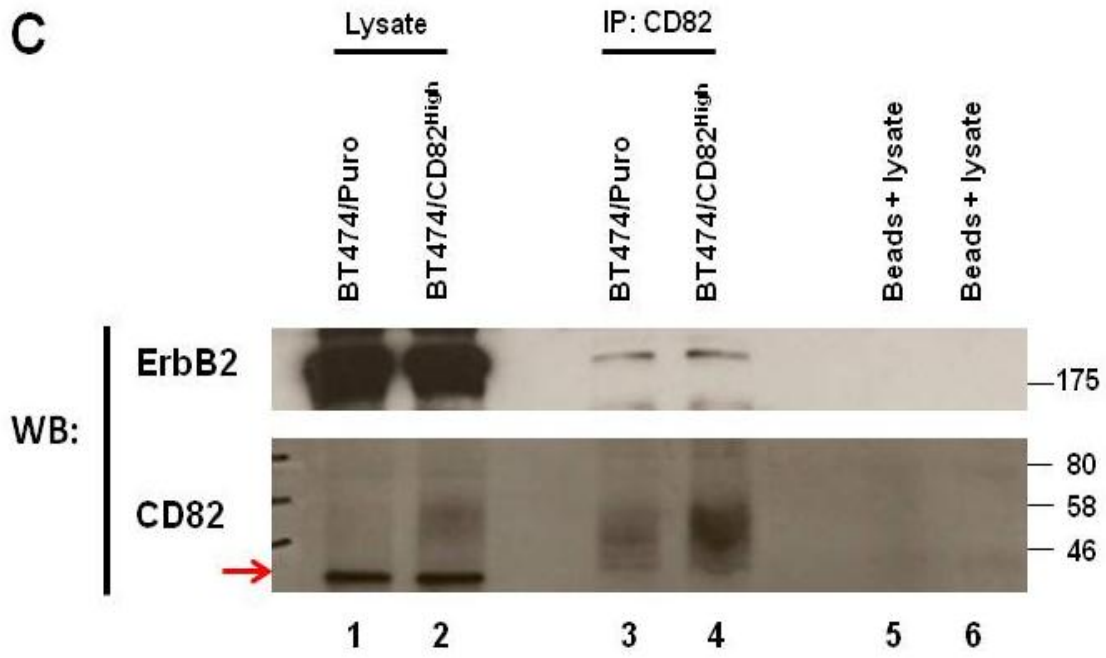
C
Lysate
IP: CD82
BT474/Puro
BT474/CD82High
BT474/Puro
BT474/CD82High
Beads + lysate
Beads + lysate
WB:
ErbB2
CD82
175
80
58
46
1
2
3
4
5
6

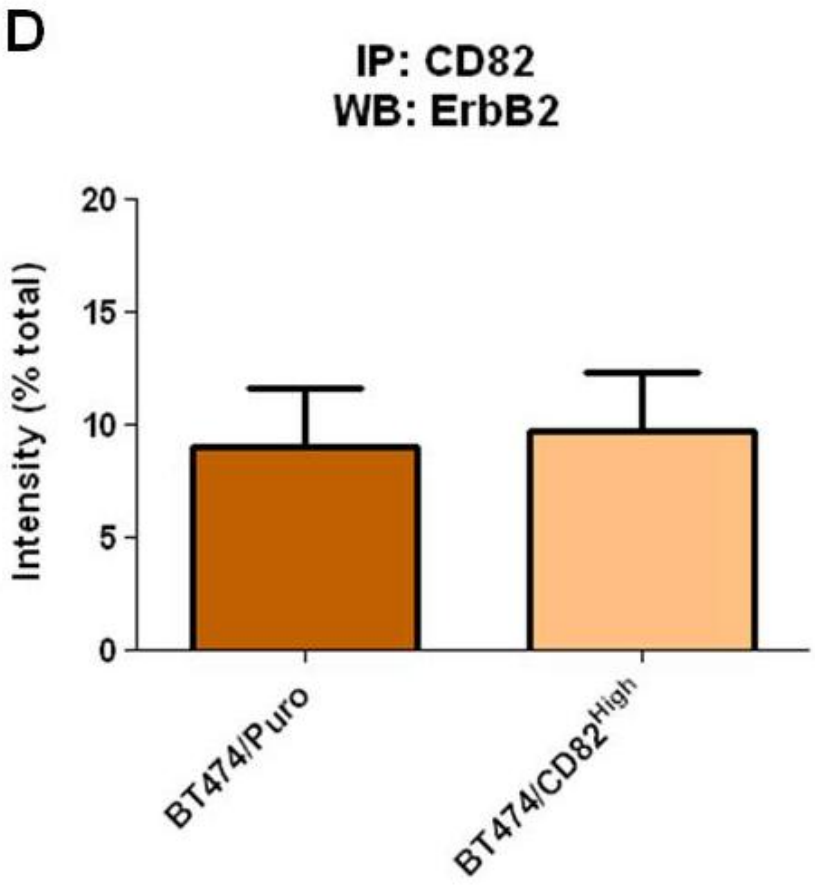
D
IP: CD82
WB: ErbB2
Intensity (% total)
20
15
10
5
0
BT474/Puro
BT474/CD82High

Figure 3.8: CD82 associates with ErbB2 in SKBR3 and BT474 cells.

(A) SKBR3 and (C) BT474 cells were prepared for the immunoprecipitation assay as described in the Materials and Methods under section 2.3.4. Cells were lysed using a mixture of 0.8% Brij-98 + 0.2% Triton X-100 lysis buffer for 4h at 4^{o}C with rotation. Immune complexes were precipitated using mouse IgG agarose beads conjugated with M104 mouse anti-CD82 mAb followed by western blot analysis using anti-ErbB2 (Ab-17) and anti-CD82 (KAI1 C-16) antibodies. (B and D) Densitometric analysis of the blots, plotted as percentage of total protein. Data shown is one representative of at least two independent experiments. Asterisks represent the statistical significance as determined by a two-tailed, unpaired Student's t test, using GraphPad Prism software. Significance was set at 0.05, whereby (*** $P<0.001$).

3.2.2 Ectopic expression of CD82 changes the compartmentalisation of ErbB2

Tetraspanins are known to affect the membrane compartmentalisation of not just tetraspanins, but also of non-tetraspanin proteins (Berditchevski 2001;Claas et al. 2001;Odintsova et al. 2003). In the present study, the role of CD82 in the membrane distribution of ErbB2 was investigated in Herceptin treated (10µg/ml; 1h) and non-treated (Herceptin-free) cells, by fractionation in a sucrose gradient as outlined in section 2.4 of the Materials and Methods. Ten fractions were collected from the top of the gradient and protein distribution within these gradient fractions was determined by western blot analysis. Following lysis with Triton X-100, any proteins distributed within low density fractions 2-5 were considered to be in membrane microdomains that are insoluble to lysis with this detergent whilst distribution within high density fractions 6-10 was considered to be in detergent-soluble membrane microdomains.

Figures 3.9A and B (top panels) illustrate that in the absence of Herceptin, 93% of ErbB2 was distributed within the dense detergent-soluble fractions, 6-10 in SKBR3/Zeo cells. No ErbB2 was detected in the detergent-insoluble fractions, 1-5. A similar distribution of CD82 was observed under the same conditions in these cells, whereby 96% of CD82 was detected in fractions 6-10 (Figures 3.9C and D, top panel). However, 4% of total CD82 was also detected in the buoyant fraction 5 (Figure 3.9C, upper top panel). Treatment of these cells with Herceptin resulted in a change in the distribution of both ErbB2 and CD82. By

comparing the distribution of ErbB2 in non-treated and treated cells, we found that Herceptin treatment caused redistribution of ErbB2 to the heavier fractions; whereby significantly ($P<0.05$) less ErbB2 was detected in fraction 6 of the Herceptin-treated SKBR3/Zeo cells compared to that in same fraction of non-treated cells (Figure 3.9A upper top panel; lane 6). On the other hand, CD82 was redistributed to the light membrane fractions following Herceptin treatment (Figure 3.9C upper top panel, lane 5). Densitometric analysis of the blots revealed that the amount of CD82 redistributed to fraction 5 following Herceptin treatment was increased by ~6% when compared to that of non-treated SKBR3/Zeo cells (Figure 3.9D, top graph, compare the dark blue bar to the purple bar).

Interestingly, we found that in SKBR3/CD82^{High} cells, the amount of ErbB2 in fraction 6 was markedly decreased with the concomitant increase of the protein in fraction 3 (Figure 3.9A top panel; compare lanes 3 and 6 of SKBR3/Zeo and SKBR3/CD82^{High} cells). Densitometric analysis of the blots revealed that at least 1.5% of total ErbB2 was redistributed to fraction 3 in non-treated SKBR3/CD82^{High} cells. Furthermore, we found that treatment with Herceptin (10µg/ml, 1h) increased the amount of ErbB2 in this fraction by 8-fold, when compared to the amount in the same fraction of non-treated cells (Figure 3.9B top panel, fraction 3; compare the light blue bar to the green bar). No signal was detected in the first two fractions. Similarly, we found that CD82 was distributed in both dense and light membrane fractions in non-treated and Herceptin-treated SKBR3/CD82^{High} cells (Figure 3.9C, lower top panel). 86% of total CD82 was detected in dense fractions, 6-10; whilst 14% of CD82 was detected in the

light fractions, 2 and 3 in the non-treated cells (Figure 3.9D top panel, light blue bars). Treatment with Herceptin induced further redistribution of CD82 into fractions 4 and 5, which was hardly detectable in non-treated cells (Figure 3.9C, lower top panel). Similar observations were made when cells were lysed under different lysis conditions (Appendix IV, Supplementary Figure 3).

We also investigated the membrane distribution of other tetraspanins (CD9, CD151 and CD63) (Figure 3.10). Similar to the distribution of CD82, we found that CD9 was distributed in both detergent-insoluble and soluble fractions. Specifically, in SKBR3/Zeo cells, CD9 was detected in the detergent-insoluble fractions 2, 3 and 5; as well as in the detergent-soluble fractions 6-10. However, in SKBR3/CD82^{High} cells, CD9 was detected in fractions 2, 5, and 6-10, with hardly detectable amount in fraction 3 (Figure 3.10A). On the other hand, the distribution of tetraspanins CD151 and CD63 was localised only to the dense fractions, 6-10 (Figure 3.10). Notably, treatment with Herceptin did not affect the membrane distribution of CD9, CD151 and CD63 in both SKBR3/Zeo and SKBR3/CD82^{High} cells.

Contrary to the observations in SKBR3 cells, ectopic expression of CD82 in BT474 cells had no effect on the distribution of ErbB2. The receptor was only distributed within the dense gradient fractions 7-10, in both control and CD82-overexpressing cells (Figures 3.9A and B, bottom panels). Furthermore, we found that treatment of these cells with Herceptin did not affect the distribution of ErbB2. Similar to the distribution of ErbB2, CD82 was only detected in the dense gradient fractions, with majority (69% and 66%) being detected in

fractions 7, 8 and 9 in BT474/Puro and BT474/CD82^{High} cells, respectively (Figure 3.9C, bottom panel). However, treatment with Herceptin induced a shift in the distribution of CD82 into heavier fractions, with less amount of CD82 (8% and 2%) being detected in fraction 6 following Herceptin treatment in both BT474/Puro and BT474/CD82^{High} cells, respectively (Figure 3.9C bottom panel, lane 6; and Figure 3.9D).

The distribution pattern of flotillin-2, a component of lipid rafts (Bickel et al. 1997;Salzer and Prohaska 2001;Slaughter et al. 2003;Zhao et al. 2011) was also analysed. Like ErbB2 and CD82, we found that flotillin-2 was also distributed in the low-density fractions 2, 3 and 4; and in the high-density fractions mainly 7-10, in both SKBR3 and BT474 cells (Figure 3.9E). Densitometric analysis of the blots revealed that treatment with Herceptin resulted in redistribution of flotillin-2. Specifically, the amount of flotillin-2 detected in fractions 2, 3 and 4 was increased by at least 3-fold, following Herceptin treatment in the SKBR3/CD82^{High} cells when compared to that of non-treated cells (Figure 3.9F, top panel). This effect appeared to be cell-type specific, since it was not observed in the BT474 cells (Figure 3.9F, bottom panel). Based on the distribution pattern of flotillin-2 in the low-density fractions in both SKBR3 and BT474 cells, we concluded that fractions 2 and 3 are the typical raft fractions, insoluble following lysis with 1% Triton X-100.

The fact that ectopic expression of CD82 resulted in redistribution of ErbB2 to raft microdomains, particularly in SKBR3/CD82^{High} cells and not in BT474/CD82^{High} cells suggests that this CD82-mediated effect could be cell-

type specific. In addition, the fact that Herceptin treatment increased the amount of ErbB2 and flotillin-2 distributed within these raft fractions, particularly in fraction 2 implies that the distribution of ErbB2 to these microdomains could be functionally significant in the regulation of this receptor.

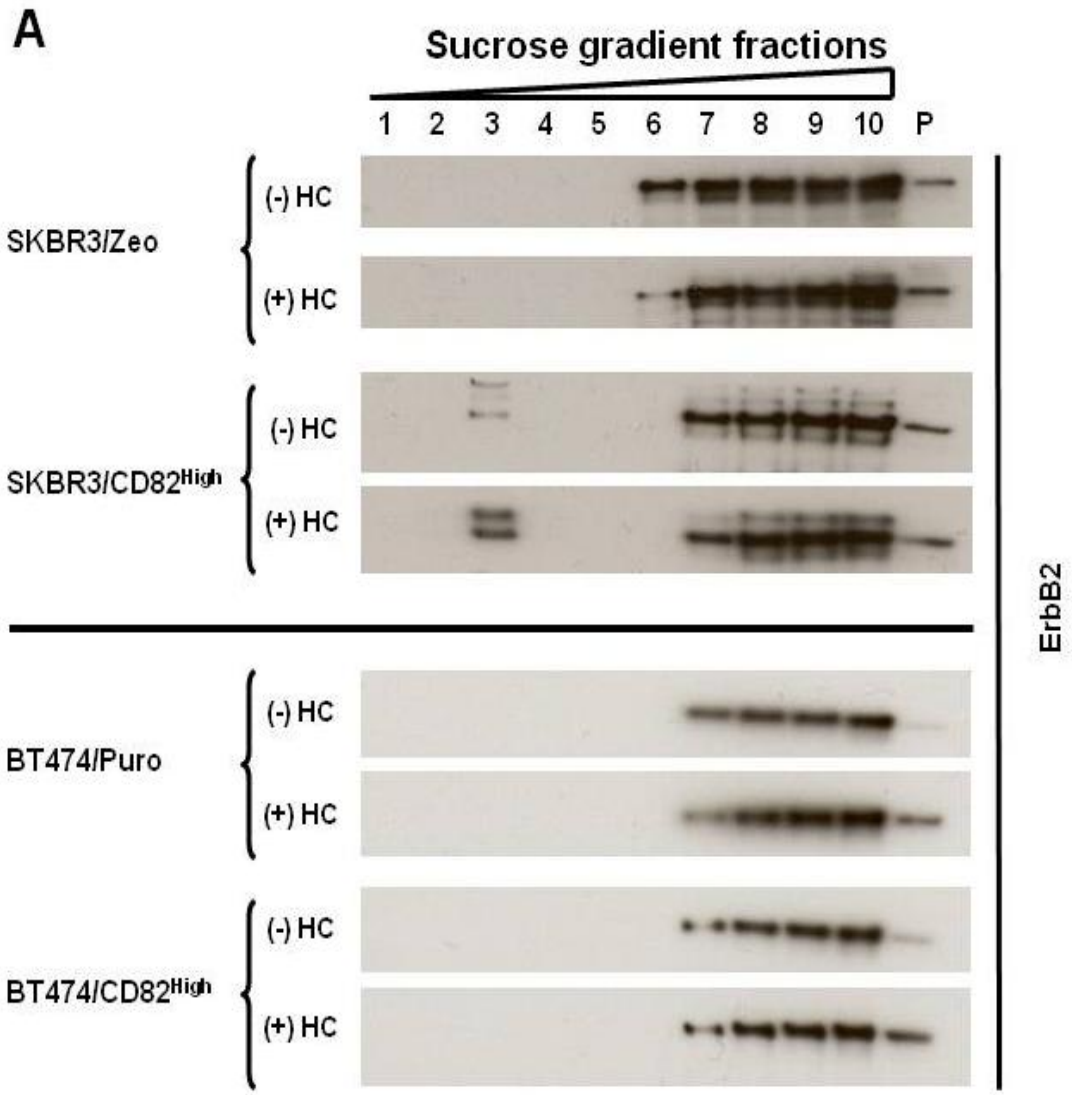
A
Sucrose gradient fractions
1 2 3 4 5 6 7 8 9 10 P
SKBR3/Zeo
(-) HC
(+) HC
SKBR3/CD82High
(-) HC
(+) HC
BT474/Puro
(-) HC
(+) HC
BT474/CD82High
(-) HC
(+) HC
ErbB2

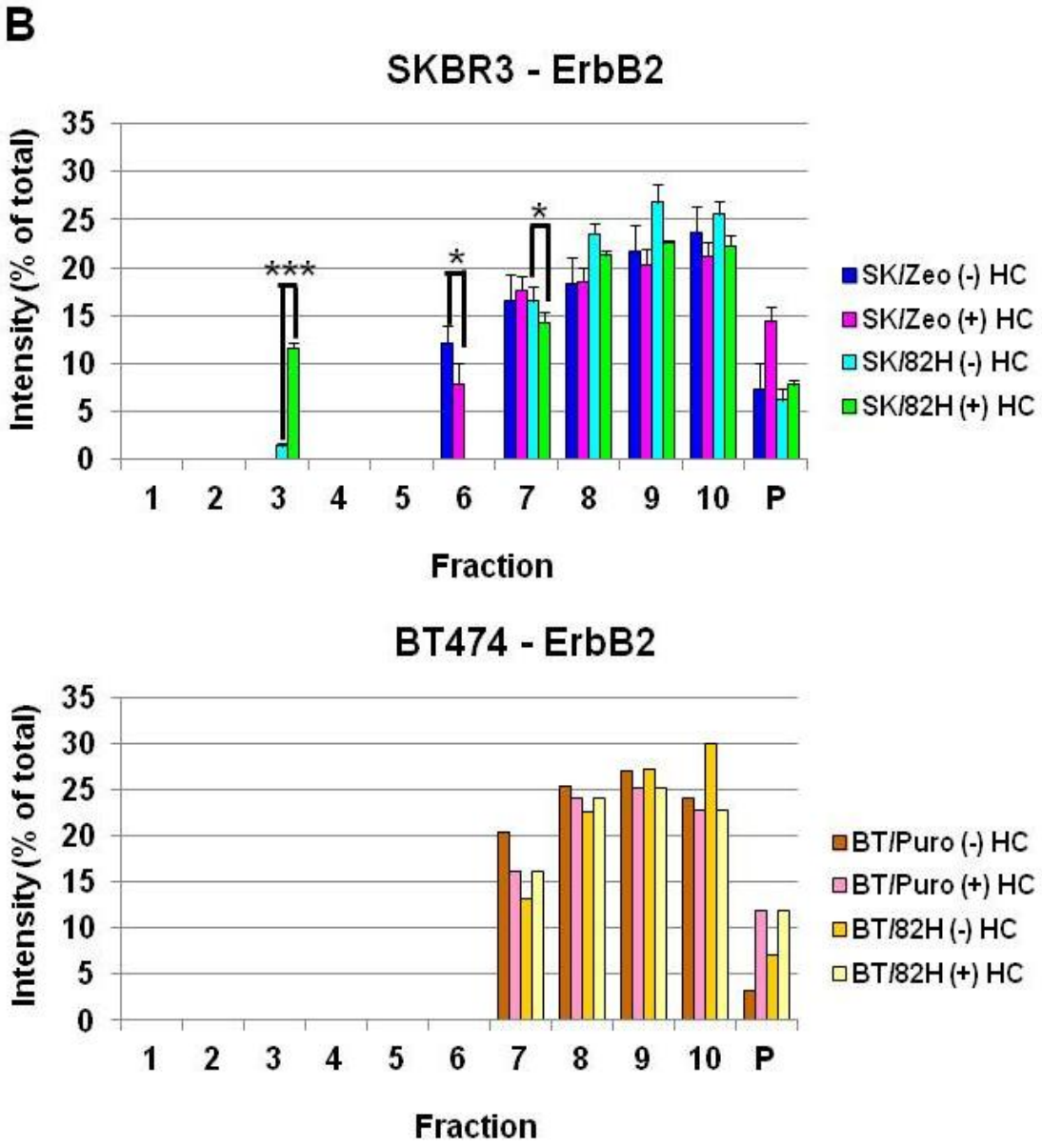
B
SKBR3 - ErbB2
Intensity (% of total)
35
30
25
20
15
10
5
0
***
*
*
1 2 3 4 5 6 7 8 9 10 P
Fraction
SK/Zeo (-) HC
SK/Zeo (+) HC
SK/82H (-) HC
SK/82H (+) HC
BT474 - ErbB2
Intensity (% of total)
35
30
25
20
15
10
5
0
1 2 3 4 5 6 7 8 9 10 P
Fraction
BT/Puro (-) HC
BT/Puro (+) HC
BT/82H (-) HC
BT/82H (+) HC

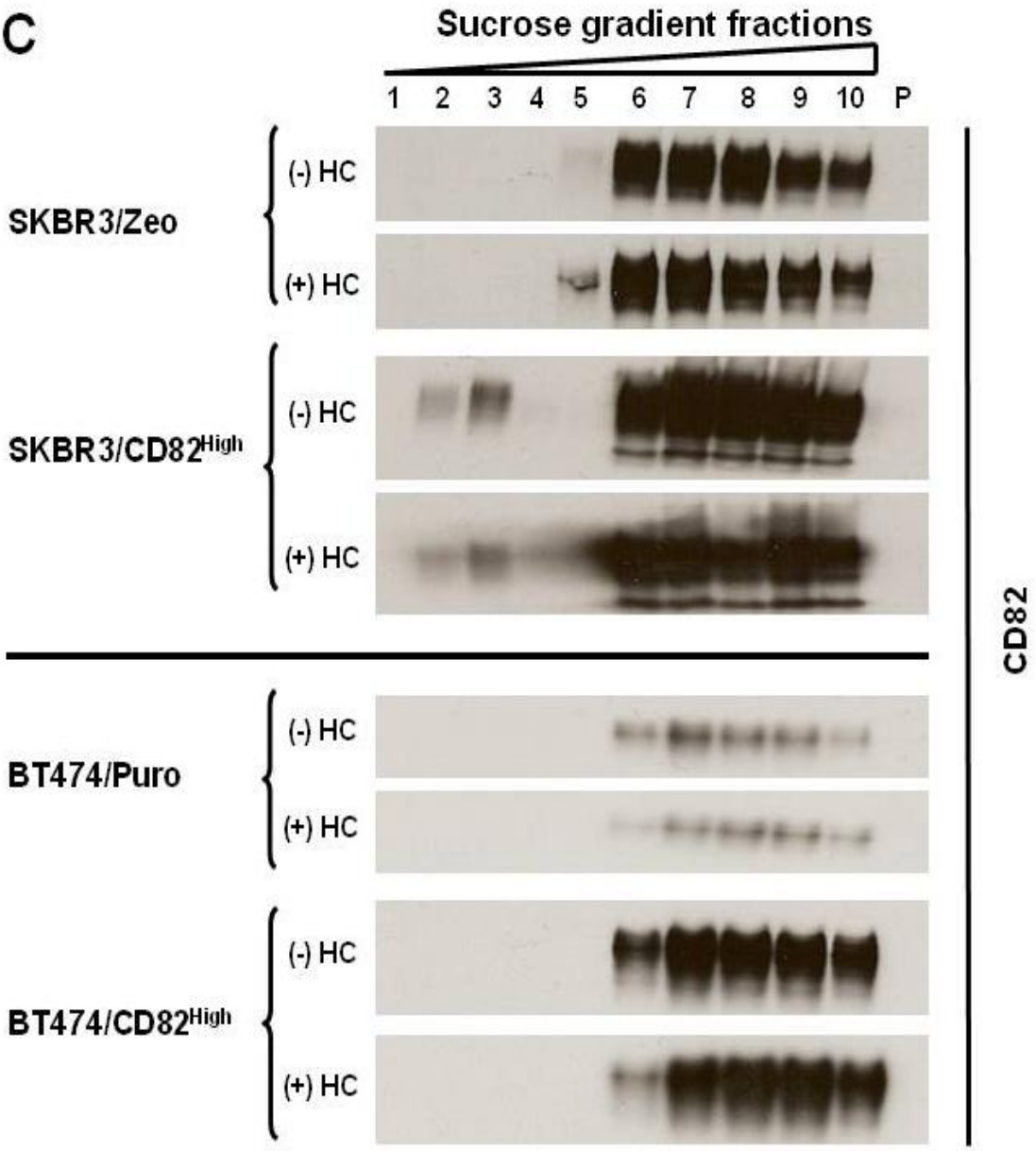
C
Sucrose gradient fractions
1 2 3 4 5 6 7 8 9 10 P
SKBR3/Zeo
(-) HC
(+) HC
SKBR3/CD82High
(-) HC
(+) HC
BT474/Puro
(-) HC
(+) HC
BT474/CD82High
(-) HC
(+) HC
CD82

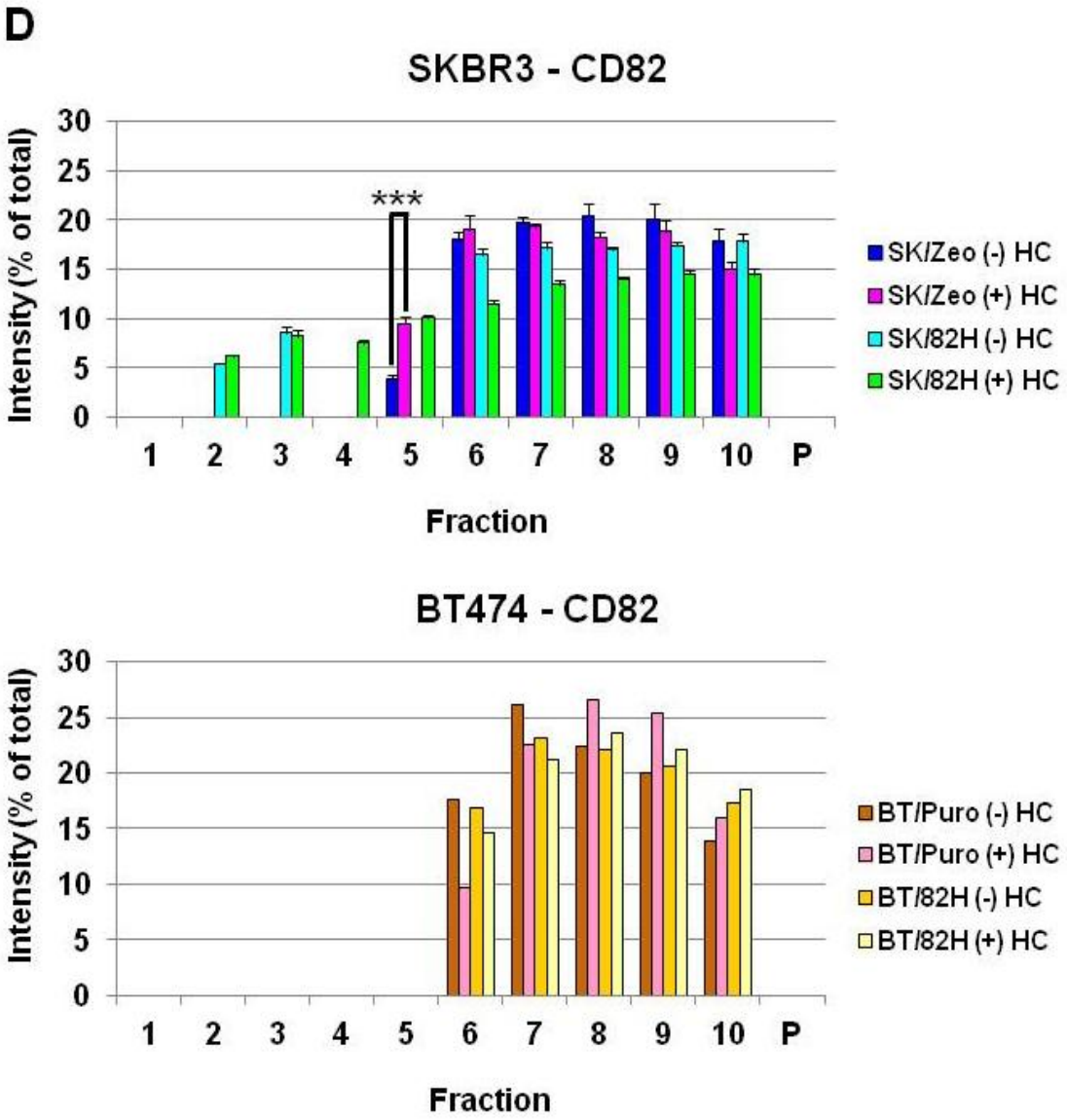
D
SKBR3 - CD82
Intensity (% of total)
30
25
20
15
10
5
0
***
1
2
3
4
5
6
7
8
9
10
P
Fraction
SK/Zeo (-) HC
SK/Zeo (+) HC
SK/82H (-) HC
SK/82H (+) HC
BT474 - CD82
Intensity (% of total)
Fraction
BT/Puro (-) HC
BT/Puro (+) HC
BT/82H (-) HC
BT/82H (+) HC

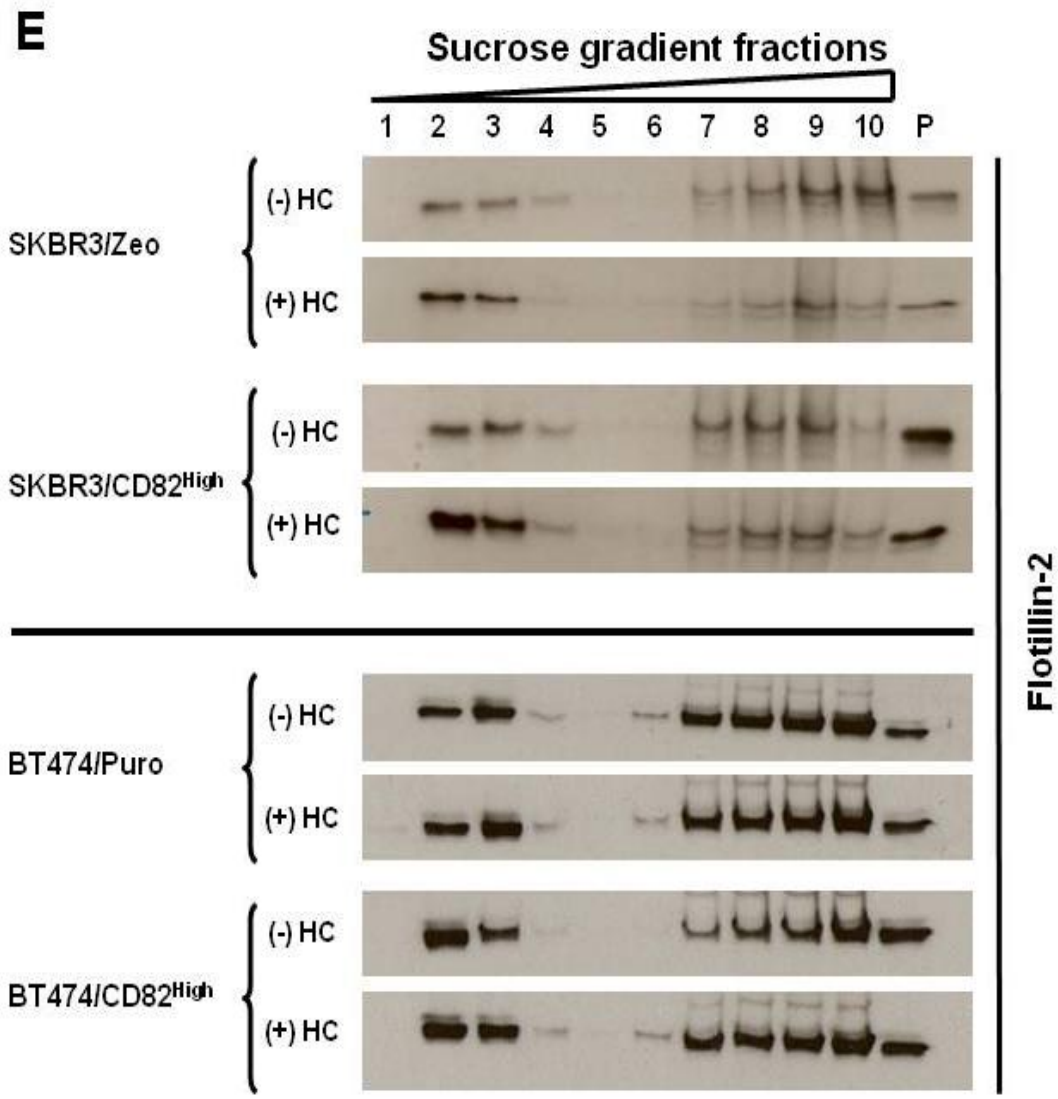
E
Sucrose gradient fractions
1 2 3 4 5 6 7 8 9 10 P
SKBR3/Zeo
(-) HC
(+) HC
SKBR3/CD82High
(-) HC
(+) HC
BT474/Puro
(-) HC
(+) HC
BT474/CD82High
(-) HC
(+) HC
Flotillin-2

F

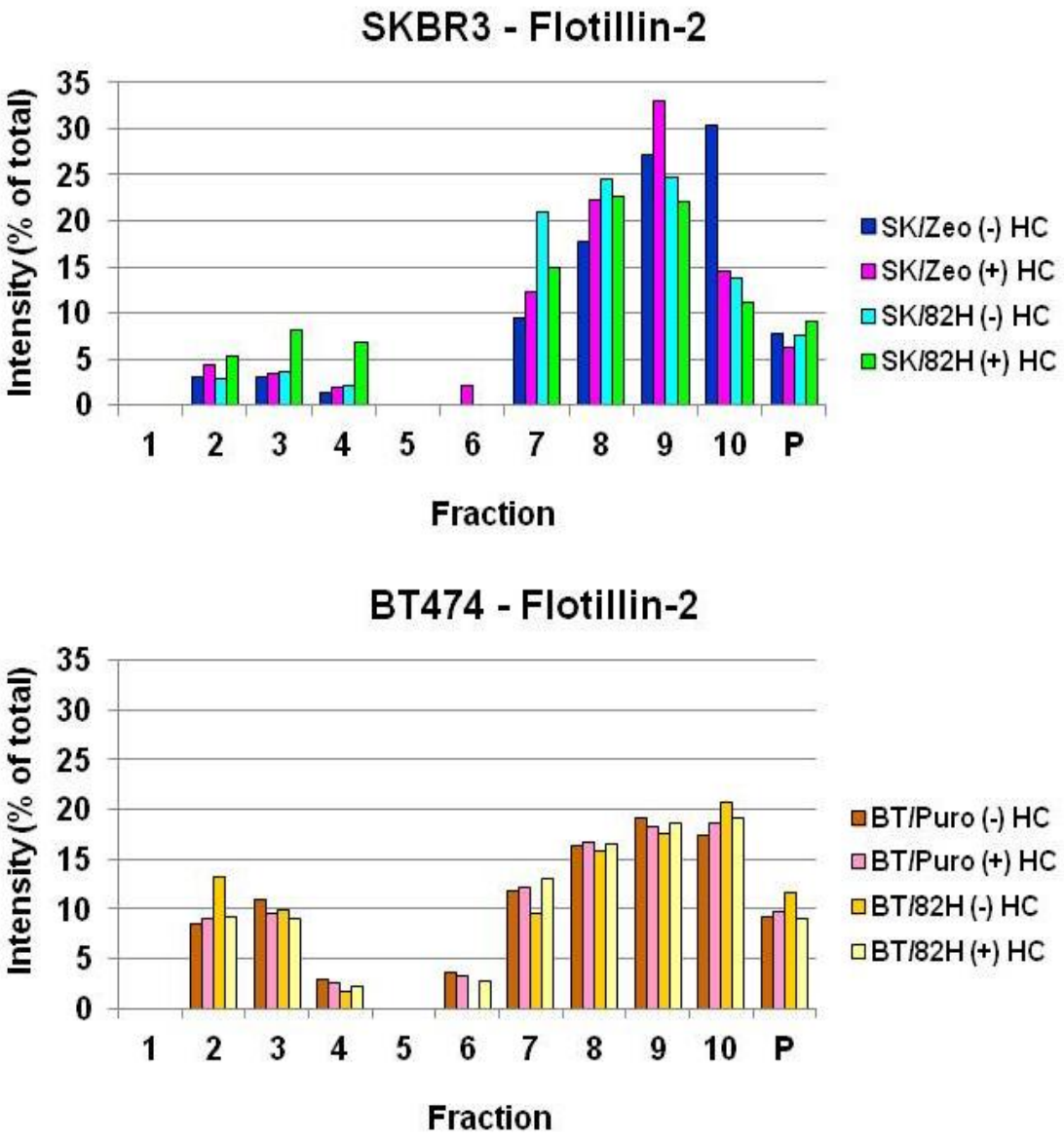
SKBR3 - Flotillin-2
Intensity (% of total)
35
30
25
20
15
10
5
0
1
2
3
4
5
6
7
8
9
10
P
Fraction
SK/Zeo (-) HC
SK/Zeo (+) HC
SK/82H (-) HC
SK/82H (+) HC
BT474 - Flotillin-2
Intensity (% of total)
Fraction
BT/Puro (-) HC
BT/Puro (+) HC
BT/82H (-) HC
BT/82H (+) HC

Figure 3.9: CD82 changes the compartmentalisation of ErbB2.

SKBR3 and BT474 cells were treated with Herceptin (10µg/ml) for 1h prior to lysis. Non-treated and treated cells were lysed in ice-cold 1% Triton X-100 and the resulting homogenate of equal protein concentration was centrifuged in a discontinuous sucrose density gradient composed of 90%, 35% and 5% (w/v) sucrose. 10 fractions were collected from the meniscus of the gradient and the pellet was resuspended in Laemmli buffer supplemented with protease and phosphatase inhibitors. Equal amounts of each fraction were mixed with 4X Laemmli loading buffer and the protein distribution was analysed by SDS-PAGE under reducing and non-reducing conditions followed by western blot analysis using antibodies against (A) ErbB2 (Ab-17); (C) CD82 (TS82b); and (E) Flotillin-2 (C42A3). (B; D and F) Summary of density ratios, plotted as percentage of total protein from at least two independent experiments. Asterisks represent the statistical significance as determined by the one-way ANOVA multiple comparison test with the Tukey-Kramer post-test, using GraphPad Prism software. Significance was set at 0.05, whereby (*P<0.05) and (*** P<0.001). Abbreviations: SK - SKBR3; BT - BT474; 82H - $CD82^{High}$; HC - Herceptin; P - pellet.

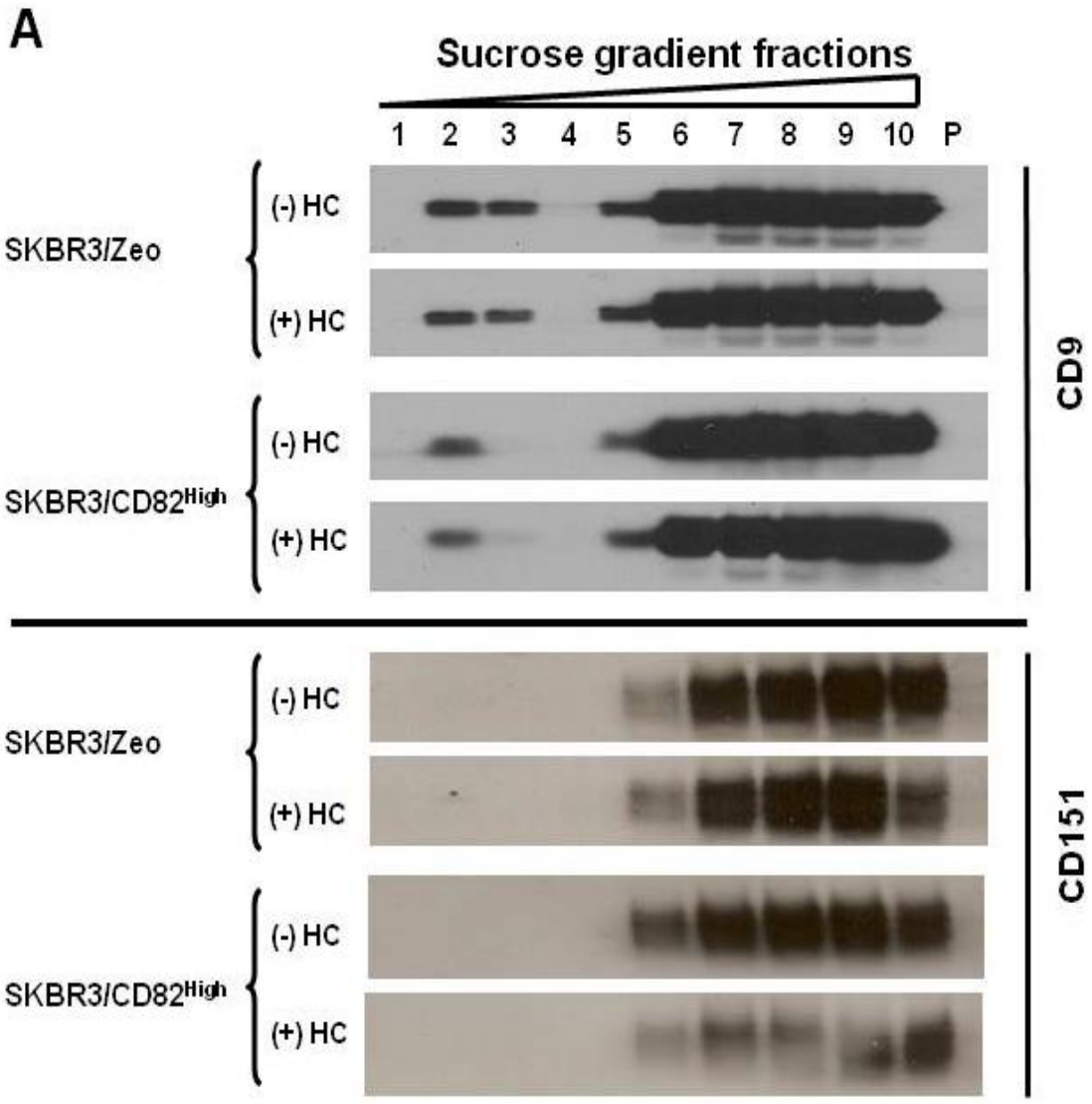
A
Sucrose gradient fractions
1 2 3 4 5 6 7 8 9 10 P
SKBR3/Zeo
(-) HC
(+) HC
SKBR3/CD82High
(-) HC
(+) HC
CD9
SKBR3/Zeo
(-) HC
(+) HC
SKBR3/CD82High
(-) HC
(+) HC
CD151

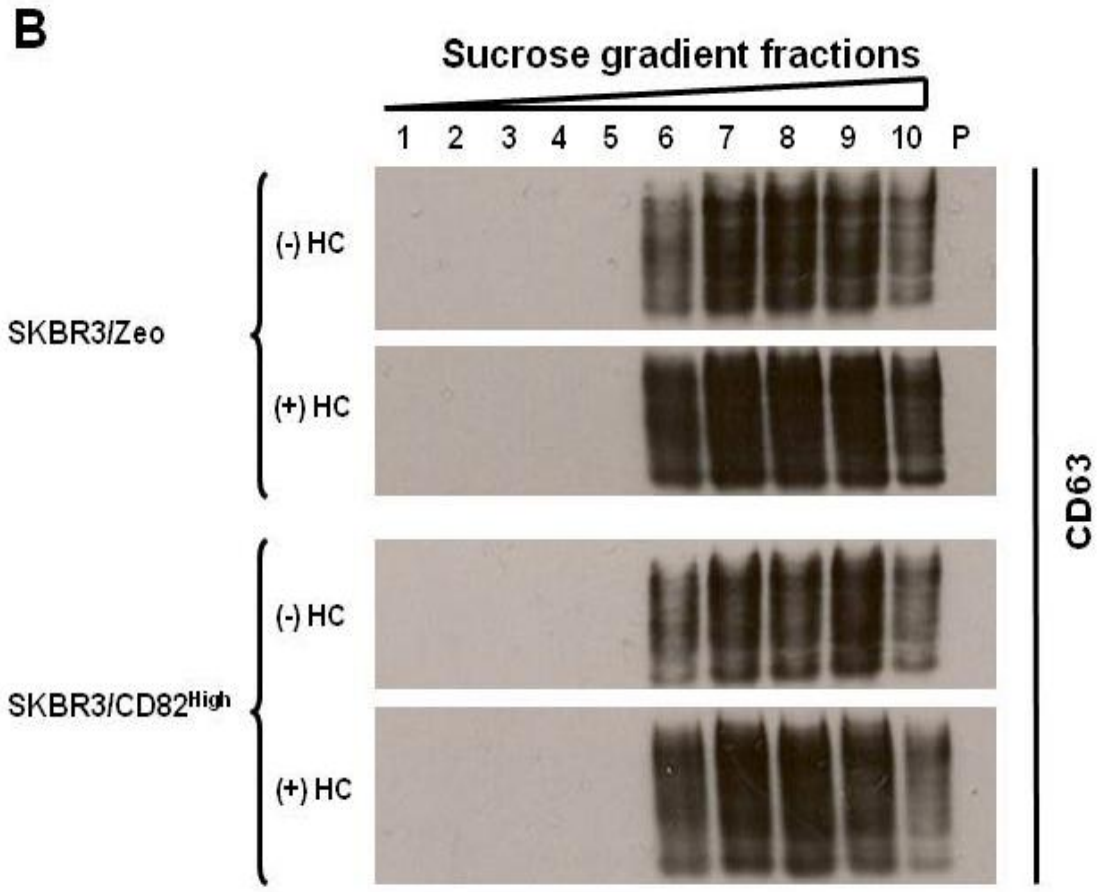

Figure 3.10: The effects of CD82 expression and Herceptin treatment on the distribution of other tetraspanins following lysis with Triton X-100.

SKBR3/Zeo and SKBR3/CD82^{High} cells were treated with Herceptin (10µg/ml) for 1h prior to lysis. Non-treated and treated cells were lysed in ice-cold 1% Triton X-100 followed by fractionation as described in the Materials and Methods under section 2.4. The resulting homogenate of equal protein concentration was centrifuged in a discontinuous sucrose density gradient composed of 90%, 35% and 5% (w/v) sucrose. 10 fractions were collected from the meniscus of the gradient and the pellet was resuspended in Laemmli buffer supplemented with protease and phosphatase inhibitors. Equal amounts of each fraction were mixed with loading buffer and the protein distribution was analysed by SDS-PAGE under non-reducing conditions followed by western blot analysis and probing for the indicated proteins.

3.2.3 The use of fluorescence recovery after photobleaching (FRAP) to monitor the membrane dynamics of ErbB receptors in live cells

3.2.3.1 Herceptin reduces the mobility of ErbB2 in the plasma membrane

FRAP experiments were performed on live cells expressing fluorescent-tagged proteins. A region of the cell was irreversibly bleached using a high laser power followed by monitoring the diffusion of non-bleached fluorescent molecules from the surrounding area into the bleached region. The diffusion of non-bleached molecules into the bleached region is termed fluorescence recovery (Lippincott-Schwartz et al. 2001;Reits and Neefjes 2001). Herein FRAP analysis was performed in order to monitor the membrane dynamics of GFP-tagged ErbB2 and EGFR receptors transfected into cells stably expressing CD82. These experiments were performed in non-treated and Herceptin-treated cells. Where indicated, Herceptin (10µg/ml) was added to the cells at least 1h prior to FRAP analysis. Two parameters were deduced from these experiments; the mobile fraction and the rate of mobility of fluorescent molecules within a defined region of interest (ROI). Both these parameters were determined from the fluorescence recovery curve. Specifically, we aimed to determine the effect of Herceptin on the mobility of ErbB2 and also to determine whether CD82 affected the mobility of EGFR and ErbB2 receptors. SKBR/Zeo and SKBR3/CD82^{High} cells were transiently transfected with GFP-tagged ErbB2. Details of FRAP analysis are outlined in the Materials and Methods under section 2.5.2.

Representative images captured during FRAP analysis are shown in Figure 3.11A. For each FRAP experiment, 10-12 cells expressing similar levels of ErbB2-GFP in the absence and presence of Herceptin were analysed. The images on the left show fluorescence within the region of interest (ROI) (rectangle) before bleaching; central images were acquired immediately after bleaching; and images on the right represent recovery at a given time point after bleaching. From these images, it is clear that ErbB2-GFP was highly expressed on the plasma membrane prior to bleaching and that photobleaching of greater than 50% was achieved in the region of interest, plus a clear indication of fluorescence recovery of ErbB2-GFP molecules into this region over time. Additionally, these images clearly demonstrate that photobleaching was restricted only to the defined ROI and did not bleach the entire cell. Furthermore, these data illustrate that non-treated cells recovered faster than the Herceptin-treated cells (Figure 3.11A; compare top right image to the bottom right).

Figure 3.11B is a representative graph of typical raw data plotted as fluorescence intensity against time. It shows that fluorescence recovery normalised from the pre-bleach fluorescence values (F_i) can be plotted against time. Such analysis was adapted for all FRAP data; therefore, all subsequent FRAP plots herein represent normalised fluorescence recovery plotted against time. Figure 3.12A shows the fluorescence recovery curve of ErbB2-GFP in non-treated and Herceptin-treated SKBR3/Zeo and SKBR3/CD82^{High} cells of pooled results from three independent experiments. These experiments

revealed that ErbB2 is highly mobile, as represented by fluorescence recovery of at least 80% and high mobile fraction values of non-treated cells (Figure 3.12A, top plots and Figure 3.12B). Notably, we found that the mobility of ErbB2 was comparable in both SKBR3/Zeo and SKBR3/CD82^{High} cells. The fluorescence recovery plots for both cell lines superimposed onto one another, indicative that ectopic expression of CD82 does not affect the mobility of ErbB2 in the plasma membrane (Figure 3.12A, top plots). Furthermore, calculations of the mobile fractions were in agreement with the plotted data, whereby 72.5% and 64.4% of ErbB2 was mobile in non-treated SKBR3/Zeo and SKBR3/CD82^{High} cells, respectively (Figure 3.12B and Figure 3.12C; compare the dark blue-filled bar to the light blue-filled bar). Analysis of the statistical significance of the marginal difference in the mobile fraction values revealed that this difference was not statistically significant. In addition, no statistical difference was found between the T_D values (the diffusion time at half fluorescence recovery) of non-treated SKBR3/Zeo and SKBR3/CD82^{High} cells, 88.8s and 78.5s, respectively (Figure 3.12B).

On the other hand, we found that treatment with Herceptin significantly impeded ErbB2 fluorescence recovery in both cell lines. Only 60% fluorescence recovery was detected within the bleached region of both SKBR3/Zeo and SKBR3/CD82^{High} cells following Herceptin treatment (Figure 3.12A, comparing both top plots to the bottom plots). This was also reflected in the mobile fraction calculations, whereby the fraction of mobile ErbB2 was consistently found to be lower in the Herceptin treated cells compared to that of non-treated cells; 41.3% and 42% in treated SKBR3/Zeo and SKBR3/CD82^{High} cells compared to 72.5%

and 64.4% in non-treated cells, respectively (Figure 3.12B and Figure 3.12C). Statistical analysis carried out on these data revealed that the percentage of mobile ErbB2 in each cell line was significantly reduced ($P<0.001$), following Herceptin treatment (Figure 3.12C). Consequently, Herceptin treatment resulted in an increase in recovery time as represented by T_D, the diffusion time at half fluorescence recovery. Non-bleached ErbB2-GFP molecules in Herceptin treated cells took longer to diffuse into the bleached region to achieve half fluorescence recovery than in the non-treated cells. Specifically, in Herceptin-treated SKBR3/Zeo and SKBR3/CD82^{High} cells, the diffusion time at which half of the fluorescence was recovered was 102s and 95s compared to 89s and 79s in non-treated cells, respectively (Figure 3.12B). However, differences between T_D values of non-treated verses treated or indeed between control verses CD82-overexpressing cells were found not be statistically significant. These data demonstrate that even though Herceptin treatment reduces the mobility of ErbB2 within the plasma membrane, the rate of diffusion was comparable between control and CD82-overexpressing cells.

Collectively, these data demonstrate that treatment with Herceptin reduced the mobility of ErbB2 in the plasma membrane, thus suggesting that Herceptin may function by immobilising ErbB2.

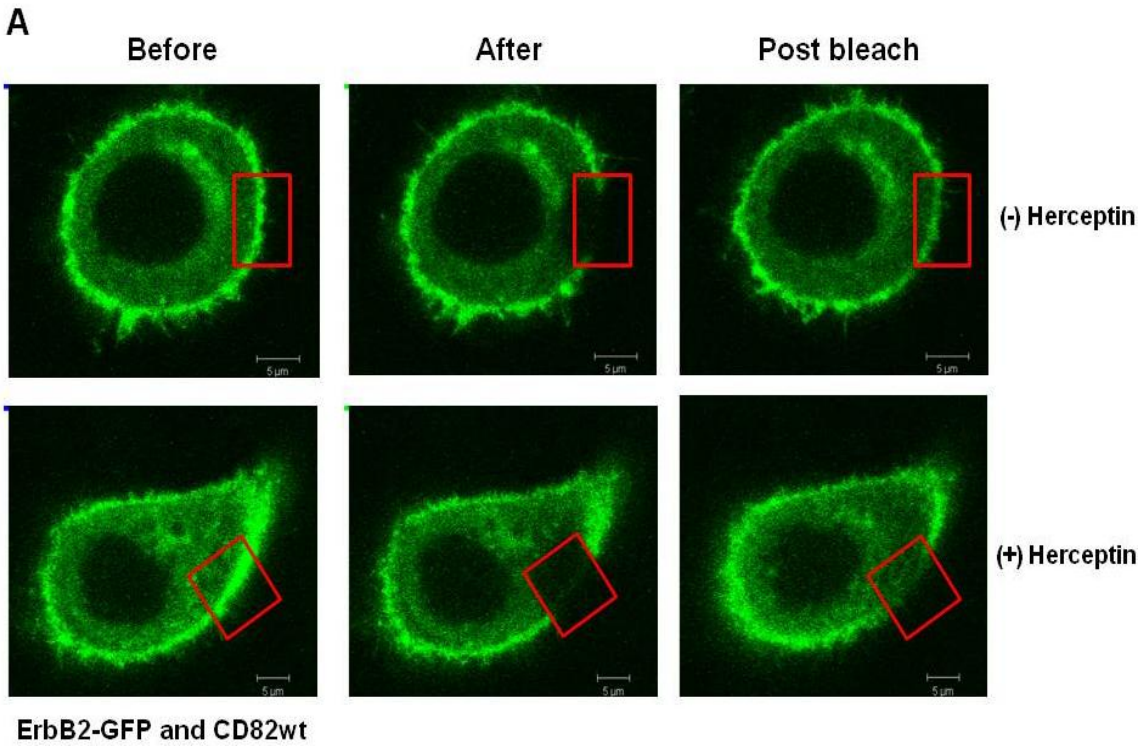
A
Before
After
Post bleach
(-) Herceptin
(+) Herceptin
ErbB2-GFP and CD82wt

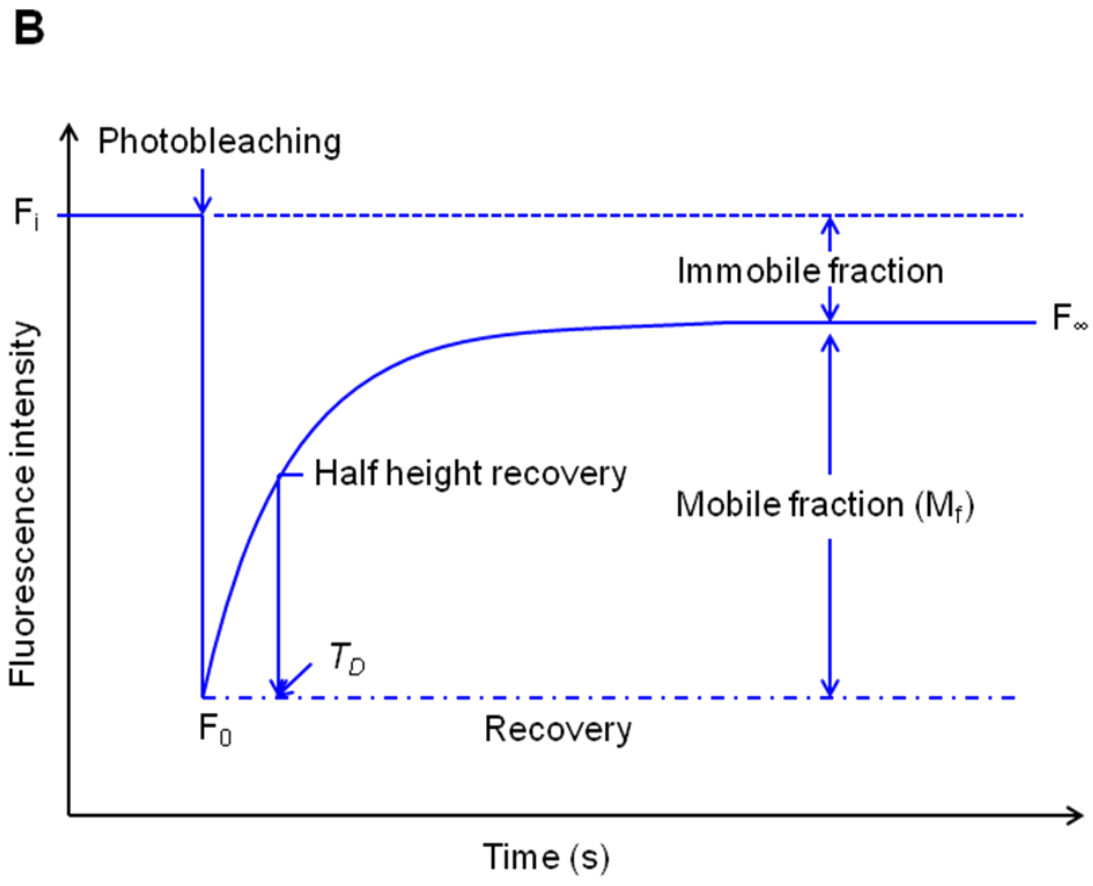
B
Photobleaching
F_i
Immobile fraction
F_∞
Fluorescence intensity
Half height recovery
Mobile fraction (M_f)
T_D
F_0
Recovery
Time (s)

Figure 3.11: Kinetic analysis of fluorescence recovery after Photobleaching (FRAP).

(A) An example of the images used during FRAP analysis. It illustrates non-treated and Herceptin-treated (10µg/ml, minimum 1h) cells before bleaching; immediately after bleaching; and an image at any given time (seconds) postbleaching ErbB2 fluorescence in a region of interest (rectangle). Scale bar = 5µm. (B) An illustration of a typical raw data plot explaining the kinetic analysis of FRAP plotted as fluorescence intensity against time. Figure was adapted from Lippincott-Schwartz et al. and Reits et al. (Lippincott-Schwartz et al. 2001;Reits and Neefjes 2001). The mobile fraction was calculated using the following equation: $M_f = (F_\infty - F_0) / F_i - F_0)$; whereby F_i is the initial fluorescence intensity prior to bleaching; F_0 is the fluorescence intensity immediately after bleaching; and F_∞ is the fluorescence intensity at the point when recovery reaches a plateau, as previously described by Axelrod et al. (Axelrod et al. 1976). T_D is the diffusion time at half fluorescence recovery.

A

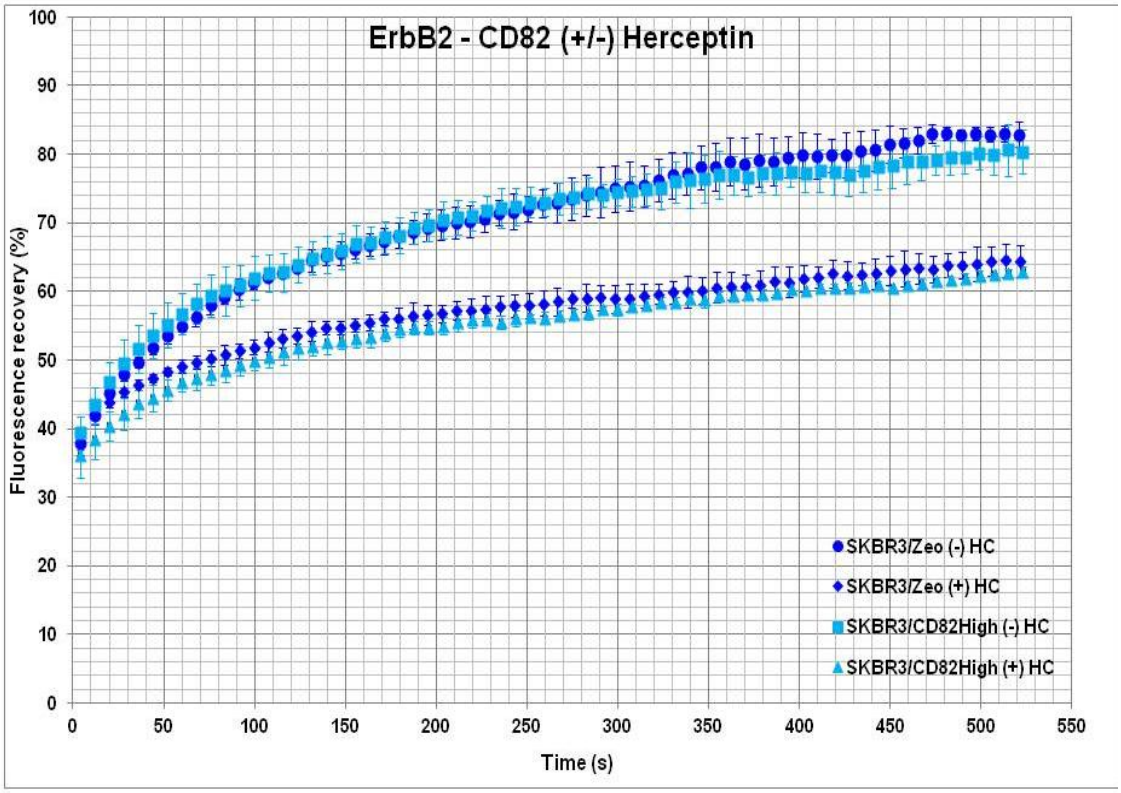

B

ErbB2 – CD82 (+/-) Herceptin

	SK/Zeo (-) HC	SD	SK/Zeo (+) HC	SD	SK/CD82^{High} (-) HC	SD	SK/CD82^{High} (+) HC	SD
Mobile fraction (M_f)	72.5	4.5	41.3	2.2	64.4	3.4	42.0	5.8
T_D	88.8	4.7	102.2	12.0	78.5	9.5	94.5	3.9

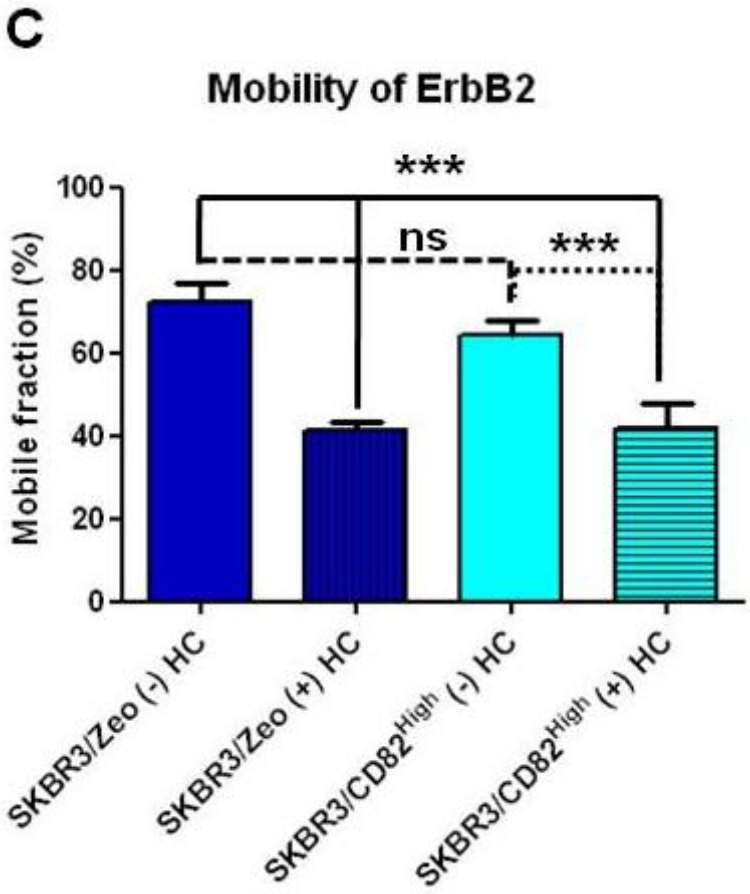

Figure 3.12: The effects of CD82 and Herceptin on the membrane dynamics of ErbB2.

(A) SKBR3/Zeo and SKBR3/CD82^{High} cells stably expressing CD82 were transiently transfected with a plasmid encoding ErbB2-GFP. All cell lines were prepared for FRAP as described in section 2.5.2 of the Materials and Methods. Fluorescence recovery in a bleached region of live cells was monitored by scanning 70 frames per cell, at 7 seconds intervals until 550 seconds post bleach. For each experiment, 10-12 individual cells were bleached and scanned under the same conditions. Shown is pooled data from three independent experiments. (B) Summary of the mobile fraction values. (C) Statistical analysis of the mobile fraction values. Asterisks represent statistical significance as determined by the one-way ANOVA multiple comparison test with the Tukey-Kramer post-test, using GraphPad Prism software. Significance was set at 0.05, whereby (***P<0.001). Data shown as mean ± standard deviation (SD). Abbreviations: ns – not significant; HC – Herceptin.

3.2.3.2 The effect of CD82 in regulating the dynamics of EGFR on the plasma membrane

EGFR, another member of the ErbB family also associates with CD82; and it has previously been reported that CD82 attenuates EGFR signalling partly by changing the compartmentalisation of EGFR (Odintsova et al. 2000;Odintsova et al. 2003). As an additional control for the experiments described above for ErbB2, the same experiments were carried out using EGFR. In these experiments, SKBR3/Zeo and SKBR3/CD82^{High} cells stably expressing CD82 were transiently transfected with EGFR-GFP followed by FRAP analysis. As illustrated in Figures 3.13A and C, expression of CD82 had a subtle negative effect on the mobility of EGFR in the plasma membrane. The percentage of mobile EGFR-GFP was marginally reduced in SKBR3/CD82^{High} cells when compared to that in SKBR3/Zeo cells; 15.4% and 24.1%, respectively (Figure 3.13B). However, statistical analysis of this data revealed no statistical difference between the two cell lines. Thus, these data indicate that under our experimental conditions, we were not able to detect any influence of tetraspanin CD82 in modulation of the membrane dynamics of ErbB2 and EGFR.

A

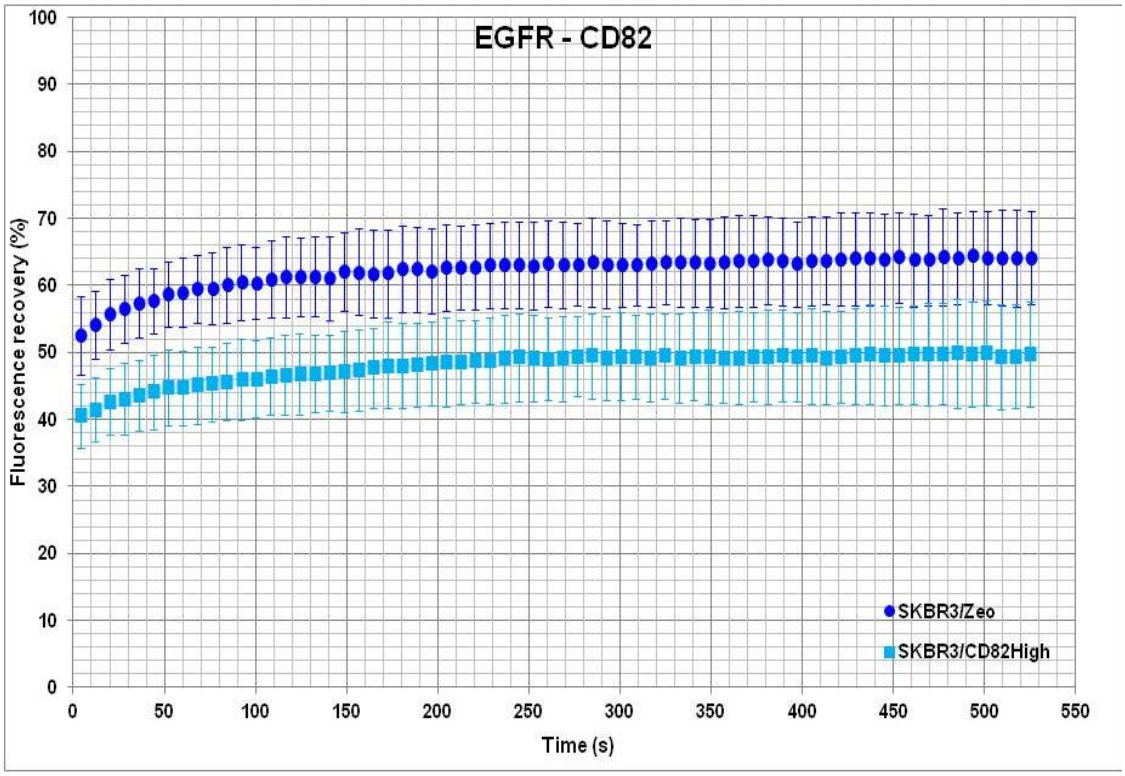

B

EGFR – CD82				
	SKBR3/Zeo	SD	SKBR3/CD82^{High}	SD
Mobile fraction (M_f)	24.1	1.6	15.4	4.4
T_D	52.1	0.0	64.1	16.9

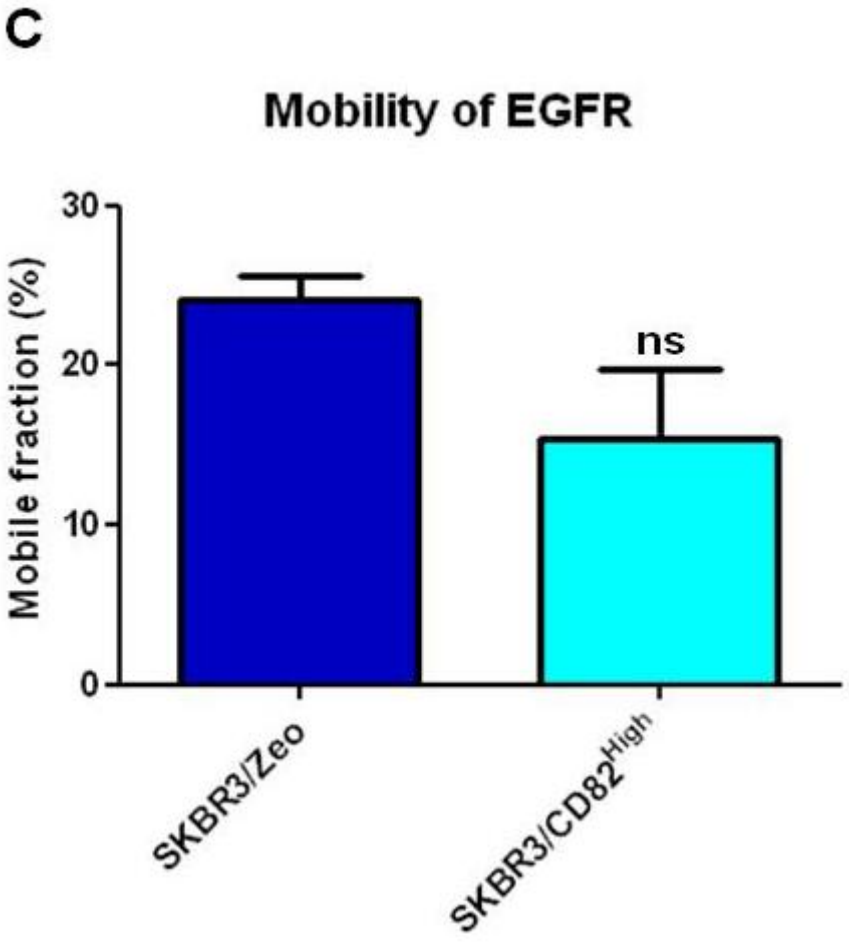

Figure 3.13: The effect of CD82 on the membrane dynamics of EGFR.

(A) SKBR3/Zeo and SKBR3/CD82^{High} cells stably expressing CD82 were transiently transfected with a plasmid encoding EGFR-GFP. All cell lines were prepared for FRAP as described in section 2.5.2 of the Materials and Methods. Fluorescence recovery in a bleached region of live cells was monitored by scanning 70 frames per cell, at 7 seconds intervals until 550 seconds post bleach. At least 10 individual cells were bleached and scanned under the same conditions for each FRAP assay; and 3 individual experiments were carried out. (B) Summary of the mobile fraction values. (C) Statistical analysis of the mobile fraction values as determined by the two-tailed unpaired Student's t-test, using GraphPad Prism software. Significance was set at 0.05. Data shown as mean ± standard deviation (SD). Abbreviation: ns – not significant.

3.2.4 Discussion

Our earlier experiments demonstrated that CD82 modulates the cellular response of ErbB2-positive breast cancer cells to Herceptin treatment. Consequently, we postulated that CD82 could be exerting these effects by regulating the distribution and downstream signalling of the ErbB2 receptor. We explored these hypotheses by initially investigating the effect of CD82 expression on the distribution and dynamics of ErbB2. Since the association of CD82 and ErbB2 was previously reported to be cell type specific (Odintsova et al. 2000), we begun by determining whether this interaction occurred in our model system of SKBR3 and BT474 cells. From our immunoprecipitation experiments, we demonstrated that CD82 associated with ErbB2 in both SKBR3 and BT474 cells. In SKBR3 cells, the amount of ErbB2 in complex with CD82 was higher in the CD82-overexpressing cells than in vector control cells. Contrary however, in BT474 cells, both control and CD82-overexpressing cells had comparable levels of ErbB2 in complex with CD82. The fact that the ErbB2-CD82 interaction was detected in control cells (SKBR3/Zeo and BT474/Puro cells) suggests that the association is not an artefact as a result of CD82 overexpression. In addition, the fact that no significant increase in the amount of ErbB2 in complex with CD82 was observed in BT474/CD82^{High} cells when compared to BT474/Puro cells, as was observed between SKBR3/Zeo and SKBR3/CD82^{High} cells suggests that the increase in the association could be cell-type specific in terms of complex composition and distribution. In view of the fact that the ErbB2-CD82 interaction is disrupted under stringent detergent

conditions and thus suggesting that the association is not direct, it is possible that components of the ErbB2-CD82 complex are different between SKBR3 and BT474 cells. It is possible that in SKBR3/CD82^{High} cells, the membrane distribution of ErbB2 favours its association with CD82 more than its distribution in BT474/CD82^{High} cells. Indeed, the distribution of ErbB2 within membrane fractions was found to be different between SKBR3 and BT474 cells, as discussed below.

It has previously been reported that CD82 changes the compartmentalisation of both EGFR and ErbB2 as assessed by fractionation in a sucrose gradient in other cell lines (Odintsova et al. 2003). Here, we found that ectopic expression of CD82 in ErbB2-overexpressing cells resulted in a change in the distribution of both ErbB2 and CD82 from detergent-soluble microdomains to detergent-insoluble membrane raft microdomains. Notably, we observed that the proportion of ErbB2 redistributed to the raft microdomains was enriched by at least 8-fold following Herceptin treatment. The fact that ErbB2 and CD82 had similar distribution characteristics particularly in the detergent-insoluble fractions suggests that both proteins are likely to be in the same complex. In view of the fact that the CD82-mediated distribution of ErbB2 to light membrane fractions was specifically observed in SKBR3/CD82^{High} cells but not in the BT474/CD82^{High} cells suggests that partitioning of ErbB2 to raft microdomains could be dependent on the expression levels of CD82. It is possible that the redistribution of ErbB2 in the light membrane fractions was not detected in BT474 due to differences in the expression levels of CD82 in these cells compared to that in SKBR3 cells. As previously mentioned, CD82 was

overexpressed by at least 9-fold in the SKBR3/CD82^{High} cells when compared to 2-fold in BT474/CD82^{High} cells. It is therefore feasible that overexpression of CD82 to the level observed in SKBR3/CD82^{High} cells results in changes in the distribution and/or dynamics of not only CD82 itself, but also its association partners such as ErbB2. Indeed Odintsova and colleagues previously reported a change in the distribution of both EGFR and ErbB2 to light membrane fractions in mammary epithelial HB2 cells, in which CD82 was overexpressed by ~15 fold compared to control cells (Odintsova et al. 2003).

The fact that ErbB2 was redistributed to the raft fraction and that the proportion of the receptor redistributed to this fraction was increased following Herceptin treatment suggests that Herceptin could be inducing clustering of ErbB2 within raft domains. These data also suggest a possible role of lipid rafts or components of these microdomains in modulating the function of ErbB2. Lipid rafts are cholesterol- and sphingolipid-enriched membrane microdomains, characterised by their partitioning in low density fractions of a sucrose gradient and their resistance to solubilisation by cold detergent lysis (Orr et al. 2005). Gangliosides are components of lipid rafts and have been implicated by several studies in the regulation of ErbB proteins, including ErbB2 (Milani et al. 2007;Milani et al. 2010;Nagy et al. 2002;Orr et al. 2005;Zurita et al. 2004). Specifically, Nagy and colleagues previously reported that clusters of ErbB2 co-localised with lipid rafts and that the latter influenced the association properties and activity of ErbB2. The authors found that crosslinking of lipid rafts caused segregation of ErbB2 clusters from lipid rafts, which consequently resulted in decreased ErbB2/ErbB3 heterodimerisation, reduced ligand-induced tyrosine

phosphorylation of ErbB2 and downstream adaptor molecules (Nagy et al. 2002). Others demonstrated the involvement of specific gangliosides in the membrane distribution and activity of ErbB2. For example, ganglioside GM3 was reported to colocalise with ErbB2, to play a key role in retaining the receptor in lipid rafts, and it was also found to be strongly associated with tyrosine-phosphorylated ErbB2 (Milani et al. 2007;Sottocornola et al. 2006). Moreover, CD82 has previously been reported to colocalise with gangliosides and cholesterol and to be partially distributed in low-density gradient fractions (Charrin et al. 2003;Delaguillaumie et al. 2004;Odintsova et al. 2003;Todeschini et al. 2007;Todeschini et al. 2008). Gangliosides and cholesterol have previously been reported to play a role in modulating the integrity of tetraspanin-enriched microdomains (TERMs) and the function of individual tetraspanins, as it has been shown particularly for CD82 (Charrin et al. 2003;Delaguillaumie et al. 2004;Odintsova et al. 2006;Todeschini et al. 2007;Todeschini et al. 2008). The link between CD82, gangliosides and cholesterol is reported to be crucial for the metastasis suppressive function of CD82. Disruption of lipid rafts and TERMs by cholesterol depletion or via inhibition of ganglioside biosynthesis has been shown to result in inhibition of CD82-induced adhesion, a decrease in the ability of CD82 to induce tyrosine phosphorylation of various CD82-associated proteins, and abolishes the suppressive effect of CD82 on cell migration (Delaguillaumie et al. 2004;Odintsova et al. 2006;Todeschini et al. 2007;Todeschini et al. 2008). Altogether, these reports highlight the significance of our findings that in addition to the distribution of ErbB2 and CD82 into TERMs, approximately 1.5% and 14%, respectively of these proteins are redistributed to the raft microdomains upon ectopic expression of CD82 in

SKBR3/CD82^{High} cells, which is increased following Herceptin treatment. These findings thus suggest a probable functional relevance of this distribution that warrants further investigation.

We also examined the membrane distribution of other tetraspanins under the same conditions to those mentioned above. Notably, we found that tetraspanin CD9 also partitioned in both light and heavy membrane fractions of a sucrose gradient as CD82, but was not affected by Herceptin treatment. Additionally, we observed that the membrane distribution of tetraspanins CD151 and CD63 was solely detected in the detergent-soluble membrane fractions (Figure 3.10). The fact that we observed two distinct patterns of membrane distribution for the panel of tetraspanins that we studied in this project, not only demonstrates the specificity of our results but also demonstrates that our findings are not an artefact induced by overexpression of CD82. Furthermore, our results are in agreement with other reports and further corroborate the notion of the existence of distinct tetraspanin-enriched microdomains. In this regard, the evidence presented herein supports the existence of CD82-enriched microdomains, as previously proposed by Odintsova and colleagues (Odintsova et al. 2006), whereby they differ from the classical detergent-soluble tetraspanin-enriched microdomains by partially partitioning in the detergent-insoluble gradient fractions; they vary in the tetraspanin content; and are also likely to consist of gangliosides, ErbB2, tetraspanin CD9 amongst other molecules.

Since our fractionation experiments demonstrated that expression of CD82 changed the compartmentalisation of ErbB2, FRAP analysis was performed in

order to examine the membrane dynamics of ErbB2 and EGFR. These experiments were specifically performed in order to determine the effects of CD82 expression and Herceptin treatment on the dynamics of these receptors. We found that both proteins were mobile, but displayed different diffusion characteristics; whereby ErbB2 was found to be more mobile than EGFR. The mobility of each protein was determined from calculations of the mobile fraction based on the fluorescence recovery after photobleaching within a defined region of interest. From these values, we found that a higher fraction of ErbB2 was mobile compared to that of EGFR in both control and CD82-overexpressing cells. Notably, we found that the membrane dynamics of both ErbB2 and EGFR were not affected by expression of CD82 under our experimental conditions; since the lateral diffusion of the receptors on the plasma membrane was comparable in both SKBR3/Zeo and SKBR3/CD82^{High} cells. Although we were unable to detect any CD82-mediated effect on the membrane dynamics of EGFR and ErbB2 under these experimental conditions, it is still possible that CD82 may have a role in modulating the membrane mobility of these receptors under different experimental conditions. Indeed, the effect of CD82 on the diffusion of EGFR has previously been investigated by Danglot and colleagues whereby they demonstrated that depletion of TI-VAMP, a membrane protein or depletion of its cargo, CD82 in HeLa cells resulted in decreased mobility of activated EGFR (Danglot et al. 2010). Additionally, it is widely known that tetraspanins including CD82 are palmitoylated; and several studies have previously demonstrated the importance of palmitoylation for the stability and formation of tetraspanin-enriched microdomains (TERMs) (Berditchevski et al. 2002;Charrin et al. 2002;Yang et al. 2002;Zhou et al. 2004). Specifically,

palmitoylation of CD82 has been shown to regulate not only the compartmentalisation of CD82, but also its association with other tetraspanins, ultimately affecting its cellular function. Moreover, it has previously been reported that disruption of CD82 palmitoylation reverses the functions of wild-type CD82 (Zhou et al. 2004). Since palmitoylation is important for the assembly of TERMs, we postulate that disruption of CD82 palmitoylation may affect the compartmentalisation and/or the membrane dynamics of ErbB proteins. It would be interesting to investigate this further using a palmitoylation-deficient CD82 mutant in comparison to the effects of wild-type CD82.

FRAP experiments in which the cells where treated with Herceptin revealed a decrease in the cell surface dynamics of ErbB2. These observations suggest that Herceptin could be functioning by immobilising ErbB2 possibly by inducing the formation of immobile surface aggregates of the receptor and/or by inducing internalisation of the receptor under our experimental conditions. However, both of these notions are opposed by data from a previously published extensive study by Austin and colleagues into the dynamics of Herceptin-bound ErbB2, whereby the authors demonstrated that Herceptin-bound ErbB2 is not a static pool, but is rather dynamic, undergoing slow internalisation and is efficiently recycled to the cell surface. Furthermore, the authors found no significant effect of Herceptin on the surface levels of ErbB2, thereby opposing the notion of receptor degradation (Austin et al. 2004). It should be noted that although this study by Austin was carried out using SKBR3 cells like we have used herein, there were differences between our present study and theirs which could explain the opposing effects described above. Firstly, in their study, SKBR3

cells were seeded on to poly-L-lysine-coated glass slides, whilst in our study the cells were cultured on non-coated coverglass chambers. Secondly, they used radiolabelled and fluorescence-labelled Herceptin to monitor the dynamics of endogenous ErbB2 whilst we studied transiently transfected GFP-tagged ErbB2 and non-labelled Herceptin. Thirdly, the study by Austin was carried out using flow cytometry to monitor the effect of Herceptin on the surface levels of ErbB2 whilst herein we used FRAP. Finally, both studies differed in the duration of the assays: we monitored the surface dynamics of ErbB2 within approximately 10 minutes whilst the time-points in Austin's study were in hours. It is difficult to draw conclusions since both studies differ in the experimental design. Thus at this stage of our current study, it remains unclear as to the reason behind the decrease in the surface mobility of ErbB2 following Herceptin treatment.

Taken together, these data highlight a profound ability of CD82 to modulate the distribution of ErbB2. These data also suggest that Herceptin may function by affecting the compartmentalisation and diffusion of ErbB2. Furthermore, the CD82-mediated redistribution of ErbB2 to the raft fractions suggests a possible role of CD82 in ErbB2 signalling and will thus be investigated further in the following section.

3.3 The effects of CD82 and Herceptin on cell signalling downstream of the ErbB2 receptor

3.3.1 Ectopic expression of CD82 results in increased MAPK signalling at basal level

The EGF-family of growth factor ligands including heregulin can lead to activation of the ligandless ErbB2 and kinase-dead ErbB3 receptors through heterodimerisation. Once activated the ErbB receptors can in turn activate two key signalling pathways, the PI3K/Akt and MAPK pathways (Figures 1.4 and 1.6, respectively) (Hynes and MacDonald 2009). In order to verify whether ectopic expression of CD82 affects heregulin-induced ErbB signalling, SKBR3/Zeo and SKBR3/CD82^{High} cells were serum-starved overnight prior to stimulation with heregulin for the indicated time intervals. Lysates were collected at the end of each time point followed by western blot analysis for the phosphorylation pattern of various proteins of the PI3K and MAPK signalling pathways.

The C-terminal domain of ErbB3 contains six YXXM motifs, which when phosphorylated serve as a docking site for the SH2 domain of p85 (Olayioye et al. 2000;Smirnova et al. 2012). The tyrosine residue 1289 of ErbB3 resides within the YXXM sequence motif. Thus phosphorylation of ErbB3 at this site (Y1289) would couple the receptor to the PI3K pathway. As shown in Figure 3.14A, both SKBR3/Zeo and SKBR3/CD82^{High} cells displayed comparable

levels of phosphorylated ErbB3 (Y1289) at basal level (lanes 1 and 6). Stimulation with heregulin, a ligand for ErbB3 (and ErbB4) resulted in elevated levels of phosphorylated ErbB3. However, the phosphorylation pattern was different between control and CD82-overexpressing cells. Specifically, in SKBR3/Zeo cells, stimulation of cells with heregulin resulted in a gradual increase in ErbB3 phosphorylation, which peaked at 5 minutes of heregulin stimulation followed by a steady decrease over time (Figure 3.14A). In contrast, the highest level of phosphorylated ErbB3 was observed as early as 2 minutes of heregulin stimulation in SKBR3/CD82^{High} cells followed by a gradual decrease at 5 and 15 minutes, before dephosphorylation occurred by 30 minutes post stimulation (Figure 3.14A). Figure 3.14B (top graph) shows the densitometric analysis of the blots. Akt, which is phosphorylated following activation of ErbB3, displayed a similar kinetic pattern to that of phosphorylated ErbB3; with comparable levels of phosphorylated protein at basal level in both control and CD82-overexpressing cells (Figures 3.14A and B, bottom graph). These data suggest that ectopic expression of CD82 could have a role in modulating the formation of heregulin-induced ErbB3 heterodimers with other ErbB receptors that leads to activation of ErbB3 and its downstream PI3K pathway.

Analysis of the phosphorylation pattern of ErbB2 revealed that this receptor was constitutively active in both control and CD82-overexpressing cells. Interestingly, we observed a difference in phosphorylation of ErbB2 at basal level between the two cell lines; whereby the CD82-overexpressing cells displayed significantly high levels of activated ErbB2 when compared to control

cells (Figure 3.14A, compare lanes 1 and 6). This definitive result was observed with two different antibodies targeting separate phosphorylation sites of ErbB2, namely tyrosines 877 and 1221/1222.

Phosphorylation of ErbB2 at Y877 couples the receptor to Src and its downstream targets including focal adhesion kinase (FAK) and the pro-migratory $p130^{CAS}$-CrkII complex (Cabodi et al. 2010;Muthuswamy et al. 1999). In accordance to this, analysis of Src phosphorylation at Y416 revealed a similar pattern to that observed for pErbB2 (Y877), whereby high levels of pSrc were detected in SKBR3/$CD82^{High}$ cells than those in SKBR3/Zeo cells, at basal level (Figure 3.14A and Figure 3.14C).

Phosphorylation of ErbB2 at Y1221/1222 couples the receptor to the MAPK signalling pathway through binding of Shc, a scaffolding protein which when phosphorylated leads to the recruitment of Grb2, an adaptor molecule; and SOS, a Ras guanosine nucleotide exchange factor (Alroy and Yarden 1997;Muthuswamy et al. 1999). Accordingly, we examined the phosphorylation pattern of MEK1/2, Erk1/2, p38 and JNK MAPK proteins. Similar to ErbB2 phosphorylation, we observed that all MAPK proteins listed above were phosphorylated at higher basal level in the CD82-overexpressing cells when compared to control cells (Figure 3.14A, compare lanes 1 and 6 of corresponding blots). In addition to differences in levels of phosphorylated proteins at the basal level between control and CD82-overexpressing cells, we also observed differences in the phosphorylation kinetics of signalling proteins downstream of ErbB2 following heregulin stimulation. Specifically, we found that

in SKBR3/Zeo cells, the levels of phosphorylated ErbB2 detected at basal level were maintained 2 minutes after stimulation before dephosphorylation by 5 minutes, to almost undetectable levels (Figure 3.14A). Dephosphorylation was maintained 15 minutes post stimulation, but the level of phosphorylated protein began to marginally rise again by 30 minutes of stimulation. In contrast, equal levels of phosphorylated ErbB2 were detected in SKBR3/CD82^{High} cells after 2 and 5 minutes of ligand stimulation. Receptor dephosphorylation occurred within 15 minutes of stimulation and was maintained by 30 minutes. Phosphorylated ErbB2 after 15 and 30 minutes of stimulation was still clearly detectable in the SKBR3/CD82^{High} cells compared to SKBR3/Zeo cells (Figure 3.14A). Notably, the phosphorylation kinetics of activated ErbB2 was comparable for both phosphorylation sites Y877 and Y1221/1222 (Figure 3.14A; Figures 3.14C and D, top graphs). However, the phosphorylation kinetic pattern of activated MAPK proteins was different to that of pErbB2. Stimulation with heregulin resulted in a steady increase in the levels of phosphorylated MAPK proteins in SKBR3/Zeo cells. In contrast however, the level of phosphorylated MAPK proteins remained comparable to the basal levels in SKBR3/CD82^{High} cells (Figure 3.14A and D). A representative densitometric plot for the MAPK proteins is shown for phosphorylated Erk1/2 (Figure 3.14D, bottom plot). These data suggest a possibility of alternative signalling between the control cells and CD82-overexpressing cells. In order to ensure that the difference in phosphorylation levels observed at basal level in both cell lines was not due to changes in total protein expression levels, we also examined the expression levels of total proteins under the same conditions. As shown in Figure 3.14E, no changes in the expression levels of total proteins were observed between

control and CD82-overexpressing cells. Particularly, both cell lines displayed comparable levels of total proteins at basal level (Figure 3.14E, compare lanes 1 and 6).

Analysis of the total tyrosine phosphorylation profile following heregulin stimulation revealed a similar pattern of high protein phosphorylation at basal level in the CD82-overexpressing cells when compared to control cells (Figure 3.14F, compare lanes 1 and 6). Of key interest were the bands detected above 175 kilodaltons (kDa) and at around 60kDa, which could correspond to the ErbB receptors (185kDa) and Src family kinases (60kDa) (Figure 3.14F, red arrows).

In order to determine whether the above described increase in phosphorylation of ErbB2 and MAPK proteins at basal level observed in the CD82-overexpressing cells was a result of serum-starvation, we assessed the phosphorylation levels of ErbB2 and MAPK proteins in cells maintained under complete growth medium without serum starvation. As shown in Figure 3.14G, elevated levels of phosphorylated ErbB2, MEK and Erk proteins were detected in the CD82-overexpressing cells when compared to that of control cells. These findings were thus indicative that the observed phenomenon of CD82-mediated increase in phosphorylation of ErbB2 and MAPK proteins was not an artefact of serum starvation.

Collectively, these data indicate that whilst ectopic expression of CD82 does not affect basal phosphorylation of ErbB3, it does facilitate ligand-induced receptor heterodimerisation and thus activation of ErbB3 and its downstream PI3K/Akt

pathway. Additionally, we present evidence here suggesting that ectopic expression of CD82 in ErbB2-positive breast cancer cells results in elevated ErbB2 phosphorylation under both serum-free and normal culture conditions, which subsequently leads to activation of Src family kinases and the MAPK signalling cascade. These findings thus imply a possible role of CD82 in regulating ErbB signalling.

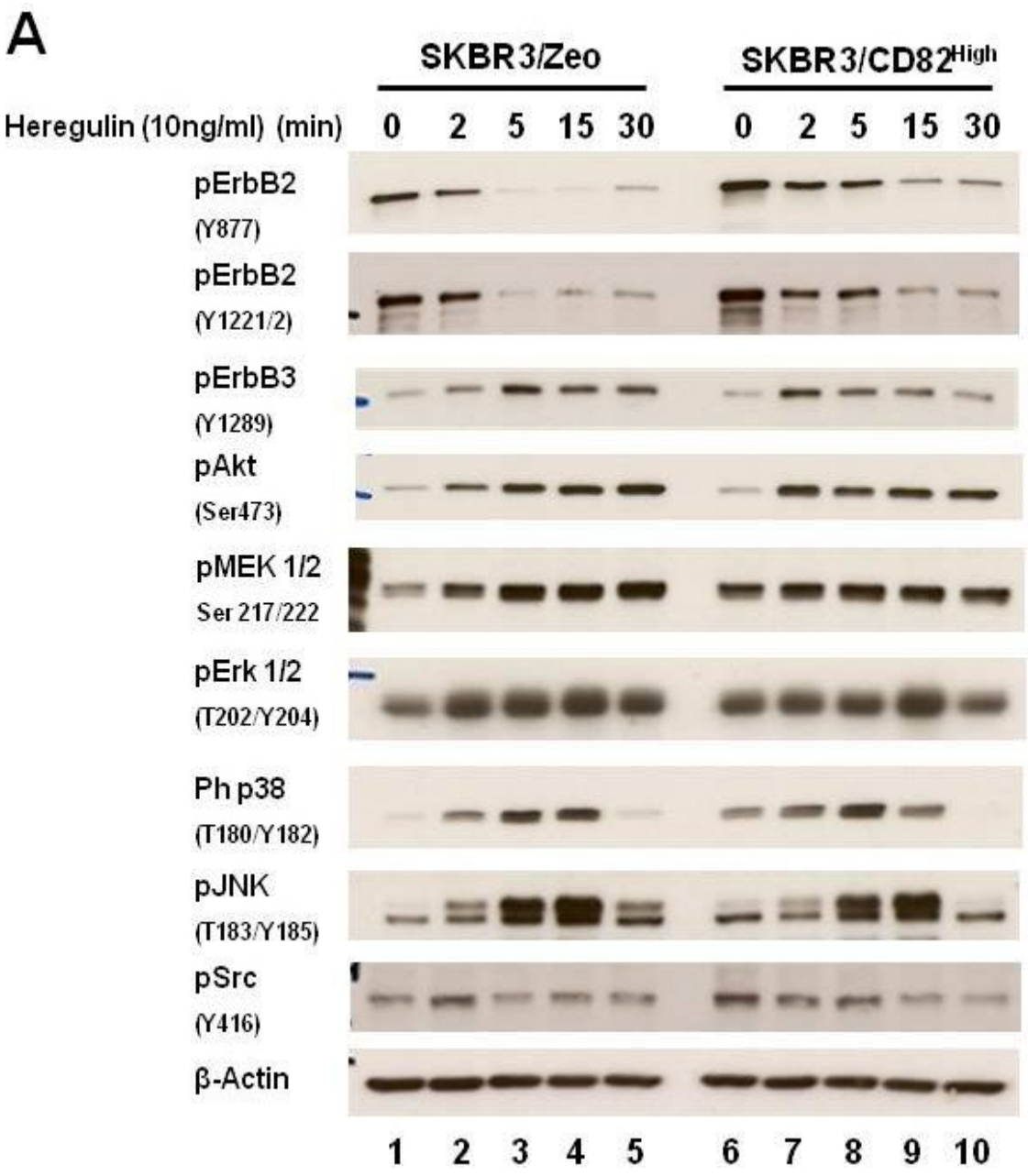
A
SKBR3/Zeo
SKBR3/CD82High
Heregulin (10ng/ml) (min)
0 2 5 15 30 0 2 5 15 30
pErbB2 (Y877)
pErbB2 (Y1221/2)
pErbB3 (Y1289)
pAkt (Ser473)
pMEK 1/2 Ser 217/222
pErk 1/2 (T202/Y204)
Ph p38 (T180/Y182)
pJNK (T183/Y185)
pSrc (Y416)
β-Actin
1 2 3 4 5 6 7 8 9 10

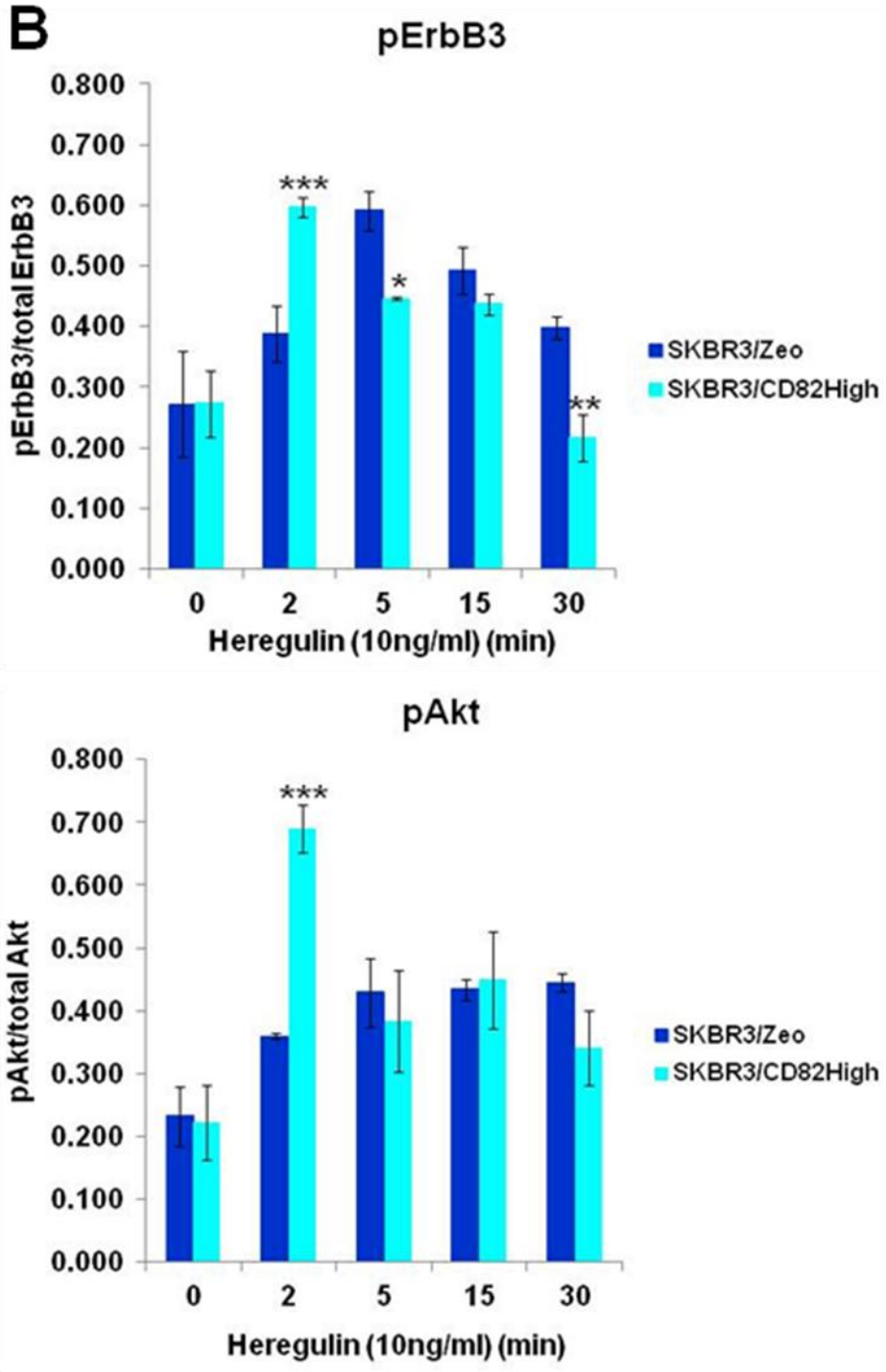
B
pErbB3
pErbB3/total ErbB3
0.800
0.700
0.600
0.500
0.400
0.300
0.200
0.100
0.000
***
*
**
0
2
5
15
30
Heregulin (10ng/ml) (min)
SKBR3/Zeo
SKBR3/CD82High
pAkt
pAkt/total Akt
0.800
0.700
0.600
0.500
0.400
0.300
0.200
0.100
0.000
***
0
2
5
15
30
Heregulin (10ng/ml) (min)
SKBR3/Zeo
SKBR3/CD82High

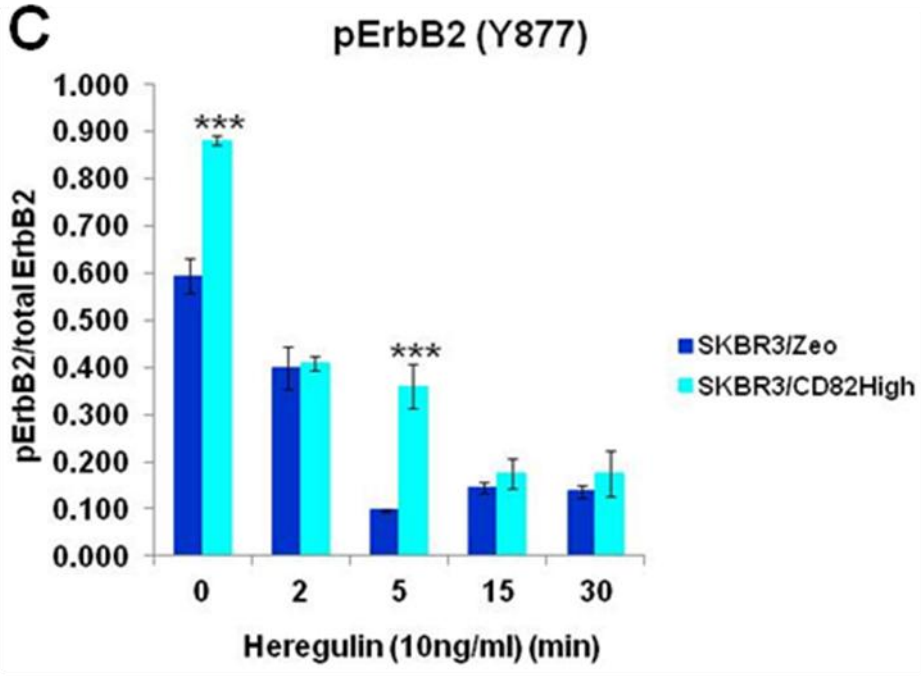
C
pErbB2 (Y877)
pErbB2/total ErbB2
1.000
0.900
0.800
0.700
0.600
0.500
0.400
0.300
0.200
0.100
0.000
***
***
0
2
5
15
30
Heregulin (10ng/ml) (min)
SKBR3/Zeo
SKBR3/CD82High

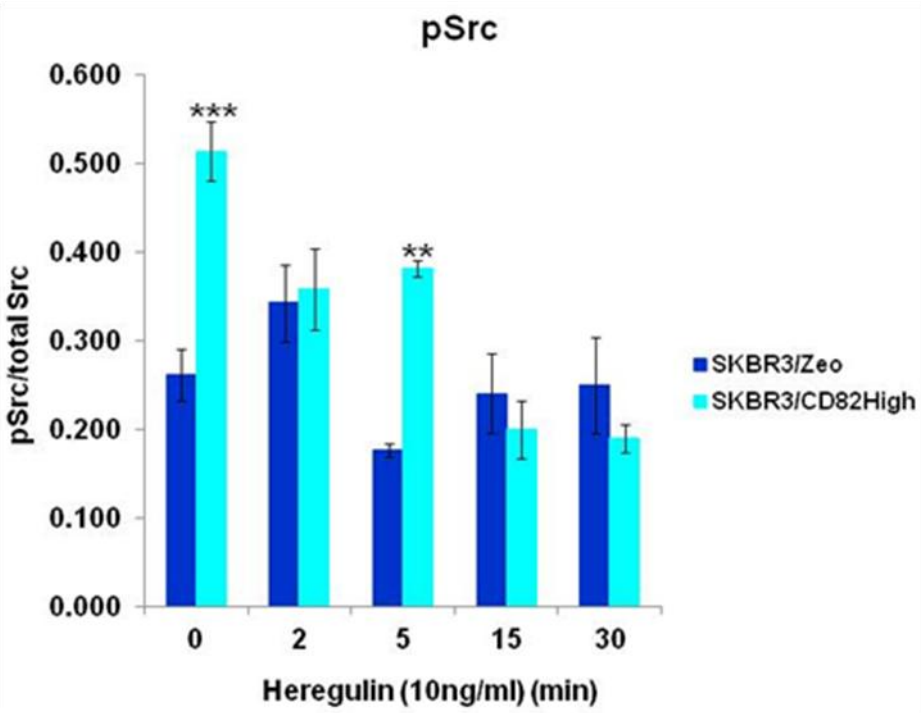
pSrc
pSrc/total Src
0.600
0.500
0.400
0.300
0.200
0.100
0.000
***
**
0
2
5
15
30
Heregulin (10ng/ml) (min)
SKBR3/Zeo
SKBR3/CD82High

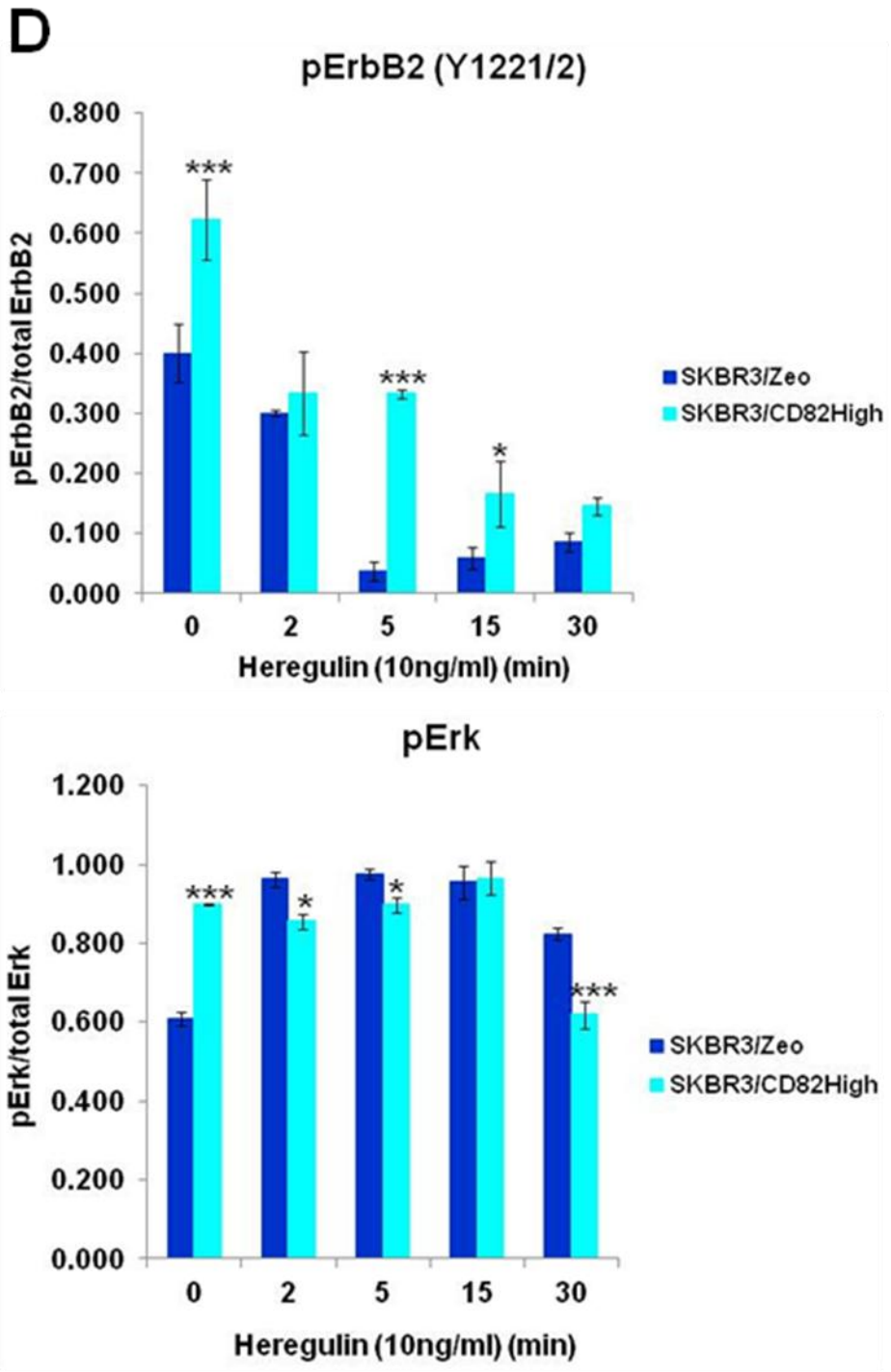
D
pErbB2 (Y1221/2)
pErbB2/total ErbB2
0.800
0.700
0.600
0.500
0.400
0.300
0.200
0.100
0.000
***
***
*
0
2
5
15
30
Heregulin (10ng/ml) (min)
SKBR3/Zeo
SKBR3/CD82High
pErk
pErk/total Erk
1.200
1.000
0.800
0.600
0.400
0.200
0.000
***
*
*
***
0
2
5
15
30
Heregulin (10ng/ml) (min)
SKBR3/Zeo
SKBR3/CD82High

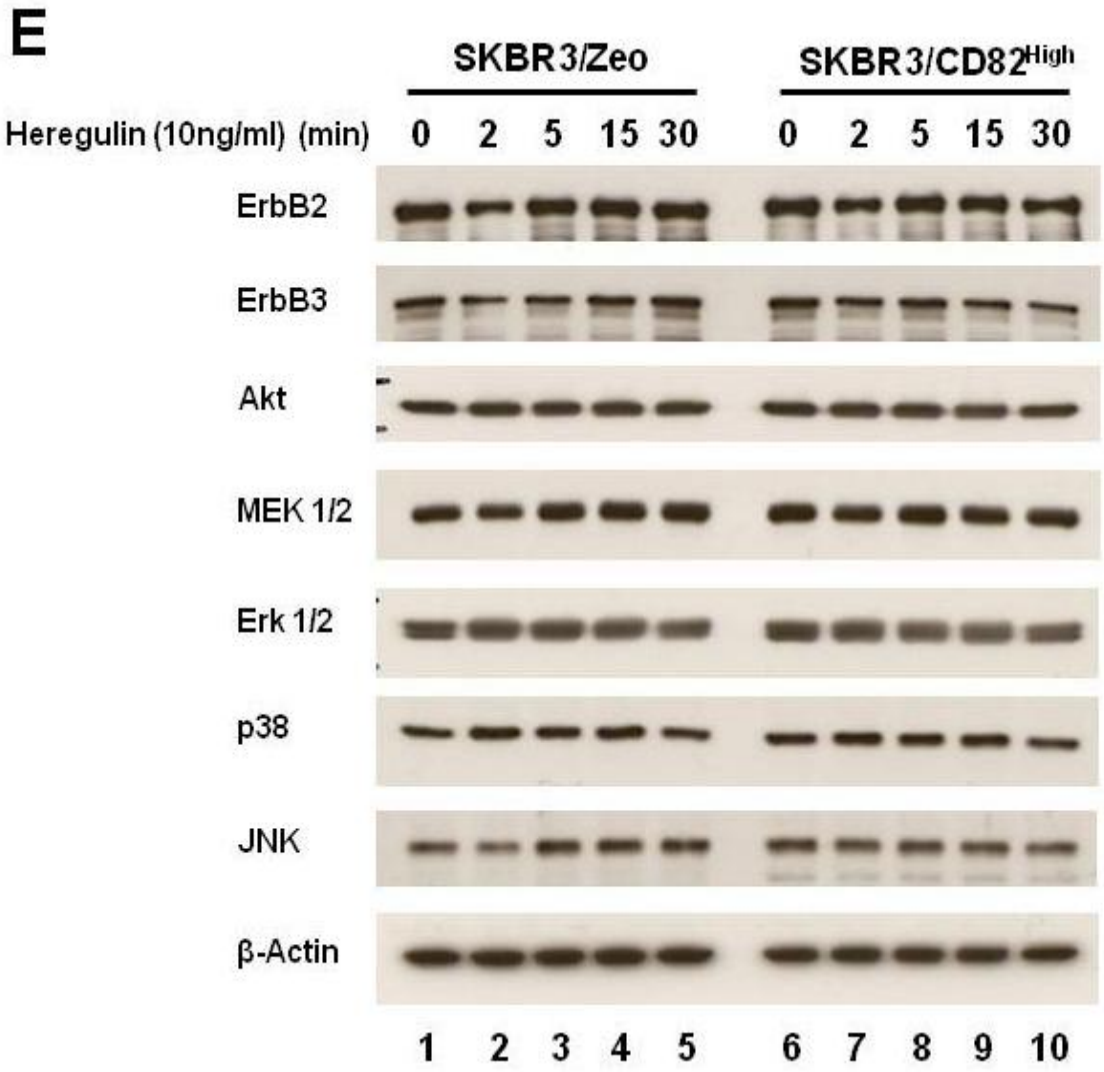
E
SKBR3/Zeo
SKBR3/CD82High
Heregulin (10ng/ml) (min)
0 2 5 15 30
0 2 5 15 30
ErbB2
ErbB3
Akt
MEK 1/2
Erk 1/2
p38
JNK
β-Actin
1 2 3 4 5 6 7 8 9 10

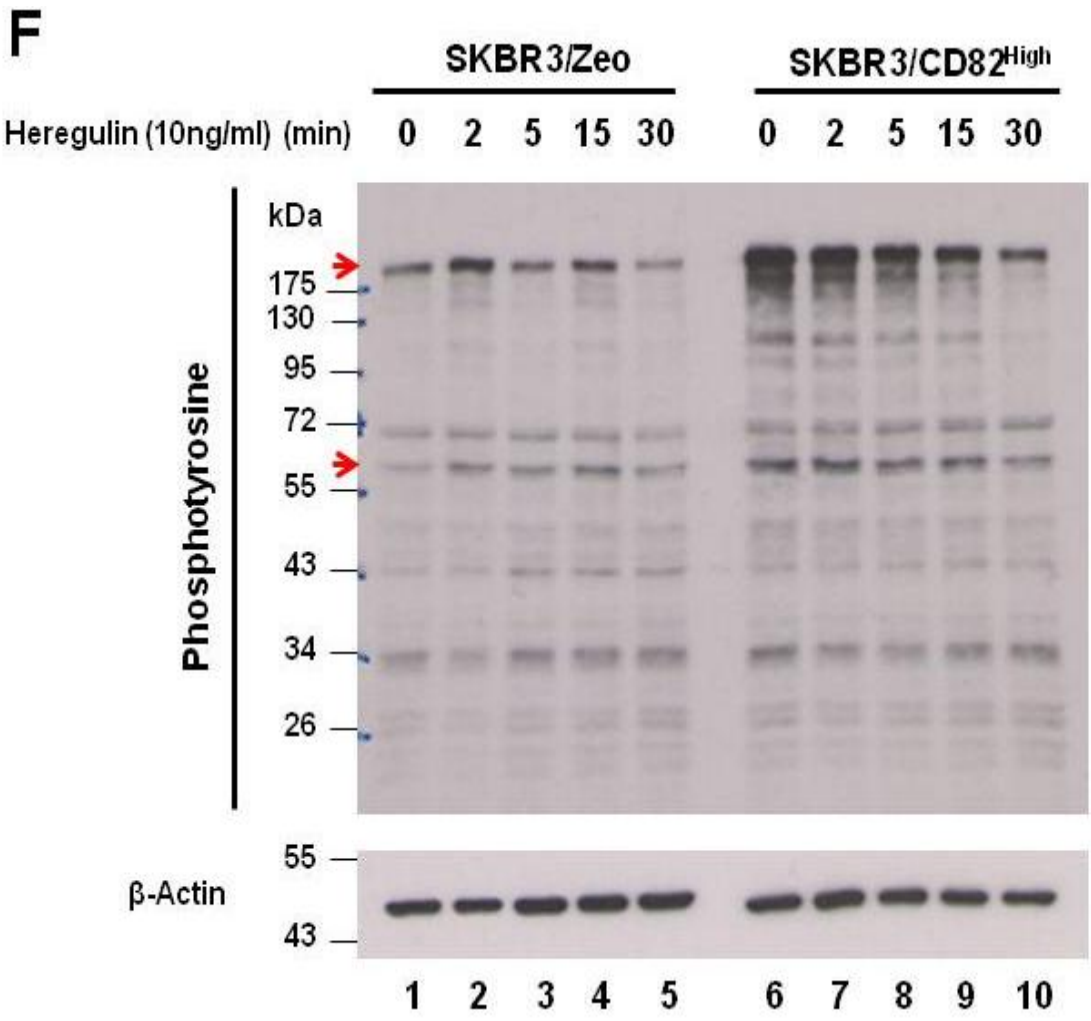
F
SKBR3/Zeo
SKBR3/CD82High
Heregulin (10ng/ml) (min)
0 2 5 15 30
0 2 5 15 30
kDa
175
130
95
72
55
43
34
26
Phosphotyrosine
55
43
β-Actin
1 2 3 4 5 6 7 8 9 10

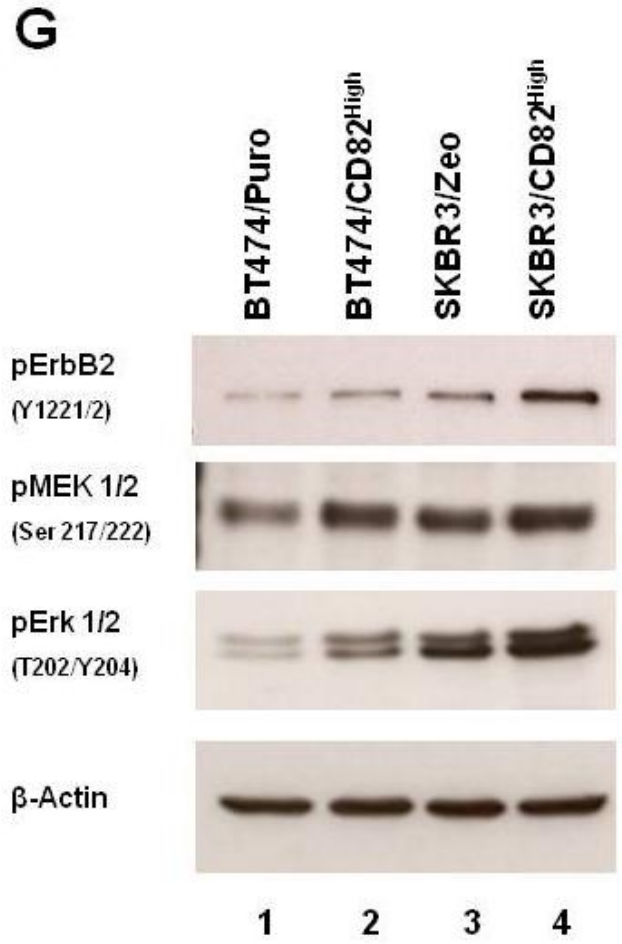

Figure 3.14: The effect of CD82 expression on heregulin-induced signalling.

SKBR3/Zeo and SKBR3/CD82^{High} cells were seeded on plastic until log phase. The cells were serum-starved overnight prior to stimulation with heregulin (10ng/ml) for the indicated time intervals. Lysates were collected at the end of each time-point and subsequently blotted for the indicated molecules using antibodies specific for: (A) phosphorylated proteins; (E) total protein levels; and (F) phosphotyrosine. Shown are representative blots from at least three independent experiments. (B-D) Summary of protein density ratios determined as phosphorylated/total protein from at least three independent experiments. Data shown as mean ± standard deviation. Asterisks represent the statistical significance as determined by the one-way ANOVA multiple comparison test with the Tukey-Kramer post-test, using GraphPad Prism software. Significance was set at 0.05, whereby (*P<0.05), (**P<0.01) and (***P<0.001). (G) Blots demonstrating the expression levels of phosphorylated ErbB2, MEK and Erk proteins from lysates collected from cells cultured in complete growth medium without serum starvation.

3.3.2 The effects of CD82 expression and Herceptin treatment on ErbB signalling

Since the data presented above implied a possible role of CD82 in modulating ErbB2 signalling under serum-free and normal culture conditions, we investigated this further with a specific aim to determine whether ectopic expression of CD82 affected the Herceptin-mediated effect on ErbB2 signalling under serum-free conditions. SKBR3/Zeo and SKBR3/CD82^{High} cells were serum-starved overnight prior to treatment with Herceptin (10µg/ml) for the indicated time intervals. At the end of the incubation period, lysates were collected and the phosphorylation pattern of ErbB2 and ErbB3 along with various downstream target molecules of the PI3K and MAPK pathways was assessed.

Treatment with Herceptin for 30 minutes had minimal effect on ErbB2 phosphorylation in both cell lines. The level of ErbB2 phosphorylation detected after 30 minutes of Herceptin treatment was comparable to that of non-treated cells (Figure 3.15A, compare lanes 1 & 2; lanes 5 & 6). On the other hand, longer incubations of cells with the drug resulted in a gradual decrease in protein phosphorylation levels in a time-dependent manner. Specifically, treatment with Herceptin for 1h caused ~50% reduction in phosphorylated ErbB2 in both cell lines, which was maintained even after 4h incubation (Figures 3.15A, compare lanes 3 & 4; 7 & 8). Densitometry analysis is presented in Figures 3.15B and C. Notably, ErbB2 phosphorylation at Y877 and Y1221/1222

residues displayed a similar kinetic pattern of marginal change to the level of protein phosphorylation within 30 minutes of Herceptin treatment, followed by dephosphorylation after 1h of treatment.

ErbB2 is the preferred heterodimerisation partner for all ErbB members (Yarden and Sliwkowski 2001). The fact that the C-terminal tail of activated ErbB3 contains six docking sites for p85 regulatory subunit of PI3K, makes it a potent receptor for recruiting p85 and thus activation of the PI3K signalling pathway; ultimately leading to phosphorylation of Akt. Therefore, formation of ErbB2/ErbB3 heterodimers would potently lead to activation of the PI3K pathway. One of the proposed mechanisms of action for Herceptin is its ability to inhibit PI3K signalling by promoting Akt dephosphorylation through enhanced PTEN phosphatase activity (Nagata et al. 2004;Valabrega et al. 2007). Indeed, several studies have demonstrated the Herceptin-mediated inhibitory effect on PI3K/Akt signalling (Le et al. 2005a;Nagata et al. 2004). In this regard, we proceeded with experiments to examine the cellular response of CD82-overexpressing cells to Herceptin treatment in comparison to control cells by use of western blot analysis. In agreement with previously published reports, we found that treatment of SKBR3/Zeo and SKBR3/CD82^{High} cells with Herceptin resulted in a decline in the levels of phosphorylated ErbB3 in a time-dependent manner. Specifically, treatment for 30 minutes had minimal effect on the level of phosphorylated ErbB3 in both cell lines (Figure 3.15D; compare lanes 1 & 2; 5 &6). On the other hand, we found that longer incubation of cells with the drug for up to 4h resulted in dephosphorylation of ErbB3 to almost undetectable levels (Figures 3.15D and E). Notably, no differences in the amount of

phosphorylated ErbB3 at basal level were observed between SKBR3/Zeo and SKBR3/CD82^{High} cells (Figure 3.15D, lanes 1 and 5). Additionally, both cell lines responded to Herceptin in a similar manner with comparable kinetics (Figure 3.15E).

Assessment of the effects of CD82 expression and Herceptin treatment on the phosphorylation of Akt revealed similar results to those described above for phosphorylated ErbB3. Firstly, we found that ectopic expression of CD82 did not affect the phosphorylation of Akt at basal level; since comparable levels of phosphorylated Akt were detected in non-treated SKBR3/Zeo and SKBR3/CD82^{High} cells (Figure 3.15D, compare lanes 1 and 5). Secondly, treatment with Herceptin resulted in a time-dependent inhibition of Akt phosphorylation, with a kinetic pattern that was comparable in both control and CD82-overexpressing cells (Figures 3.15D and F). The effect of Herceptin on Akt phosphorylation was more pronounced 4h after treatment - at least a 60% decrease in phosphorylated Akt was observed at this time-point compared to a 24% reduction observed after 1h treatment in both cell lines (Figure 3.15F).

In addition to PI3K signalling, we also investigated the effects of CD82 and Herceptin on MAPK signalling. Consistent with our previously described data, we observed higher levels of phosphorylated MAPK proteins in non-treated CD82-overexpressing cells when compared to non-treated control cells (Figure 3.15G, compare lanes 1 and 5). In general, both cell lines had a similar kinetic pattern in their response to Herceptin treatment; whereby treatment with Herceptin for 30 minutes induced an initial increase in phosphorylation of MAPK

proteins that decreased over time. Besides the initial observation of higher levels of phosphorylated proteins at basal level in the CD82-overexpressing cells when compared to controls, we did not observe any CD82-mediated effect on the cellular response to Herceptin between the cell lines, under these experimental conditions. Assessment of the effect of Herceptin on protein phosphorylation relative to the phosphorylation levels of non-treated cells revealed no differences between SKBR3/Zeo and SKBR3/CD82^{High} cells in their response to Herceptin under these experimental conditions (Figure 3.15I). Although the CD82-overexpressing cells show higher levels of phosphorylated proteins when compared to control cells following Herceptin treatment (Figure 3.15G), further analysis of the data relative to non-treated controls revealed that this was in accordance to the initially high basal levels (Figure 3.15I).

Similar results were observed with BT474 cells under the same conditions. These experiments revealed a similar CD82-mediated effect of elevated phosphorylation of ErbB2 and MAPK proteins at basal level in BT474/CD82^{High} cells when compared to BT474/Puro cells. Additionally, treatment with Herceptin resulted in Akt dephosphorylation in the BT474 cells, albeit with a kinetic pattern different to that observed in SKBR3 cells (Appendix IV, Supplementary Figure 4).

A

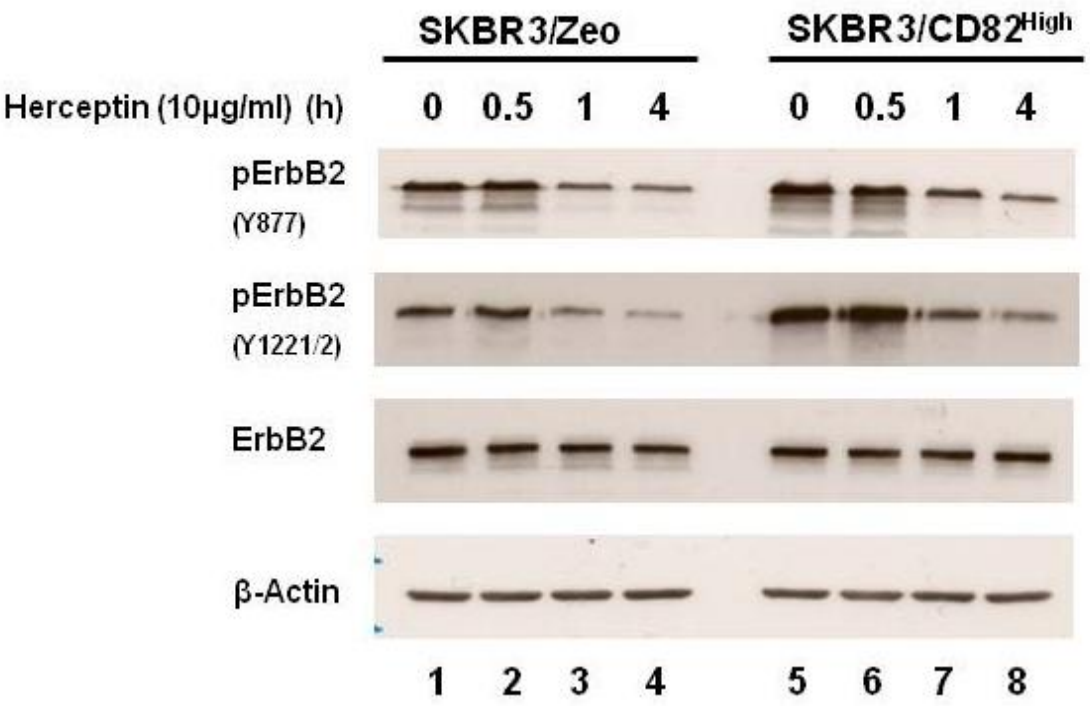
SKBR3/Zeo
SKBR3/CD82High
Herceptin (10µg/ml) (h)
0 0.5 1 4
0 0.5 1 4
pErbB2
(Y877)
pErbB2
(Y1221/2)
ErbB2
β-Actin
1 2 3 4 5 6 7 8

B

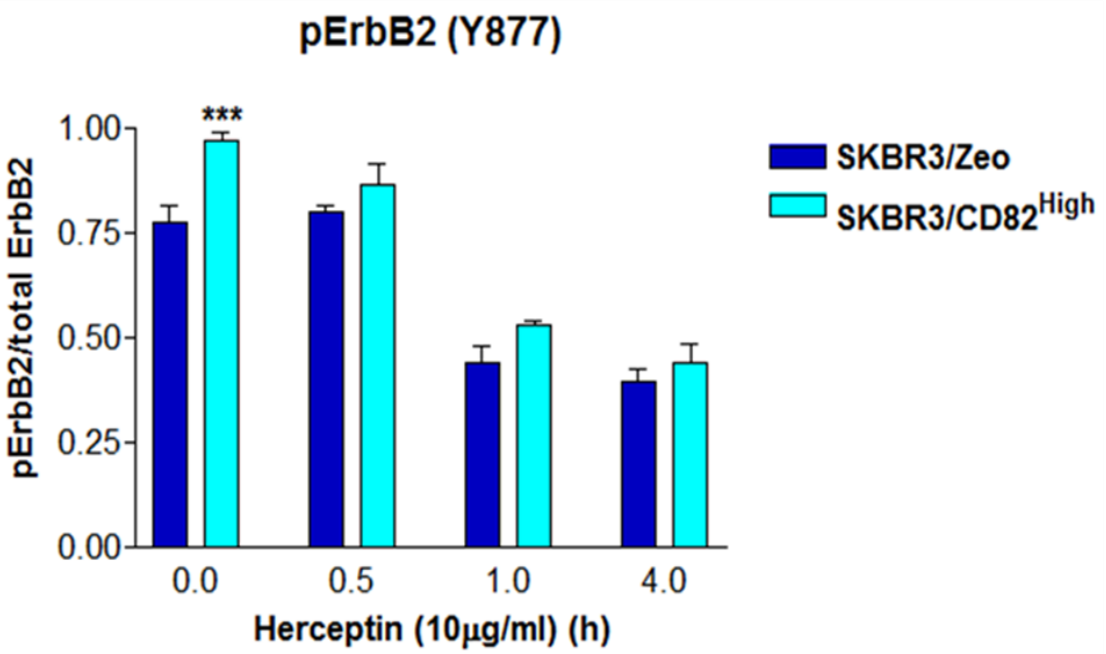
pErbB2 (Y877)
pErbB2/total ErbB2
1.00
0.75
0.50
0.25
0.00
***
0.0
0.5
1.0
4.0
Herceptin (10µg/ml) (h)
SKBR3/Zeo
SKBR3/CD82High

C

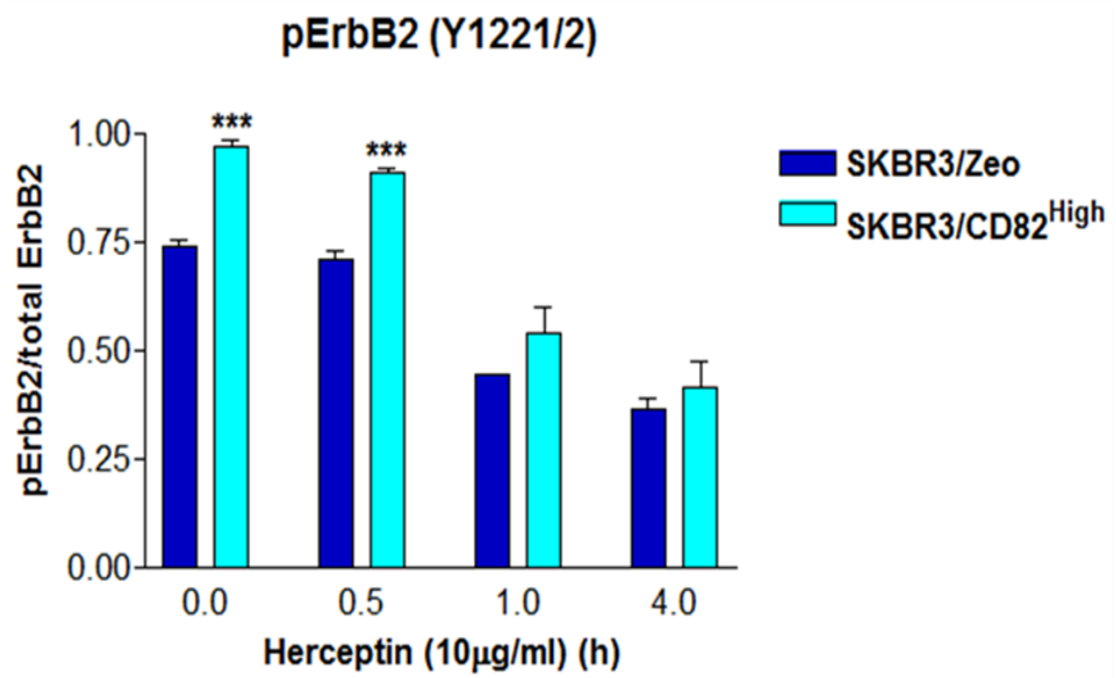
pErbB2 (Y1221/2)
pErbB2/total ErbB2
1.00
0.75
0.50
0.25
0.00
***
***
0.0
0.5
1.0
4.0
Herceptin (10µg/ml) (h)
SKBR3/Zeo
SKBR3/CD82High

D

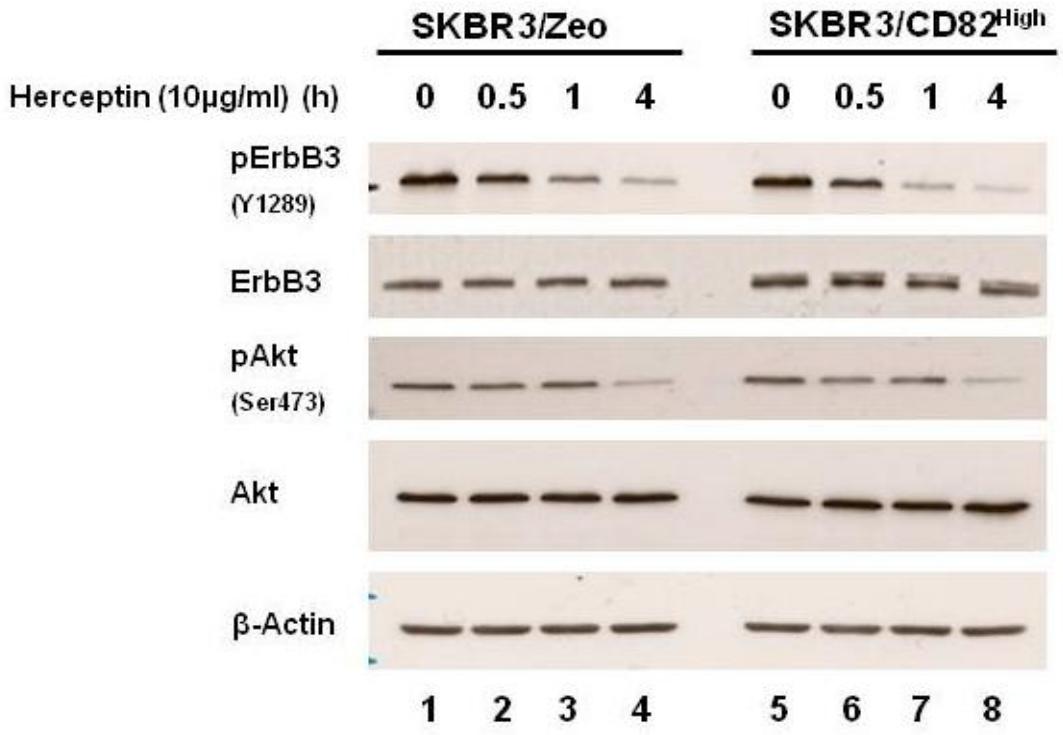
SKBR3/Zeo
SKBR3/CD82High
Herceptin (10µg/ml) (h)
0 0.5 1 4
0 0.5 1 4
pErbB3
(Y1289)
ErbB3
pAkt
(Ser473)
Akt
β-Actin
1 2 3 4 5 6 7 8

E

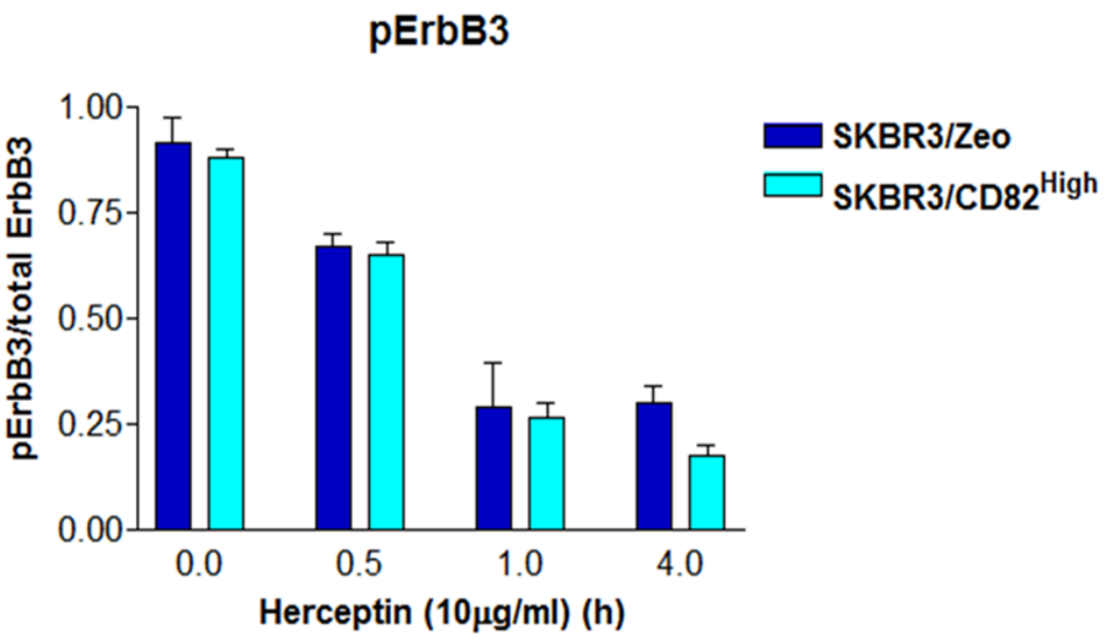
pErbB3
pErbB3/total ErbB3
1.00
0.75
0.50
0.25
0.00
0.0
0.5
1.0
4.0
Herceptin (10µg/ml) (h)
SKBR3/Zeo
SKBR3/CD82High

F

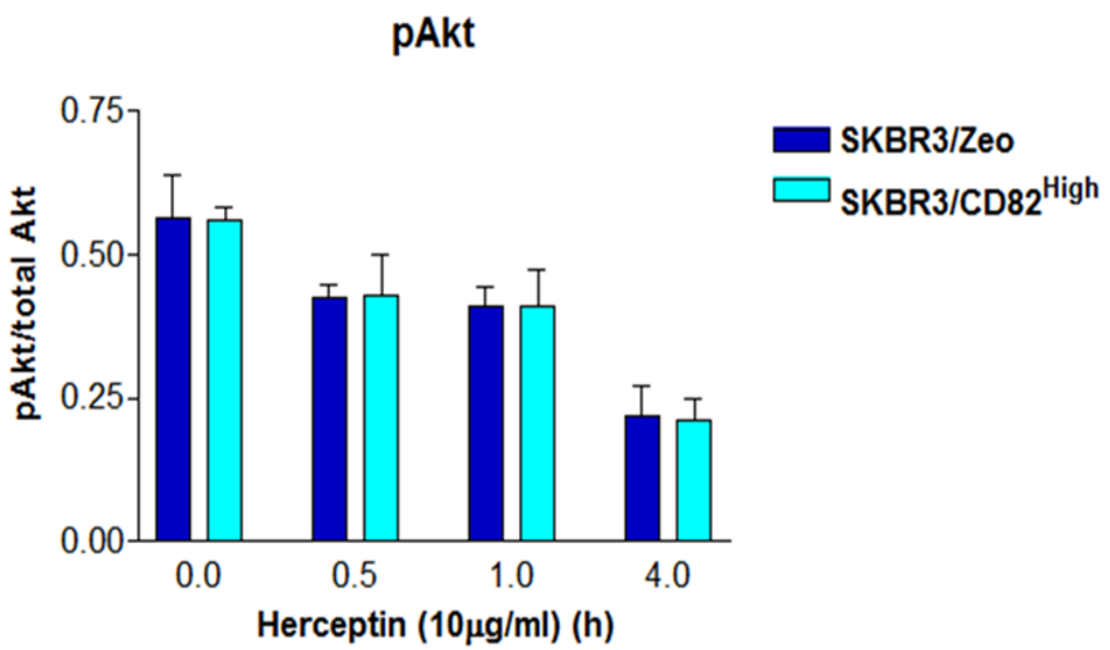
pAkt
pAkt/total Akt
0.75
0.50
0.25
0.00
0.0
0.5
1.0
4.0
Herceptin (10µg/ml) (h)
SKBR3/Zeo
SKBR3/CD82High

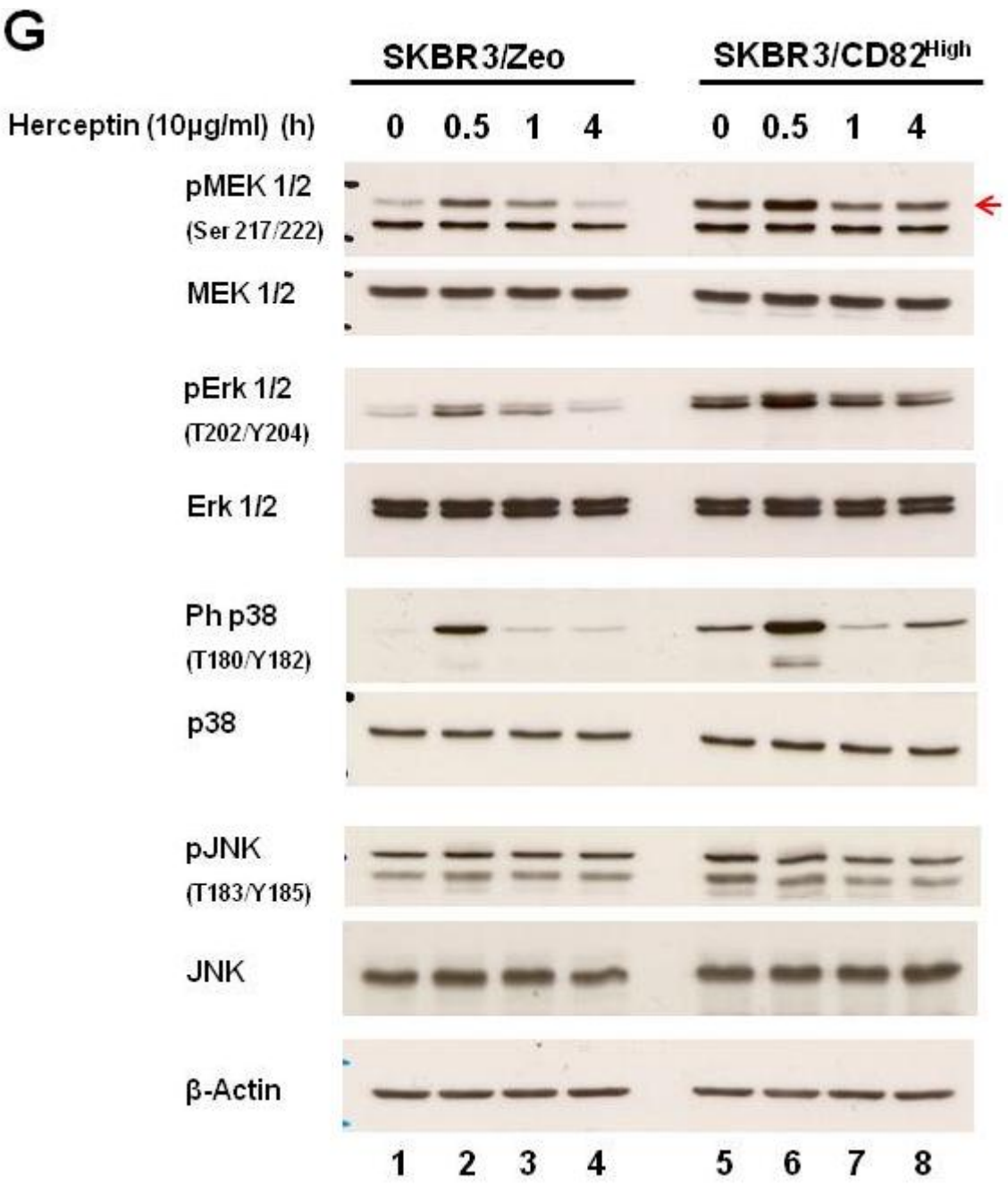
G
SKBR3/Zeo
SKBR3/CD82High
Herceptin (10µg/ml) (h)
0 0.5 1 4
0 0.5 1 4
pMEK 1/2
(Ser 217/222)
MEK 1/2
pErk 1/2
(T202/Y204)
Erk 1/2
Ph p38
(T180/Y182)
p38
pJNK
(T183/Y185)
JNK
β-Actin
1 2 3 4 5 6 7 8

H

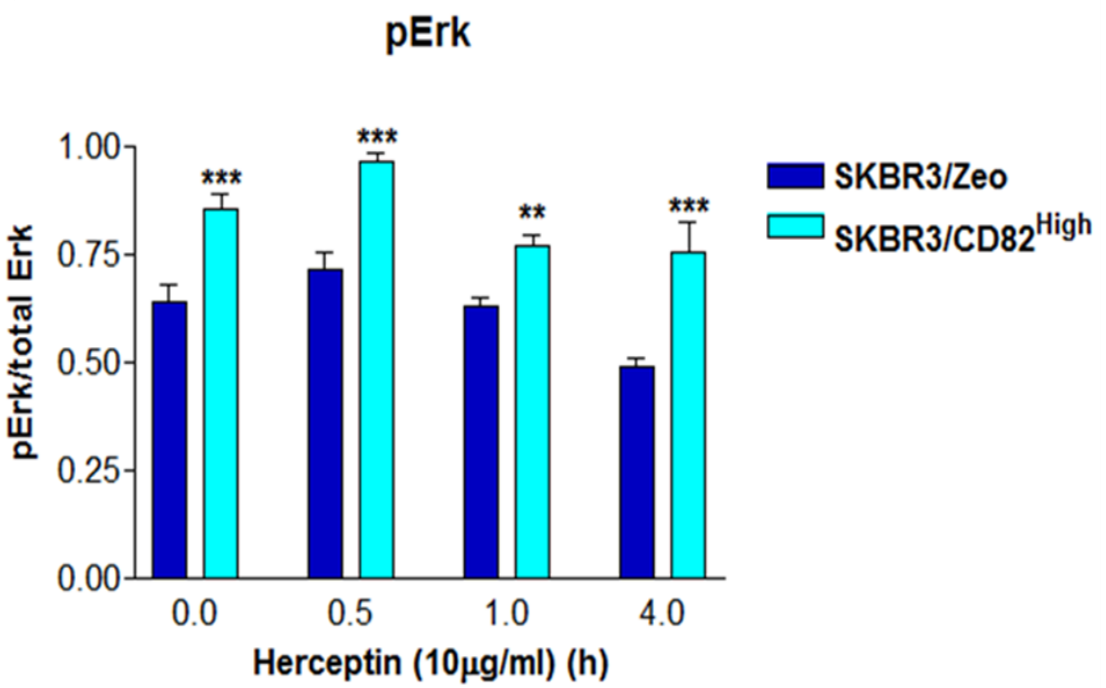
pErk
pErk/total Erk
1.00
0.75
0.50
0.25
0.00
***
***
**
***
0.0
0.5
1.0
4.0
Herceptin (10µg/ml) (h)
SKBR3/Zeo
SKBR3/CD82High

I

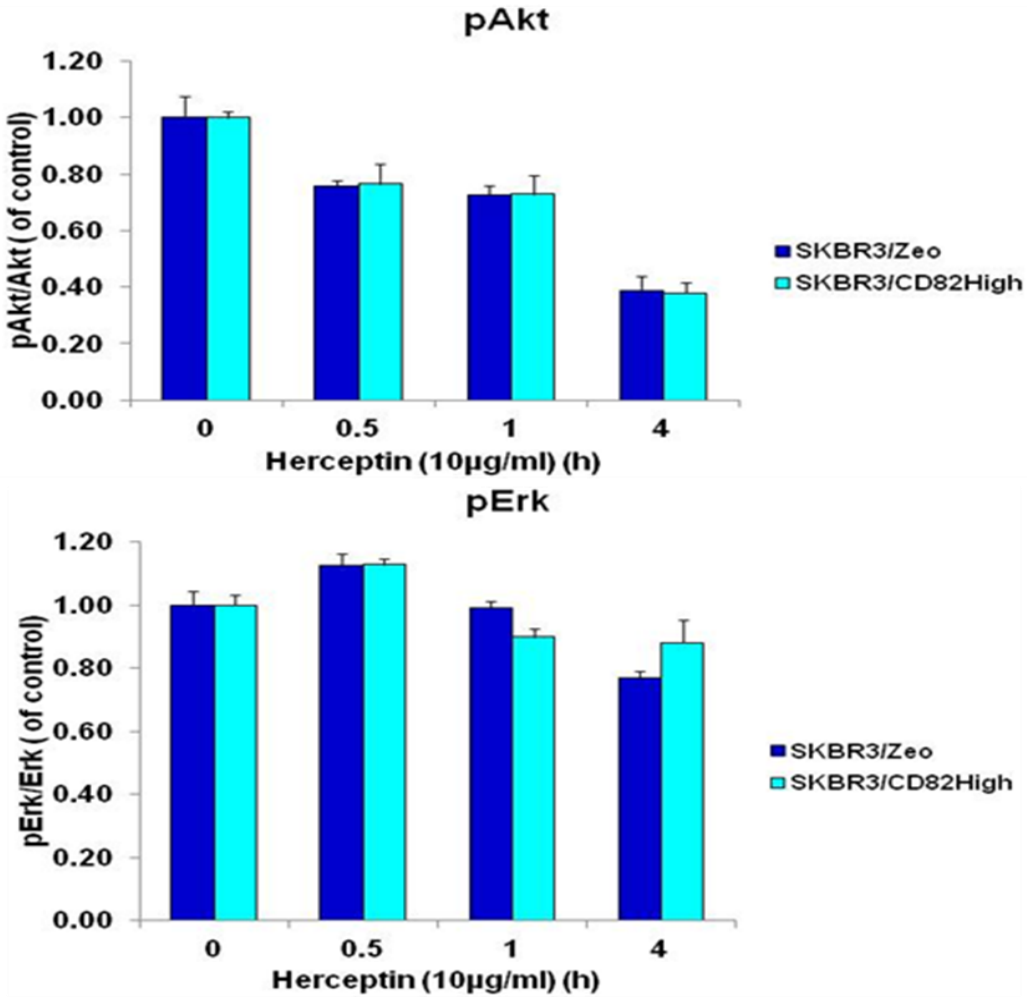

Figure 3.15: The effects of CD82 expression and short incubations of Herceptin on ErbB signalling.

SKBR3/Zeo and SKBR3/CD82^{High} cells in log phase were serum-starved overnight prior to treatment with Herceptin (10µg/ml) for the indicated time intervals. Lysates were collected at the end of each time-point and subsequently blotted for the indicated molecules in order to evaluate: (A) ErbB2 phosphorylation; (D) PI3K/Akt signalling; and (G) MAPK signalling. (B; C; E; F and H) Summary of protein density ratios determined as phosphorylated/total protein from three independent experiments. (I) Densitometry ratios of pAkt and pErk determined as phosphorylated/total protein, relative to non-treated control. Data shown as mean ± standard deviation. Asterisks represent the statistical significance as determined by the one-way ANOVA multiple comparison test with the Tukey-Kramer post-test, using GraphPad Prism software. Significance was set at 0.05, whereby (**P<0.01) and (*** P<0.001).

In addition to the short time-course experiments of Herceptin treatment described above, analysis of signalling was performed after longer incubations of cells with Herceptin (treatment for up to 72h). From these experiments, it was clear that the previously described inhibitory effect of Herceptin on Akt phosphorylation was maintained for up to 48h of treatment, in both SKBR3/Zeo and SKBR3/CD82^{High} cells. However, we observed that by 72h of Herceptin treatment the phosphorylation levels of Akt had increased to levels observed at baseline in both cell lines (Figures 3.16A and B). In contrast, longer incubations of cells with Herceptin had minimal inhibitory effect on MAPK signalling at 24 and 48h in SKBR3/Zeo cells (Figures 3.16A, C and D). In fact, we observed that in the SKBR3/Zeo, but not SKBR3/CD82^{High} cells, prolonged treatment with Herceptin resulted in a switch in signalling pathways. Specifically, MAPK signalling became more prominent with increased levels of phosphorylated MAPK proteins being observed especially at 24 and 48h of Herceptin treatment when Akt phosphorylation was significantly inhibited (Figures 3.16A and D). Conversely, in the CD82-overexpressing cells, treatment with Herceptin for longer incubations resulted in a time-dependent gradual decrease in phosphorylation levels of MAPK proteins (Figures 3.16A and D). These data thus suggest a CD82-mediated effect of modulating the cellular response to prolonged treatment with Herceptin.

These experiments were also performed in BT474/Puro and BT474/CD82^{High} cells albeit with somewhat contrasting findings. Specifically, the phosphorylated level of Akt after 24h of Herceptin treatment was comparable to that detected at

baseline in both cell lines (Appendix IV, Supplementary Figure 5, compare lane 1 &2; 5 & 6). The Herceptin-mediated Akt dephosphorylation occurred at 48h and 72h of treatment. Notably, the switch in signalling pathways from the inhibited PI3K to MAPK signalling as observed in the SKBR3/Zeo cells was not apparent in BT474 cells. Phosphorylation of MAPK proteins and Akt followed a similar kinetic pattern in both BT474/Puro and BT474/CD82^{High} cells (Appendix IV, Supplementary Figure 5).

Collectively, these findings further support the notion of a possible role of CD82 in modulating ErbB signalling that is specific for the MAPK signalling cascade. Additionally, these data demonstrate the ability of Herceptin to inhibit not only the PI3K/Akt signalling pathway, but also the MAPK signalling cascade.

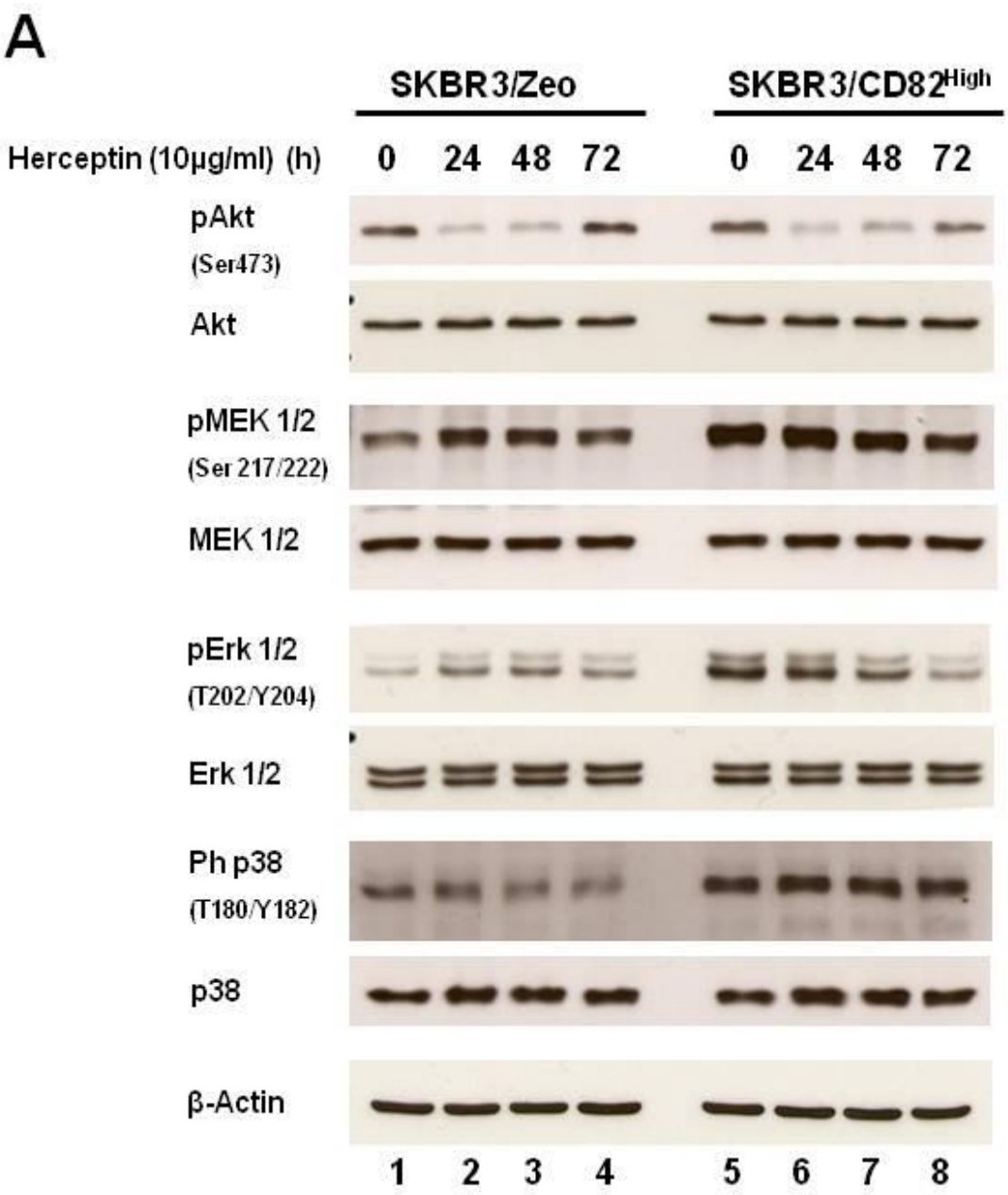
A
SKBR3/Zeo
SKBR3/CD82High
Herceptin (10µg/ml) (h)
0 24 48 72
0 24 48 72
pAkt
(Ser473)
Akt
pMEK 1/2
(Ser 217/222)
MEK 1/2
pErk 1/2
(T202/Y204)
Erk 1/2
Ph p38
(T180/Y182)
p38
β-Actin
1 2 3 4 5 6 7 8

B

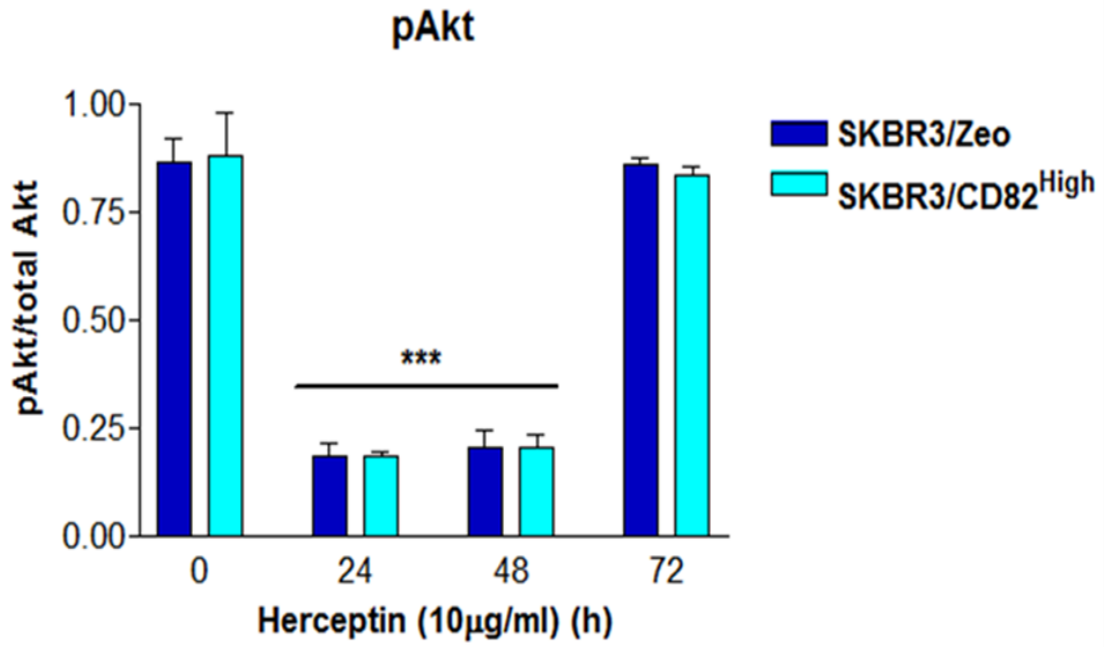
pAkt
pAkt/total Akt
1.00
0.75
0.50
0.25
0.00
***
0
24
48
72
Herceptin (10µg/ml) (h)
SKBR3/Zeo
SKBR3/CD82High

C

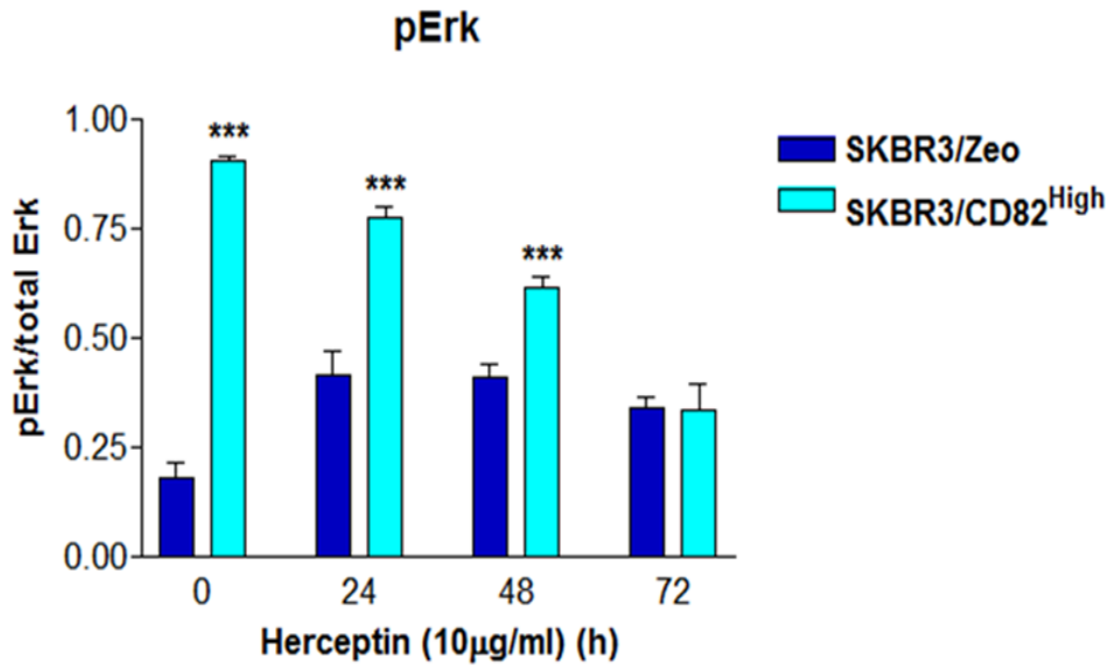
pErk
pErk/total Erk
1.00
0.75
0.50
0.25
0.00
***
***
***
0
24
48
72
Herceptin (10µg/ml) (h)
SKBR3/Zeo
SKBR3/CD82High

D

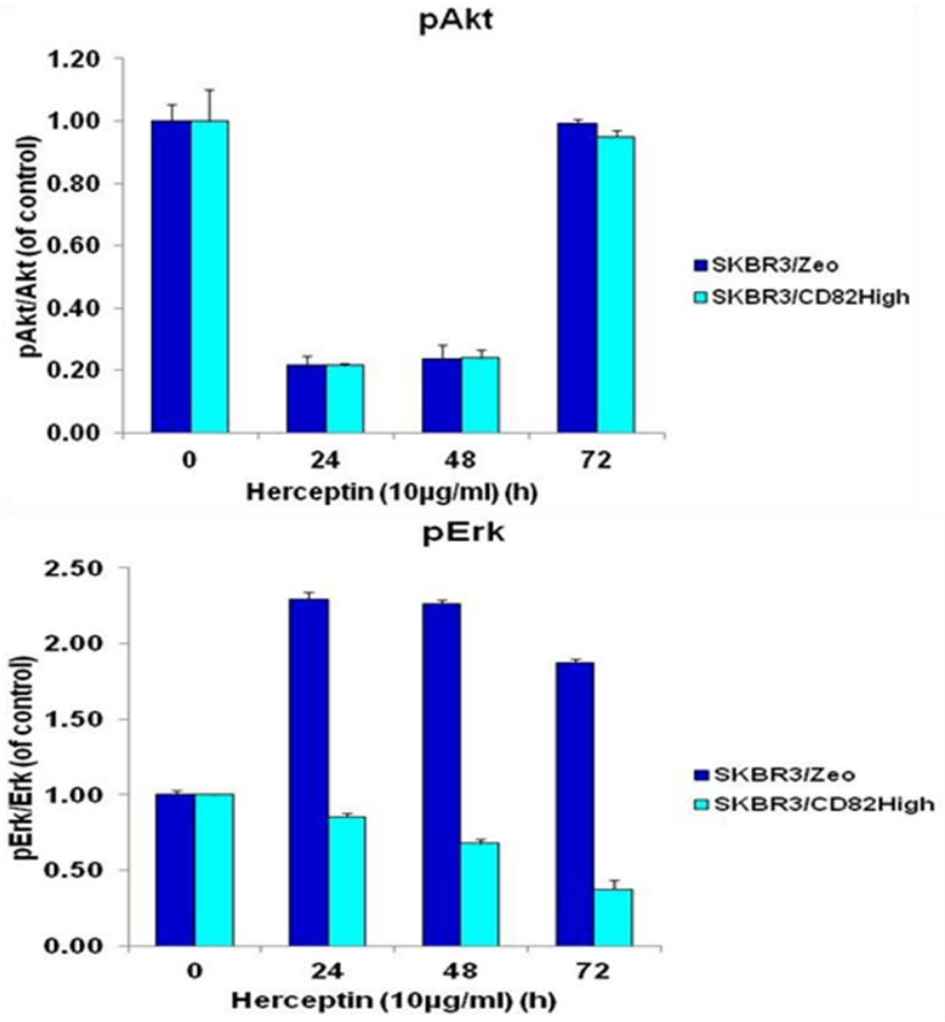

Figure 3.16: The effects of CD82 expression and long incubations of Herceptin on ErbB signalling.

SKBR3/Zeo and SKBR3/CD82^{High} cells in log phase were serum-starved overnight before treatment with Herceptin (10µg/ml) for the indicated time intervals. Lysates were collected at the end of each time-point and subsequently blotted for the indicated molecules in order to evaluate: (A) PI3K/Akt and MAPK signalling. (B and C) Summary of protein density ratios determined as phosphorylated/total protein from three independent experiments. (D) Densitometry ratios of pAkt and pErk determined as phosphorylated/total protein, relative to non-treated control. Data shown as mean ± standard deviation. Asterisks represent the statistical significance as determined by the one-way ANOVA multiple comparison test with the Tukey-Kramer post-test, using GraphPad Prism software. Significance was set at 0.05, whereby (*** P<0.001).

3.3.2.1 The effect of CD82 depletion on the basal levels of phosphorylated Erk

In order to verify whether the high basal levels of phosphorylated MAPK proteins previously observed in CD82-overexpressing cells was CD82-dependent; we assessed Erk phosphorylation in CD82-depleted cells under the same conditions. ErbB2-positive breast cancer cells depleted in CD82 (ZR75.30/shCD82) were generated via a lentiviral transduction method using lentiviral constructs containing short hairpin RNA (shRNA) that specifically targets wild-type CD82 as described in section 2.1.5 of the Materials and Methods. Control cell lines (ZR75.30/GFP) expressing an empty vector were also generated. Western blot analysis shows that the level of CD82 was decreased by at least 80% in ZR75.30/shCD82 cells compared to control cells (Figure 3.17A). The cells were serum-starved overnight; and where indicated, Herceptin (10µg/ml) was added for the indicated time intervals. Analysis of Erk phosphorylation in the CD82-depleted cells revealed no sign of high levels of basal phosphorylated Erk that was consistently observed previously in the CD82-overexpressing cells. Rather, in three independent experiments, we consistently observed comparable levels of phosphorylated Erk at basal level in ZR75.30/shCD82 when compared to control cells (Figure 3.17B, compare lanes 1 and 5). Densitometry analysis is presented in Figure 3.15C. Notably, the response to Herceptin of both ZR75.30/GFP and ZR75.30/shCD82 cells was comparable. The fact that depletion of CD82 had no effect on the

phosphorylation levels of Erk in these cells suggests cell type specific mechanisms.

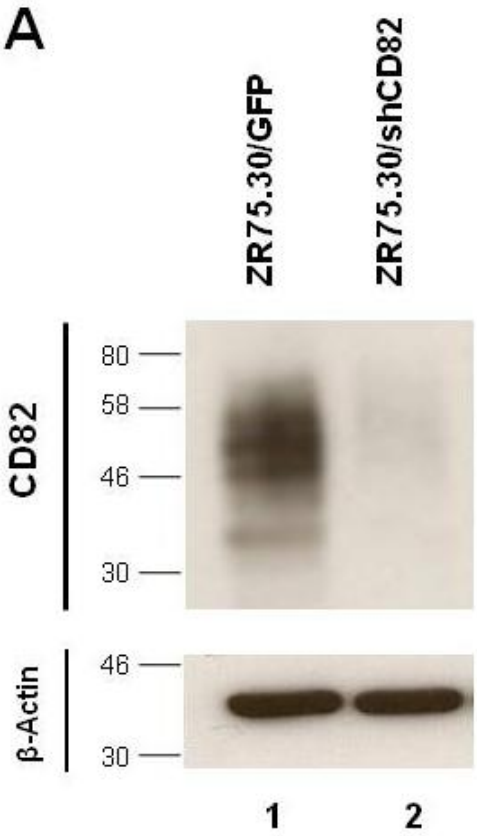

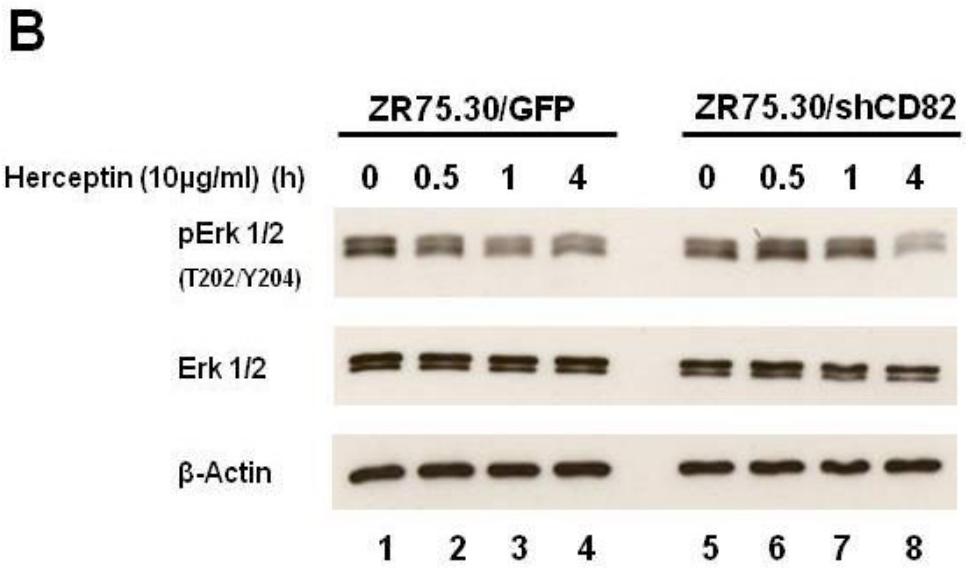

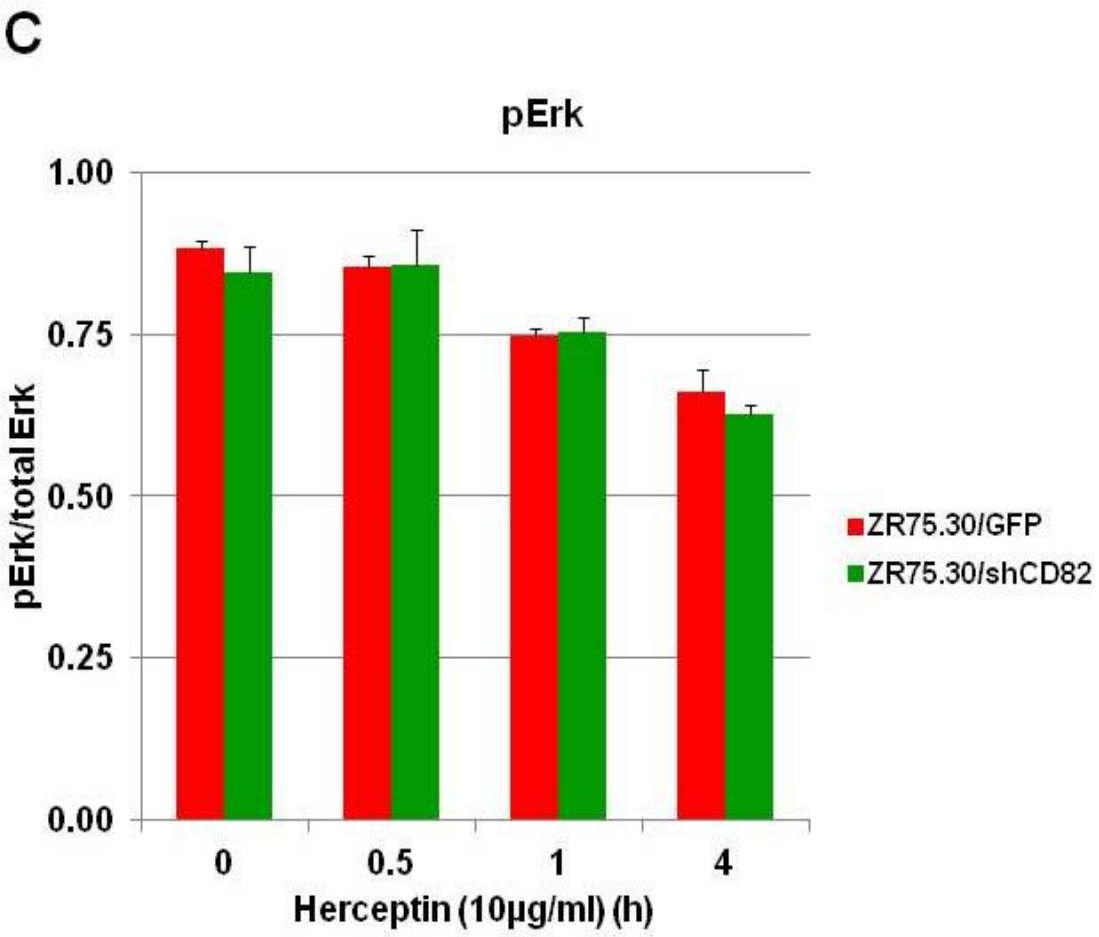

Figure 3.17: The effect of CD82 depletion on the basal levels of phosphorylated Erk1/2.

ZR75.30/shCD82 cells stably expressing low levels of CD82 were generated by lentiviral transduction using lentiviral constructs containing short hairpin RNA (shRNA) that specifically target wild-type CD82. (A) Knockdown of CD82 was confirmed by western blot analysis from lysates of sorted cells. (B) ZR75.30/GFP and ZR75.30/shCD82 cells in log phase were serum-starved overnight before treatment with Herceptin (10µg/ml) for the indicated time intervals. Lysates were collected at the end of each time-point and subsequently blotted for the indicated molecules. (C) Summary of protein density ratios determined as phosphorylated/total protein. Shown are representative blots from three independent experiments.

3.3.3 Suppression of heregulin-induced Ras activation in CD82-overexpressing cells

Since the data presented above indicate an increase in phosphorylation of ErbB2 and MAPK proteins in this model system of CD82-overexpressing breast cancer cells, we next examined whether CD82 affected the activity of Ras, a small GTPase upstream of the MAPK pathway, but downstream of the ErbB2 receptor. As outlined in Figures 1.4 and 1.6, MAPK signalling propagates extracellular signals upon receptor activation. Ras plays a central role in activating several signalling pathways downstream of receptor tyrosine kinases including the PI3K and MAPK signalling pathways. We examined the activity of Ras in serum-starved and heregulin-stimulated SKBR3/Zeo and SKBR3/CD82^{High} cells using a commercially available kit as outlined in the Materials and Methods, section 2.3.2. This is a pull-down assay involving the use of sepharose beads conjugated with the Ras Binding Domain (RBD) region of Raf-1 kinase (Raf-RBD beads). Raf-1 kinase is one of the downstream targets of activated Ras and was thus used as an affinity substrate. In parallel to the test samples, control samples were also prepared whereby lysates were loaded with either a non-hydrolysable GTP analogue, GTPγS or GDP in order to activate or inactivate Ras, respectively.

As shown in Figure 3.18A (lanes 2 and 7), comparable levels of active Ras were detected in the whole cell lysates of both SKBR3/Zeo and SKBR3/CD82^{High} cells. And as expected, pre-loading samples with GTPγS

resulted in elevated levels of active Ras. Notably; this was comparable in both control and CD82-overexpressing cells (Figure 3.18A, compare lanes 3 and 8). Accordingly, pre-loading the samples with GDP resulted in decreased levels of active Ras in both cell lines (Figure 3.18A, compare lanes 3 & 4; 8 & 9). Surprisingly, comparable levels of active Ras were observed under serum-starved basal conditions in both control and CD82-overexpressing cells (Figure 3.18A, lanes 5 & 10; Figure 3.18B, compare the dark blue filled bar with the light blue chequered bar). This particular result implies that the previously described CD82-mediated effect on MAPK signalling could be downstream of Ras proteins.

Interestingly, differences in Ras activity were observed between the cell lines upon heregulin stimulation. Significantly ($P<0.001$) lower levels of active Ras were detected in heregulin-stimulated SKBR3/CD82^{High} cells when compared to SKBR3/Zeo cells (Figure 3.18A, compare lanes 6 & 11; Figure 3.18B, compare the dark blue bar of vertical lines with the line blue bar of horizontal lines). Densitometric analysis of the immunoblots revealed at least a 78% decrease in Ras activity in SKBR3/CD82^{High} cells upon stimulation with heregulin for 30 minutes when compared to stimulated control cells (Figure 3.18B). This reduction in heregulin-induced Ras activity in the CD82-overexpressing cells can be correlated to our previously described results that demonstrated a decrease in phosphorylated MAPK proteins in SKBR3/CD82^{High} cells following stimulation with heregulin for 30 minutes, compared to control SKBR3/Zeo cells (Figure 3.14A, compare lanes 5 & 10).

Collectively, these findings imply that the CD82-mediated effect on MAPK signalling could be independent of Ras. In addition, these findings also indicate a possible dual modulatory role of CD82 in MAPK signalling that is dependent on the physiological conditions; a stimulatory role during resting cellular states and an inhibitory role in conditions of prolonged ligand stimulation. The fact that we observed herein a CD82-mediated increase in ErbB2 and MAPK phosphorylation, but no corresponding increase in Ras activity at basal level suggests a possibility of CD82 modulating an intermediary molecule that can in turn modulate MAPK signalling independent of Ras.

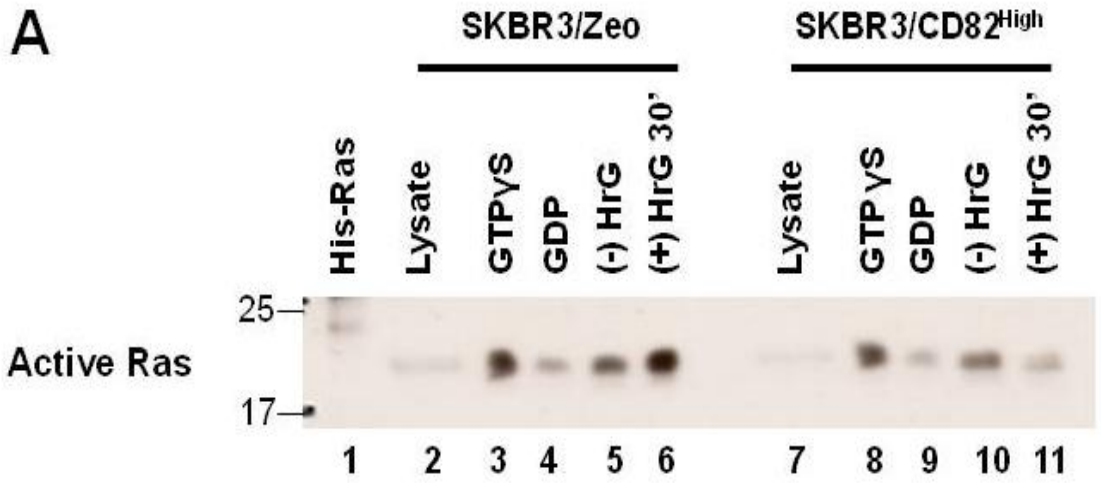
A
SKBR3/Zeo
SKBR3/CD82High
His-Ras
Lysate
GTPγS
GDP
(-) HrG
(+) HrG 30'
Lysate
GTPγS
GDP
(-) HrG
(+) HrG 30'
Active Ras
25
17
1 2 3 4 5 6 7 8 9 10 11

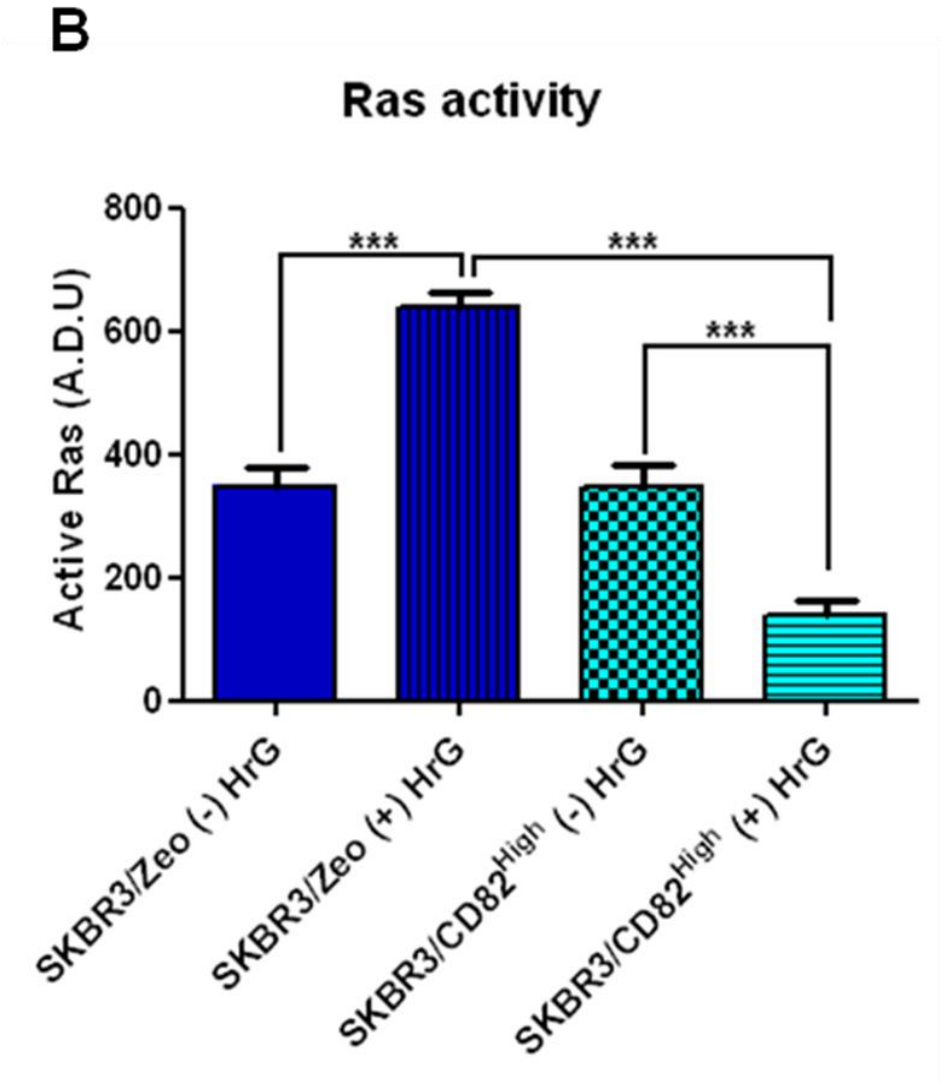
B
Ras activity
Active Ras (A.D.U)
800
600
400
200
0
***
***
***
SKBR3/Zeo (-) HrG
SKBR3/Zeo (+) HrG
SKBR3/CD82High (-) HrG
SKBR3/CD82High (+) HrG

Figure 3.18: Suppression of heregulin-induced Ras activation in CD82-overexpressing cells.

SKBR3/Zeo and SKBR3/CD82^{High} cells were serum-starved overnight; and where indicated, heregulin (HrG) (10ng/ml) was added for 30 minutes prior to lysis. The cells were lysed and assayed for Ras activity using a pull-down method involving sepharose beads conjugated with the Ras binding domain of Raf-1 kinase as an affinity substrate as described in the Materials and Methods under section 2.3.2. Controls included whole cell lysates; histidine-tagged Ras (His-Ras); GTPγS- and GDP-loaded lysates for endogenous, active and inactive Ras, respectively. (A) Samples were resolved by 12% SDS-PAGE under reducing conditions and blotted for active Ras using the anti-pan-Ras mAb. (B) Densitometric analysis of active Ras in non-stimulated and heregulin-stimulated samples for the results shown in (A). A.D.U. = arbitrary densitometry units. Shown are representative blots with mean ± standard deviation from four independent experiments. Asterisks represent the statistical significance as determined by the one-way ANOVA multiple comparison test with the Tukey-Kramer post-test, using GraphPad Prism software. Significance was set at 0.05, whereby (***P<0.001).

3.3.4 No interaction was detected between CD82 and kinase suppressor of Ras 1 (KSR1)

Since the above described Ras activity data implies that the CD82-mediated effect on MAPK signalling could be downstream of the Ras protein, we next assessed whether CD82 affected MAPK signalling by modulating KSR1 (kinase suppressor of Ras 1). As previously discussed, KSR1 is a scaffold protein that binds all three-tier MAPK proteins (Raf-MEK-Erk) of the Erk signalling pathway, downstream of Ras. In resting cells, KSR1 is retained in the cytoplasm through its association in a multi-protein complex that includes MEK (Figure 1.6). Upon Ras activation, KSR1 translocates to the plasma membrane where it interacts with Raf thus leading to Erk phosphorylation (Fehrenbacher et al. 2009). Specifically, we investigated whether CD82 associated with KSR1 under serum-free and heregulin-stimulated conditions in transiently transfected cells. SKBR3 parental cells were co-transfected with HA-KSR1 and non-tagged CD82, followed by immunoprecipitation using anti-HA antibodies and blotting for both HA and CD82. As shown in Figure 3.19A (lanes 3 and 4), no association between KSR1 and CD82 was detected in both non-stimulated and heregulin-stimulated cells under these experimental conditions. These data indicate that CD82 does not affect Ras activity at basal conditions and neither does it directly interact with KSR1 under these experimental conditions. These data thus imply a possible alternative pathway that differs from the classical linear Ras-Raf-MEK-Erk signalling pathway in our model system. It is possible that in CD82-overexpressing cells, MAPK signalling occurs in a manner involving the growth

factor receptors, but with a caveat that signal propagation is in part independent of Ras.

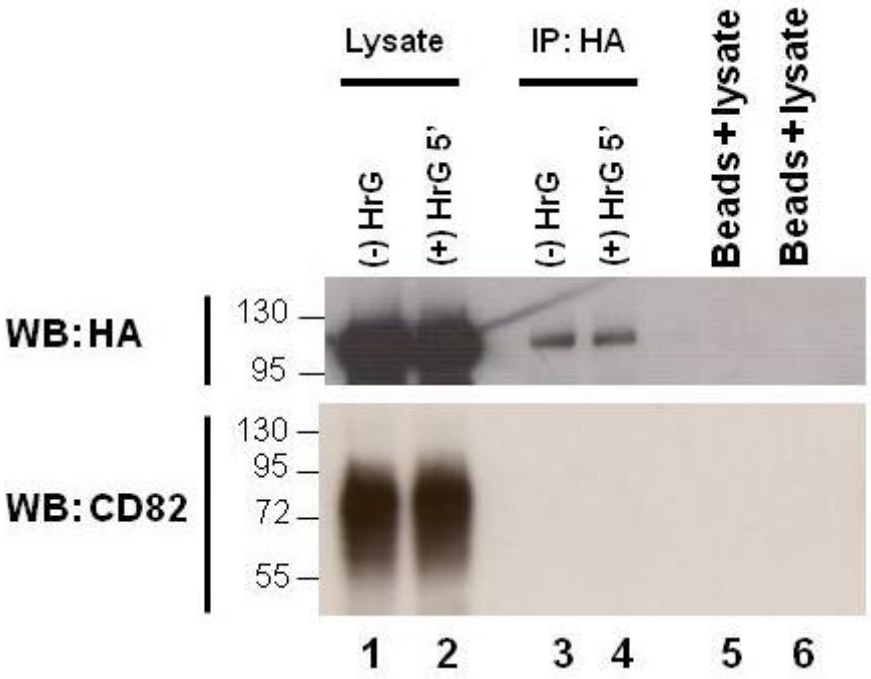

Figure 3.19: No direct association between CD82 and KSR1 was detected.

SKBR3 parental cells were transiently co-transfected with HA-tagged kinase suppressor of Ras 1 (HA-KSR1) and non-tagged CD82. The cells were serum-starved overnight; and where indicated, stimulated with heregulin (10ng/ml) for 5 minutes. Lysates were subjected to immunoprecipitation with anti-HA antibodies and subsequently blotted for the indicated molecules.

3.3.5 Suppression of the MEK/Erk pathway leads to alternative MAPK signalling

Since the above described data indicated that the CD82-mediated increase in phosphorylated MAPK proteins could be downstream of Ras, we next examined the point of regulation within the Erk pathway. The aim of these experiments was to determine the point at which signalling from the growth factor receptors converges with the MAPK signalling cascade, downstream of Ras. As a starting point, we looked at targeting the kinase activity of MEK1/2, the MAPKK upstream of Erk MAPK, but downstream of Ras. The selective and potent MEK inhibitor, U0126 (10μM) was used as described in the Materials and Methods under section 2.1.12 followed by assessment of its effects on Erk phosphorylation. Initially, a pilot experiment was performed in order to determine the optimal time point for the basis of the inhibition assays. Serum-starved SKBR3/Zeo and SKBR3/CD82^{High} cells were treated with U0126 (10μM) for 30 minutes, 1h and 6h followed by western blot analysis for the detection of phosphorylated Erk.

As shown in Figure 3.20A, there was complete inhibition of Erk phosphorylation in both cell lines, following treatment with U0126. Furthermore, this negative effect of U0126 on Erk phosphorylation was evident as early as 30 minutes of treatment with the inhibitor (Figure 3.20A, lanes 2 and 6) and was maintained even up to 6h of treatment (Figure 3.20A, lanes 4 and 8). Notably, U0126 was equally effective at inhibiting Erk phosphorylation in both control and CD82-

overexpressing cells, thereby abolishing the CD82-mediated increase in basal phosphorylation of Erk. Furthermore, U0126 treatment did not affect the expression levels of total Erk (Figure 3.20A).

Interestingly, we observed that inhibition of Erk phosphorylation with U0126 for 30 minutes resulted in an increase in p38 MAPK phosphorylation in both control and CD82-overexpressing cells (Figure 3.20A, compare lanes 1 and 2; 5 and 6). However, this U0126-mediated induction of p38 MAPK signalling was time dependent, as it was abolished by 1h of treatment (Figure 3.20A, lanes 3 and 7). Furthermore, the levels of phosphorylated p38 MAPK returned back to baseline levels by 6h treatment with U0126 (Figure 3.20A; compare lanes 1 and 4; 5 and 8). This U0126-mediated effect on the phosphorylation kinetics of p38 MAPK was confirmed by densitometric analysis of the blots (Figure 3.20B). Since treatment with U0126 for 30 minutes was sufficient to inhibit Erk phosphorylation whilst affecting the p38 MAPK signalling pathway, this time point was thus adopted for the subsequent inhibition assays.

Further to the observation in the pilot experiment that inhibition of the Erk pathway with U0126 for 30 minutes led to elevated p38 MAPK phosphorylation, we next used these conditions to determine whether this compound affected any other MAPK signalling pathways. From these experiments, we were able to confirm that indeed treatment of cells with U0126 for 30 minutes resulted in a significant ($P<0.01$) increase in phosphorylation of p38 MAPK in both control and CD82-overexpressing cells (Figure 3.20C, lanes 2 and 4; Figure 3.20D). In addition, we observed that the p38 MAPK pathway was not the only MAPK

pathway affected; since a similar effect was observed for the JNK signalling pathway (Figure 3.20C). These observations were confirmed by densitometric analysis of the blots from two independent experiments (Figures 3.20D and E). Notably, there was no indication of any CD82-mediated effect on the cellular response to the MEK1/2 inhibitor, since both control and CD82-overexpressing cells responded similarly to U0126 treatment.

Collectively, these data are indicative that the CD82-mediated effect on Erk phosphorylation at basal level is not due to a direct effect on Erk1/2, but is rather localised to a target(s) upstream of Erk1/2. These data also further supports the notion that the regulatory target for the CD82-mediated effect on Erk phosphorylation is downstream of Ras. The fact that inhibition of the Erk pathway induced p38 and JNK MAPK signalling further demonstrates crosstalk between the MAPK signalling pathways.

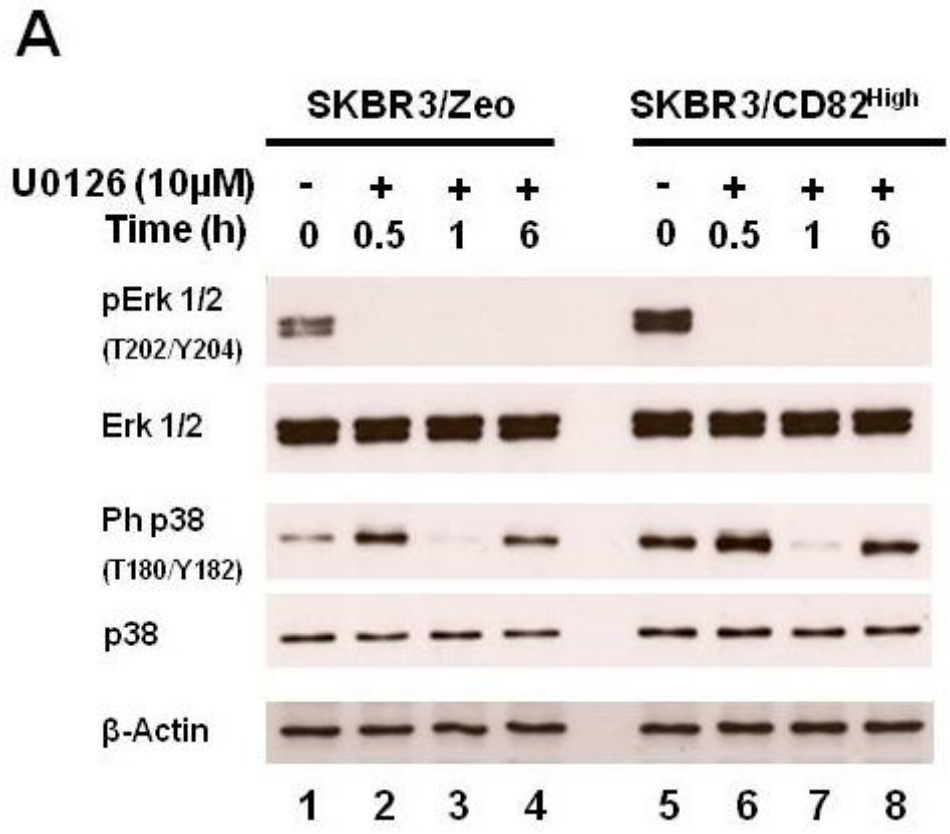
A
SKBR3/Zeo
SKBR3/CD82High
U0126 (10µM) - + + + - + + +
Time (h) 0 0.5 1 6 0 0.5 1 6
pErk 1/2
(T202/Y204)
Erk 1/2
Ph p38
(T180/Y182)
p38
β-Actin
1 2 3 4 5 6 7 8

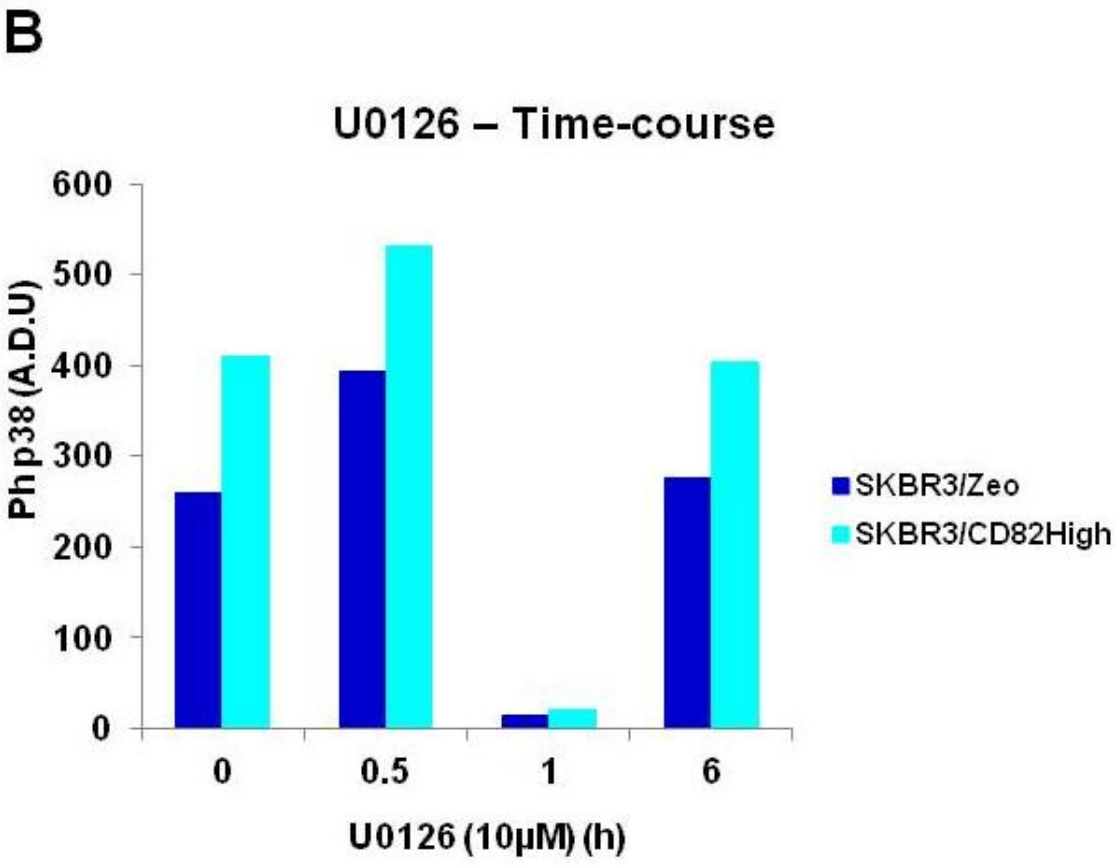
B
U0126 – Time-course
Ph p38 (A.D.U)
600
500
400
300
200
100
0
0
0.5
1
6
U0126 (10µM) (h)
SKBR3/Zeo
SKBR3/CD82High

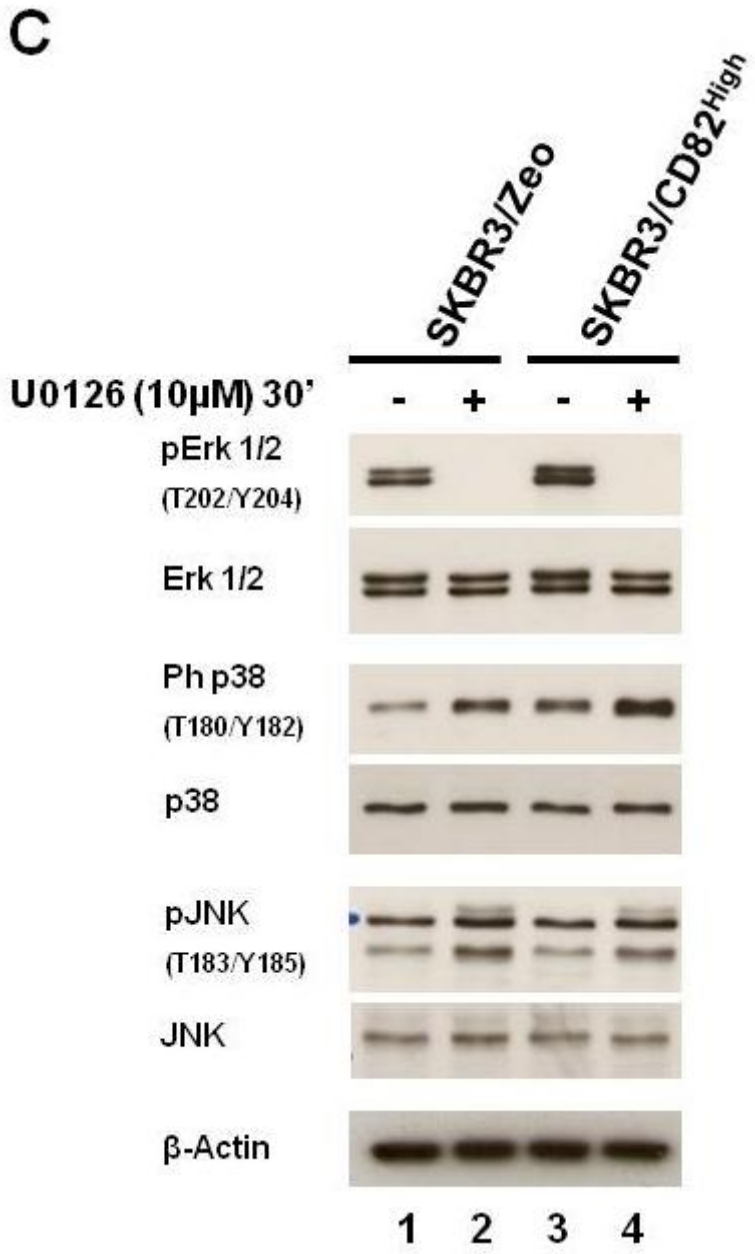
C
SKBR3/Zeo
SKBR3/CD82High
U0126 (10µM) 30'
- + - +
pErk 1/2
(T202/Y204)
Erk 1/2
Ph p38
(T180/Y182)
p38
pJNK
(T183/Y185)
JNK
β-Actin
1 2 3 4

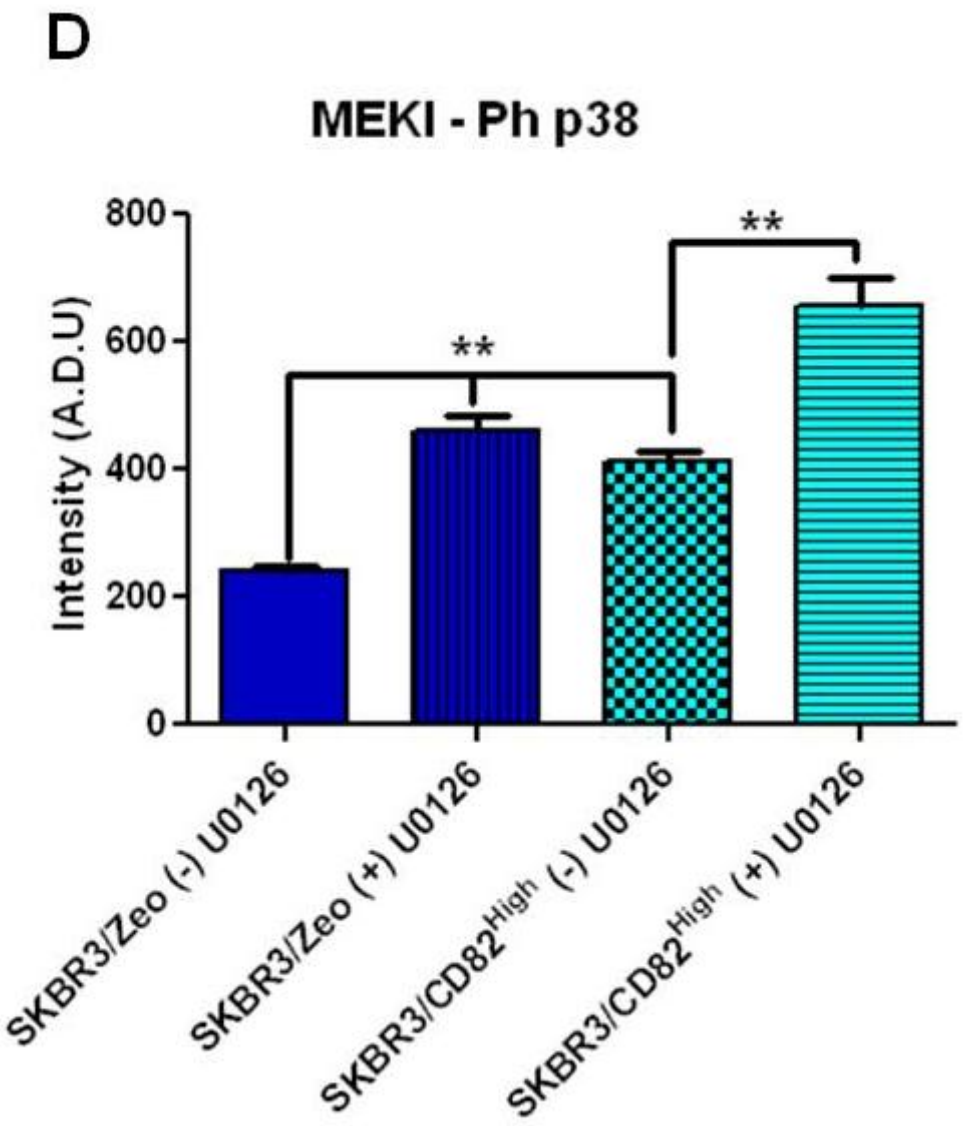
D
MEKI - Ph p38
Intensity (A.D.U)
800
600
400
200
0
**
**
SKBR3/Zeo (-) U0126
SKBR3/Zeo (+) U0126
SKBR3/CD82High (-) U0126
SKBR3/CD82High (+) U0126

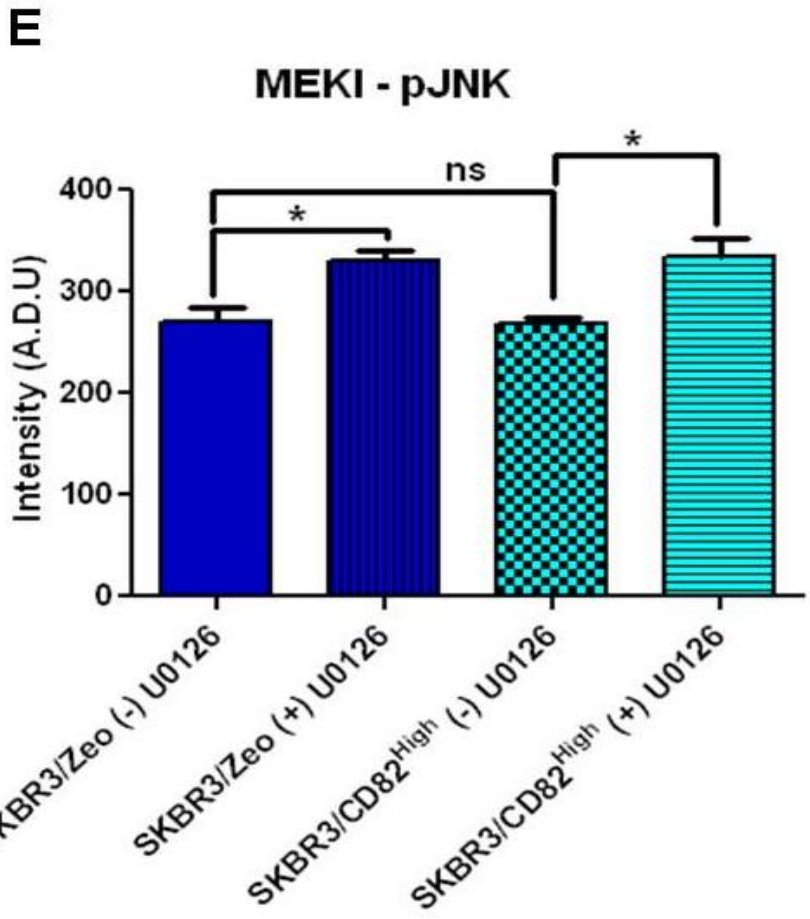

Figure 3.20: Suppression of the MEK/Erk pathway with U0126 leads to alternative MAPK signalling.

SKBR3/Zeo and SKBR3/CD82^{High} cells in log phase were serum-starved overnight prior to the assay. The next day, the cells were treated with the MEK1/2 inhibitor, U0126 (10µM) for (A) 30 minutes, 1h and 4h at 37^{o}C, 5% CO_2. (C) The cells were treated with U0126 for 30 minutes followed by western blot analysis. U0126 was prepared in dimethyl sulfoxide (DMSO) as a 10mM stock solution and was diluted in serum-free medium to a working concentration of 10µM prior to use. DMSO diluted in serum-free medium to the same solvent concentration as in the inhibitor preparations was added to the inhibitor-free controls. At the end of the incubation period, the cells were lysed. Lysates of equal protein concentration were subjected to SDS-PAGE under reducing conditions followed by western blot analysis for the detection of the indicated molecules. (B, D and E) Densitometric analysis of the blots; A.D.U. = arbitrary densitometry units. Shown are representative blots with mean ± standard deviation from two independent experiments. Asterisks represent the statistical significance as determined by the one-way ANOVA multiple comparison test with the Tukey-Kramer post-test, using GraphPad Prism software. Significance was set at 0.05, whereby (*P<0.05) and (**P<0.01). ns – not significant.

3.3.6 Discussion

Having demonstrated that ectopic expression of CD82 and Herceptin treatment resulted in changes in the membrane distribution of ErbB2, we next investigated the effects of CD82 expression and Herceptin treatment on ErbB signalling under various experimental conditions. We assessed the impact of CD82 expression on the phosphorylation of ErbB receptors and signalling molecules of the PI3K and MAPK pathways in heregulin stimulated and non-stimulated cells. From these experiments we found that ectopic expression of CD82 did not affect the basal phosphorylation levels of ErbB3. Our data demonstrate that both control and CD82-overexpressing cells had similar levels of activated ErbB3 at basal level. However, differences were observed between the cell lines in the kinetic pattern of ErbB3 phosphorylation upon stimulation with heregulin. Specifically, the highest levels of phosphorylated ErbB3 were observed at 5 minutes following heregulin stimulation in the control cells compared to 2 minutes in the CD82-overexpressing cells. These data suggest that CD82 could have a role in modulating the formation of heregulin-induced ErbB3 heterodimers leading to receptor activation. It should be noted that ErbB3 has a defective kinase domain, whereby its activation occurs as a result of heterodimerisation with other ErbB receptors, induced by ligand binding (Olayioye et al. 2000;Roskoski, Jr. 2004). Since SKBR3 cells also express EGFR and ErbB2, it is possible that ectopic expression of CD82 facilitates rapid heterodimerisation of ErbB3 with either EGFR and/or ErbB2 upon ligand stimulation. However, in view of the fact that ErbB2 is reported to be the

preferred heterodimerisation partner for members of the EGFR family (Hynes and Lane 2005), it is thus possible that the ligand-induced phosphorylation of ErbB3 is due to ErbB2/ErbB3 heterodimers under these experimental conditions.

The observation, that CD82 appears to have a modulatory role in facilitating heregulin-induced ErbB3 phosphorylation and thus its heterodimerisation in our model system of breast cancer cells is an interesting observation. An earlier report by Odintsova and colleagues using another model system of breast cancer cell lines (MCF-7) in which CD82 was overexpressed, it was demonstrated that CD82 did not affect ErbB2/ErbB3 heterodimerisation in cells stimulated with heregulin (Odintsova et al. 2003). It should be noted that MCF-7 cells express low levels of ErbB2 (Kao et al. 2009), whilst we have demonstrated herein that SKBR3 cells overexpress the ErbB2 receptor. Therefore, our findings herein and in conjunction with the observations by Odintsova and colleagues thus imply that CD82 modulates ErbB receptor dimerisation based on the expression status of ErbB2, whereby it facilitates ligand-induced ErbB2/ErbB3 heterodimerisation in cells overexpressing ErbB2. Interestingly, in the same study by Odintsova and colleagues, the authors also demonstrated that CD82 negatively affected ligand-induced EGFR/ErbB2 heterodimerisation in cells expressing comparable levels of EGFR, ErbB2 and ErbB3 (Odintsova et al. 2003).

The C-terminal tail of activated ErbB3 contains six docking sites for p85 regulatory subunit of PI3K, thereby making it a potent receptor for recruiting p85

and thus activation of the PI3K signalling pathway; ultimately leading to phosphorylation of Akt. In this regard, we assessed the phosphorylation pattern of Akt in both control and CD82-overexpressing cells. We found that phosphorylated Akt followed the same kinetic pattern as that described of activated ErbB3 upon heregulin stimulation. Similarly, CD82 expression did not affect Akt phosphorylation at basal level, as both control and CD82-overexpressing cells had comparable baseline levels of phosphorylated Akt.

On the other hand, assessment of the impact of CD82 expression and heregulin stimulation on ErbB2 activity not only revealed that this receptor is highly constitutively active in SKBR3 and BT474 cells, but also revealed some novel findings that implicate CD82 in the regulation of ErbB2. We found that ectopic expression of CD82 resulted in enhanced ErbB2 phosphorylation at Y877 and Y1221/1222 sites. Stimulation with heregulin resulted in a gradual dephosphorylation of ErbB2. However, we observed that the rate of ErbB2 dephosphorylation was slower in the CD82-overexpressing cells when compared to control cells, thus suggesting implications on downstream signalling.

Y877 is localised in the kinase domain of ErbB2 and is homologous to Y416 of Src. Phosphorylation of ErbB2 at this site couples the receptor to Src and its downstream targets including focal adhesion kinase (FAK) and the pro-migratory $p130^{CAS}$-CrkII complex (Cabodi et al. 2010;Muthuswamy et al. 1999). Our data demonstrate high Src activity correlating with ErbB2 (Y877) phosphorylation, particularly in the CD82-overexpressing cells when compared

to control cells. Furthermore, analysis of tyrosine phosphorylation supported the CD82-mediated effect on ErbB2 phosphorylation. These data also revealed two additional protein mobility masses (130kDa and 60kDa) whereby differences between control and CD82-overexpressing cells were observed. A phosphotyrosine mobility mass of 60kDa could correspond to Src family kinases; whilst a mobility mass of 130kDa could correspond to several proteins including FAK and $p130^{CAS}$. These observations indicate that ectopic expression of CD82 not only modulates ErbB2 phosphorylation, but also key downstream signalling molecules such as Src, with ultimate implications on cell migration. Hence, these observations imply a higher migratory potential of CD82-overexpressing cells compared to control cells. However, work by others and our previously described data herein demonstrated that CD82 strongly suppressed cell migration and invasion in the CD82-overexpressing cells when compared to controls. In fact, it has been previously proposed that CD82 suppresses migration by downregulating the expression levels of $p130^{CAS}$, consequently inhibiting the formation of the pro-migratory $p130^{CAS}$-CrkII complex and thus inhibiting cell migration (Zhang et al. 2003a). At this stage, the mechanism by which CD82 suppresses migration and invasion in our model system of SKBR3 cells is unclear. The fact that ectopic expression of CD82 in these cells results in suppression of cell migration even though CD82 overexpression also resulted in increased phosphorylation of various molecules implicated in cell motility, including Src, suggests an alternative mechanism(s). In addition to the adhesion-dependent signalling, Src can also modulate other signalling pathways including the MAPK pathway (Olayioye et al. 2001).

Phosphorylation of ErbB2 at Y1221/1222 autophosphorylation site couples the receptor to the MAPK signalling pathway through binding of Shc, a scaffolding protein which when phosphorylated leads to the recruitment of effector molecules such as Grb2 and SOS (Alroy and Yarden 1997;Muthuswamy et al. 1999). Accordingly, we found that ErbB2 phosphorylation at Y1221/1222 correlated with the phosphorylation of MAPK proteins, particularly at basal level. The CD82-mediated increase in ErbB2 phosphorylation at basal level was also observed for phosphorylated MAPK proteins.

The fact that ectopic expression of CD82 specifically affected the basal phosphorylation levels of only the ErbB2 receptor and its downstream signalling pathways and that it was not also observed for the ErbB3 receptor or the PI3K pathway, implies that the proportion of ErbB2 modulated by CD82 is not in a heterodimer complex with ErbB3. Since SKBR3 and BT474 cells express EGFR in addition of ErbB2 and ErbB3, it is possible that the CD82-mediated effect on ErbB2 and its downstream signalling is a result of modulating homodimerisation or the formation of a heterodimer with EGFR. This notion is further supported by our observations that control cells and CD82-overexpressing cells responded differently to heregulin stimulation. Specifically, control cells responded positively to heregulin stimulation as represented by an increase in protein phosphorylation. However in the CD82-overexpressing cells, the phosphorylation levels of MAPK proteins remained similar to the baseline levels even in the presence of heregulin stimulation. This was particularly observed for the MAPK proteins affected by the ectopic expression of CD82, namely MEK, Erk and p38. These data imply that the compartmentalisation and possibly the

dimers from which MAPK signalling is emanating are different between control cells and CD82-overexpressing cells. It is feasible that CD82-enriched microdomains facilitate various associations of the ErbB receptors, thereby modulating downstream signalling pathways. Indeed, our data presented herein and reports from others (Danglot et al. 2010;Odintsova et al. 2003;Odintsova et al. 2006) have demonstrated the importance of the membrane compartmentalisation of ErbB receptors for the CD82-mediated regulation of their activity. We have also demonstrated that the proportion of ErbB2 distributed within these microdomains is increased by Herceptin treatment. Together, these findings suggest that ectopic expression of CD82 (and to some extent Herceptin treatment) induces clustering of ErbB receptors, particularly ErbB2 and possibly EGFR, thereby facilitating the activation of alternative signalling pathways, such as Src and MAPK signalling.

Since the CD82-mediated effect on ErbB2 signalling at basal level was more pronounced in lysates from serum-starved cells than from cells maintained in complete medium, it is conceivable that in non-stimulated CD82-overexpressing cells, the proportion of ErbB2 redistributed to the CD82-enriched microdomains is higher; and/or that the ErbB2/ErbB2 and ErbB2/EGFR associations are enhanced in serum-free conditions. Conversely, it is possible that stimulation or serum conditions decrease the proportion of ErbB2 in these microdomains and/or disperse the homo-associations and ErbB2/EGFR hetero-associations. This is supported by data in the literature demonstrating that ErbB2 and EGFR interact in non-stimulated and stimulated cells (Milani et al. 2007;Yang et al. 2007); furthermore, that the proportion of EGFR distributed in lipid rafts is higher

in non-stimulated cells than in stimulated cells (Sottocornola et al. 2006). Moreover, our data herein with heregulin stimulation suggest a possible role of CD82 in facilitating ErbB2/ErbB3 heterodimerisation upon ligand stimulation.

Based on the observation of an increase in phosphorylation of ErbB2 and MAPK proteins in our model system of CD82-overexpressing breast cancer cells, we next examined whether CD82 affected the activity of Ras, a small GTPase upstream of the MAPK pathway, but is downstream of the ErbB receptors. Ras activity was assessed in heregulin-stimulated and non-stimulated cells. We found no evidence of ectopic CD82 expression affecting Ras activity in non-stimulated cells, since comparable levels of active Ras were detected in non-stimulated control and CD82-overexpressing cells. This observation implies that the point at which CD82 regulates MAPK signalling could be downstream of the Ras proteins. This was later investigated further as discussed below. From these experiments, we also observed that heregulin-induced Ras activation was suppressed in the SKBR3/CD82^{High} cells when compared to SKBR3/Zeo cells. In control experiments whereby cell lysates were loaded with a non-hydrolysable GTP analogue (GTPγS), comparable levels of active Ras were detected in both SKBR3/Zeo and SKBR3/CD82^{High} cells (Figure 3.18A, lanes 3 and 8). However in samples stimulated with heregulin, the level of active Ras detected in SKBR3/CD82^{High} cells was significantly lower when compared to that in SKBR3/Zeo cells (Figure 3.18A, compare lanes 6 and 11). These data imply a possibility that the GTPase activity of Ras proteins is elevated in the CD82-overexpressing cells than in control cells under these experimental conditions. The activation state of Ras is

tightly controlled partly by its intrinsic GTPase activity through the action of GTPase activating proteins (GAPs), which increase the catalytic activity of Ras to hydrolyse and thus revert from the GTP-bound active state to the inactive GDP-bound state (Ahearn et al. 2012;Fehrenbacher et al. 2009). It is possible that this process is enhanced in CD82-overexpressing cells after prolonged ligand stimulation, whereby ligand-induced GTP bound to Ras is more readily hydrolysed in these cells than in control cells.

The effect of CD82 on the activation of small GTPase proteins has previously been demonstrated (Delaguillaumie et al. 2002;Takahashi et al. 2007). Specifically, a study by Takahashi and colleagues demonstrated that ectopic expression of CD82 in a non-small cell lung carcinoma cell line resulted in inhibition of ligand-induced Ras activation, which was specific for c-Met signalling following stimulation with hepatocyte growth factor (HGF) (Takahashi et al. 2007). Moreover, CD82 is not the only tetraspanin to be implicated in Ras activation. Indeed, a study by Sawada and colleagues previously demonstrated that expression of tetraspanin CD151 specifically attenuated the adhesion-dependent activation of Ras and diminished the activation of downstream signalling molecules, namely Erk1/2 and Akt (Sawada et al. 2003). Furthermore, the authors in that study proposed that the CD151-mediated negative effect on Ras activation was indicative of low levels of GTP-bound active Ras (Sawada et al. 2003). Based on the data presented herein and the reports described above, it is clear that tetraspanins are capable of influencing signalling pathways at various stages of a signalling cascade including regulation of the receptors and downstream signalling molecules.

Scaffold proteins regulate MAPK signalling by mediating the structural and functional organisation of the three-tier MAPK module (Dhanasekaran et al. 2007;Sacks 2006). Kinase suppressor of Ras 1 (KSR1) is one of the scaffold proteins that regulate Erk signalling. It binds all three-tier MAPK proteins (Raf-MEK-Erk) of the Erk signalling pathway, downstream of Ras. Since the above described data implied that the CD82-mediated effect on MAPK signalling is likely to be downstream of the Ras proteins, we next assessed whether CD82 affected MAPK signalling by modulating KSR1. Specifically, we examined whether CD82 associated with KSR1 by use of immunoprecipitation. From these experiments however, we were unable to detect any possible CD82/KSR1 interaction in our experimental conditions. However, these findings do not rule out the possibility of CD82 modulating KSR1 or indeed other scaffold proteins. It is possible that although CD82 and KSR1 do not interact directly, they could still be localised within the same complex or compartment. Moreover, we have demonstrated herein that CD82 associates with ErbB2. Although the association of ErbB2 and KSR1 has not yet been reported in literature to date, it is feasible that these two molecules could interact or colocalise; and in such a case, CD82 could then modulate MAPK signalling via this interaction. Indeed, the association of ErbB2 and another MAPK scaffold has previously been demonstrated, resulting in modulation of MAPK signalling. A recent study by White and colleagues demonstrated that scaffold protein IQGAP1 is overexpressed in ErbB2-positive breast cancer tissue and Herceptin-resistant breast cancer cells. These authors further demonstrated that IQGAP1 directly associated with ErbB2 thereby regulating its expression, phosphorylation and

signalling. They showed that knocking down of IQGAP1 resulted in decreased expression and phosphorylation of ErbB2 in addition to decreased phosphorylation of downstream signalling molecules, including Akt and Erk (White et al. 2011). It would thus be interesting to determine whether ErbB2 associated with KSR1, particularly in the CD82-overexpressing cells.

In an effort to determine the point at which signalling from the growth factor receptors converges with the MAPK signalling cascade, downstream of Ras, we proceeded by assessing the effect of targeting MEK, the MAPKK which is downstream of Ras, but upstream of Erk. A previously described (Favata et al. 1998) selective and potent MEK inhibitor, U0126 was used in these assays. This compound has previously been shown to be selective at inhibiting the kinase activity of MEK without affecting the kinase activity of other kinases (Favata et al. 1998). From these experiments, we found that U0126 completely inhibited Erk phosphorylation in both control and CD82-overexpressing cells. The inhibitory effect of U0126 was evident as early as 30 minutes of treatment and was maintained by up to 6h of treatment with the inhibitor in both cell lines. The fact that U0126 was effective at abolishing Erk phosphorylation in both control and CD82-overexpressing cells is indicative that our previous observations of increased Erk phosphorylation in the CD82-overexpressing cells are not a result of direct modulation of Erk, but rather of upstream targets, possibly MEK. These findings thus suggest that the CD82-mediated point of regulation in the MAPK signalling cascade in this model system is localised in the region between the receptor level and MEK, but downstream or independent of the Ras proteins.

Interestingly, we also observed that Erk inhibition with U0126 resulted in a time-dependent activation of p38 MAPK in both control and CD82-overexpressing cells. Treatment with U0126 for 30 minutes resulted in elevated levels of p38 followed by dephosphorylation at 1h and subsequently returning back to baseline levels by 6h of treatment (Figure 3.20A). A similar effect was observed with JNK phosphorylation following 30 minutes of treatment with U0126 in both control and CD82-overexpressing cells. The p38 and JNK signalling pathways can be activated by cellular stress (Roberts and Der 2007). Thus these data suggest that treatment with U0126 for short incubations such as 30 minutes could induce cellular stress, which in turn would lead to activation of p38 and JNK signalling pathways. This could ultimately lead to cell death. Indeed, a previous study by Monick and colleagues demonstrated that inhibition of constitutive Erk activity with U0126 resulted in a rapid loss of mitochondrial membrane potential and a decrease in ATP levels. These authors also found that prolonged inhibition of Erk subsequently led to cell death (Monick et al. 2008). It would thus be interesting to determine whether treatment with U0126 induces apoptosis in our model system.

Whilst the data presented herein are intriguing, we were not able to identify the point at which the signal converges with the MAPK signalling cascade. At this point, it is not yet clear whether MEK is the point of regulation or indeed Raf, which is upstream of MEK, but downstream of Ras. A detailed assessment into the effects of targeting Raf is required in order to identify the key players in the CD82-mediated effect on MAPK signalling. This could be approached by the

use of Raf inhibitors such as vemurafanib (a B-Raf inhibitor), sorafenib (a C-Raf inhibitor) or RAF265 (a pan-Raf inhibitor) followed by analysis of effects on downstream signalling in both control and CD82-overexpressing cells. Such studies would not only determine whether CD82 overexpression affects Raf, but would also identify which Raf isoform(s) (if any) is affected.

It is possible that the point of convergence is at the level of Raf, whereby Src family kinases serve as a link between the activated receptors and the MAPK signalling cascade, possibly at the level of Raf. Indeed, Src has previously been implicated in MAPK signalling. A study by Olayioye and colleagues using two breast cancer cell lines, including SKBR3 cells demonstrated the sensitivity of Erk activation to Src inhibition; whereby treatment of cells with the c-Src tyrosine kinase inhibitor (CPG77675) resulted in complete inhibition of Erk activation (Olayioye et al. 2001). In addition to observing a constitutive association of Src and Shc, these authors also demonstrated that in the presence of the Src inhibitor, ligand-induced Shc phosphorylation and the Shc-Grb2 interaction was reduced. Interestingly, these authors found that in cells stimulated with high levels of ligand, Erk activation was not sensitive to Src inhibition (Olayioye et al. 2001). This study demonstrates that Src is able to influence MAPK signalling at the receptor level and their findings suggest that Src could play an important role in activating this signalling cascade under low levels of ligand. Moreover, the ability of Src to influence MAPK signalling through other downstream targets has also previously been demonstrated by several studies. Specifically, earlier studies demonstrated the involvement of Src in Raf phosphorylation; whereby it was shown that both Ras and Src activity

were required for the maximal activation of Raf-1 and A-Raf, whilst the activation of B-Raf required only Ras (Fabian et al. 1993;Marais et al. 1995;Marais et al. 1997;Mason et al. 1999;Tran and Frost 2003).

In addition to Src directly phosphorylating Raf, it can also indirectly influence MAPK signalling via protein kinase C (PKC), a family of serine/threonine kinases. A study by Tan and colleagues demonstrated that Src kinase activity played a critical role in the ErbB2-mediated upregulation and activation of PKCα (Tan et al. 2006). Moreover, an isotype of PKC (PKCδ) has previously been shown to activate the MAPK pathway in a manner that was independent of the Ras protein, but dependent on Raf (Ueda et al. 1996). Furthermore, the classic isoforms of PKC (α, β and γ) have previously been implicated in the induction of *CD82* transcription in a manner that was independent of Ras, but required the activation of MEK1/2 and Erk1/2 (Rowe et al. 2008). These pathways are summarised in Figure 3.21. It would thus be interesting to determine whether Src and/or PKC family kinases are involved in the CD82-mediated effect on MAPK signalling in our model system and to identify which isoforms are involved.

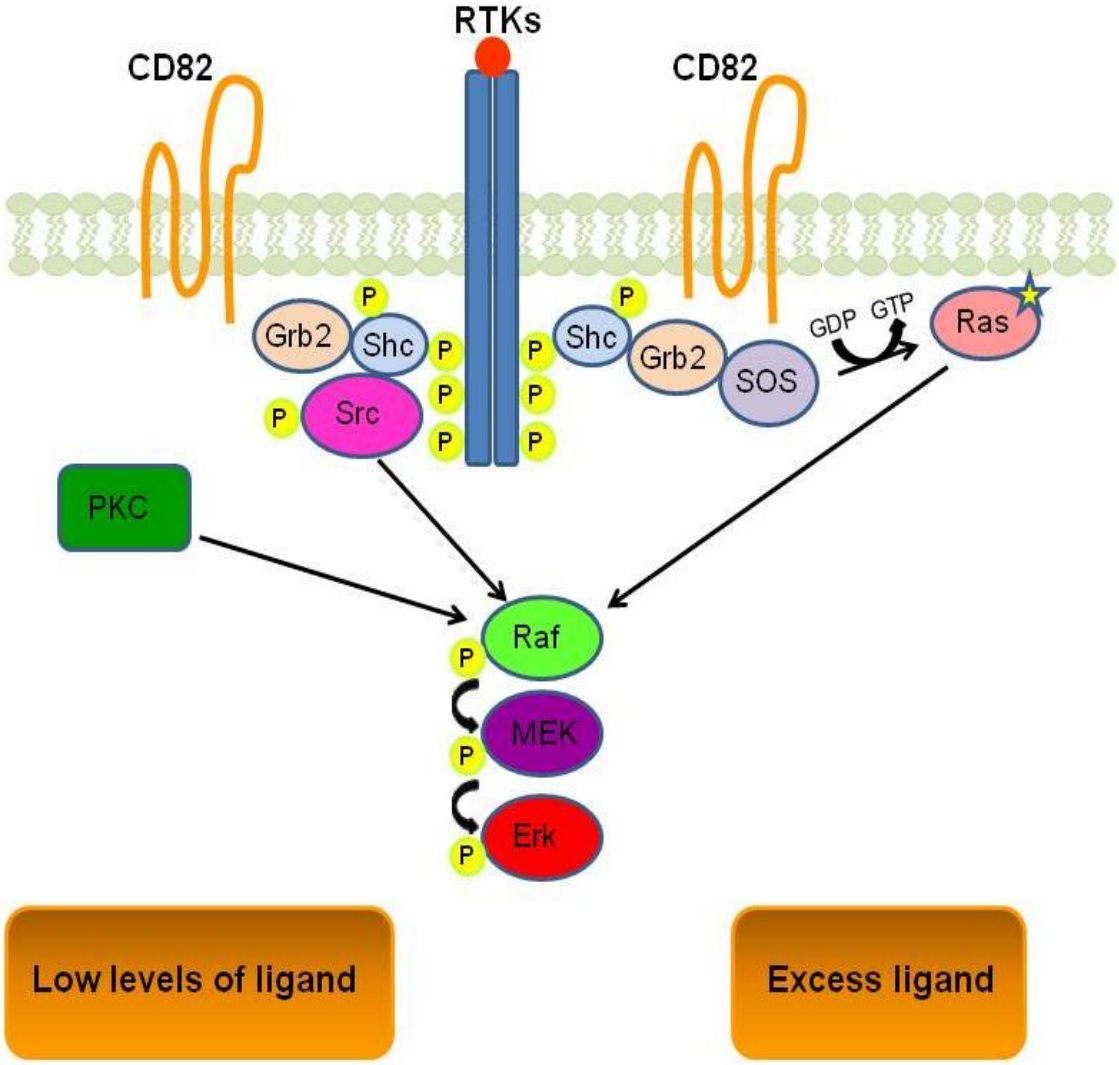

Figure 3.21: Summary of the proposed CD82-mediated influence on MAPK signalling.

Ectopic expression of CD82 results in an increase in basal levels of phosphorylated ErbB2, Src and MAPK proteins. Under conditions of low ligand levels, the MAPK pathway is likely to be activated independently of the Ras proteins but involving Src family kinases and/or protein kinase C. Under conditions of excess ligand, MAPK signalling is likely to be dependent of the Ras proteins. Data presented herein implies a possible dual modulatory role of CD82 on MAPK signalling that is dependent on the conditions: a stimulatory role during conditions of low ligand levels; and an inhibitory role in conditions of excess ligand.

The notion that a Src family kinase(s) could be the link between the receptors and Raf, is supported by our own observations presented herein showing a basal increase in pan-Src phosphorylation (Y416) in the CD82-overexpressing cells when compared to controls, similar to that observed for phosphorylated ErbB2 and MAPK proteins (Figure 3.14). This is an interesting observation since Src activation has recently been implicated in Herceptin resistance (Zhang et al. 2011). By using a model system of ErbB2-positive breast cancer cells that had developed resistance to Herceptin, Zhang and colleagues demonstrated a resistant phenotype that differed from the parental cells, whereby the resistant cell lines prominently expressed high levels of EGFR, ErbB3 and IGF-1R which correlated with increased Src phosphorylation at Y416 (Zhang et al. 2011). In addition, these authors demonstrated that increased Src activity was sufficient to confer Herceptin resistance; and that inhibition of Src activity effectively blocked receptor activation and downstream signalling. Furthermore, these authors demonstrated that Src inhibition sensitised Herceptin-resistant cells to Herceptin (Zhang et al. 2011). This study by Zhang highlights the key role played by Src in modulating Herceptin response. Indeed, identifying Src as one of the central modulators of Herceptin response can offer some explanation to some of our observations presented herein. It is possible that the poor response to Herceptin observed in the CD82-overexpressing cells is due to increased Src activity in these cells. Thus response to Herceptin in these cells could be improved by the use of Src inhibitors. Moreover, we have demonstrated herein that Erk activation in both control and particularly in CD82-overexpressing cells was sensitive to MEK inhibition. This is indicative that

targeting other signalling molecules within key pathways in conjunction with Herceptin could be an effective approach to improve the cellular response to Herceptin. Indeed, this approach has recently been demonstrated in the literature (Ferguson et al. 2012;Lu et al. 2007;Zhang et al. 2011;Zhang and Yu 2012).

Collectively, the data presented here demonstrate that CD82 modulates ErbB2 phosphorylation leading to activation of downstream signalling, particularly the MAPK signalling pathway. Additionally, the point at which CD82 modulates MAPK signalling is likely to be independent of Ras proteins.

4 GENERAL DISCUSSION AND FUTURE WORK

In this study we have endeavoured to determine the role of tetraspanin CD82 in Herceptin-mediated cellular responses. Our findings have identified several avenues in need of further investigation in order to fully understand the contribution of CD82 in the efficacy of Herceptin in ErbB2-overexpressing cells. Firstly, our data demonstrate that ectopic expression of CD82 resulted in a poor response to Herceptin treatment. Specifically, the antiproliferative effect of Herceptin was observed in control cells when cultured in various 3D extracellular matrices, whilst the CD82-overexpressing cells, in particular the BT474/CD82^{High} cells showed resistance to Herceptin in these culture conditions. Thus these data suggest that CD82 and components of the extracellular matrix (ECM) may indeed cooperate in regulating sensitivity of cells to Herceptin treatment. Integrins are important receptors for specific components of ECM used in 3D culturing experiments; for example integrins α2β1 (collagen I) and α6β1/α6β4 for laminin-1, a component of Matrigel. BT474 cells express higher levels of these integrins compared to SKBR3 cells. The fact that a higher level of resistance to Herceptin was observed in the BT474/CD82^{High} cells suggests a functional relationship between CD82 and these integrin receptors in mediating the response to Herceptin. Thus, functional studies involving cells cultured on various ECM matrices and knockdown experiments would be valuable in verifying the roles of these proteins and CD82 in the cellular response to Herceptin. In this respect, a recent study by Yang and colleagues demonstrated the involvement of

tetraspanin CD151 and ECM proteins in regulating sensitivity of cells to Herceptin. In this study, the authors demonstrated that ErbB2-positive breast cancer cells were resistant to Herceptin when cultured on laminin-5 and that knockdown of CD151 and the laminin-binding integrins restored Herceptin sensitivity (Yang et al. 2010). Similar studies could be applied to our CD82 model system in order to identify the ECM molecules involved in the CD82-mediated effect on Herceptin sensitivity.

Secondly, we show here that expression of CD82 results in changes in the compartmentalisation of ErbB2 whereby the receptor is redistributed to light gradient fractions; and that treatment with Herceptin increased the amount of ErbB2 redistributed in these fractions. This effect of Herceptin was obvious in CD82-overexpressing cells but not in control cells; however the significance of CD82-mediated redistribution of ErbB2 to these microdomains and thus implications on the efficacy of Herceptin remains to be elucidated. Several studies have previously demonstrated the importance of gangliosides in the function of CD82 (Odintsova et al. 2003;Odintsova et al. 2006;Todeschini et al. 2007). For example, the report by Odintsova and colleagues demonstrated a correlation of CD82 expression levels and gangliosides, whereby they found that ectopic expression of CD82 resulted in an increase in surface expression of gangliosides GD1a and GM1 which correlated with the redistribution of EGFR and ErbB2 on the plasma membrane (Odintsova et al. 2003;Odintsova et al. 2006). The same group also reported the importance of gangliosides in regulating the stability and organisation of CD82-enriched microdomains by demonstrating that depletion of gangliosides led to a decrease in CD82 protein-

protein interactions and also caused a redistribution of CD82-associated proteins (Odintsova et al. 2006). Moreover, a study by Sottocornola and colleagues investigated the role of gangliosides in the association of ErbB2 with lipid rafts; specifically, they demonstrated that ErbB2 co-localised with ganglioside GM3 and that depletion of gangliosides led to redistribution of ErbB2 into detergent-soluble high density sucrose gradient fractions. These authors also found that although GM3 was important for the localisation of ErbB2 into lipid rafts in their model system, it did not affect the phosphorylation of the receptor (Sottocornola et al. 2006). In regard to all these reports and our current data, it is clear that CD82 plays a role in the distribution of ErbB2 into light gradient fractions and also that gangliosides are important for the localisation of ErbB2 into these microdomains. However, it remains to be verified as to which ganglioside(s) is (are) important for the CD82-mediated compartmentalisation of ErbB2 to these microdomains and also the effects of this distribution on the efficacy of Herceptin. Thus, further studies are required to clarify these issues, using the current knowledge in the literature as a starting point.

Thirdly, our data demonstrate for the first time that ectopic expression of CD82 results in an increase in ErbB2-mediated MAPK signalling without affecting the PI3K pathway. As an initial step towards elucidating the mechanism(s) by which CD82 exerts this effect, we investigated whether the expression of CD82 affected Ras activity, a small GTPase upstream of the MAPK pathway; and whether CD82 affected the assembly of the three-tier MAPK proteins, by assessing its possible interaction with KSR1, a scaffold protein that binds all

three MAPK proteins (Raf-MEK-Erk). However, we found that expression of CD82 did not affect Ras activity; and no interaction was observed between CD82 and KSR1 under our experimental conditions, thus implying that the point at which CD82 modulates MAPK signalling could be independent of Ras. Further studies are therefore required in order to determine whether expression of CD82 affects the recruitment of signalling molecules to the activated receptor that can couple the receptor to the MAPK signalling cascade. Since we observed CD82-mediated changes to the phosphorylation of ErbB2 in particular at Y1221/1222 phosphorylation site that couples the receptor to the MAPK pathway, we propose that the recruitment of adaptor proteins Shc and Grb2 to this site should be investigated, as a starting point.

In addition, we found that expression of CD82 affected phosphorylation of ErbB2 at another site, Y877 which couples the receptor to Src-mediated signalling. As we have discussed in the previous section, Src family kinases influence several signalling pathways including the MAPK signalling pathway; and they have been reported to play a critical role in modulating resistance to Herceptin. In view of the facts that we observed an increase in Src phosphorylation (using a pan-Src antibody) in the CD82-overexpressing cells and that we consistently observed a poor response to Herceptin in CD82-overexpressing cells, it would be interesting to investigate the impact of targeting the activity of members of the Src family kinases on downstream signalling and also how this would affect the response of CD82-overexpressing cells to Herceptin treatment. This could be approached by the use of inhibitors such as saracatinib (a c-Src inhibitor); dasatinib (a pan-Src kinase inhibitor) or

indeed by the use of siRNA targeted against specific members of the Src family kinases. This would be useful to identify the family member(s) influenced by CD82 expression.

Finally, in view of the fact that ectopic expression of CD82 correlated with enhanced ErbB2 phosphorylation and MAPK activation, it would be interesting to investigate the biological significance of this by determining whether ectopic expression of CD82 sensitises ErbB2-positive breast cancer cells to other ErbB2-targeted therapies such as Lapatinib, a tyrosine kinase inhibitor that targets the kinase activity of both EGFR and ErbB2. Results from such experiments, together with our current findings could be the building blocks in verifying whether tetraspanin CD82 could be a possible biomarker in identifying breast cancer patients with ErbB2-positive disease that could benefit or respond better to ErbB2-targeted therapies including Herceptin.

In conclusion, the data presented here demonstrate that CD82 modulates the cellular response of ErbB2-positive breast cancer cells to Herceptin treatment by regulating not only the distribution of the ErbB2 receptor, but also its phosphorylation and activation of downstream signalling pathways, particularly the MAPK pathway.

5 APPENDICES

5.1 Appendix I: Cell culture media and supplements

BT474

RPMI 1640
10% HI FBS
10µg/ml Insulin
50 units Penicillin/ 50µg/ml Streptomycin
± 1µg/ml Puromycin

SKBR3

DMEM
10% HI FBS
50 units Penicillin/ 50µg/ml Streptomycin
± 100µg/ml Zeocin

ZR75-30

RPMI 1640
10% HI FBS
50 units Penicillin/ 50µg/ml Streptomycin

Freeze mix

10% DMSO
90% HI FBS

5.2 Appendix II: Materials

Product	Supplier	Catalogue number
10X Tris/Glycine	Geneflow	EC-880
10X Trypsin-EDTA	Invitrogen	15400-054
2-Mercaptoethanol	Sigma	M7522
6.5mm Transwell® with 8.0µm pore polycarbonate membrane insert	Corning	3422
Amersham Hyperfilm™ MP	GE Healthcare	28-9068-46
Ammonium persulfate	Sigma	A6761
Anti-Mouse IgG (whole molecule)-Agarose	Sigma	A6531
Aprotinin	Sigma	A1153
BD Matrigel™	BD Biosciences	354230
Bio-Rad D_c protein assay Reagent A	Bio-Rad Laboratories	500-0113
Bio-Rad D_c protein assay Reagent B	Bio-Rad Laboratories	500-0114
Bio-Rad D_c protein assay Reagent S	Bio-Rad Laboratories	500-0115
BioTrace™ pure nitrocellulose blotting membrane	PALL Life Sciences	P/N 66485
BM-Cyclin	Roche	10799050001
Bromophenol blue	Fisher Scientific	B/4630/44
Calcium chloride (dihydrate)	Sigma	C5080
Cell dissociation buffer	Invitrogen	13151-014
CellTrics® disposable filters	PARTEC	04-004-2327
Collagen, Type I	Sigma	C7661
Dimethyl sulphoxide	Sigma	D2650
DMEM without Phenol Red	Biological Industries	01-053-1A
Dulbecco's Modified Eagle's Medium	Sigma	D6429
Ethanol	Fisher Scientific	E/0650DF/P17
Fetal bovine serum	PAA Laboratories	A15-101
Fibronectin form bovine plasma	Sigma	F1141
Fluorescent mounting medium	Dako	S3023
FuGene® 6	Roche	11814 443001
GeneJammer	Agilent Technologies	204130
Glycerol	Fisher Scientific	G/0650/08
Glycine	Sigma	G8898
Haemocytometer	Fisher Scientific	MNK-420-010N
HEPES solution	Sigma	H0887
Hoechst 33342	Invitrogen	H3570
Insulin	Sigma	I6634
Lab-Tek™ chambered coverglass (4-wells)	Nunc	155383
Leupeptin	Sigma	L2023
Magnesium chloride	Fisher Scientific	M/0600/53
Methanol	Sigma	24229
MycoAlert® mycoplasma detection kit	Lonza	LT07-418
Paraformaldehyde powder	Park Scientific	30525-89-4
Penicillin/Streptomycin	Invitrogen	15070-063
Phenylmethanesulfonyl fluoride	Sigma	P7626
Plasmid pLVTHM	Addgene	12247
Plasmid pMD2.G	Addgene	12259
Plasmid psPAX2	Addgene	12260
Polybrene®	Sigma	AL-118
Precision red advanced protein assay reagent	Cytoskeleton	ADV02A

Pre-stained protein markers	New England Biolabs	P7708L
ProLong® gold antifade reagent	Invitrogen	P36934
Protein A agarose	Sigma	P9269
Protein-G Agarose	Sigma	P4691
ProtoGel® Acrylamide	Geneflow	EC-890
Puromycin dihydrochloride	Sigma	P8833
Ras activation assay kit	Cytoskeleton	BK008
RPMI-1640	Sigma	R8758
Sodium acetate trihydrate	Sigma	S7670
Sodium azide	Fisher Scientific	S/2380/48
Sodium chloride	BDH	10241AP
Sodium citrate tribasic dihydrate	Sigma	C3434
Sodium dodecyl sulphate	BDH	444464T
Sodium hydroxide	Sigma	S8045
Sodium orthovanadate	Sigma	S6508
Sucrose	Sigma	S0389
Tetramethylethylenediamine	Sigma	T2,250-0
Tris(hydroxymethyl)methylamine	BDH	271195Y
Triton® X-100	Sigma	T9284
Trypan blue solution	Sigma	T8154
Tween® 80	Sigma	P1754
U0126	Calbiochem	662005
Zeocin™	Invitrogen	P/N 46-0509
β-Morpholino-ethansulfonsaeure	Janssen Chimica	17-259-90

5.3 Appendix III: Components of reagents used in this study

1% Triton X-100

495ml	1X PBS
5ml	Triton X-100
1mM	$MgCl_2$
0.5mM	$CaCl_2$

1% Brij-98

495ml	1X PBS
5ml	Brij-98
1mM	$MgCl_2$
0.5mM	$CaCl_2$

1M Tris-HCl at pH 6.8 and pH 8.8

121.14g	Tris-HCl (mw: 121.14g/mol)
800ml	dH_2O

- Adjust pH to pH 6.8 or pH 8.8
- Make up to 1L with dH_2O

2% Paraformaldehyde (PFA)

18ml	dH_2O
10µl	10M NaOH
0.4g	PFA
2ml	10X PBS
8.5µl	Concentrated HCl
1mM	$MgCl_2$
0.5mM	$CaCl_2$
0.6g	Sucrose

Blocking solution for immunofluorescence

For 20ml:

4ml	HINGS (goat serum)
16ml	PBS
40µl	10% sodium azide (NaN_3)

4X Laemmli buffer

8ml	20% SDS
8ml	Glycerol
6.5ml	Tris-HCl pH 6.8
3.1ml	dH_2O

- A small amount of Bromophenol blue was added to the sample buffer

10% ammonium persulfate (APS)

10ml	dH_2O
1g	APS

10X Running buffer for electrophoresis

700ml	dH_2O
144.3g	Glycine
30.3g	Tris
10g	SDS

- Make up to 1L with dH_2O

10X TBS-T

800ml	dH_2O
12.11g	Tris
87.66g	NaCl
5ml	Tween-80

- Adjust pH to pH 7.5 with concentrated HCl (+/- NaOH)
- Make up to 1L with dH_2O

PBS-T

1L	dH_2O
10	PBS tablets
1ml	Tween-80

Transfer buffer

700ml	dH_2O
200ml	Methanol
100ml	10X Tris/Glycine

MES buffer

1L	dH_2O
4.88g	MES hydrate
8.77g	NaCl
1.02g	$MgCl_2$

- Adjust pH to pH 6.5 with concentrated HCl (+/- NaOH)

5.4 Appendix IV: Supplementary figures

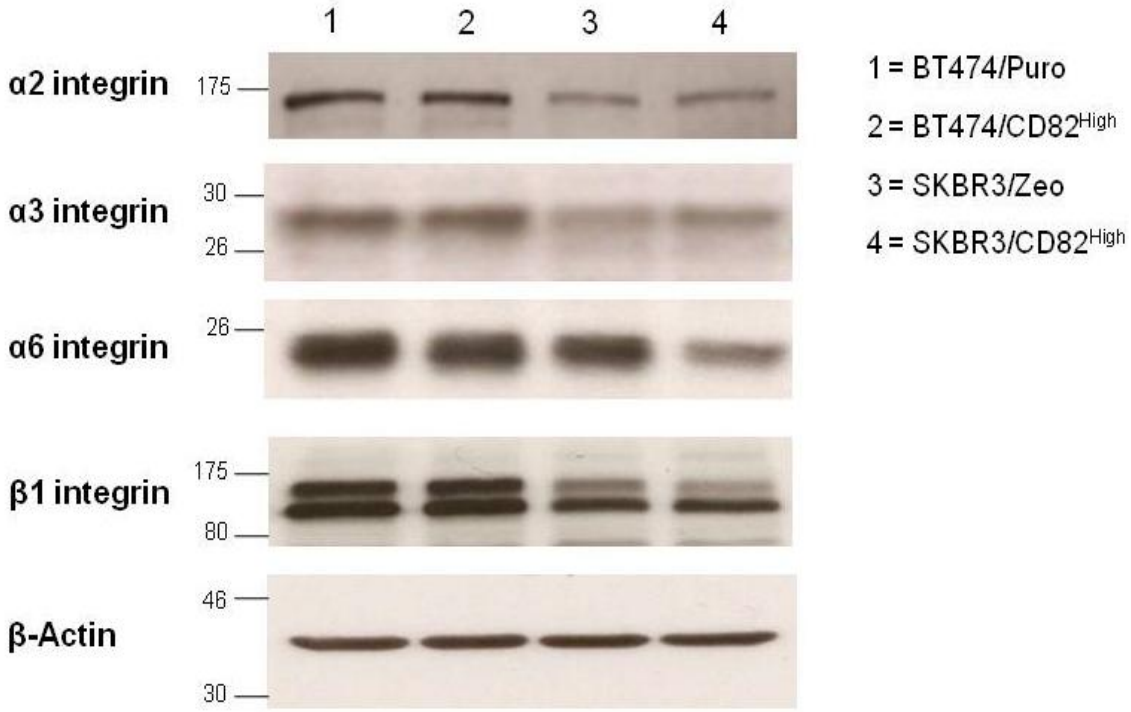

Supplementary Figure 1: Expression levels of integrins in a breast cancer model system of CD82-overexpressing cells.

The expression levels of integrins were analysed by western blotting. Lysates of equal protein concentration were resolved by 10% SDS-PAGE under reducing conditions and blotted for the indicated molecules. Shown are representative blots from at least two independent experiments.

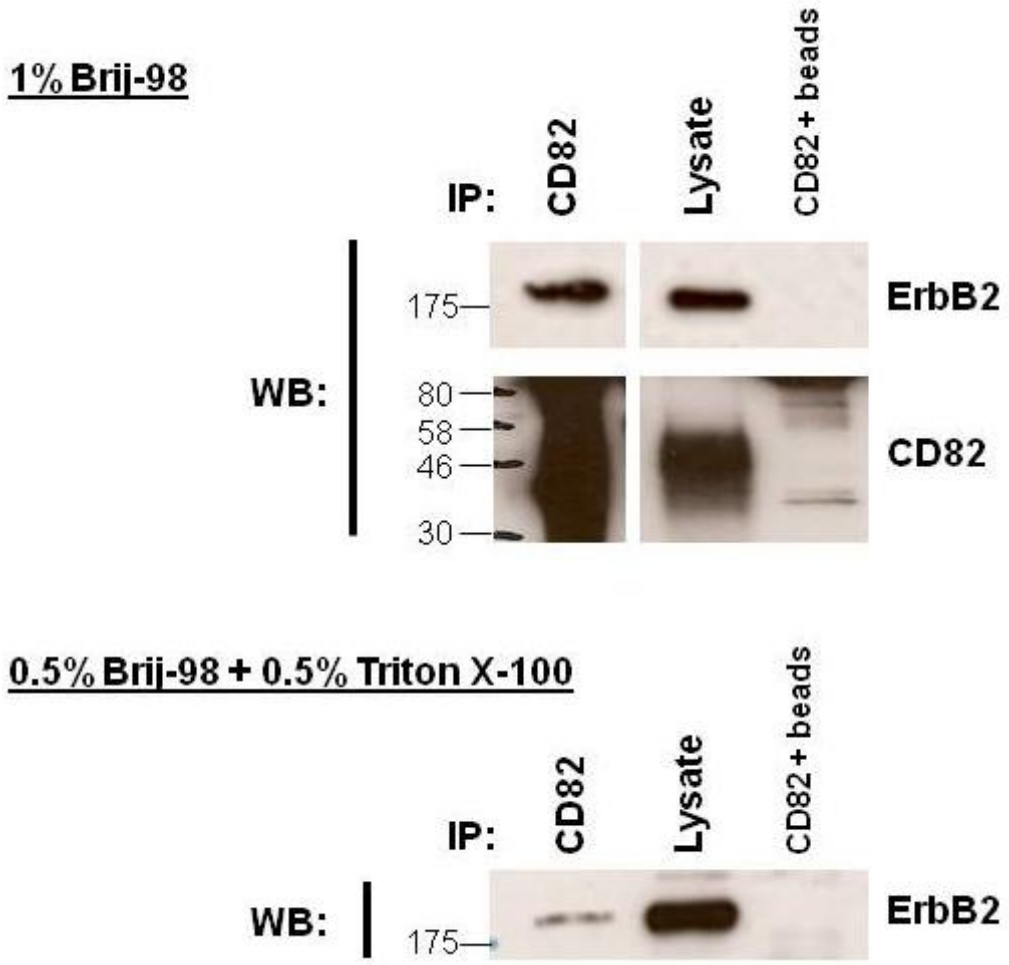

Supplementary Figure 2: The association of CD82 with ErbB2 in SKBR3/CD82^{High} cells following lysis with other detergents.

SKBR3/CD82^{High} cells were prepared for the immunoprecipitation assay as described in the Materials and Methods under section 2.3.4. Cells were lysed using either 1% Brij-98 or a mixture of 0.5% Brij-98 + 0.5% Triton X-100 lysis buffer for 4h at 4^{o}C with rotation. Immune complexes were precipitated using mouse IgG agarose beads conjugated with M104 anti-CD82 mouse mAb followed by western blot analysis using anti-ErbB2 (Ab-17) and anti-CD82 (KAI1 C-16) antibodies.

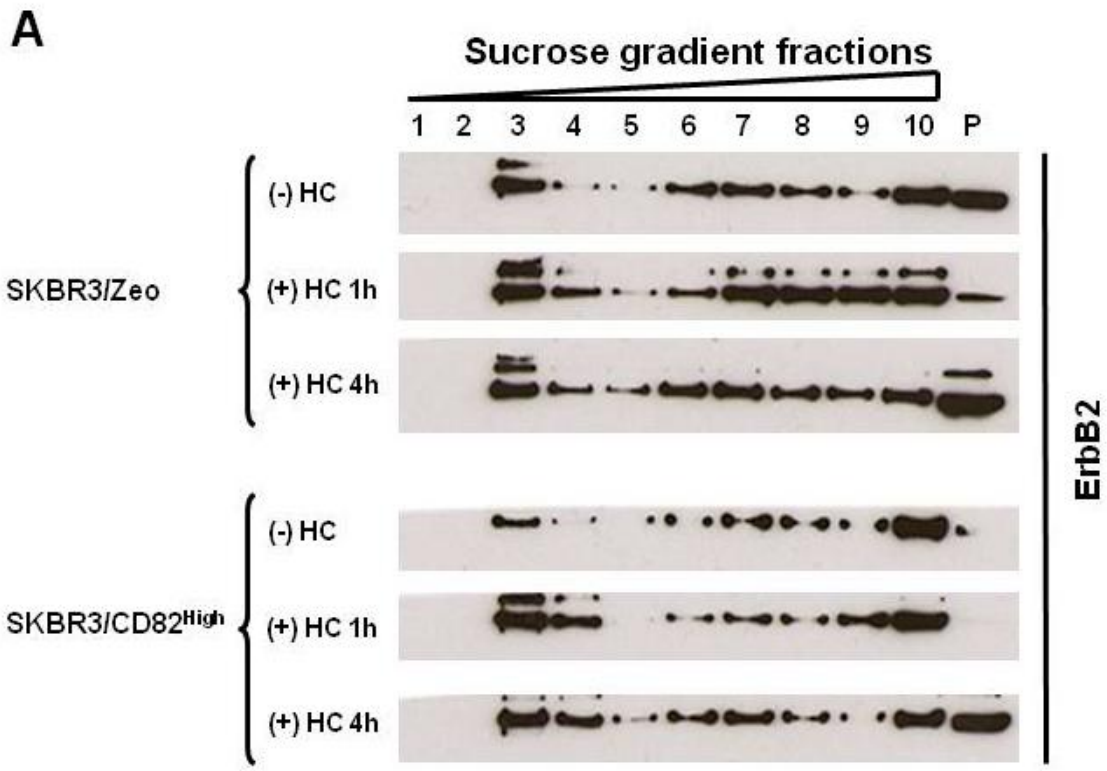
A
Sucrose gradient fractions
1 2 3 4 5 6 7 8 9 10 P
SKBR3/Zeo
(-) HC
(+) HC 1h
(+) HC 4h
SKBR3/CD82High
(-) HC
(+) HC 1h
(+) HC 4h
ErbB2

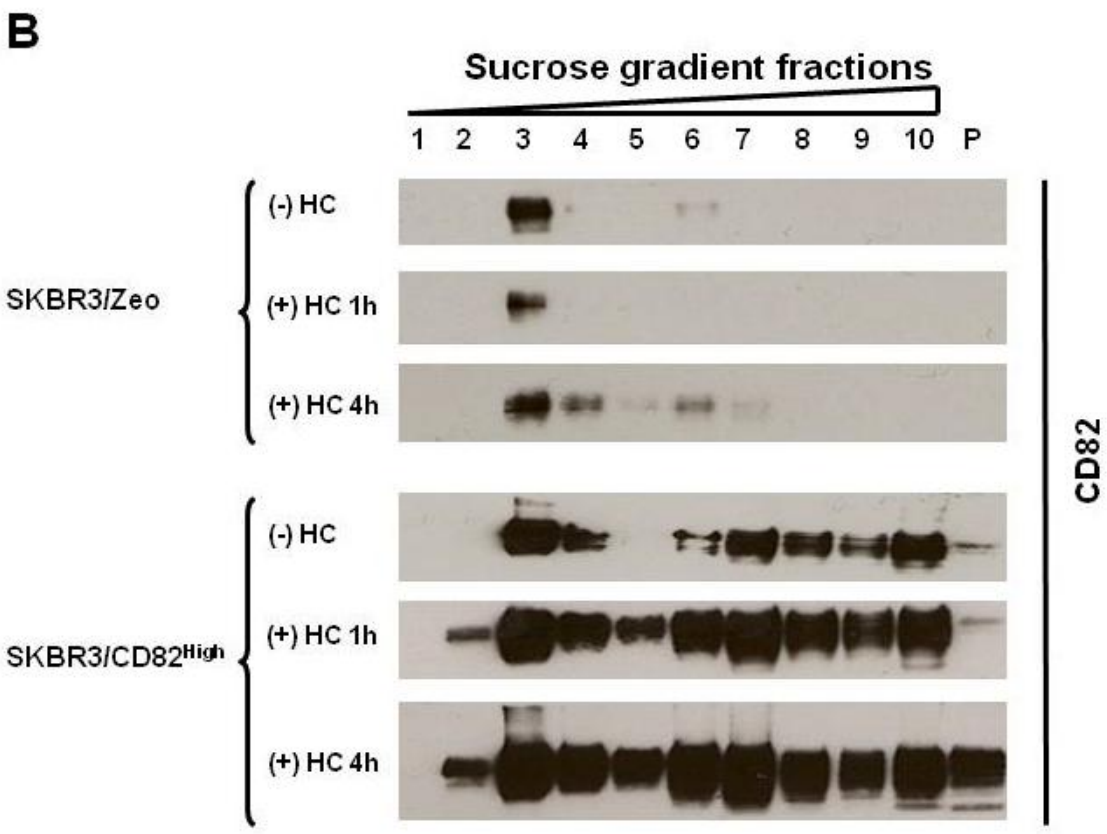
B
Sucrose gradient fractions
1 2 3 4 5 6 7 8 9 10 P
SKBR3/Zeo
(-) HC
(+) HC 1h
(+) HC 4h
SKBR3/CD82High
(-) HC
(+) HC 1h
(+) HC 4h
CD82

Supplementary Figure 3: The effect of Herceptin treatment on the distribution of ErbB2 and CD82 following detergent-free lysis.

SKBR3/Zeo and SKBR3/CD82^{High} cells were treated with Herceptin (10µg/ml) for the indicated time intervals prior to lysis. Not-treated and treated cells were mechanically lysed without any detergent followed by fractionation as described in the Materials and Methods under section 2.4. The resulting homogenate of equal protein concentration was centrifuged in a discontinuous sucrose density gradient composed of 90%, 35% and 5% (w/v) sucrose. 10 fractions were collected from the meniscus of the gradient and the pellet was resuspended in Laemmli buffer supplemented with protease and phosphatase inhibitors. Equal amounts of each fraction were mixed with loading buffer and the protein distribution was analysed by SDS-PAGE under reducing and non-reducing conditions followed by western blot analysis using antibodies against (A) ErbB2 (Ab-17); and (B) CD82 (TS82b).

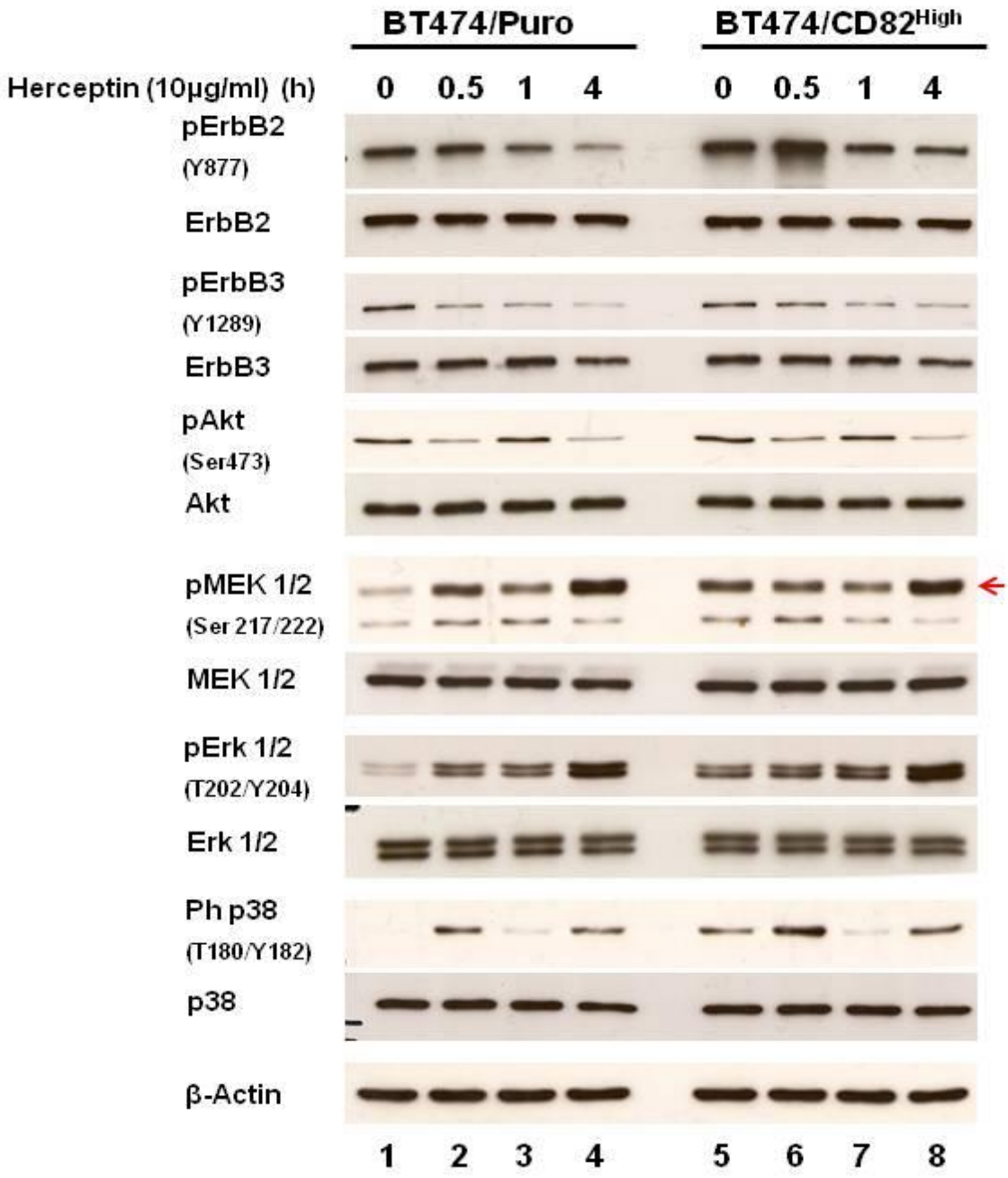

Supplementary Figure 4: The effects of CD82 expression and short incubations of Herceptin treatment on the PI3K and MAPK signalling pathways in BT474 cells.

BT474/Puro and BT474/CD82^{High} cells in log phase were serum-starved overnight prior to treatment with Herceptin (10µg/ml) for the indicated time intervals. Lysates were collected at the end of each time-point and subsequently blotted for the indicated molecules of the PI3K and MAPK signalling pathways. Shown are representative blots from three independent experiments.

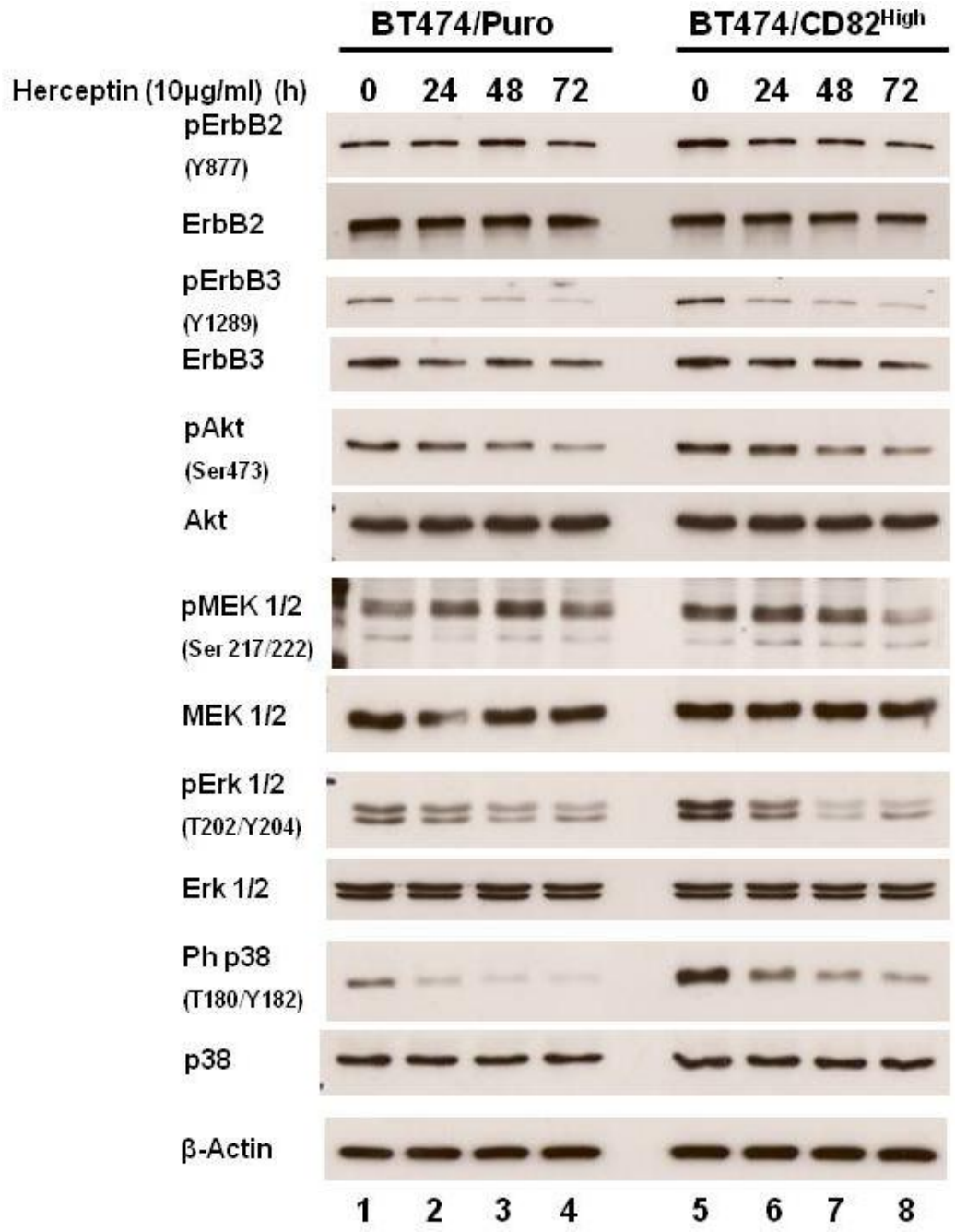

Supplementary Figure 5: The effects of CD82 expression and long incubations of Herceptin on the PI3K and MAPK signalling pathways in BT474 cells.

BT474/Puro and BT474/CD82^{High} cells in log phase were serum-starved overnight prior to treatment with Herceptin (10µg/ml) for the indicated time intervals. Lysates were collected at the end of each time-point and subsequently blotted for the indicated molecules of the PI3K and MAPK signalling pathways. Shown are representative blots from three independent experiments.

6 LIST OF REFERENCES

Ahearn, I.M., Haigis, K., Bar-Sagi, D., & Philips, M.R. 2012. Regulating the regulator: post-translational modification of RAS. *Nat.Rev.Mol.Cell Biol.*, 13, (1) 39-51.

Alroy, I. & Yarden, Y. 1997. The ErbB signaling network in embryogenesis and oncogenesis: signal diversification through combinatorial ligand-receptor interactions. *FEBS Lett.*, 410, (1) 83-86.

Alvarado, D., Klein, D.E., & Lemmon, M.A. 2009. ErbB2 resembles an autoinhibited invertebrate epidermal growth factor receptor. *Nature*, 461, (7261) 287-291.

Austin, C.D., De Maziere, A.M., Pisacane, P.I., van Dijk, S.M., Eigenbrot, C., Sliwkowski, M.X., Klumperman, J., & Scheller, R.H. 2004. Endocytosis and sorting of ErbB2 and the site of action of cancer therapeutics trastuzumab and geldanamycin. *Mol.Biol.Cell*, 15, (12) 5268-5282.

Axelrod, D., Koppel, D.E., Schlessinger, J., Elson, E., & Webb, W.W. 1976. Mobility measurement by analysis of fluorescence photobleaching recovery kinetics. *Biophys.J.*, 16, (9) 1055-1069.

Bandyopadhyay, S., Zhan, R., Chaudhuri, A., Watabe, M., Pai, S.K., Hirota, S., Hosobe, S., Tsukada, T., Miura, K., Takano, Y., Saito, K., Pauza, M.E., Hayashi, S., Wang, Y., Mohinta, S., Mashimo, T., Iiizumi, M., Furuta, E., & Watabe, K. 2006. Interaction of KAI1 on tumor cells with DARC on vascular endothelium leads to metastasis suppression. *Nat.Med.*, 12, (8) 933-938.

Bari, R., Zhang, Y.H., Zhang, F., Wang, N.X., Stipp, C.S., Zheng, J.J., & Zhang, X.A. 2009. Transmembrane Interactions Are Needed for KAI1/CD82-Mediated Suppression of Cancer Invasion and Metastasis. *American Journal of Pathology*, 174, (2) 647-660.

Barros, F.F., Powe, D.G., Ellis, I.O., & Green, A.R. 2010. Understanding the HER family in breast cancer: interaction with ligands, dimerization and treatments. *Histopathology*, 56, (5) 560-572.

Baselga, J. 2011. Targeting the phosphoinositide-3 (PI3) kinase pathway in breast cancer. *Oncologist.*, 16 Suppl 1, 12-19.

Baselga, J., Tripathy, D., Mendelsohn, J., Baughman, S., Benz, C.C., Dantis, L., Sklarin, N.T., Seidman, A.D., Hudis, C.A., Moore, J., Rosen, P.P., Twaddell, T., Henderson, I.C., & Norton, L. 1996. Phase II study of weekly intravenous recombinant humanized anti-p185HER2 monoclonal antibody in patients with

HER2/neu-overexpressing metastatic breast cancer. *J.Clin.Oncol.*, 14, (3) 737-744.

Berditchevski, F. 2001. Complexes of tetraspanins with integrins: more than meets the eye. *Journal of Cell Science*, 114, (23) 4143-4151.

Berditchevski, F., Gilbert, E., Griffiths, M.R., Fitter, S., Ashman, L., & Jenner, S.J. 2001. Analysis of the CD151-alpha3beta1 integrin and CD151-tetraspanin interactions by mutagenesis. *J.Biol.Chem.*, 276, (44) 41165-41174.

Berditchevski, F. & Odintsova, E. 1999. Characterization of integrin-tetraspanin adhesion complexes: Role of tetraspanins in integrin signaling. *Journal of Cell Biology*, 146, (2) 477-492.

Berditchevski, F. & Odintsova, E. 2007. Tetraspanins as regulators of protein trafficking. *Traffic*, 8, (2) 89-96.

Berditchevski, F., Odintsova, E., Sawada, S., & Gilbert, E. 2002. Expression of the palmitoylation-deficient CD151 weakens the association of alpha(3)beta(1) integrin with the tetraspanin-enriched microdomains and affects integrin-dependent signaling. *Journal of Biological Chemistry*, 277, (40) 36991-37000.

Berditchevski, F., Tolias, K.F., Wong, K., Carpenter, C.L., & Hemler, M.E. 1997. A novel link between integrins, transmembrane-4 superfamily proteins (CD63 and CD81), and phosphatidylinositol 4-kinase. *J.Biol.Chem.*, 272, (5) 2595-2598.

Berditchevski, F., Zutter, M.M., & Hemler, M.E. 1996. Characterization of novel complexes on the cell surface between integrins and proteins with 4 transmembrane domains (TM4 proteins). *Mol.Biol.Cell*, 7, (2) 193-207.

Bessman, N.J. & Lemmon, M.A. 2012. Finding the missing links in EGFR. *Nat.Struct.Mol.Biol.*, 19, (1) 1-3.

Bickel, P.E., Scherer, P.E., Schnitzer, J.E., Oh, P., Lisanti, M.P., & Lodish, H.F. 1997. Flotillin and epidermal surface antigen define a new family of caveolae-associated integral membrane proteins. *J.Biol.Chem.*, 272, (21) 13793-13802.

Bienstock, R.J. & Barrett, J.C. 2001. KAI1, a prostate metastasis suppressor: prediction of solvated structure and interactions with binding partners; integrins, cadherins, and cell-surface receptor proteins. *Mol.Carcinog.*, 32, (3) 139-153.

Bissell, M.J., Weaver, V.M., Lelievre, S.A., Wang, F., Petersen, O.W., & Schmeichel, K.L. 1999. Tissue structure, nuclear organization, and gene expression in normal and malignant breast. *Cancer Res.*, 59, (7 Suppl) 1757-1763s.

Blume-Jensen, P. & Hunter, T. 2001. Oncogenic kinase signalling. *Nature*, 411, (6835) 355-365.

Boucheix, C. & Rubinstein, E. 2001. Tetraspanins. *Cellular and Molecular Life Sciences*, 58, (9) 1189-1205.

Brenton, J.D., Carey, L.A., Ahmed, A.A., & Caldas, C. 2005. Molecular classification and molecular forecasting of breast cancer: ready for clinical application? *J.Clin.Oncol.*, 23, (29) 7350-7360.

Bublil, E.M. & Yarden, Y. 2007. TheEGF receptor family: spearheading a merger of signaling and therapeutics. *Current Opinion in Cell Biology*, 19, (2) 124-134.

Burgess, A.W., Cho, H.S., Eigenbrot, C., Ferguson, K.M., Garrett, T.P., Leahy, D.J., Lemmon, M.A., Sliwkowski, M.X., Ward, C.W., & Yokoyama, S. 2003. An open-and-shut case? Recent insights into the activation of EGF/ErbB receptors. *Mol.Cell*, 12, (3) 541-552.

Cabodi, S., del, P.C.-L., Di, S.P., & Defilippi, P. 2010. Integrin signalling adaptors: not only figurants in the cancer story. *Nat.Rev.Cancer*, 10, (12) 858-870.

Carey, L.A. 2010. Through a glass darkly: advances in understanding breast cancer biology, 2000-2010. *Clin.Breast Cancer*, 10, (3) 188-195.

Carey, L.A., Perou, C.M., Livasy, C.A., Dressler, L.G., Cowan, D., Conway, K., Karaca, G., Troester, M.A., Tse, C.K., Edmiston, S., Deming, S.L., Geradts, J., Cheang, M.C., Nielsen, T.O., Moorman, P.G., Earp, H.S., & Millikan, R.C. 2006. Race, breast cancer subtypes, and survival in the Carolina Breast Cancer Study. *JAMA*, 295, (21) 2492-2502.

Chang, H.R. 2010. Trastuzumab-based neoadjuvant therapy in patients with HER2-positive breast cancer. *Cancer*, 116, (12) 2856-2867.

Charrin, S., Le Naour, F., Silvie, O., Milhiet, P.E., Boucheix, C., & Rubinstein, E. 2009. Lateral organization of membrane proteins: tetraspanins spin their web. *Biochemical Journal*, 420, 133-154.

Charrin, S., Manie, S., Oualid, M., Billard, M., Boucheix, C., & Rubinstein, E. 2002. Differential stability of tetraspanin/tetraspanin interactions: role of palmitoylation. *Febs Letters*, 516, (1-3) 139-144.

Charrin, S., Manie, S., Thiele, C., Billard, M., Gerlier, D., Boucheix, C., & Rubinstein, E. 2003. A physical and functional link between cholesterol and tetraspanins. *Eur.J.Immunol.*, 33, (9) 2479-2489.

Cho, H.S., Mason, K., Ramyar, K.X., Stanley, A.M., Gabelli, S.B., Denney, D.W., & Leahy, D.J. 2003. Structure of the extracellular region of HER2 alone and in complex with the Herceptin Fab. *Nature*, 421, (6924) 756-760.

Choi, U.J., Jee, B.K., Lim, Y., & Lee, K.H. 2009. KAI1/CD82 decreases Rac1 expression and cell proliferation through PI3K/Akt/mTOR pathway in H1299 lung carcinoma cells. *Cell Biochem.Funct.*, 27, (1) 40-47.

Chow, L.M. & Baker, S.J. 2006. PTEN function in normal and neoplastic growth. *Cancer Lett.*, 241, (2) 184-196.

Christgen, M., Bruchhardt, H., Ballmaier, M., Krech, T., Langer, F., Kreipe, H., & Lehmann, U. 2008. KAI1/CD82 is a novel target of estrogen receptor-mediated gene repression and downregulated in primary human breast cancer. *International Journal of Cancer*, 123, (10) 2239-2246.

Christgen, M., Christgen, H., Heil, C., Krech, T., Langer, F., Kreipe, H., & Lehmann, U. 2009. Expression of KAI1/CD82 in distant metastases from estrogen receptor-negative breast cancer. *Cancer Sci.*, 100, (9) 1767-1771.

Citri, A. & Yarden, Y. 2006. EGF-ERBB signalling: towards the systems level. *Nature Reviews Molecular Cell Biology*, 7, 505-516.

Claas, C., Stipp, C.S., & Hemler, M.E. 2001. Evaluation of prototype transmembrane 4 superfamily protein complexes and their relation to lipid rafts. *Journal of Biological Chemistry*, 276, (11) 7974-7984.

Clynes, R.A., Towers, T.L., Presta, L.G., & Ravetch, J.V. 2000. Inhibitory Fc receptors modulate in vivo cytotoxicity against tumor targets. *Nat.Med.*, 6, (4) 443-446.

Cobleigh, M.A., Vogel, C.L., Tripathy, D., Robert, N.J., Scholl, S., Fehrenbacher, L., Wolter, J.M., Paton, V., Shak, S., Lieberman, G., & Slamon, D.J. 1999. Multinational study of the efficacy and safety of humanized anti-HER2 monoclonal antibody in women who have HER2-overexpressing metastatic breast cancer that has progressed after chemotherapy for metastatic disease. *J.Clin.Oncol.*, 17, (9) 2639-2648.

Cook, K.M. & Figg, W.D. 2010. Angiogenesis inhibitors: current strategies and future prospects. *CA Cancer J.Clin.*, 60, (4) 222-243.

Danglot, L., Chaineau, M., Dahan, M., Gendron, M.C., Boggetto, N., Perez, F., & Galli, T. 2010. Role of TI-VAMP and CD82 in EGFR cell-surface dynamics and signaling. *J.Cell Sci.*, 123, (Pt 5) 723-735.

de Vos, A.M., Ultsch, M., & Kossiakoff, A.A. 1992. Human growth hormone and extracellular domain of its receptor: crystal structure of the complex. *Science*, 255, (5042) 306-312.

Delaguillaumie, A., Harriague, J., Kohanna, S., Bismuth, G., Rubinstein, E., Seigneuret, M., & Conjeaud, H. 2004. Tetraspanin CD82 controls the association of cholesterol-dependent microdomains with the actin cytoskeleton in T lymphocytes: relevance to co-stimulation. *Journal of Cell Science*, 117, (22) 5269-5282.

Delaguillaumie, A., Lagaudriere-Gesbert, C., Popoff, M.R., & Conjeaud, H. 2002. Rho GTPases link cytoskeletal rearrangements and activation processes induced via the tetraspanin CD82 in T lymphocytes. *J.Cell Sci.*, 115, (Pt 2) 433-443.

Dhanasekaran, D.N., Kashef, K., Lee, C.M., Xu, H., & Reddy, E.P. 2007. Scaffold proteins of MAP-kinase modules. *Oncogene*, 26, (22) 3185-3202.

Dhillon, A.S., Hagan, S., Rath, O., & Kolch, W. 2007. MAP kinase signalling pathways in cancer. *Oncogene*, 26, (22) 3279-3290.

Dillon, R.L., White, D.E., & Muller, W.J. 2007. The phosphatidyl inositol 3-kinase signaling network: implications for human breast cancer. *Oncogene*, 26, (9) 1338-1345.

Dong, J.T., Isaacs, W.B., Barrett, J.C., & Isaacs, J.T. 1997. Genomic organization of the human KAI1 metastasis-suppressor gene. *Genomics*, 41, (1) 25-32.

Dong, J.T., Lamb, P.W., Rinkerschaeffer, C.W., Vukanovic, J., Ichikawa, T., Isaacs, J.T., & Barrett, J.C. 1995. Kai1, A Metastasis Suppressor Gene for Prostate-Cancer on Human-Chromosome 11P11.2. *Science*, 268, (5212) 884-886.

El Touny, L.H. & Banerjee, P.P. 2007. Genistein induces the metastasis suppressor kangai-1 which mediates its anti-invasive effects in TRAMP cancer cells. *Biochem.Biophys.Res.Commun.*, 361, (1) 169-175.

Espenel, C., Margeat, E., Dosset, P., Arduise, C., Le, G.C., Royer, C.A., Boucheix, C., Rubinstein, E., & Milhiet, P.E. 2008. Single-molecule analysis of CD9 dynamics and partitioning reveals multiple modes of interaction in the tetraspanin web. *J.Cell Biol.*, 182, (4) 765-776.

Esteva, F.J., Guo, H., Zhang, S., Santa-Maria, C., Stone, S., Lanchbury, J.S., Sahin, A.A., Hortobagyi, G.N., & Yu, D. 2010. PTEN, PIK3CA, p-AKT, and p-p70S6K status: association with trastuzumab response and survival in patients with HER2-positive metastatic breast cancer. *Am.J.Pathol.*, 177, (4) 1647-1656.

Fabian, J.R., Daar, I.O., & Morrison, D.K. 1993. Critical tyrosine residues regulate the enzymatic and biological activity of Raf-1 kinase. *Mol.Cell Biol.*, 13, (11) 7170-7179.

Favata, M.F., Horiuchi, K.Y., Manos, E.J., Daulerio, A.J., Stradley, D.A., Feeser, W.S., Van Dyk, D.E., Pitts, W.J., Earl, R.A., Hobbs, F., Copeland, R.A., Magolda, R.L., Scherle, P.A., & Trzaskos, J.M. 1998. Identification of a novel inhibitor of mitogen-activated protein kinase kinase. *J.Biol.Chem.*, 273, (29) 18623-18632.

Fehrenbacher, N., Bar-Sagi, D., & Philips, M. 2009. Ras/MAPK signaling from endomembranes. *Mol.Oncol.*, 3, (4) 297-307.

Fendly, B.M., Winget, M., Hudziak, R.M., Lipari, M.T., Napier, M.A., & Ullrich, A. 1990. Characterization of murine monoclonal antibodies reactive to either the human epidermal growth factor receptor or HER2/neu gene product. *Cancer Res.*, 50, (5) 1550-1558.

Ferguson, J., Arozarena, I., Ehrhardt, M., & Wellbrock, C. 2012. Combination of MEK and SRC inhibition suppresses melanoma cell growth and invasion. *Oncogene*.

Ferguson, K.M., Berger, M.B., Mendrola, J.M., Cho, H.S., Leahy, D.J., & Lemmon, M.A. 2003. EGF activates its receptor by removing interactions that autoinhibit ectodomain dimerization. *Mol.Cell*, 11, (2) 507-517.

Freudenberg, J.A., Wang, Q., Katsumata, M., Drebin, J., Nagatomo, I., & Greene, M.I. 2009. The role of HER2 in early breast cancer metastasis and the origins of resistance to HER2-targeted therapies. *Exp.Mol.Pathol.*, 87, (1) 1-11.

Fukudome, K., Furuse, M., Imai, T., Nishimura, M., Takagi, S., Hinuma, Y., & Yoshie, O. 1992. Identification of membrane antigen C33 recognized by monoclonal antibodies inhibitory to human T-cell leukemia virus type 1 (HTLV-1)-induced syncytium formation: altered glycosylation of C33 antigen in HTLV-1-positive T cells. *J.Virol.*, 66, (3) 1394-1401.

Garrett, T.P., McKern, N.M., Lou, M., Elleman, T.C., Adams, T.E., Lovrecz, G.O., Kofler, M., Jorissen, R.N., Nice, E.C., Burgess, A.W., & Ward, C.W. 2003. The crystal structure of a truncated ErbB2 ectodomain reveals an active conformation, poised to interact with other ErbB receptors. *Mol.Cell*, 11, (2) 495-505.

Gaugitsch, H.W., Hofer, E., Huber, N.E., Schnabl, E., & Baumruker, T. 1991. A new superfamily of lymphoid and melanoma cell proteins with extensive homology to Schistosoma mansoni antigen Sm23. *Eur.J.Immunol.*, 21, (2) 377-383.

Gehart, H., Kumpf, S., Ittner, A., & Ricci, R. 2010. MAPK signalling in cellular metabolism: stress or wellness? *EMBO Rep.*, 11, (11) 834-840.

Gennari, R., Menard, S., Fagnoni, F., Ponchio, L., Scelsi, M., Tagliabue, E., Castiglioni, F., Villani, L., Magalotti, C., Gibelli, N., Oliviero, B., Ballardini, B., Da, P.G., Zambelli, A., & Costa, A. 2004. Pilot study of the mechanism of action of preoperative trastuzumab in patients with primary operable breast tumors overexpressing HER2. *Clin.Cancer Res.*, 10, (17) 5650-5655.

Geyer, F.C., Marchio, C., & Reis-Filho, J.S. 2009. The role of molecular analysis in breast cancer. *Pathology*, 41, (1) 77-88.

Gil, M.L., Vita, N., Lebel-Binay, S., Miloux, B., Chalon, P., Kaghad, M., Marchiol-Fournigault, C., Conjeaud, H., Caput, D., Ferrara, P., & . 1992. A member of the tetra spans transmembrane protein superfamily is recognized by a monoclonal antibody raised against an HLA class I-deficient, lymphokine-activated killer-susceptible, B lymphocyte line. Cloning and preliminary functional studies. *J.Immunol.*, 148, (9) 2826-2833.

Ginestier, C., Adelaide, J., Goncalves, A., Repellini, L., Sircoulomb, F., Letessier, A., Finetti, P., Geneix, J., Charafe-Jauffret, E., Bertucci, F., Jacquemier, J., Viens, P., & Birnbaum, D. 2007. ERBB2 phosphorylation and trastuzumab sensitivity of breast cancer cell lines. *Oncogene*, 26, (50) 7163-7169.

Haining, E.J., Yang, J., & Tomlinson, M.G. 2011. Tetraspanin microdomains: fine-tuning platelet function. *Biochem.Soc.Trans.*, 39, (2) 518-523.

Hanahan, D. & Weinberg, R.A. 2000. The hallmarks of cancer. *Cell*, 100, (1) 57-70.

Hanahan, D. & Weinberg, R.A. 2011. Hallmarks of cancer: the next generation. *Cell*, 144, (5) 646-674.

He, B., Liu, L., Cook, G.A., Grgurevich, S., Jennings, L.K., & Zhang, X.A. 2005. Tetraspanin CD82 attenuates cellular morphogenesis through down-regulating integrin alpha 6-mediated cell adhesion. *Journal of Biological Chemistry*, 280, (5) 3346-3354.

Hemler, M.E. 2001. Specific tetraspanin functions. *Journal of Cell Biology*, 155, (7) 1103-1107.

Hemler, M.E. 2003. Tetraspanin proteins mediate cellular penetration, invasion, and fusion events and define a novel type of membrane microdomain. *Annual Review of Cell and Developmental Biology*, 19, 397-422.

Hemler, M.E. 2005. Tetraspanin functions and associated microdomains. *Nature Reviews Molecular Cell Biology*, 6, (10) 801-811.

Hemler, M.E. 2008. Targeting of tetraspanin proteins - potential benefits and strategies. *Nature Reviews Drug Discovery*, 7, (9) 747-758.

Hoeflich, K.P., O'Brien, C., Boyd, Z., Cavet, G., Guerrero, S., Jung, K., Januario, T., Savage, H., Punnoose, E., Truong, T., Zhou, W., Berry, L., Murray, L., Amler, L., Belvin, M., Friedman, L.S., & Lackner, M.R. 2009. In vivo antitumor activity of MEK and phosphatidylinositol 3-kinase inhibitors in basal-like breast cancer models. *Clin.Cancer Res.*, 15, (14) 4649-4664.

Hoorn, T., Paul, P., Janssen, L., Janssen, H., & Neefjes, J. 2012. Dynamics within tetraspanin pairs affect MHC class II expression. *J.Cell Sci.*, 125, (Pt 2) 328-339.

Horvath, G., Serru, V., Clay, D., Billard, M., Boucheix, C., & Rubinstein, E. 1998. CD19 is linked to the integrin-associated tetraspans CD9, CD81, and CD82. *J.Biol.Chem.*, 273, (46) 30537-30543.

Huang, H., Groth, J., Sossey-Alaoui, K., Hawthorn, L., Beall, S., & Geradts, J. 2005. Aberrant expression of novel and previously described cell membrane markers in human breast cancer cell lines and tumors. *Clin.Cancer Res.*, 11, (12) 4357-4364.

Huang, X., Gao, L., Wang, S., McManaman, J.L., Thor, A.D., Yang, X., Esteva, F.J., & Liu, B. 2010. Heterotrimerization of the growth factor receptors erbB2, erbB3, and insulin-like growth factor-i receptor in breast cancer cells resistant to herceptin. *Cancer Res.*, 70, (3) 1204-1214.

Hudis, C.A. 2007. Drug therapy: Trastuzumab - Mechanism of action and use in clinical practice. *New England Journal of Medicine*, 357, (1) 39-51.

Hughes, C.S., Postovit, L.M., & Lajoie, G.A. 2010. Matrigel: a complex protein mixture required for optimal growth of cell culture. *Proteomics.*, 10, (9) 1886-1890.

Hynes, N.E. & Lane, H.A. 2005. ERBB receptors and cancer: The complexity of targeted inhibitors. *Nature Reviews Cancer*, 5, (5) 341-354.

Hynes, N.E. & MacDonald, G. 2009. ErbB receptors and signaling pathways in cancer. *Current Opinion in Cell Biology*, 21, (2) 177-184.

Ignatiadis, M., Desmedt, C., Sotiriou, C., de, A.E., & Piccart, M. 2009. HER-2 as a target for breast cancer therapy. *Clin.Cancer Res.*, 15, (6) 1848-1852.

Imai, T., Fukudome, K., Takagi, S., Nagira, M., Furuse, M., Fukuhara, N., Nishimura, M., Hinuma, Y., & Yoshie, O. 1992. C33 antigen recognized by monoclonal antibodies inhibitory to human T cell leukemia virus type 1-induced syncytium formation is a member of a new family of transmembrane proteins including CD9, CD37, CD53, and CD63. *J.Immunol.*, 149, (9) 2879-2886.

Imai, T. & Yoshie, O. 1993. C33 antigen and M38 antigen recognized by monoclonal antibodies inhibitory to syncytium formation by human T cell leukemia virus type 1 are both members of the transmembrane 4 superfamily and associate with each other and with CD4 or CD8 in T cells. *J.Immunol.*, 151, (11) 6470-6481.

Izumi, Y., Xu, L., di, T.E., Fukumura, D., & Jain, R.K. 2002. Tumour biology: herceptin acts as an anti-angiogenic cocktail. *Nature*, 416, (6878) 279-280.

Jackson, P., Marreiros, A., & Russell, P.J. 2005. KAI1 tetraspanin and metastasis suppressor. *International Journal of Biochemistry & Cell Biology*, 37, (3) 530-534.

Jee, B.K., Lee, J.Y., Lim, Y., Lee, K.H., & Jo, Y.H. 2007. Effect of KAI1/CD82 on the beta1 integrin maturation in highly migratory carcinoma cells. *Biochem.Biophys.Res.Commun.*, 359, (3) 703-708.

Jin, Q. & Esteva, F.J. 2008. Cross-talk between the ErbB/HER family and the type I insulin-like growth factor receptor signaling pathway in breast cancer. *J.Mammary.Gland.Biol.Neoplasia.*, 13, (4) 485-498.

Jorissen, R.N., Walker, F., Pouliot, N., Garrett, T.P., Ward, C.W., & Burgess, A.W. 2003. Epidermal growth factor receptor: mechanisms of activation and signalling. *Exp.Cell Res.*, 284, (1) 31-53.

Joshi, B., Li, L., & Nabi, I.R. 2010. A role for KAI1 in promotion of cell proliferation and mammary gland hyperplasia by the gp78 ubiquitin ligase. *J.Biol.Chem.*, 285, (12) 8830-8839.

Junge, H.J., Yang, S., Burton, J.B., Paes, K., Shu, X., French, D.M., Costa, M., Rice, D.S., & Ye, W. 2009. TSPAN12 regulates retinal vascular development by promoting Norrin- but not Wnt-induced FZD4/beta-catenin signaling. *Cell*, 139, (2) 299-311.

Junttila, T.T., Akita, R.W., Parsons, K., Fields, C., Phillips, G.D.L., Friedman, L.S., Sampath, D., & Sliwkowski, M.X. 2009. Ligand-Independent HER2/HER3/PI3K Complex Is Disrupted by Trastuzumab and Is Effectively Inhibited by the PI3K Inhibitor GDC-0941. *Cancer Cell*, 15, (5) 429-440.

Kao, J., Salari, K., Bocanegra, M., Choi, Y.L., Girard, L., Gandhi, J., Kwei, K.A., Hernandez-Boussard, T., Wang, P., Gazdar, A.F., Minna, J.D., & Pollack, J.R. 2009. Molecular profiling of breast cancer cell lines defines relevant tumor models and provides a resource for cancer gene discovery. *PLoS.One.*, 4, (7) e6146.

Karamatic, C., V, Burton, N., Kagan, A., Green, C.A., Levene, C., Flinter, F., Brady, R.L., Daniels, G., & Anstee, D.J. 2004. CD151, the first member of the tetraspanin (TM4) superfamily detected on erythrocytes, is essential for the correct assembly of human basement membranes in kidney and skin. *Blood*, 104, (8) 2217-2223.

Kawakami, Y., Kawakami, K., Steelant, W.F., Ono, M., Baek, R.C., Handa, K., Withers, D.A., & Hakomori, S. 2002. Tetraspanin CD9 is a "proteolipid," and its interaction with alpha 3 integrin in microdomain is promoted by GM3 ganglioside, leading to inhibition of laminin-5-dependent cell motility. *J.Biol.Chem.*, 277, (37) 34349-34358.

Kim, H.J. & Bar-Sagi, D. 2004. Modulation of signalling by Sprouty: a developing story. *Nat.Rev.Mol.Cell Biol.*, 5, (6) 441-450.

Kim, J.M., Bak, E.J., Chang, J.Y., Kim, S.T., Park, W.S., Yoo, Y.J., & Cha, J.H. 2011a. Effects of HB-EGF and epiregulin on wound healing of gingival cells in vitro. *Oral Dis.*, 17, (8) 785-793.

Kim, J.S., Bak, E.J., Lee, B.C., Kim, Y.S., Park, J.B., & Choi, I.G. 2011b. Neuregulin induces HaCaT keratinocyte migration via Rac1-mediated NADPH-oxidase activation. *J.Cell Physiol*, 226, (11) 3014-3021.

Kitadokoro, K., Bordo, D., Galli, G., Petracca, R., Falugi, F., Abrignani, S., Grandi, G., & Bolognesi, M. 2001. CD81 extracellular domain 3D structure: insight into the tetraspanin superfamily structural motifs. *Embo Journal*, 20, (1-2) 12-18.

Kleinman, H.K. & Martin, G.R. 2005. Matrigel: basement membrane matrix with biological activity. *Semin.Cancer Biol.*, 15, (5) 378-386.

Klemke, R.L., Leng, J., Molander, R., Brooks, P.C., Vuori, K., & Cheresh, D.A. 1998. CAS/Crk coupling serves as a "molecular switch" for induction of cell migration. *J.Cell Biol.*, 140, (4) 961-972.

Kolch, W. 2005. Coordinating ERK/MAPK signalling through scaffolds and inhibitors. *Nat.Rev.Mol.Cell Biol.*, 6, (11) 827-837.

Kovalenko, O.V., Yang, X., Kolesnikova, T.V., & Hemler, M.E. 2004. Evidence for specific tetraspanin homodimers: inhibition of palmitoylation makes cysteine residues available for cross-linking. *Biochem.J.*, 377, (Pt 2) 407-417.

Krementsov, D.N., Rassam, P., Margeat, E., Roy, N.H., Schneider-Schaulies, J., Milhiet, P.E., & Thali, M. 2010. HIV-1 assembly differentially alters dynamics and partitioning of tetraspanins and raft components. *Traffic.*, 11, (11) 1401-1414.

Kroep, J.R., Linn, S.C., Boven, E., Bloemendal, H.J., Baas, J., Mandjes, I.A., van den Bosch, J., Smit, W.M., de, G.H., Schroder, C.P., Vermeulen, G.J., Hop, W.C., & Nortier, J.W. 2010. Lapatinib: clinical benefit in patients with HER 2-positive advanced breast cancer. *Neth.J.Med.*, 68, (9) 371-376.

Kruser, T.J. & Wheeler, D.L. 2010. Mechanisms of resistance to HER family targeting antibodies. *Exp.Cell Res.*, 316, (7) 1083-1100.

Kwon, M.J., Park, S., Choi, J.Y., Oh, E., Kim, Y.J., Park, Y.H., Cho, E.Y., Kwon, M.J., Nam, S.J., Im, Y.H., Shin, Y.K., & Choi, Y.L. 2012. Clinical significance of CD151 overexpression in subtypes of invasive breast cancer. *Br.J.Cancer*, 106, (5) 923-930.

Lagaudriere-Gesbert, C., Lebel-Binay, S., Hubeau, C., Fradelizi, D., & Conjeaud, H. 1998. Signaling through the tetraspanin CD82 triggers its association with the cytoskeleton leading to sustained morphological changes and T cell activation. *Eur.J.Immunol.*, 28, (12) 4332-4344.

Lagaudriere-Gesbert, C., Lebel-Binay, S., Wiertz, E., Ploegh, H.L., Fradelizi, D., & Conjeaud, H. 1997. The tetraspanin protein CD82 associates with both free HLA class I heavy chain and heterodimeric beta 2-microglobulin complexes. *J.Immunol.*, 158, (6) 2790-2797.

Lane, H.A., Beuvink, I., Motoyama, A.B., Daly, J.M., Neve, R.M., & Hynes, N.E. 2000. ErbB2 potentiates breast tumor proliferation through modulation of p27(Kip1)-Cdk2 complex formation: receptor overexpression does not determine growth dependency. *Mol.Cell Biol.*, 20, (9) 3210-3223.

Lapalombella, R., Yeh, Y.Y., Wang, L., Ramanunni, A., Rafiq, S., Jha, S., Staubli, J., Lucas, D.M., Mani, R., Herman, S.E., Johnson, A.J., Lozanski, A., Andritsos, L., Jones, J., Flynn, J.M., Lannutti, B., Thompson, P., Algate, P., Stromatt, S., Jarjoura, D., Mo, X., Wang, D., Chen, C.S., Lozanski, G., Heerema, N.A., Tridandapani, S., Freitas, M.A., Muthusamy, N., & Byrd, J.C. 2012. Tetraspanin CD37 Directly Mediates Transduction of Survival and Apoptotic Signals. *Cancer Cell*, 21, (5) 694-708.

Lau, L.M., Wee, J.L., Wright, M.D., Moseley, G.W., Hogarth, P.M., Ashman, L.K., & Jackson, D.E. 2004. The tetraspanin superfamily member CD151

regulates outside-in integrin alphaIIbbeta3 signaling and platelet function. *Blood*, 104, (8) 2368-2375.

Lazo, P.A. 2007. Functional implications of tetraspanin proteins in cancer biology. *Cancer Sci.*, 98, (11) 1666-1677.

Le, N.F., Rubinstein, E., Jasmin, C., Prenant, M., & Boucheix, C. 2000. Severely reduced female fertility in CD9-deficient mice. *Science*, 287, (5451) 319-321.

Le, X.F., Claret, F.X., Lammayot, A., Tian, L., Deshpande, D., LaPushin, R., Tari, A.M., & Bast, R.C., Jr. 2003. The role of cyclin-dependent kinase inhibitor p27Kip1 in anti-HER2 antibody-induced G1 cell cycle arrest and tumor growth inhibition. *J.Biol.Chem.*, 278, (26) 23441-23450.

Le, X.F., Lammayot, A., Gold, D., Lu, Y., Mao, W., Chang, T., Patel, A., Mills, G.B., & Bast, R.C., Jr. 2005a. Genes affecting the cell cycle, growth, maintenance, and drug sensitivity are preferentially regulated by anti-HER2 antibody through phosphatidylinositol 3-kinase-AKT signaling. *J.Biol.Chem.*, 280, (3) 2092-2104.

Le, X.F., Pruefer, F., & Bast, R.C., Jr. 2005b. HER2-targeting antibodies modulate the cyclin-dependent kinase inhibitor p27Kip1 via multiple signaling pathways. *Cell Cycle*, 4, (1) 87-95.

Lebel-Binay, S., Lagaudriere, C., Fradelizi, D., & Conjeaud, H. 1995. CD82, member of the tetra-span-transmembrane protein family, is a costimulatory protein for T cell activation. *J.Immunol.*, 155, (1) 101-110.

Leber, M.F. & Efferth, T. 2009. Molecular principles of cancer invasion and metastasis (review). *Int.J.Oncol.*, 34, (4) 881-895.

Lee, C.C., Putnam, A.J., Miranti, C.K., Gustafson, M., Wang, L.M., Vande Woude, G.F., & Gao, C.F. 2004a. Overexpression of sprouty 2 inhibits HGF/SF-mediated cell growth, invasion, migration, and cytokinesis. *Oncogene*, 23, (30) 5193-5202.

Lee, J.H., Park, S.R., Chay, K.O., Seo, Y.W., Kook, H., Ahn, K.Y., Kim, Y.J., & Kim, K.K. 2004b. KAI1 COOH-terminal interacting tetraspanin (KITENIN), a member of the tetraspanin family, interacts with KAI1, a tumor metastasis suppressor, and enhances metastasis of cancer. *Cancer Res.*, 64, (12) 4235-4243.

Lemmon, M.A., Bu, Z., Ladbury, J.E., Zhou, M., Pinchasi, D., Lax, I., Engelman, D.M., & Schlessinger, J. 1997. Two EGF molecules contribute additively to stabilization of the EGFR dimer. *EMBO J.*, 16, (2) 281-294.

Levy, S. & Shoham, T. 2005a. Protein-protein interactions in the tetraspanin web. *Physiology*, 20, 218-224.

Levy, S. & Shoham, T. 2005b. The tetraspanin web modulates immune-signalling complexes. *Nature Reviews Immunology*, 5, (2) 136-148.

Li, E. & Hristova, K. 2010. Receptor tyrosine kinase transmembrane domains: Function, dimer structure and dimerization energetics. *Cell Adh.Migr.*, 4, (2) 249-254.

Lin, S., Yu, L., Yang, J., Liu, Z., Karia, B., Bishop, A.J., Jackson, J., Lozano, G., Copland, J.A., Mu, X., Sun, B., & Sun, L.Z. 2011. Mutant p53 Disrupts Role of ShcA Protein in Balancing Smad Protein-dependent and -independent Signaling Activity of Transforming Growth Factor-beta (TGF-beta). *J.Biol.Chem.*, 286, (51) 44023-44034.

Linggi, B. & Carpenter, G. 2006. ErbB receptors: new insights on mechanisms and biology. *Trends Cell Biol.*, 16, (12) 649-656.

Lingwood, D. & Simons, K. 2010. Lipid rafts as a membrane-organizing principle. *Science*, 327, (5961) 46-50.

Lippincott-Schwartz, J., Snapp, E., & Kenworthy, A. 2001. Studying protein dynamics in living cells. *Nat.Rev.Mol.Cell Biol.*, 2, (6) 444-456.

Liu, H., Radisky, D.C., Wang, F., & Bissell, M.J. 2004a. Polarity and proliferation are controlled by distinct signaling pathways downstream of PI3-kinase in breast epithelial tumor cells. *J.Cell Biol.*, 164, (4) 603-612.

Liu, P., Sudhaharan, T., Koh, R.M., Hwang, L.C., Ahmed, S., Maruyama, I.N., & Wohland, T. 2007. Investigation of the dimerization of proteins from the epidermal growth factor receptor family by single wavelength fluorescence cross-correlation spectroscopy. *Biophys.J.*, 93, (2) 684-698.

Liu, W.M. & Zhang, X.A. 2006. KAI1/CD82, a tumor metastasis suppressor. *Cancer Letters*, 240, (2) 183-194.

Liu, Y., Li, R., & Ladisch, S. 2004b. Exogenous ganglioside GD1a enhances epidermal growth factor receptor binding and dimerization. *J.Biol.Chem.*, 279, (35) 36481-36489.

Lu, C.H., Wyszomierski, S.L., Tseng, L.M., Sun, M.H., Lan, K.H., Neal, C.L., Mills, G.B., Hortobagyi, G.N., Esteva, F.J., & Yu, D. 2007. Preclinical testing of clinically applicable strategies for overcoming trastuzumab resistance caused by PTEN deficiency. *Clin.Cancer Res.*, 13, (19) 5883-5888.

Lu, Y., Zi, X., & Pollak, M. 2004. Molecular mechanisms underlying IGF-I-induced attenuation of the growth-inhibitory activity of trastuzumab (Herceptin) on SKBR3 breast cancer cells. *Int.J.Cancer*, 108, (3) 334-341.

Lu, Y., Zi, X., Zhao, Y., Mascarenhas, D., & Pollak, M. 2001. Insulin-like growth factor-I receptor signaling and resistance to trastuzumab (Herceptin). *J.Natl.Cancer Inst.*, 93, (24) 1852-1857.

Maecker, H.T., Todd, S.C., & Levy, S. 1997. The tetraspanin superfamily: Molecular facilitators. *Faseb Journal*, 11, (6) 428-442.

Manning, B.D. & Cantley, L.C. 2007. AKT/PKB signaling: navigating downstream. *Cell*, 129, (7) 1261-1274.

Mannion, B.A., Berditchevski, F., Kraeft, S.K., Chen, L.B., & Hemler, M.E. 1996. Transmembrane-4 superfamily proteins CD81 (TAPA-1), CD82, CD63, and CD53 specifically associated with integrin alpha 4 beta 1 (CD49d/CD29). *J.Immunol.*, 157, (5) 2039-2047.

Marais, R., Light, Y., Paterson, H.F., & Marshall, C.J. 1995. Ras recruits Raf-1 to the plasma membrane for activation by tyrosine phosphorylation. *EMBO J.*, 14, (13) 3136-3145.

Marais, R., Light, Y., Paterson, H.F., Mason, C.S., & Marshall, C.J. 1997. Differential regulation of Raf-1, A-Raf, and B-Raf by oncogenic ras and tyrosine kinases. *J.Biol.Chem.*, 272, (7) 4378-4383.

Marreiros, A., Czolij, R., Yardley, G., Crossley, M., & Jackson, P. 2003. Identification of regulatory regions within the KAI1 promoter: a role for binding of AP1, AP2 and p53. *Gene*, 302, (1-2) 155-164.

Marreiros, A., Dudgeon, K., Dao, V., Grimm, M.O., Czolij, R., Crossley, M., & Jackson, P. 2005. KAI1 promoter activity is dependent on p53, junB and AP2: evidence for a possible mechanism underlying loss of KAI1 expression in cancer cells. *Oncogene*, 24, (4) 637-649.

Marshall, C.J. 1995. Specificity of receptor tyrosine kinase signaling: transient versus sustained extracellular signal-regulated kinase activation. *Cell*, 80, (2) 179-185.

Mason, C.S., Springer, C.J., Cooper, R.G., Superti-Furga, G., Marshall, C.J., & Marais, R. 1999. Serine and tyrosine phosphorylations cooperate in Raf-1, but not B-Raf activation. *EMBO J.*, 18, (8) 2137-2148.

Massague, J. 2008. TGFbeta in Cancer. *Cell*, 134, (2) 215-230.

Matheny, S.A., Chen, C., Kortum, R.L., Razidlo, G.L., Lewis, R.E., & White, M.A. 2004. Ras regulates assembly of mitogenic signalling complexes through the effector protein IMP. *Nature*, 427, (6971) 256-260.

Mazurov, D., Heidecker, G., & Derse, D. 2007. The inner loop of tetraspanins CD82 and CD81 mediates interactions with human T cell lymphotrophic virus type 1 Gag protein. *J.Biol.Chem.*, 282, (6) 3896-3903.

McCubrey, J.A., Steelman, L.S., Chappell, W.H., Abrams, S.L., Wong, E.W., Chang, F., Lehmann, B., Terrian, D.M., Milella, M., Tafuri, A., Stivala, F., Libra, M., Basecke, J., Evangelisti, C., Martelli, A.M., & Franklin, R.A. 2007. Roles of the Raf/MEK/ERK pathway in cell growth, malignant transformation and drug resistance. *Biochim.Biophys.Acta*, 1773, (8) 1263-1284.

Mebratu, Y. & Tesfaigzi, Y. 2009. How ERK1/2 activation controls cell proliferation and cell death: Is subcellular localization the answer? *Cell Cycle*, 8, (8) 1168-1175.

Mi, L.Z., Lu, C., Li, Z., Nishida, N., Walz, T., & Springer, T.A. 2011. Simultaneous visualization of the extracellular and cytoplasmic domains of the epidermal growth factor receptor. *Nat.Struct.Mol.Biol.*, 18, (9) 984-989.

Milani, S., Sottocornola, E., Zava, S., Berselli, P., Berra, B., & Colombo, I. 2007. Ganglioside GM(3) is stably associated to tyrosine-phosphorylated ErbB2/EGFR receptor complexes and EGFR monomers, but not to ErbB2. *Biochim.Biophys.Acta*, 1771, (7) 873-878.

Milani, S., Sottocornola, E., Zava, S., Galbiati, M., Berra, B., & Colombo, I. 2010. Gangliosides influence EGFR/ErbB2 heterodimer stability but they do not modify EGF-dependent ErbB2 phosphorylation. *Biochim.Biophys.Acta*, 1801, (6) 617-624.

Miljan, E.A. & Bremer, E.G. 2002. Regulation of growth factor receptors by gangliosides. *Sci.STKE.*, 2002, (160) re15.

Millikan, R.C., Newman, B., Tse, C.K., Moorman, P.G., Conway, K., Dressler, L.G., Smith, L.V., Labbok, M.H., Geradts, J., Bensen, J.T., Jackson, S., Nyante, S., Livasy, C., Carey, L., Earp, H.S., & Perou, C.M. 2008. Epidemiology of basal-like breast cancer. *Breast Cancer Res.Treat.*, 109, (1) 123-139.

Min, G.W., Wang, H.B., Sun, T.T., & Kong, X.P. 2006. Structural basis for tetraspanin functions as revealed by the cryo-EM structure of uroplakin complexes at 6-A resolution. *Journal of Cell Biology*, 173, (6) 975-983.

Miranti, C.K. 2009. Controlling cell surface dynamics and signaling: How CD82/KAI1 suppresses metastasis. *Cellular Signalling*, 21, (2) 196-211.

Molina, M.A., Codony-Servat, J., Albanell, J., Rojo, F., Arribas, J., & Baselga, J. 2001. Trastuzumab (herceptin), a humanized anti-Her2 receptor monoclonal antibody, inhibits basal and activated Her2 ectodomain cleavage in breast cancer cells. *Cancer Res.*, 61, (12) 4744-4749.

Mollinedo, F., Fontan, G., Barasoain, I., & Lazo, P.A. 1997. Recurrent infectious diseases in human CD53 deficiency. *Clin.Diagn.Lab Immunol.*, 4, (2) 229-231.

Monick, M.M., Powers, L.S., Barrett, C.W., Hinde, S., Ashare, A., Groskreutz, D.J., Nyunoya, T., Coleman, M., Spitz, D.R., & Hunninghake, G.W. 2008. Constitutive ERK MAPK activity regulates macrophage ATP production and mitochondrial integrity. *J.Immunol.*, 180, (11) 7485-7496.

Mor, A. & Philips, M.R. 2006. Compartmentalized Ras/MAPK signaling. *Annu.Rev.Immunol.*, 24, 771-800.

Mu, Z., Wang, H., Zhang, J., Li, Q., Wang, L., & Guo, X. 2008. KAI1/CD82 suppresses hepatocyte growth factor-induced migration of hepatoma cells via upregulation of Sprouty2. *Sci.China C.Life Sci.*, 51, (7) 648-654.

Mukohara, T. 2011. Mechanisms of resistance to anti-human epidermal growth factor receptor 2 agents in breast cancer. *Cancer Sci.*, 102, (1) 1-8.

Muthuswamy, S.K., Gilman, M., & Brugge, J.S. 1999. Controlled dimerization of ErbB receptors provides evidence for differential signaling by homo- and heterodimers. *Mol.Cell Biol.*, 19, (10) 6845-6857.

Nagata, Y., Lan, K.H., Zhou, X., Tan, M., Esteva, F.J., Sahin, A.A., Klos, K.S., Li, P., Monia, B.P., Nguyen, N.T., Hortobagyi, G.N., Hung, M.C., & Yu, D. 2004. PTEN activation contributes to tumor inhibition by trastuzumab, and loss of PTEN predicts trastuzumab resistance in patients. *Cancer Cell*, 6, (2) 117-127.

Nagy, P., Friedlander, E., Tanner, M., Kapanen, A.I., Carraway, K.L., Isola, J., & Jovin, T.M. 2005. Decreased accessibility and lack of activation of ErbB2 in JIMT-1, a herceptin-resistant, MUC4-expressing breast cancer cell line. *Cancer Res.*, 65, (2) 473-482.

Nagy, P., Vereb, G., Sebestyen, Z., Horvath, G., Lockett, S.J., Damjanovich, S., Park, J.W., Jovin, T.M., & Szollosi, J. 2002. Lipid rafts and the local density of ErbB proteins influence the biological role of homo- and heteroassociations of ErbB2. *J.Cell Sci.*, 115, (Pt 22) 4251-4262.

Nahta, R. & Esteva, F.J. 2007. Trastuzumab: triumphs and tribulations. *Oncogene*, 26, (25) 3637-3643.

Nahta, R., Yuan, L.X., Zhang, B., Kobayashi, R., & Esteva, F.J. 2005. Insulin-like growth factor-I receptor/human epidermal growth factor receptor 2 heterodimerization contributes to trastuzumab resistance of breast cancer cells. *Cancer Res.*, 65, (23) 11118-11128.

Nakamura, K., Mitamura, T., Takahashi, T., Kobayashi, T., & Mekada, E. 2000. Importance of the major extracellular domain of CD9 and the epidermal growth factor (EGF)-like domain of heparin-binding EGF-like growth factor for up-regulation of binding and activity. *J.Biol.Chem.*, 275, (24) 18284-18290.

Nichols, T.C., Guthridge, J.M., Karp, D.R., Molina, H., Fletcher, D.R., & Holers, V.M. 1998. Gamma-glutamyl transpeptidase, an ecto-enzyme regulator of intracellular redox potential, is a component of TM4 signal transduction complexes. *Eur.J.Immunol.*, 28, (12) 4123-4129.

Novitskaya, V., Romanska, H., Dawoud, M., Jones, J.L., & Berditchevski, F. 2010. Tetraspanin CD151 regulates growth of mammary epithelial cells in three-dimensional extracellular matrix: implication for mammary ductal carcinoma in situ. *Cancer Res.*, 70, (11) 4698-4708.

Odintsova, E., Butters, T.D., Monti, E., Sprong, H., van Meer, G., & Berditchevski, F. 2006. Gangliosides play an important role in the organization of CD82-enriched microdomains. *Biochemical Journal*, 400, 315-325.

Odintsova, E., Sugiura, T., & Berditchevski, F. 2000. Attenuation of EGF receptor signaling by a metastasis suppressor, the tetraspanin CD82/KAI-1. *Current Biology*, 10, (16) 1009-1012.

Odintsova, E., Voortman, J., Gilbert, E., & Berditchevski, F. 2003. Tetraspanin CD82 regulates compartmentalisation and ligand-induced dimerization of EGFR. *Journal of Cell Science*, 116, (22) 4557-4566.

Olayioye, M.A., Badache, A., Daly, J.M., & Hynes, N.E. 2001. An essential role for Src kinase in ErbB receptor signaling through the MAPK pathway. *Exp.Cell Res.*, 267, (1) 81-87.

Olayioye, M.A., Neve, R.M., Lane, H.A., & Hynes, N.E. 2000. The ErbB signaling network: receptor heterodimerization in development and cancer. *EMBO J.*, 19, (13) 3159-3167.

Olopade, O.I., Grushko, T.A., Nanda, R., & Huo, D. 2008. Advances in breast cancer: pathways to personalized medicine. *Clin.Cancer Res.*, 14, (24) 7988-7999.

Omerovic, J. & Prior, I.A. 2009. Compartmentalized signalling: Ras proteins and signalling nanoclusters. *FEBS J.*, 276, (7) 1817-1825.

Orr, G., Hu, D., Ozcelik, S., Opresko, L.K., Wiley, H.S., & Colson, S.D. 2005. Cholesterol dictates the freedom of EGF receptors and HER2 in the plane of the membrane. *Biophys.J.*, 89, (2) 1362-1373.

Park, C.C., Zhang, H., Pallavicini, M., Gray, J.W., Baehner, F., Park, C.J., & Bissell, M.J. 2006. Beta1 integrin inhibitory antibody induces apoptosis of breast cancer cells, inhibits growth, and distinguishes malignant from normal phenotype in three dimensional cultures and in vivo. *Cancer Res.*, 66, (3) 1526-1535.

Pegram, M., Hsu, S., Lewis, G., Pietras, R., Beryt, M., Sliwkowski, M., Coombs, D., Baly, D., Kabbinavar, F., & Slamon, D. 1999. Inhibitory effects of combinations of HER-2/neu antibody and chemotherapeutic agents used for treatment of human breast cancers. *Oncogene*, 18, (13) 2241-2251.

Pegram, M.D., Konecny, G.E., O'Callaghan, C., Beryt, M., Pietras, R., & Slamon, D.J. 2004. Rational combinations of trastuzumab with chemotherapeutic drugs used in the treatment of breast cancer. *J.Natl.Cancer Inst.*, 96, (10) 739-749.

Pegram, M.D., Lipton, A., Hayes, D.F., Weber, B.L., Baselga, J.M., Tripathy, D., Baly, D., Baughman, S.A., Twaddell, T., Glaspy, J.A., & Slamon, D.J. 1998. Phase II study of receptor-enhanced chemosensitivity using recombinant humanized anti-p185HER2/neu monoclonal antibody plus cisplatin in patients with HER2/neu-overexpressing metastatic breast cancer refractory to chemotherapy treatment. *J.Clin.Oncol.*, 16, (8) 2659-2671.

Perou, C.M., Sorlie, T., Eisen, M.B., van de Rijn, M., Jeffrey, S.S., Rees, C.A., Pollack, J.R., Ross, D.T., Johnsen, H., Akslen, L.A., Fluge, O., Pergamenschikov, A., Williams, C., Zhu, S.X., Lonning, P.E., Borresen-Dale, A.L., Brown, P.O., & Botstein, D. 2000. Molecular portraits of human breast tumours. *Nature*, 406, (6797) 747-752.

Pickl, M. & Ries, C.H. 2009. Comparison of 3D and 2D tumor models reveals enhanced HER2 activation in 3D associated with an increased response to trastuzumab. *Oncogene*, 28, (3) 461-468.

Reits, E.A. & Neefjes, J.J. 2001. From fixed to FRAP: measuring protein mobility and activity in living cells. *Nat.Cell Biol.*, 3, (6) E145-E147.

Richardson, M.M., Jennings, L.K., & Zhang, X.A. 2011. Tetraspanins and tumor progression. *Clin.Exp.Metastasis*, 28, (3) 261-270.

Roberts, P.J. & Der, C.J. 2007. Targeting the Raf-MEK-ERK mitogen-activated protein kinase cascade for the treatment of cancer. *Oncogene*, 26, (22) 3291-3310.

Robinson, D.R., Wu, Y.M., & Lin, S.F. 2000. The protein tyrosine kinase family of the human genome. *Oncogene*, 19, (49) 5548-5557.

Romanska, H.M. & Berditchevski, F. 2011. Tetraspanins in human epithelial malignancies. *J.Pathol.*, 223, (1) 4-14.

Roskoski, R., Jr. 2004. The ErbB/HER receptor protein-tyrosine kinases and cancer. *Biochem.Biophys.Res.Commun.*, 319, (1) 1-11.

Routledge, H.C., Rea, D.W., & Steeds, R.P. 2006. Monitoring the introduction of new drugs--Herceptin to cardiotoxicity. *Clin.Med.*, 6, (5) 478-481.

Rowe, A., Weiske, J., Kramer, T.S., Huber, O., & Jackson, P. 2008. Phorbol ester enhances KAI1 transcription by recruiting Tip60/Pontin complexes. *Neoplasia.*, 10, (12) 1421-32, following.

Rubinstein, E., Le, N.F., Lagaudriere-Gesbert, C., Billard, M., Conjeaud, H., & Boucheix, C. 1996. CD9, CD63, CD81, and CD82 are components of a surface tetraspan network connected to HLA-DR and VLA integrins. *Eur.J.Immunol.*, 26, (11) 2657-2665.

Rubinstein, E., Ziyyat, A., Prenant, M., Wrobel, E., Wolf, J.P., Levy, S., Le, N.F., & Boucheix, C. 2006. Reduced fertility of female mice lacking CD81. *Dev.Biol.*, 290, (2) 351-358.

Runge, K.E., Evans, J.E., He, Z.Y., Gupta, S., McDonald, K.L., Stahlberg, H., Primakoff, P., & Myles, D.G. 2007. Oocyte CD9 is enriched on the microvillar membrane and required for normal microvillar shape and distribution. *Dev.Biol.*, 304, (1) 317-325.

Ruseva, Z., Geiger, P.X.C., Hutzler, P., Kotzsch, M., Luber, B., Schmitt, M., Gross, E., & Reuning, U. 2009. Tumor suppressor KAI1 affects integrin alpha v beta 3-mediated ovarian cancer cell adhesion, motility, and proliferation. *Experimental Cell Research*, 315, (10) 1759-1771.

Sacks, D.B. 2006. The role of scaffold proteins in MEK/ERK signalling. *Biochem.Soc.Trans.*, 34, (Pt 5) 833-836.

Sadej, R., Romanska, H., Baldwin, G., Gkirtzimanaki, K., Novitskaya, V., Filer, A.D., Krcova, Z., Kusinska, R., Ehrmann, J., Buckley, C.D., Kordek, R., Potemski, P., Eliopoulos, A.G., Lalani, e., & Berditchevski, F. 2009. CD151 regulates tumorigenesis by modulating the communication between tumor cells and endothelium. *Mol.Cancer Res.*, 7, (6) 787-798.

Sadej, R., Romanska, H., Kavanagh, D., Baldwin, G., Takahashi, T., Kalia, N., & Berditchevski, F. 2010. Tetraspanin CD151 regulates transforming growth factor beta signaling: implication in tumor metastasis. *Cancer Res.*, 70, (14) 6059-6070.

Salzer, U. & Prohaska, R. 2001. Stomatin, flotillin-1, and flotillin-2 are major integral proteins of erythrocyte lipid rafts. *Blood*, 97, (4) 1141-1143.

Sawada, S., Yoshimoto, M., Odintsova, E., Hotchin, N.A., & Berditchevski, F. 2003. The tetraspanin CD151 functions as a negative regulator in the adhesion-dependent activation of Ras. *J.Biol.Chem.*, 278, (29) 26323-26326.

Scaltriti, M., Rojo, F., Ocana, A., Anido, J., Guzman, M., Cortes, J., Di, C.S., Matias-Guiu, X., Cajal, S., Arribas, J., & Baselga, J. 2007. Expression of p95HER2, a truncated form of the HER2 receptor, and response to anti-HER2 therapies in breast cancer. *J.Natl.Cancer Inst.*, 99, (8) 628-638.

Schmeichel, K.L. & Bissell, M.J. 2003. Modeling tissue-specific signaling and organ function in three dimensions. *J.Cell Sci.*, 116, (Pt 12) 2377-2388.

Schmitt, F. 2009. HER2+ breast cancer: how to evaluate? *Adv.Ther.*, 26 Suppl 1, S1-S8.

Schnitt, S.J. 2010. Classification and prognosis of invasive breast cancer: from morphology to molecular taxonomy. *Mod.Pathol.*, 23 Suppl 2, S60-S64.

Shattuck, D.L., Miller, J.K., Carraway, K.L., III, & Sweeney, C. 2008. Met receptor contributes to trastuzumab resistance of Her2-overexpressing breast cancer cells. *Cancer Res.*, 68, (5) 1471-1477.

Simons, K. & Gerl, M.J. 2010. Revitalizing membrane rafts: new tools and insights. *Nat.Rev.Mol.Cell Biol.*, 11, (10) 688-699.

Simons, K. & Ikonen, E. 1997. Functional rafts in cell membranes. *Nature*, 387, (6633) 569-572.

Simons, K. & Sampaio, J.L. 2011. Membrane organization and lipid rafts. *Cold Spring Harb.Perspect.Biol.*, 3, (10) a004697.

Slaughter, N., Laux, I., Tu, X., Whitelegge, J., Zhu, X., Effros, R., Bickel, P., & Nel, A. 2003. The flotillins are integral membrane proteins in lipid rafts that contain TCR-associated signaling components: implications for T-cell activation. *Clin.Immunol.*, 108, (2) 138-151.

Smirnova, T., Zhou, Z.N., Flinn, R.J., Wyckoff, J., Boimel, P.J., Pozzuto, M., Coniglio, S.J., Backer, J.M., Bresnick, A.R., Condeelis, J.S., Hynes, N.E., &

Segall, J.E. 2012. Phosphoinositide 3-kinase signaling is critical for ErbB3-driven breast cancer cell motility and metastasis. *Oncogene*, 31, (6) 706-715.

Smyth, M.J., Cretney, E., Kelly, J.M., Westwood, J.A., Street, S.E., Yagita, H., Takeda, K., van Dommelen, S.L., Degli-Esposti, M.A., & Hayakawa, Y. 2005. Activation of NK cell cytotoxicity. *Mol.Immunol.*, 42, (4) 501-510.

Sottocornola, E., Misasi, R., Mattei, V., Ciarlo, L., Gradini, R., Garofalo, T., Berra, B., Colombo, I., & Sorice, M. 2006. Role of gangliosides in the association of ErbB2 with lipid rafts in mammary epithelial HC11 cells. *FEBS J.*, 273, (8) 1821-1830.

Spector, N.L. & Blackwell, K.L. 2009. Understanding the mechanisms behind trastuzumab therapy for human epidermal growth factor receptor 2-positive breast cancer. *J.Clin.Oncol.*, 27, (34) 5838-5847.

Stern, D.F. 2008. ERBB3/HER3 and ERBB2/HER2 duet in mammary development and breast cancer. *Journal of Mammary Gland Biology and Neoplasia*, 13, (2) 215-223.

Stipp, C.S. 2010. Laminin-binding integrins and their tetraspanin partners as potential antimetastatic targets. *Expert.Rev.Mol.Med.*, 12, e3.

Takahashi, M., Sugiura, T., Abe, M., Ishii, K., & Shirasuna, K. 2007. Regulation of c-Met signaling by the tetraspanin KAI-1/CD82 affects cancer cell migration. *International Journal of Cancer*, 121, 1919-1929.

Tan, M., Li, P., Sun, M., Yin, G., & Yu, D. 2006. Upregulation and activation of PKC alpha by ErbB2 through Src promotes breast cancer cell invasion that can be blocked by combined treatment with PKC alpha and Src inhibitors. *Oncogene*, 25, (23) 3286-3295.

Tarrant, J.M., Robb, L., van Spriel, A.B., & Wright, M.D. 2003. Tetraspanins: molecular organisers of the leukocyte surface. *Trends Immunol.*, 24, (11) 610-617.

Tavassoli, F.A. 2010. Correlation between gene expression profiling-based molecular and morphologic classification of breast cancer. *Int.J.Surg.Pathol.*, 18, (3 Suppl) 167S-169S.

Todeschini, A.R., Dos Santos, J.N., Handa, K., & Hakolmori, S.I. 2008. Ganglioside GM2/GM3 complex affixed on silica nanospheres strongly inhibits cell motility through CD82/cMet-mediated pathway. *Proceedings of the National Academy of Sciences of the United States of America*, 105, (6) 1925-1930.

Todeschini, A.R., Dos Santos, J.N., Handa, K., & Hakomori, S. 2007. Ganglioside GM2-tetraspanin CD82 complex inhibits met and its cross-talk with integrins, providing a basis for control of cell motility through glycosynapse. *Journal of Biological Chemistry*, 282, (11) 8123-8133.

Tonoli, H. & Barrett, J.C. 2005. CD82 metastasis suppressor gene: a potential target for new therapeutics? *Trends in Molecular Medicine*, 11, (12) 563-570.

Tran, N.H. & Frost, J.A. 2003. Phosphorylation of Raf-1 by p21-activated kinase 1 and Src regulates Raf-1 autoinhibition. *J.Biol.Chem.*, 278, (13) 11221-11226.

Tseng, P.H., Wang, Y.C., Weng, S.C., Weng, J.R., Chen, C.S., Brueggemeier, R.W., Shapiro, C.L., Chen, C.Y., Dunn, S.E., Pollak, M., & Chen, C.S. 2006. Overcoming trastuzumab resistance in HER2-overexpressing breast cancer cells by using a novel celecoxib-derived phosphoinositide-dependent kinase-1 inhibitor. *Molecular Pharmacology*, 70, (5) 1534-1541.

Ueda, Y., Hirai, S., Osada, S., Suzuki, A., Mizuno, K., & Ohno, S. 1996. Protein kinase C activates the MEK-ERK pathway in a manner independent of Ras and dependent on Raf. *J.Biol.Chem.*, 271, (38) 23512-23519.

Valabrega, G., Montemurro, F., & Aglietta, M. 2007. Trastuzumab: mechanism of action, resistance and future perspectives in HER2-overexpressing breast cancer. *Ann.Oncol.*, 18, (6) 977-984.

van Zelm, M.C., Smet, J., Adams, B., Mascart, F., Schandene, L., Janssen, F., Ferster, A., Kuo, C.C., Levy, S., van Dongen, J.J., & van der Burg, M. 2010. CD81 gene defect in humans disrupts CD19 complex formation and leads to antibody deficiency. *J.Clin.Invest*, 120, (4) 1265-1274.

van, S.S., Westerveld, A., de Jong, P.T., Bleeker-Wagemakers, E.M., & Bergen, A.A. 1999. Retinitis pigmentosa: defined from a molecular point of view. *Surv.Ophthalmol.*, 43, (4) 321-334.

Vogel, C.L., Cobleigh, M.A., Tripathy, D., Gutheil, J.C., Harris, L.N., Fehrenbacher, L., Slamon, D.J., Murphy, M., Novotny, W.F., Burchmore, M., Shak, S., Stewart, S.J., & Press, M. 2002. Efficacy and safety of trastuzumab as a single agent in first-line treatment of HER2-overexpressing metastatic breast cancer. *J.Clin.Oncol.*, 20, (3) 719-726.

Wang, F., Weaver, V.M., Petersen, O.W., Larabell, C.A., Dedhar, S., Briand, P., Lupu, R., & Bissell, M.J. 1998. Reciprocal interactions between beta1-integrin and epidermal growth factor receptor in three-dimensional basement membrane breast cultures: a different perspective in epithelial biology. *Proc.Natl.Acad.Sci.U.S.A*, 95, (25) 14821-14826.

Wang, X.Q., Yan, Q., Sun, P., Liu, J.W., Go, L., McDaniel, S.M., & Paller, A.S. 2007. Suppression of epidermal growth factor receptor signaling by protein kinase C-alpha activation requires CD82, caveolin-1, and ganglioside. *Cancer Research*, 67, 9986-9995.

Weaver, V.M., Petersen, O.W., Wang, F., Larabell, C.A., Briand, P., Damsky, C., & Bissell, M.J. 1997. Reversion of the malignant phenotype of human breast cells in three-dimensional culture and in vivo by integrin blocking antibodies. *J.Cell Biol.*, 137, (1) 231-245.

Weigelt, B. & Bissell, M.J. 2008. Unraveling the microenvironmental influences on the normal mammary gland and breast cancer. *Seminars in Cancer Biology*, 18, (5) 311-321.

Weigelt, B., Lo, A.T., Park, C.C., Gray, J.W., & Bissell, M.J. 2010. HER2 signaling pathway activation and response of breast cancer cells to HER2-targeting agents is dependent strongly on the 3D microenvironment. *Breast Cancer Res.Treat.*, 122, (1) 35-43.

Westermarck, J., Li, S.P., Kallunki, T., Han, J., & Kahari, V.M. 2001. p38 mitogen-activated protein kinase-dependent activation of protein phosphatases 1 and 2A inhibits MEK1 and MEK2 activity and collagenase 1 (MMP-1) gene expression. *Mol.Cell Biol.*, 21, (7) 2373-2383.

White, A., Lamb, P.W., & Barrett, J.C. 1998. Frequent downregulation of the KAI1(CD82) metastasis suppressor protein in human cancer cell lines. *Oncogene*, 16, (24) 3143-3149.

White, C.D., Li, Z., Dillon, D.A., & Sacks, D.B. 2011. IQGAP1 protein binds human epidermal growth factor receptor 2 (HER2) and modulates trastuzumab resistance. *J.Biol.Chem.*, 286, (34) 29734-29747.

Whyte, J., Bergin, O., Bianchi, A., McNally, S., & Martin, F. 2009. Key signalling nodes in mammary gland development and cancer. Mitogen-activated protein kinase signalling in experimental models of breast cancer progression and in mammary gland development. *Breast Cancer Res.*, 11, (5) 209.

Witherden, D.A., Boismenu, R., & Havran, W.L. 2000. CD81 and CD28 costimulate T cells through distinct pathways. *J.Immunol.*, 165, (4) 1902-1909.

Wright, M.D., Geary, S.M., Fitter, S., Moseley, G.W., Lau, L.M., Sheng, K.C., Apostolopoulos, V., Stanley, E.G., Jackson, D.E., & Ashman, L.K. 2004a. Characterization of mice lacking the tetraspanin superfamily member CD151. *Mol.Cell Biol.*, 24, (13) 5978-5988.

Wright, M.D., Moseley, G.W., & van Spriel, A.B. 2004b. Tetraspanin microdomains in immune cell signalling and malignant disease. *Tissue Antigens*, 64, (5) 533-542.

Xu, C., Zhang, Y.H., Thangavel, M., Richardson, M.M., Liu, L., Zhou, B., Zheng, Y., Ostrom, R.S., & Zhang, X.A. 2009. CD82 endocytosis and cholesterol-dependent reorganization of tetraspanin webs and lipid rafts. *FASEB J.*, 23, (10) 3273-3288.

Yamamoto, Y., Ibusuki, M., Nakano, M., Kawasoe, T., Hiki, R., & Iwase, H. 2009. Clinical significance of basal-like subtype in triple-negative breast cancer. *Breast Cancer*, 16, (4) 260-267.

Yanez-Mo, M., Barreiro, O., Gordon-Alonso, M., Sala-Valdes, M., & Sanchez-Madrid, F. 2009. Tetraspanin-enriched microdomains: a functional unit in cell plasma membranes. *Trends Cell Biol.*, 19, (9) 434-446.

Yang, H., Xiao, X., Li, S., Mai, G., & Zhang, Q. 2011. Novel TSPAN12 mutations in patients with familial exudative vitreoretinopathy and their associated phenotypes. *Mol.Vis.*, 17, 1128-1135.

Yang, S., Raymond-Stintz, M.A., Ying, W., Zhang, J., Lidke, D.S., Steinberg, S.L., Williams, L., Oliver, J.M., & Wilson, B.S. 2007. Mapping ErbB receptors on breast cancer cell membranes during signal transduction. *J.Cell Sci.*, 120, (Pt 16) 2763-2773.

Yang, X., Claas, C., Kraeft, S.K., Chen, L.B., Wang, Z., Kreidberg, J.A., & Hemler, M.E. 2002. Palmitoylation of tetraspanin proteins: modulation of CD151 lateral interactions, subcellular distribution, and integrin-dependent cell morphology. *Mol.Biol.Cell*, 13, (3) 767-781.

Yang, X.H., Flores, L.M., Li, Q., Zhou, P., Xu, F., Krop, I.E., & Hemler, M.E. 2010. Disruption of laminin-integrin-CD151-focal adhesion kinase axis sensitizes breast cancer cells to ErbB2 antagonists. *Cancer Res.*, 70, (6) 2256-2263.

Yang, X.H., Richardson, A.L., Torres-Arzayus, M.I., Zhou, P., Sharma, C., Kazarov, A.R., Andzelm, M.M., Strominger, J.L., Brown, M., & Hemler, M.E. 2008. CD151 accelerates breast cancer by regulating alpha 6 integrin function, signaling, and molecular organization. *Cancer Res.*, 68, (9) 3204-3213.

Yang, X.H., Wei, L.L., Tang, C., Slack, R., Mueller, S., & Lippman, M.E. 2001. Overexpression of KAI1 suppresses in vitro invasiveness and in vivo metastasis in breast cancer cells. *Cancer Research*, 61, (13) 5284-5288.

Yarden, Y. & Sliwkowski, M.X. 2001. Untangling the ErbB signalling network. *Nature Reviews Molecular Cell Biology*, 2, (2) 127-137.

Yeon, C.H. & Pegram, M.D. 2005. Anti-erbB-2 antibody trastuzumab in the treatment of HER2-amplified breast cancer. *Invest New Drugs*, 23, (5) 391-409.

Yuan, T.L. & Cantley, L.C. 2008. PI3K pathway alterations in cancer: variations on a theme. *Oncogene*, 27, (41) 5497-5510.

Zemni, R., Bienvenu, T., Vinet, M.C., Sefiani, A., Carrie, A., Billuart, P., McDonell, N., Couvert, P., Francis, F., Chafey, P., Fauchereau, F., Friocourt, G., des, P., V, Cardona, A., Frints, S., Meindl, A., Brandau, O., Ronce, N., Moraine, C., van, B.H., Ropers, H.H., Sudbrak, R., Kahn, A., Fryns, J.P., Beldjord, C., & Chelly, J. 2000. A new gene involved in X-linked mental retardation identified by analysis of an X;2 balanced translocation. *Nat.Genet.*, 24, (2) 167-170.

Zhang, S., Huang, W.C., Li, P., Guo, H., Poh, S.B., Brady, S.W., Xiong, Y., Tseng, L.M., Li, S.H., Ding, Z., Sahin, A.A., Esteva, F.J., Hortobagyi, G.N., & Yu, D. 2011. Combating trastuzumab resistance by targeting SRC, a common node downstream of multiple resistance pathways. *Nat.Med.*, 17, (4) 461-469.

Zhang, S. & Yu, D. 2012. Targeting Src family kinases in anti-cancer therapies: turning promise into triumph. *Trends Pharmacol.Sci.*, 33, (3) 122-128.

Zhang, X., Gureasko, J., Shen, K., Cole, P.A., & Kuriyan, J. 2006. An allosteric mechanism for activation of the kinase domain of epidermal growth factor receptor. *Cell*, 125, (6) 1137-1149.

Zhang, X.A., Bontrager, A.L., & Hemler, M.E. 2001. Transmembrane-4 superfamily proteins associate with activated protein kinase C (PKC) and link PKC to specific beta(1) integrins. *J.Biol.Chem.*, 276, (27) 25005-25013.

Zhang, X.A., He, B., Zhou, B., & Liu, L. 2003a. Requirement of the p130CAS-Crk coupling for metastasis suppressor KAI1/CD82-mediated inhibition of cell migration. *J.Biol.Chem.*, 278, (29) 27319-27328.

Zhang, X.A., Lane, W.S., Charrin, S., Rubinstein, E., & Liu, L. 2003b. EWI2/PGRL associates with the metastasis suppressor KAI1/CD82 and inhibits the migration of prostate cancer cells. *Cancer Res.*, 63, (10) 2665-2674.

Zhao, F., Zhang, J., Liu, Y.S., Li, L., & He, Y.L. 2011. Research advances on flotillins. *Virol.J.*, 8, 479.

Zhao, J. & Guan, J.L. 2009. Signal transduction by focal adhesion kinase in cancer. *Cancer Metastasis Rev.*, 28, (1-2) 35-49.

Zhou, B., Liu, L., Reddivari, M., & Zhang, X.A. 2004. The palmitoylation of metastasis suppressor KAI1/CD82 is important for its motility- and invasiveness-inhibitory activity. *Cancer Res.*, 64, (20) 7455-7463.

Zoller, M. 2009. Tetraspanins: push and pull in suppressing and promoting metastasis. *Nature Reviews Cancer*, 9, (1) 40-55.

Zurita, A.R., Crespo, P.M., Koritschoner, N.P., & Daniotti, J.L. 2004. Membrane distribution of epidermal growth factor receptors in cells expressing different gangliosides. *Eur.J.Biochem.*, 271, (12) 2428-2437.